

**Exploring the dermal immune and angiogenic
responses to *Schistosoma mansoni***

Sarah Amelia Aynsley

Thesis submitted for the degree of PhD

The University of York

Department of Biology

August 2011

Abstract

Schistosoma mansoni is a parasitic helminth which gains access to the host's vascular system by penetrating and migrating through the skin in search of a blood vessel. The aim of this thesis was to determine whether during this migration the schistosome cercariae induce blood vessel growth (angiogenesis). This was examined following both a single exposure to the parasite (1x) and four exposures (4x). After 4x infections it has been shown that the skin immune response is predominantly Th2 and may favour angiogenesis.

Utilising both imaging and molecular techniques it was shown that the vasculature of the pinnae alters and pro-angiogenic growth factors are up – regulated after infection. This was exacerbated in the pinnae of 4x infected mice with a change in the predominant growth factors up regulated. The difference in growth factors between 1x infected and 4x infected mice was in part due to the influx of haematopoietic cells into the dermis (DEC). In the 4x infected pinnae the DEC were predominately eosinophils (45%) which expressed hepatocyte growth factor (HGF) and matrix metalloproteinases (MMPs). Macrophages in the 4x infected mice were alternatively activated (up –regulating Arginase-1 and Ym1) and producing pro- vascular endothelial growth factor (VEGF) and placental growth factor (PlGF). These phenotypes were partially controlled by high levels of IL-10 in 4x pinnae, loss of which increased the expression of PlGF by macrophages. It was also shown that the cercarial secretions (0-3hrRP) have pro-angiogenic properties. Culture of human umbilical vein endothelial cells (HUVECs) with 0-3hrRP induced cell proliferation and the formation of primitive branches *in vitro*. Additionally using the Matrigel plug method it was shown that 0-3hrRP can induce the growth of new blood vessels *in vivo*. These results indicated that cercariae can directly induce blood vessel growth as well as altering the dermal innate immune response. This presents a potential therapeutic benefit in the treatment of non-healing wounds.

Contents

Abstract	2
Contents	3
List of Figures	9
List of Tables	10
Acknowledgments	11
Declaration	11
Chapter 1: General Introduction	12
Overview of the Introduction.....	13
1.1 Schistosomiasis	13
1.1.1 The disease and life cycle.....	13
1.1.2 Migration of cercariae through the skin	15
1.2 Wound healing and Angiogenesis.....	17
1.2.1 Overview of wounding and angiogenesis	17
1.2.2 The process of angiogenesis	18
1.2.3 Factors involved in angiogenesis	20
1.2.3.1 The angiopoietins.....	20
1.2.3.2 Matrix metalloproteinases.....	21
1.2.3.3 The VEGF family	21
1.2.3.4 FGF family.....	24
1.2.3.5 HGF.....	24
1.3 The immune response and angiogenesis.....	25
1.3.1 The immune response to schistosomes.....	27
1.3.2 The dermal immune response to multiple infections with <i>S.mansoni</i>	28
1.3.3 Cytokines in angiogenesis	27
1.3.4 Immune cells and angiogenesis	32
1.3.4.1 Neutrophils.....	33
1.3.4.3 Dendritic cells.....	36
1.3.4.4 Eosinophils	36
1.3.4.5 Mast cells	37
1.4 Aim of this study	38

Chapter 2: General Materials and Methods	39
2.1 General Materials and Methods	40
2.1.1 Parasite Maintenance	40
2.1.2 Infection Scheme.....	40
.....	40
2.1.3 RNA Extraction	41
2.1.4 Reverse Transcription.....	41
2.1.5 Semi-quantitative Polymerase chain reaction (SQ-PCR)	41
2.1.6 Real time Quantitative PCR (Q-PCR) of DEC.....	42
2.1.7 In vitro cultured pinnae biopsies	43
2.1.8 Enzyme linked immunosorbent assay (ELISA)	43
Chapter 3: Characterising the angiogenic response following single (1x) and multiple (4x) infections.	45
3.1 Introduction	46
3.2 Materials and Methods.....	47
3.2.1 External imaging on the pinnae and vessel quantification.....	47
3.2.2 Skin Histology	47
3.2.3 α CD31 and α CD105 vessel labelling.....	47
3.2.4 Visualisation and quantification of CD31+ and CD105+ vessels.....	48
3.2.5 Measurement of vascular leakage using the Modified Miles assay	48
3.2.6 Detection of active MMPs.....	49
3.3 Results	50
3.3.1 Vessels become more visible following infection	50
3.3.2 The epidermis and dermis are disrupted and thicken following infection	52
3.3.3 The vessels of 4x pinnae are thicker and more numerous than 1x and naïve	54
3.3.4 Vessel remodelling identified by labelling with α CD105	58
3.3.5 CD105 expression is up regulated on vessels in infected pinnae	61
3.3.6 Increased vascular permeability following infection	62
.....	63
3.3.7 Angiopoietin 2 is strongly induced in 4x pinnae	64
3.3.8 4x pinnae show increased levels of active MMPs compared to 1x and naïve	65
3.3.9 Transcript levels of MMP-9 and MMP-19 increased after infection	66
3.3.10 Two isoforms of VEGF are significantly up regulated after 4x infection	68

3.3.11 Array analysis of angiogenic factors	70
3.3.12 Several pro-angiogenic growth factors were up regulated after infection	74
3.4 Discussion.....	76
3.4.1 Overview	76
3.4.2 Pinnae vasculature changes after infection.....	76
3.4.3 MMPs are up-regulated in 4x pinnae	78
3.4.4 Infection induces the release of pro-angiogenic growth factors.....	80
3.4.5 Summary	83
Chapter 4: Determining the angiogenic phenotype of the dermal innate immune response to infection	84
4.1 Introduction	85
4.2 Materials and Methods.....	88
4.2.1 Dermal Exudate Cell (DEC) retrieval and counts.....	88
4.2.2 Labelling DEC with antibodies for flow cytometric analysis	88
4.2.3 Cell sorting of DEC.....	89
4.2.4 Cytospins and DiffQuick staining	89
4.2.5 Pinnae digest	90
4.2.6 Cytokine array kit	90
4.2.7 Cytokine ELISAs	90
4.2.7.1 IFN γ , IL-1 β , IL-4, IL-5 (in house using paired antibodies from BD Pharmingen).....	91
4.2.7.2 IL-10, IL-12p40, IL-13 (Duo kits from R&D Systems)	92
4.2.7.3 Addition of final substrate	92
4.2.8 Toluidine Blue staining of pinnae sections	92
4.3 Results	93
4.3.1 1x and 4x pinnae show varying levels of cytokines and chemokines	93
4.3.1.1 Cytokines	93
4.3.1.2 Chemokines.....	94
4.3.2 4x pinnae show significantly elevated levels of Th2 cytokines.....	98
4.3.3 4x pinnae show a significant influx of DEC	100
4.3.4 The majority of DEC are CD45 ⁺	101
4.3.5 Phenotypic characterisation of the DEC	101
4.3.5.1 Neutrophils.....	102
4.3.5.2 Dendritic Cells	102
4.3.5.3 Macrophages and monocytes.....	103

4.3.5.4 Eosinophils	103
4.3.6 Phenotypic characterisation of CD45+ cells remaining in the tissue.....	108
4.3.7 More mast cells were presented in the dermis of 4x pinnae compared to 1x	114
4.3.8 4x DEC show increased expression of alternatively activated macrophage markers by PCR	115
4.3.9 DEC cell sorting into pure populations of Eosinophils, Macrophages and Dendritic Cells	116
4.3.10 DEC cells express transcript for selected growth factors and MMPs..	118
4.4 Discussion.....	120
4.4.1 Overview	120
4.4.2 Cytokine balance in the skin	120
4.4.3 The neutrophil influx was not altered between 1x and 4x infections. ...	122
4.4.4 4x macrophages express Arginase-1 and up-regulate PlGF compared to 1x.....	122
4.4.5 The majority of the 4x DEC are HGF expressing Eosinophils	124
4.4.6 Dendritic cells from 1x pinnae are more pro-angiogenic than those obtained from 4x pinnae.....	126
4.4.7 Summary	127
Chapter 5: Examining the influence of IL-10 in 4x pinnae	128
5.1 Introduction	129
5.2 Materials and Methods.....	131
5.2.1 IL-10 knock out mice	131
5.2.2 DEC retrieval and flow cytometry	131
5.2.3 Cell sorting.....	131
5.3 Results	
5.3.1 IL-10 ^{-/-} pinnae become inflamed and vessels more visible after infection	132
5.3.2 The increases vasculature in 4x IL-10 ^{-/-} is more organised than in 4x WT	134
5.3.4 Pro-angiogenic growth factors were up-regulated after infection in IL-10 ^{-/-} pinnae.....	138
5.3.5 Infection induces a significant influx of cells into the dermis.....	140
5.3.6 4x IL-10 ^{-/-} DEC contains significantly more eosinophils than 1x	141
5.3.8 Th2 cytokines are reduced in IL-10 ^{-/-} supernatants	143
5.3.8 4x IL-10 ^{-/-} pinnae contain increased levels of HGF and VEGF compared to WT	145

5.3.10 IFN γ is up regulated in IL-10 ^{-/-} pinnae	147
4.3.11 Macrophages and Eosinophils from IL-10 ^{-/-} DEC show reduced expression of Ym1 and RELM α respectively	148
5.3.12 Macrophages and dendritic cells in IL-10 ^{-/-} DEC expressed more PIGF than WT.....	150
5.4 Discussion.....	152
5.4.1 Overview	152
5.4.2 The vasculature in IL-10 ^{-/-} pinnae was increased, but displayed a more organised morphology.	152
5.4.3 Expression of pro-angiogenic growth factors in whole IL-10 ^{-/-} pinnae..	153
5.4.4 Changes in the cytokine profile of IL-10 ^{-/-} pinnae	154
5.4.5 Changes in cell recruitment in IL-10 ^{-/-} pinnae	155
5.4.6 Phenotypic changes in IL-10 ^{-/-} DEC	156
5.4.7 Summary	158
Chapter 6: Investigating the pro angiogenic potential of cercarial secretions (0-3hRP)	159
6.1 Introduction	160
6.2 Materials and Methods.....	162
6.2.1 Collection of 0-3hRP.....	162
6.2.2 L929 fibroblast culture and production of conditioned media	162
6.2.3 Bone marrow cell extraction and differentiation	162
6.2.3.1 Bone marrow derived macrophages.....	163
6.2.3.2 Bone marrow derived dendritic cells.....	163
6.2.4 Bone marrow derived cell culture with 0-3hRP.....	163
6.2.5 Transcript analysis from bone marrow derived cells.....	164
6.2.6 Wound Healing Assay.....	164
6.2.7 Culture of Human Umbilical Vein Endothelial Cells (HUVECs).....	165
6.2.8 HUVEC proliferation Assay	165
6.2.9 Proliferation assay with protease inhibition.....	166
6.2.10 Branching Assay	166
6.2.11 Staining of HUVECs with phalloidin and DAPI.....	166
6.2.12 Matrigel Plug assay	167
6.3 Results	168
6.3.1 PIGF expression is induced in bone marrow derived macrophages and dendritic cells after culture with 0-3hRP	168
6.3.1.1 Bone marrow-derived macrophages	168

6.3.1.2 Bone marrow-derived dendritic cells.....	169
6.3.2 Parasite antigens induce fibroblast migration	170
6.3.3 0-3hRP induces endothelial cell proliferation.....	172
6.3.4 Protease inhibition restores 0-3hRP induced proliferation	174
6.3.5 HUVECS form primitive branch-like structures in response to 0-3hRP .	175
6.3.6 HUVECs extend filopodia and align after culture with 0-3hRP.....	177
6.3.7 0-3hRP induces blood vessel growth into Matrigel plugs in vivo	179
6.4 Discussion 6.4.1 Overview.....	181
6.4.2 0-3hRP induced PlGF expression in bone marrow derived macrophages	181
6.4.3 0-3hRP stimulates fibroblast migration	182
6.4.4 0-3hRP induces cell endothelial proliferation and branching.....	183
6.4.5 0-3hRP induces blood vessel growth in vivo.....	185
6.4.6 Summary	187
Chapter 7: General Discussion	189
7.1 General Discussion	190
7.1.1 Overview	190
7.1.2 Pro-angiogenic growth factors in the skin following S.mansoni infection	192
7.1.3 Pro-angiogenic leukocyte influx.....	195
7.1.4 0-3hRP induced angiogenesis	197
7.1.5 Summary	199
Appendix	201
Section 1 - Primer Pairs, cycle numbers and annealing temperatures.....	201
Section 2 - Raw data from array analysis.....	203
Abbreviations	206
References.....	208

List of Figures

Figure		Page
Chapter 1		
Figure 1.1	Overview of angiogenesis	19
Chapter 2		
Figure 2.1	Timeline of Infection.	40
Chapter 3		
Figure 3.1	Imaging and quantification of blood vessels following infection	51
Figure 3.2	Thickness and histology of pinnae	53
Figure 3.3	The vessels of the dermis labelled with FITC conjugated anti CD31 mAb	55-56
Figure 3.4	Quantification of CD31 positive vessels.	57
Figure 3.5	Identification of CD105 expression on pinnae vessels	59-60
Figure 3.6	Analysis of CD105 expression	61
Figure 3.7	Vascular permeability following infection	63
Figure 3.8	Angiopoietin 1 and 2 gene expression	64
Figure 3.9	Levels of Collagenase and gelatinase MMPs in the skin.	65
Figure 3.10	Transcript analysis of MMPs.	67
Figure 3.11	Transcript and protein levels of VEGF	69
Figure 3.12	Levels of pro-angiogenic growth factor transcript from pinnae at days 1-8 after infection	74
Chapter 4		
Figure 4.1	Images and graphical representation of the cytokine and chemokine array	94-96
Figure 4.2	Cytokine ELISAs performed on skin biopsy supernatants	98
Figure 4.3	DEC counts	99
Figure 4.4	CD45+ cells in the DEC	100
Figure 4.5	Neutrophils	103
Figure 4.6	Dendritic Cells	104
Figure 4.7	Macrophages	105
Figure 4.8	Eosinophils	106
Figure 4.9	CD45+ cells in the skin	108
Figure 4.10	Neutrophils in the skin	109
Figure 4.11	Dendritic Cells in the skin	110
Figure 4.12	Macrophages in the skin	111
Figure 4.13	Eosinophils in the skin	112
Figure 4.14	Mast cells in the dermis	113
Figure 4.15	Expression by DEC of macrophage markers of activation.	114
Figure 4.16	Representative graph of parameters for cell sorting.	115
Figure 4.17	Analysis of markers of alternative activation and cytokine expression	116
Figure 4.18	Analysis of growth factor and MMP9 expression by sorted DEC	118

Chapter 5		
Figure 5.1	Images of IL-10 ^{-/-} pinnae after infection.	132
Figure 5.2	αCD31 labelled 4x IL-10 ^{-/-} and 4x WT pinnae	134
Figure 5.3	Histology of IL-10 ^{-/-} pinnae	136
Figure 5.4	Pro-angiogenic growth factor expression in IL-10 ^{-/-} whole pinnae cDNA	138
Figure 5.5	DEC cell counts from IL-10 ^{-/-} whole pinnae	139
Figure 5.6	Flow cytometric analysis of DEC from IL-10 ^{-/-} pinnae	141
Figure 5.7	Cytokine concentrations in IL-10 ^{-/-} whole pinnae supernatants	143
Figure 5.8	Comparison of growth factor expression between 4x WT and 4x IL-10 ^{-/-}	145
Figure 5.9	Comparison of IL-4, IL-13 and IFNγ concentrations between WT and IL-10 ^{-/-}	146
Figure 5.10	Alternatively activated macrophage markers in sorted IL-10 ^{-/-} DEC	148
Figure 5.11	Pro-angiogenic growth factor and MMP expression by sorted KO and WT DEC	150
Chapter 6		
Figure 6.1	Growth factor expression by bone marrow derived macrophages.	167
Figure 6.2	Growth factor expression by bone marrow derived dendritic cells.	168
Figure 6.3	Fibroblast migration in the presence of parasite antigens	170-171
Figure 6.4	HUVEC proliferation following 24hrs culture	172
Figure 6.5	HUVEC proliferation in the presence of a protease inhibitor	173
Figure 6.6	HUVEC branching after 24hr culture	175
Figure 6.7	Actin filament staining of HUVECs after 24hr culture	177
Figure 6.8	Matrigel plugs 4 days after implantation	179
Chapter 7		
Figure 7.1	Overview of experimental model	190
Figure 7.2	Parasite and Blood Vessel imaging	192

List of Tables

Chapter 3		
Table 3.1	Analysis of gene expression	72
Chapter 4		
Table 4.1	Antibodies used for DEC labelling	88
Table 4.2	Antibody pairs and kits for cytokine ELISAs	90
Table 4.3	Cell identification through surface phenotype	101
Chapter 6		
Table 6.1	Antibodies used for bone marrow derived cell labelling	163

Acknowledgments

My thanks go to Dr Adrian Mountford for his supervision and support throughout my research project. I would also like to thank my training committee, Dr Marika Kullberg and Dr Paul Genever, for their direction and criticism of my work.

Thanks also go to all the members of the Schistosomiasis group at York; including in particular Sophie, Ross and Ann for their support and help throughout my 4 years. I would also like to acknowledge the help and guidance that the imaging lab of the technology facility have provided, specifically Graeme and Karen. I would also like to thank my project and summer students, who over the years have kept me motivated and enthused. Particularly Chris Saleh, Rosie Beech, Dan Davenport and of course David Harvey.

On a personal note thanks to my friends and family for putting up with and supporting me. In particular Simon and Andy who have helped me through the pain and joy of a PhD, with the aid of many cups of tea.

Declaration

All of the research presented in this thesis is my own work with the following exceptions;

Chapter 3: External vessel quantification method was devised by Christopher .K. Saleh (University of York, Department of Biology).

Chapter 4 & Chapter 5: Cell sorting was performed by Karen Hodgkinson of the Imaging and Cytometry Labs (University of York).

Chapter 5: Some of the sorted DEC cDNA samples were originally sorted and reverse transcribed by Dr P.C.Cook

Chapter 1: General Introduction

Overview of the Introduction

This thesis aims to examine the complex process of angiogenesis during infection with Schistosomiasis mansoni (*S.mansoni*). *S.mansoni* is a parasitic helminth, which utilises blood vessels in order to infect its mammal host (Pearce 2002). The results presented here will examine changes in both the dermal vessels and the immune system in relation to angiogenesis.

The first part of this introduction will introduce schistosomiasis and the parasite's interactions with the skin during infection. The second part will give an overview of the processes involved in angiogenesis and wound healing, with particular focus on key growth factors. The final section will cover the immune response to schistosomiasis, including a description of the multiple infection model used in this study, and the influence of the immune system on angiogenesis in disease.

1.1 Schistosomiasis

1.1.1 *The disease and life cycle*

Schistosomiasis is caused by a parasitic helminth that utilises two hosts and several morphologically distinct life cycle stages (Pearce 2002). Infection is prevalent across Africa, Asia and South America (Chitsulo 2000). Schistosomiasis is a major cause of morbidity among infected populations (van der Werf 2003). There are five main species of helminth which cause schistosomiasis; one of the most prevalent and widely studied is *S.mansoni* which causes intestinal schistosomiasis in humans and is the focus of this study (Kabatereine et al 2002, Pearce 2002).

S.mansoni has a two host life cycle; snails and mammals, consisting of several morphologically distinct stages. The snail host for *S.mansoni* is the water snail *Biomphalaria glabrata* (Files 1949). Within the snails the parasite undergoes successive replication within the hepatopancreas producing thousands of the

human infective stage; the cercariae. These are shed into the water daily from the snail host dependant on temperature and light. They are composed of a head and tail and vigorously move to maintain their position in the water awaiting a permissive host. Infection of the human host occurs when bare skin comes into contact with infected water (Pearce 2002). The cercariae attach and directly penetrate the skin. During this process the tail detaches (although this is disputed and the cercariae release their gland contents. The parasite must migrate through the epidermis into the dermis in search of a blood vessel, or on occasion a lymphatic vessel (McKerrow 2002).

Upon entry into the circulatory system the schistosomula migrate to the lungs where they push through the capillaries, elongating and maturing to allow subsequent migration of the worm (Wilson 1986). The mature worms continue around the circulation to the hepatic portal system where the males and females pair up and migrate along the length of the major vessels, to as close to the intestines as possible (Miller 1980, Dean 1984). The females lay eggs which transit through the vessel wall into the lumen of the intestine and are passed out of the body in faeces. Whilst many eggs exit the body some can get backwashed into the liver or remain lodged in the intestinal wall (Doenhoff 1985). Eggs which do exit the body can hatch into the snail infective stage; miracidia upon contact with fresh water and complete the life cycle.

At several points during the schistosome life cycle the parasite is in close association with the vasculature of the host. During elongation in the lungs and egg passage through into the intestinal lumen the parasite is in direct interaction with the vessels. It has been previously shown that the eggs of *Schistosoma mansoni* secrete factors aiding their escape from the tissue (Loeffler 2002). Among these is a factor which has been shown *in vitro* to induce processes associated with angiogenesis, including endothelial cell proliferation and assembly into primitive vessels (Kanse 2005).

During the skin stage the parasite needs to find and enter a blood vessel to continue the infection process. Therefore it is possible that the cercariae as well as the eggs may induce angiogenesis or vascular remodelling.

1.1.2 Migration of cercariae through the skin

Many previous studies of *S.mansoni* have concentrated on the chronic egg stage of infection; this work will focus on the early skin interactions to the cercariae. The cercariae are approximately 250µm long consisting of a large head section (100µm) containing pre- and post- acetabular glands and a forked tail (150µm long) which allows it to move within the water (Doresy et al 2002). Invasion of the host skin requires the cercariae to attach and penetrate through the skin layers, triggered by host chemical stimuli (Haas 1994, Haas 1997).

The skin is composed of two main layers, the epidermis and dermis (Menon 2002). It is within the dermis that the blood vessels are located, and the cercariae must force through multiple epidermal layers to reach this. The outermost of these is flattened dead and dying cells whilst the lower layers are more structurally integral, composed of primarily keratinocytes which are anchored with adherent junctions to each other and the basement membrane (Menon 2002). The parasite forces its way through these epidermal layers until reaching the basement membrane which separates the epidermis and dermis (Cozzani 2001). Skin migration can be stalled here as the basement membrane which contains a thin but strong layer of collagen fibres and microfibrils (Smith 1982). Penetration and entry through the epidermis can take around 30 minutes in mice but the majority of the larvae can still be found in the dermis up to 40 hours after infection (He 2005). This timing is contentious and seems to be highly dependent on the host species and method of detection (Wilson 1987, McKerrow 2002, Curwen 2003, Whitfield 2003). During this time however the cercariae are in close contact with the keratinocytes and can cause significant damage to the epidermal layer eliciting wound healing responses.

Once through the basement membrane the cercariae move through the dermis and locate a blood vessel. In murine studies it can take the parasite 10hrs to locate a vessels and a further 8hrs to penetrate through the endothelial cell layer into the blood stream (Crabtree 1980). The dermis is composed primarily of fibroblasts which produce the extracellular matrix (ECM) the structural scaffold of the skin (Chiquet 2003). ECM is composed primarily of proteoglycans, heparin sulphate and elastin and collagen fibres (Pflieger 2006). Throughout the dermis is a well ordered network of both blood and lymphatic vessels (Menon 2002).

Migration through the dermis is associated with the release of proteolytic enzymes from the glands of the cercariae (Keene 1983, McKerrow 2002). These contain a mix of proteases, including a large amount of cercarial elastases, which can degrade the proteins that compose the extracellular matrix. (Newport 1988, Curwen 2006). Studies using models of extracellular matrix have shown cercarial secretions will degrade elastin, collagen and glycoproteins (McKerrow 1983). The timing of parasite secretion release is controversial. Some studies have shown that the acetabular glands are emptied before reaching the dermis (Curwen 2003) while others believe it is used for dermal migration (Crabtree 1985, McKerrow 2003).

After cercarial penetration of a vessel, de-granulating platelets can be found. Platelets contain a number of inflammatory mediators which could influence both activation of the immune response and inflammation driven angiogenesis (Mannaioni 2004). The movement and the release of extracellular matrix (ECM) degrading enzymes by the cercariae suggests that they have the potential to induce wound healing and angiogenesis in the skin.

1.2 Wound healing and Angiogenesis

1.2.1 Overview of wounding and angiogenesis

Wound healing comprises of a series of closely regulated steps. The process can be broken down into three phases, inflammation, proliferation and remodelling, although these are not distinct steps and *in vivo* wound healing will overlap spatially and temporally (Witte 1997).

The inflammatory phase is characterised by an influx of leukocytes and the production of pro-inflammatory cytokines e.g. Interleukin-1 β (IL-1 β), Transforming growth factor- α (TNF- α) and Interferon - γ (IFN γ). These cytokines and the release of histamines, primarily by resident immune cells and the fibroblasts of the skin, cause vasodilatation of surrounding blood vessels aiding the extravasation of leukocytes into the surrounding tissue (Neufeld 2006). There is an initial rapid neutrophil influx immediately following wounding before macrophages and then lymphocytes are recruited (Gimstad 2011). Platelets rapidly enter the site of damage and are an important source of chemokines and Platelet derived growth factor (PDGF), which is pro angiogenic (Mannaioni 2004, Gleissner 2008). In healing wounds new blood vessels sprout from the existing vasculature to supply oxygen to the new tissue (Tonnesen 2000). The damage to the skin layers releases growth factors which are sequestered in the extracellular matrix (ECM) and further growth factors are released by the cells in the skin; keratinocytes, fibroblasts and endothelial cells as well as by the haematopoietic cells recruited (Frantz 2005). After revascularisation of the wound the fibroblasts grow across the wound and deposit a provisional extracellular matrix. During this process re-epithelialisation of the epidermis occurs with epithelial cells crawling over the wound site providing cover for the new tissue to remodel and contract (Witte 1997).

1.2.2 The physiological process of angiogenesis

In a developing embryo the formation of a fully functioning vascular network is essential to survival. This process, termed vasculogenesis, utilises endothelial progenitors – angioblasts, which migrate and form networks of vessels under the guidance of several growth factors including vascular endothelial growth factor (VEGF) (Carmeliet 1996). The primitive vascular networks undergo remodelling and maturation into the quiescent functioning vasculature of an adult (Patan 2000). The term angiogenesis is used to encompass this process and the process of new blood vessel formation in the adult.

As well as being a physiological process in embryonic development, angiogenesis is important in the maintenance of the adult tissues. Local changes in the levels of pro and anti angiogenic growth factors control this process. Angiogenesis can be initiated by hypoxia, release of angiogenic growth factors by cells and from damaged tissues (Brogi 1994). It is also induced in several diseases, including cancer (Carmeliet 2000).

The process of angiogenesis itself involves a series of steps (Figure 1.1). Firstly the vessels, which are usually quiescent in the fully developed adults, undergo vasodilation. This can be initiated by nitric oxide and VEGF (Fukumura 2001). In order to allow endothelial cell proliferation and eventual migration, the junctions between endothelial cells need to loosen. The adhesion molecules, platelet endothelial cell adhesion molecule 1 (PECAM-1) and vascular endothelial cadherin (VE-cadherin), are both redistributed on the cell surface weakening the cell-cell connections (Eliceiri 1999). Excessive vasodilation is detrimental and can lead to circulatory collapse, and hypertension among others (Schermuly 2011). The angiopoietin family of genes controls the balance of vascular leakage (1.2.3.1). Angiopoietin 1 (Ang1) is constitutively expressed and maintains vascular stability whilst angiopoietin 2 (Ang 2) promotes leakage and loosening of endothelial cells and the basement membrane of vessels (Roviezzo 2005). In order to clear a path for new vessel migration the existing ECM and basement membrane of the vessels must be remodelled. This is accomplished primarily by the Matrix metalloproteinases (MMPs) (1.2.3.2). MMPs act in a cascade

promoting ECM degradation, pericyte detachment from vessels and growth factor release (Rundhaug 2005).

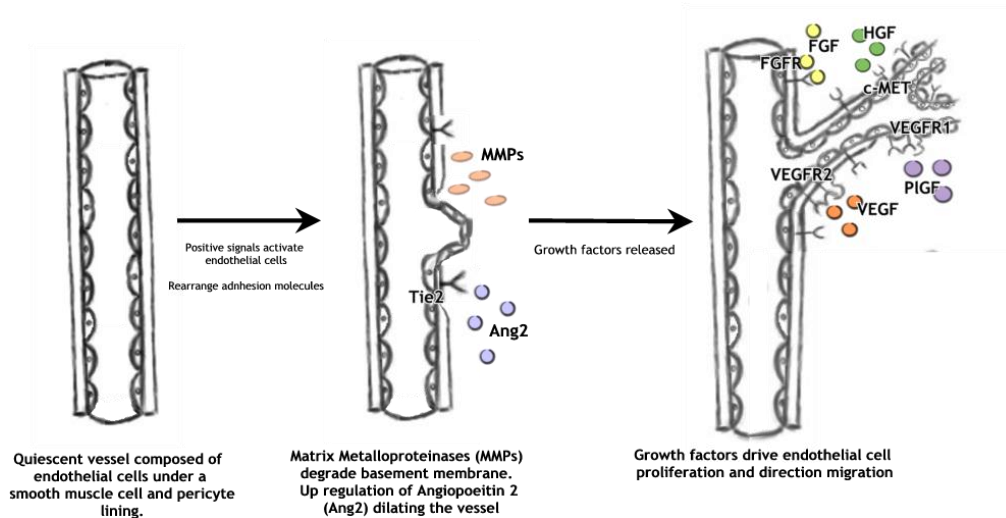


Figure 1.1: Overview of angiogenesis

Quiescent vessels are stabilised with smooth muscle cells and pericytes. When pro-angiogenic stimuli are released the endothelial cells rearrange their cell-cell adhesion molecules and become activated. MMPs degrade the basement membrane around the vessels and surrounding ECM. Growth factors released by neighbouring cells direct the proliferation and migration of endothelial. The cells of the immune system can also be a source of growth factors (1.3). After the signals are resolved the endothelial cells stabilise and up-regulate cell-cell contacts maturing with a layer of smooth muscle cells and pericytes to become quiescent again.

(HGF- hepatocyte growth factor, PIGF – Placental growth factor, FGF – fibroblast growth factors, VEGF – vascular endothelial cell growth factor)

Proliferation and migration of the endothelial cells is then induced by pro-angiogenic growth factors. Many of these are sequestered in the ECM and released by MMPs whilst others are produced by platelets (Nagase 1999). Several distinct families of growth factors can stimulate angiogenesis some with overlapping functions whilst others have a distinct role. The VEGF family of growth factors is central to angiogenesis controlling endothelial proliferation, directional migration and lumen formation (1.2.3.3). One member of the VEGF family – Placental growth factor (PIGF) is particularly associated with pathogenic angiogenesis (1.2.3.3). It and platelet-derived growth factor (PDGF) are redundant during development but induced in adult angiogenesis where they

often function to promote the recruitment of inflammatory cells to sites of remodelling (Mannaioni 2004). Hepatocyte growth factor is another factor expressed primarily in pathological angiogenesis, controlling endothelial cell mobilisation and invasiveness (1.2.3.5). Whilst the Fibroblast growth factors (FGFs) (1.2.3.4) are essential in both developmental and physiological angiogenesis. After cells have proliferated and mobilised angiogenic inhibitors suppress further proliferation and stimulate the maturation of endothelial cells into mature vessels (Moses 1991). Endothelial cells assemble as tubes which eventually form a lumen which fuses to the pre-existing vessels; the new vasculature eventually becomes quiescent.

1.2.3 Factors involved in angiogenesis

1.2.3.1 The angiopoietins

The up-regulation of pro-inflammatory cytokines and histamines can induce vessel permeability but it is also tightly controlled by the angiopoietin family . Of these there are two main genes, Ang1 and Ang2, which work antagonistically through their mutual receptor Tyrosine-protein kinase receptor (Tie 2) (Stoeltzing 2003, Maisonpierre 1997).

Ang1 is expressed constitutively in the adult and helps maintain vessel quiescence (Brindle 2006). Ang1 signalling suppresses vascular permeability by up-regulation of cell to cell adhesion molecules on the endothelial cells of the vessels, including both PECAM 1 and VE-Cadherin (Gamble 2000). Transgenic over expression of Ang1 can cause blood vessels to become leakage resistant even in the presence of VEGF (Thurston 1999).

Ang2 is expressed at sites of angiogenic sprouting and remodelling (Maisonpierre 1997). It induces vascular leakage by binding to Tie 2 and preventing Ang1 signalling. Ang2 signalling induces dissociation of the endothelial cells and inflammation of the vessels. Ang-2 must be produced constantly at high concentrations to overcome the constitutive expression of Ang-1 (Kim 2000, Roviezzo 2005).

1.2.3.2 Matrix metalloproteinases

To allow new blood vessels to form the existing ECM must be degraded, this is achieved in part by a family of zinc containing proteases called the matrix metalloproteinases (MMP). They are synthesized as inactive zymogens with a pro peptide domain which must be cleaved for the enzyme to become active (Rundhaug 2005). MMPs have various effects on the ECM including degradation to clear areas, releasing bound angiogenic factors and exposing integrin binding sites essential for the movement of growing blood vessels (Xu 2001, LeBrasseur 2002).

Among the MMPs, matrix metalloproteinase 9 (MMP-9) has been instigated as essential in the angiogenic process. Genetically modified mice lacking MMP-9 have impaired angiogenesis and impaired vascular remodelling. (Itoh 1998, Van Hinsbergh 2006). MMP-9 and MMP-2, both members of the gelatinase family, cleave type IV collagen to expose $\alpha\beta3$ integrins which are critical for pathological angiogenesis (Mahabeleshwar 2006). MMP-19 is expressed in wounded and repairing tissue and is associated with hyper proliferation of keratinocytes. MMP-19 is particularly expressed in granulation tissue by endothelial cells, fibroblasts and also the infiltrating cells (Sadowski 2003, Raza 2000). MMPs also aid in the final stage of wound repair; remodelling. Fibroblasts accumulate at the wound and deposit an array of ECM components. This provisional ECM is degraded by MMPs and replaced with an ECM of a composition more like that found in un- injured tissue. (Nagase 1999)

1.2.3.3 The VEGF family

VEGF is one of the most documented pro-angiogenic growth factors, and is widely regarded as an essential mediator in angiogenesis (Frelin 2000, Ferrara 2002, McColl 2004, Carmeliet 2005, Otrrock 2007). Its activity is largely restricted to cells of the vascular endothelium although it has been shown to stimulate macrophage migration. (Barleon 1996) VEGF stimulates endothelial cell

mitogenesis and migration as well as enhancing vascular permeability (Carmeliet 2000).

The VEGF gene family consists of seven proteins with varying and overlapping activities; VEGF-A, VEGF-B, VEGF-C, VEGF-D, VEGF-E, VEGF-F and PlGF. These each signal through one or more of the VEGF receptors; VEGFR1 (Flt-1), VEGFR2 (Flk-1), VEGFR3 (Flt-4) and Neuropilins 1 and 2. VEGF-A and PlGF are the main angiogenic mediators (see below), VEGF-B is poorly mitogenic for endothelial cells and VEGF-C and D are primarily lymphangiogenic (Otrock 2007).

VEGF-A

The primary VEGF family member is VEGF-A, also referred to as just VEGF. The gene encoding VEGF-A comprises of 8 exons, which through alternative splicing produce 4 predominant isoforms in mice: VEGF₁₂₀, VEGF₁₆₄, VEGF₁₈₈, VEGF₂₀₅ and 2 less abundant isoforms VEGF₁₄₄ and VEGF₁₈₂ (Tischer 1991). These isoforms have varying heparin binding affinity which alters their angiogenic function. The most predominant of these isoforms is VEGF₁₆₄ which partially binds heparin and is partially soluble. VEGF₁₂₀ is completely soluble whilst VEGF₁₈₈ is entirely matrix bound and sequestered in the ECM (Poltorak 1997, Krilleke 2007).

VEGF production is regulated primarily by hypoxia through activation of the Hypoxia inducible factor (HIF) -1 (Liu 1995, Detmar 1997). In addition several growth factors including TGF α , TGF β and PDGF up-regulate VEGF expression, along with pro inflammatory cytokines including IL-6 and IL-1 α (Salgado 1999, Goumans 2003, Nagineni 2003). VEGF-A signals through Flt-1 and Flk-1 which are both trans-membrane receptor tyrosine kinases (Shibuya 2001) Flt-1 undergoes phosphorylation upon VEGFA binding but does not appear to transduce a signal and was proposed to be a dummy receptor preventing binding to Flk-1 and regulating growth. However recently binding to the receptor has been associated with matrix metalloproteinase release and haematopoiesis (Wang 1998). Flk-1 is essential in developmental angiogenesis and is the main mediator of the

mitogenic effects of VEGF. Binding induces proliferation, migration and survival responses in the endothelial cells (Gerber 1998). In pathogenic conditions, VEGF up-regulation has been identified in tumour angiogenesis and associated with a high risk of subsequent metastasis. Anti VEGF treatments are currently being used to reduce vascularisation and development of tumours (Dirix 2010, Willet 2004).

PlGF

PlGF, which was originally identified in the placenta, is not essential in developmental angiogenesis but is expressed during pathological angiogenesis. (Hiratsuka 2001, Seaman 2007). PlGF signals through Flt-1 and it is theorised that it can displace bound VEGF which is then free to signal through Flk-1 and induce angiogenic responses. (Carmeliet 2001). PlGF stimulates the growth of endothelial cells (ECs) and smooth muscle cells (SMCs) (Wang 1998). Overexpression of the gene in the skin results in a significant increase in number, branching and diameter of the blood vessels (Odorisio 2002). As well as acting on endothelial cells PlGF can recruit bone marrow derived cells to neo-angiogenic sites (Carmeliet 2003). This places a central role on PlGF in many inflammatory diseases including arthritis and cancers (Yoo 2009, Taylor 2010)

VEGF-D (FIGF)

VEGF-D, also known as c-fos inducible growth factor (FIGF), activates Flk-1 and Flt-4 and has both angiogenic and lymphangiogenic properties (Byzova 2002, Saharinen 2004). FIGF is translated as an inactive precursor protein and must be proteolytically cleaved before it is active. Only fully processed forms will activate Flk-1 and induce angiogenesis (Stacker 1999). FIGF has potent angiogenic effects *in vivo* and *in vitro*. Endothelial cells stimulated with FIGF alter their morphology and proliferate, whilst overexpression of FIGF in rabbit corneas induces significant neo vascularisation (Marconcini 1999)

1.2.3.4 FGF family

The fibroblast growth factors like the VEGFs induce a wide range of responses in both developing embryos and adults. In humans 22 structurally related FGFs have been identified (Ornitz 2001). FGFs are required during development and the timing and pattern of expression varies between tissues (Maruoka 1998, Liu 2005).

The main FGF involved in angiogenesis is FGF2, mice lacking this gene have cardiovascular defects and delayed wound healing (Ortega 1998). FGF2 induces endothelial cells to organise into tubules and induces sprouting from mature vessels (Montesano 1986, Fulgham 1999, Cross 2001). As FGF2 is sequestered in the ECM through its heparin binding affinity, it can be released following wounding through proteolytic cleavage (Emoto 1998).

1.2.3.5 HGF

Hepatocyte growth factor (HGF) as its name suggests is primarily expressed in the liver, but is also found throughout several tissues in the body including the skin (Zarnegar 1995). It has supposed functions in liver regeneration but can also enhance motility and growth of endothelial cells marking it early on as a potential pro-angiogenic molecule (Matsumoto 1992, Morishita 1999). HGF is derived from a single chain glycoprotein which is proteolytically cleaved to produce a heterodimer of two subunits (Nakamura 1989). Signalling by HGF occurs through the receptor Met (Bottaro 1991, Dong 2001). This is a heterodimer which transduces multiple biological effects including mitogenesis, morphogenesis and motogenesis (Weidner 1993). HGF and VEGF work in concert to promote vessel formation from activated endothelial cells (Xin 2001). Activation of the Met receptor by HGF stimulates high levels of EC proliferation and motility, and HGF is particularly up-regulated in EC monolayers following wounding (Bussolino 1992, Camussi 1997).

1.3 The Immune response and angiogenesis

1.3.1 Pathological angiogenesis

Angiogenesis is an essential mechanism in the development and maintenance of adult vasculature during several physiological processes, including wound repair and menstruation (Smith 2001). However it can also play a distinctly pathological role. Many diseases have an angiogenic component, usually either excess new vessel growth, deformations to existing vessels or inhibition of growth (Carmeliet 2003).

One of the main differences between physiological and pathological angiogenesis is the involvement of the immune system. Platelets, monocytes/macrophages and other leukocytes are recruited to wound sites of inflammation or damage and can direct the expression of angiogenic factors (Frantz 2005). The cells themselves can also release pro-angiogenic growth factors. Several inflammatory pathological conditions show exacerbated / exaggerated angiogenesis including asthma, arthritis and psoriasis (Jackson 1997, Bos 2005, Rudolph 2005, Holt 2010).

In rheumatoid arthritis an unknown factor causes the influx of large numbers of inflammatory cells into a joint and the release of pro-inflammatory cytokines (Kinne 2007). This leads to the formation of a pannus and up-regulation of MMPs and pro angiogenic growth factors (Clavel 2003). The outer synovial layer of a normal joint is predominantly avascular and under a quiescent state. Aberrant pathological angiogenesis allows vascularisation and inflammation of the joint progressing the disease (Walsh 2001). Two predominant factors are VEGF and PlGF, which drive vessel growth and vascularisation of the joint lining and allowing more leukocytes to be recruited perpetuating the swelling and destruction in the joint (Luttun 2002). PlGF in particular is up-regulated significantly in rheumatoid arthritis and causes excessive fine vessel branching (1.2.3.3). Blocking the PlGF receptor, Flt-1, has been shown as an effective way to

reduce disease in mouse models of arthritis, by restricting revascularisation and halting disease progression (Yoo 2009).

Another disease which exhibits excess inflammation driven angiogenesis is psoriasis. This is an inflammatory disorder of the skin, characterised by excessive growth of keratinocytes, inflammatory cell accumulation in the epidermis and excessive dermal angiogenesis (Creamer 2002). Importantly it is the change in vessel morphology which characterises this disease. Capillaries of the skin become dilated and torturous elongating throughout the dermis. VEGF and Hypoxia inducible factor (HIF) are strongly up-regulated in the skin of psoriasis patients along with Ang2 which promotes vascular leakage (Simonetti 2006). Vessels in psoriasis, unlike in mature disease free skin, are thin and numerous pushing up through the dermis to the usually avascular epidermis. The change in morphology of these vessels from their native state aids in the progression of the disease (Heidenreich 2009).

In addition to a direct immune cell mediated initiation of angiogenesis, tumour cells secrete factors to promote their own growth and survival which can drive angiogenic processes (Chung 2010). As tumours grow they increase demand on nutrients and oxygen in the surrounding tissue and the centre of the tumour becomes hypoxic. The hypoxia pathway is initiated causing up regulation of VEGF and FGF-2 among other factors, and inducing angiogenesis. New vessel growth is essential for reoxygenation but is also an important step in the final stages of tumour maturation and the ability of a tumour to metastasise (Vaupel 2004). The vessels which grow into and around a tumour are morphologically different to those of normal vasculature. The vessels are often thin and densely packed and are not stabilised with pericytes and smooth muscle cells. The basement membrane is disorganised and as such the tumour vasculature is frequently leaky (Carmeliet 2000). Tumour vessels often express specific markers including CD105 (also known as Endoglin) which is a surface component of the TGF-beta receptor complex. CD105 is expressed at high density on tumour vasculature and can be used to distinguish between tumour vessels and pre-existing vessels (Seaman 2007).

S.mansoni is in close association with blood vessels throughout its life cycle, as such there it is possible that the parasite either directly or through the immune response it is inducing is causing aberrant pathological angiogenesis within the host.

1.3.2 The immune response to schistosomes

During infection with schistosomes the immune system undergoes a switch. Eggs which become lodged in the tissue elicit a vigorous immune response. This response is down regulated from a pro inflammatory Th1 driven phenotype to a regulatory Th2. The Th2 driven response encapsulates the eggs encasing them in granulomas of collagen fibres and immune cells, predominantly eosinophils and macrophages (Hoffmann et al 2000). The majority of research into schistosomiasis has concentrated on the chronic immune response to the eggs.

At the onset of egg production the body mounts a strong inflammatory response with high levels of IFN γ detectable. However as infection progresses and egg laying increases this response shows a switch to a predominantly Th2 associated response with increases in IL-10, IL-4 and IL-13 (Pearce et al 1991). This is associated with the presence of dendritic cells and macrophages around the eggs driving the Th2 phenotype. (MacDonald et al 2001) Experimental models in mice have shown that these Th2 responses are protective and beneficial for the host, mice lacking IL-4 or T cells die shortly after infection (Fallon and Dunne 1999). IL-10 dependant effects are likely to control much of the Th1 to Th2 switch as IL-10 deficient mice (IL-10KO) develop an unchecked Th1 response and exacerbated pathology and mortality (Sadler et al 2003).

There are fewer papers focusing on the skin response to infection and those which do often look in conjunction with monitoring downstream pathologies. There are few that have focused on the immune response in relation to the skin's ability to recover and the angiogenic effects in the skin. The passage of the cercariae through the skin will cause both damage and also invoke an innate immune response which may impact on downstream immune regulation.

Invasion of the skin by cercariae causes an inflammatory cytokine release and localised oedema, vasodilation and inflammatory cell influx. The epidermis of the skin thickens early (~6hours post infection) and remains thickened for several days after infection (Iceni 1984, Hogg 2003). Granulocytes can be seen infiltrating into the epidermis, these are primarily neutrophils but eosinophils are also present (Iceni 1984, Ward 1988). After infection the dermis shows considerable oedema, leukocyte infiltration and vasodilation (Mastin 1983, Wheater 1979). The cell influx contains initially neutrophils accompanied later by macrophages, dendritic cells and eosinophils which peak at day 4 (Hogg 2003). The phagocytic cells of this influx (macrophages and dendritic cells) can capture the parasite antigen and migrate to skin draining lymph nodes which will lead to initiation of the adaptive immune response and alter the phenotype of the cells (Paveley 2011).

After infection many inflammatory mediators are found in the dermis including IL-6, IL-1 β , MIP1 α and eotaxin (He 2002, Wolowczuk 1997). This is an immediate innate response to the parasite induced wounding of the skin. This initial response develops and other cytokines including IL-12 and IL-10 are expressed (Angeli 2001). IL-10 has known regulatory functions and as discussed previously has been implicated as beneficial in the modulation of the host immune response to schistosomes (Dewals 2010). Skin resident cells including keratinocytes and fibroblasts are both potential sources of the IL-10 (Ramaswamy 2000). The influx of leukocytes may also make and respond to the IL-10 regulating the immune response in the skin.

1.3.3 The dermal immune response to multiple infections with *S.mansoni*

Just prior to beginning this project the laboratory showed that the immune response in the skin after multiple infections showed a similar switch to that seen after egg deposition. Individuals living in infected regions are likely to be

repeatedly exposed to schistosomes, as they come into contact with contaminated water sources through daily tasks *e.g.* collecting water and washing. Human studies document increasing resistance to reinfection and lower infection intensities in high risk areas, potentially as a result of re infection. (Caldas et al 2000). Infected children in these areas show elevated IL-10 levels perhaps indicative of an immune switch from multiple infections (Van der Biggelaar 2000).

Unfortunately the murine host, used predominantly in experimental models, cannot survive multiple infections due to the pathology caused by egg accumulation. Several studies have used non-human primates to determine whether multiple infections can alter the host responsiveness to infection and subsequently confer protection (Sturrock 1984, Farah 1997). These studies showed that the multiple infected animals had delayed pathology and re stimulated peripheral blood mononuclear cells (PBMC) induced increased levels of IL-4, IL-5 and IL-10 compared to a single infection (Farah 2000, Nyindo 1999). However these studies have not focused on whether multiple infections affect the initial immune response at the skin infection site.

Two infection regimes have been utilised in the mouse model in order to examine multiple infections in the skin; infection with radiation attenuated (RA) cercariae or the bird schistosome *Trichobilharzia regenti* (*T.regenti*).

RA cercariae have severely reduced migration through the skin (Mastin 1983, Mountford 1988). Vaccination with RA cercariae induces immune-mediated protection against challenge infection (Hewitson 2005). Exposure of the skin to RA cercariae induces rapid inflammation as seen with infection of un-attenuated cercariae (Riengrojpitak 1998, Elsaghier 1989). Infection with a single dose of RA cercariae induces a Th-1 dependant response with high levels of IFN γ and IL-2, whereas multiple infections induced increased levels of IL-5, IL-4 and IgG1 which are associated with a Th2 response (Caulada-Benedetti 1991). Dense foci of eosinophils and mononuclear cells were detected in multiply exposed pinnae suggesting a hypersensitivity reaction (Chang 1986, McLaren 1990)

Infection with the bird schistosome *T.regenti* causes cercarial dermatitis in humans. The skin pathology after infection is similar to that seen in murine skin. (Horak 2002). The skin thickens and the acute phase cytokines, IL-6 and IL-1 β , are expressed followed by increasing amounts of IL-12 (Kouřilová 2004). In comparison, re-exposure of the skin to *T.regenti* induces the release of IL-4 and IL-10 alongside a sudden release of histamine from mast cells in the skin (Kouřilová 2004). This suggests that the re-exposure results in an allergic type response in the skin.

Previous experiments in the laboratory, just prior to the start of this work, have used a multiple infection model exposing the pinnae of mice to ~150 cercariae once a week for four weeks (2.2.2). The immune response in the pinnae and skin draining lymph nodes has been shown to change after this regime (Cook 2011). After multiple exposure to *S. mansoni* cercariae both IL-4 and IL-13 were up-regulated in the skin alongside an increase in IL-10 and significant influx of cells, particularly eosinophils, into the skin site.

The cytokines and cell types up-regulated following multiple exposure in all three of these models are all heavily associated with angiogenesis and altered wound healing in both skin and other tissue sites in diseases including psoriasis, asthma and arthritis. The cytokine levels and cell types recruited to the skin after these multiple infections causes change in the immune response but may also affect the wound healing and angiogenic potential of the skin.

1.3.4 Cytokines in angiogenesis

As well as modulating immune responses, cytokines and chemokines can have direct and indirect angiogenic properties. A number of cytokines released during inflammatory conditions can be involved in the angiogenic process, these include, IL-1, IL-8, IL-6 and TNF α . Both IL-1 and IL-6 can induce angiogenesis through the activation of VEGF, and have been implicated as essential in the production of an angiogenic response in some tumours (Kim 2003, Margetts 2002). In rheumatoid arthritis inflammatory cytokines activate macrophages

contributing to the unbalanced inflammatory response by releasing growth factors, matrix metalloproteinase, cytokine and chemokines. There is matrix destruction and angiogenesis which disrupts the natural structure and integrity of the joint (Smeets 2003, Felsmann 1996, Wakisaka 1998, Firestein 2003).

IL-8, which was originally described as a macrophage derived pro-angiogenic factor, is up regulated in hypoxia and can lead to changes in the cytoskeletal organisation of cells controlling cell retraction (Tamm 1998). It also increases the production of matrix metalloproteinases 2 and 9 by endothelial cells. (Hirani 2001, Aihua 2003).

TNF- α stimulates the synthesis of platelet-activating factor (PAF) by monocytes and endothelial cells. This factor causes vasodilatation and recruitment of platelets which are important in angiogenesis. (Mannanioni 2004, Nurden 2011). The inflammatory response in the skin following schistosome infection may influence the delicate balance between pro and anti angiogenic factors which maintains the quiescence of the vessels.

Th2 cytokines can also affect the pro/anti- angiogenic balance. IL-4 is often found up-regulated alongside IL-13 in diseases which have high levels of angiogenic induction (Munitz 2008). IL-4's angiogenic properties are conflicting with several studies categorising it as anti-angiogenic whilst others show it is pro-angiogenic. Indeed IL-4 can induce a pro-angiogenic phenotype in macrophages (Mantovani 2002). With regards to wound healing IL-4 levels increase the first 4 days after wounding stimulating collagen production by fibroblasts (Salmon-Her 2000). Culture of aortic endothelial cells with IL-4 significantly stimulates the formation of tube-like structures which could be inhibited by blocking the IL-4 receptor (Fukushi 2000). Administration of IL-4 to the cornea of rats induces neo vascularisation *in vivo* (Fukushi 1998). These studies used concentrations of 250ng of IL-4 injected directly into the cornea. An alternative study injected 10ng/ml IL-4 alongside FGF2 into rat corneas and blocked the neo vascularisation (Volpert 1998). This work also showed that endothelial cell migration was only induced when stimulated with small amounts of IL-4(0.01ng/ml). Both IL-4 and

IL-13 induce up-regulation of mRNA for VCAM -1 in vascular endothelial cells. Soluble VCAM-1 can induce angiogenesis and is correlated with increased metastasis in tumours (Ding 2003). IL-13, like IL-4, is instigated as anti-angiogenic but is a major inducer of fibrosis and tissue remodelling particularly following wounding (Kaviratne 2004, Fichtner-Feigl 2005). IL-13 addition in capillary tube assays leads to inhibition of tube formation (Nishimura 2008). IL-13 stimulates eosinophilic inflammation and remodelling in lungs and induces up-regulation of MMP-9 and resulted in alveolar remodelling in asthma (Lanone 2002). In *S.mansoni* infections, IL-13 drives liver fibrosis and remodelling independent of MMP-9 and TGF β (Kaviratne 2004)

IL-10 is directly associated with both wound healing and angiogenesis. It is expressed following wounding and associated with wound viability (Peranteau 2008, Werner 2003). However, in relation of angiogenesis, IL-10 also has anti- and pro-angiogenic properties. IL-10 inhibits blood vessel growth in ischemic conditions which show high levels of pro inflammatory cytokines (Silvestre 2000). It appears to function primarily in the resolution of inflammation and thereby probably acts primarily to reduce angiogenesis. However IL-10 stimulated macrophages produce VEGF and nitric oxide and can induce retinal angiogenesis (Dace 2008).

1.3.5 Immune cells and angiogenesis

The skin is the first barrier to schistosome infection and the innate immune response mounted here will impact later in the regulation of the infection and development of an adaptive immune response. The immune cells recruited in this response may not only function to prime the adaptive immune response and defend against the parasite infection but influence also the angiogenic/ wound healing response (Frantz 2005, Yu 2003). Increased VEGF expression will cause increased vascular permeability in addition to stimulating endothelial cell proliferation and migration (1.2.3.3). This increased permeability will enable immune effector cells to egress from vessels into the surrounding tissue

(Aghajanian 2008). The cells which influx into the site will determine the response produced. Innate immune responses to infection have been shown to affect the angiogenic response in a tissue. Following schistosome infection a large influx of cells is present in the dermis. These include eosinophils, mast cells, dendritic cells, and macrophages all of which have angiogenic properties (1.3.1).

1.3.5.1 Neutrophils

Neutrophils primarily function as the first responders to injury or infection (Weiss 1989, Dovi 2004). Within the skin they respond immediately following wounding, whether by an infectious agent or penetration of the skin with a needle, and can produce inflammatory cytokines which will increase vascular permeability and the recruitment of further immune effector cells (Ng, 2011). Neutrophils play an important role in physiological angiogenesis. During the menstrual cycle they are a potent source of VEGF supporting growth and proliferation of the endometrial tissue (Lathbury 2000). In addition, in pathological conditions, neutrophils are thought to provide an early angiogenic switch in the tissue site (Nozawa 2006). Neutrophils cultured with combinations of LPS, TNF α and IL-1 β are stimulated to release VEGF (McCourt 1999). In addition to growth factors, neutrophils also represent a source of pro-angiogenic proteases. MMP-9 expressing neutrophils are found in and around tumours and provide the initial switch to a pro-angiogenic tumour in the early stages of gastric carcinogenesis (Nozawa 2006).

1.3.5.2 Macrophages

Macrophages are present in virtually all tissues and have a diverse range of functions, primarily repair and protection (Lucas 2010). Following wounding, macrophages will scavenge and phagocytose cellular debris during tissue remodelling. Macrophages have been found in close association with vessels in pro-inflammatory conditions when the level of VEGF present is high (Sunderkötter 1994, Ausprunk 1977). Within tumour studies the depletion of monocytes leads to reduced vascularisation of the tumour (Lewis 2006).

Macrophage secretions alone can induce angiogenesis indicating a molecule produced by macrophages is the angiogenic mediator and activation of the macrophages is essential for this release (Sunderkötter 1991, Crowther 2001).

Proliferation of endothelial cells following wounding is up-regulated briefly and quickly down-regulated. Thus to allow continued neo-vascularisations e.g in tumours, the endothelial cells must be activated for longer, macrophages are potential activators of this (Delavary 2011). Macrophages release several proteases which can cleave the ECM into pro-angiogenic components e.g fibrin and releasing ECM stored growth factors (Russell 2002, Skjøt-Arkil 2010). They can also induce vascular permeability due to the release of vasoactive substances including prostaglandins (Coussens 2002). Growth factor expression by macrophages can directly induce the endothelial cell growth and vessel formation releasing, PDGF, VEGF, TNF- α and TGF β among others (Assoian 1987, Bottomely 1999, Ligresti 2011).

Macrophage activation is currently a widely researched topic. The activation status of macrophages is influenced strongly by the cytokine milieu they are subjected to (Mantovani 2004, Nathan 1984, Mosser 2003). Macrophages were originally thought to be solely pro-inflammatory activated by IFN γ and producing nitric oxide, among other radicals, to remove pathogens after infection and present antigen to T cells (Zhang 2008). However several 'alternative' macrophages have been phenotyped including the alternatively activated macrophages (AAM Φ) which are induced by the Th2 associated cytokines IL-4 and/or IL-13 and heavily associated with helminth infections. (Gordon 2003, Noël 2004, Rodriguez-Sosa 2002).

AAM Φ s process arginine with the enzyme arginase as opposed to inducible nitric oxide synthase and produce anti-inflammatory agents such as Transforming TGF β , IL-10, Ym-1 and RELM α (Edwards 2006). This leads to the production of polyamines and proline which are components of the extracellular matrix and required for remodelling. Polyamines also affect fibroblast differentiation

promoting wound healing. It is thought that these macrophages can also express growth factors promoting angiogenesis (Sunderkotter 1994).

AAM Φ are particularly associated in helminth infections (Anthony 2006, Noël 2004, Gordon 2003). In schistosome infections AAM Φ are essential in the down-regulation of the pro inflammatory response and host survival as the infection progresses to a chronic phase (Herbert 2004). Recently it has been suggested that they are in fact an innate and rapid response to tissue injury, which most parasites cause (Loke 2007, Allen 2011).

In addition to IL-4/IL-13 stimulated 'alternative' macrophages a 'regulatory' phenotype has been described. (Mosser 2008). These can be stimulated by IL-10, immune complexes, prostaglandins and apoptotic cells (Kono 2008, Erwig 2007). These regulatory macrophages express large amounts of IL-10 and down regulate IL-12 production instigating them as potent down regulators of inflammation. Unlike the AAM Φ , regulatory macrophages do not contribute to ECM production but do produce TGF β which has a functional role in angiogenesis (Edwards 2006, Martinez 2008). Large scale gene expression studies comparing IL-10 stimulated and IL-4 stimulated macrophages revealed that only 18% of the genes overlap between the two suggesting significant difference in the phenotype of IL-10 activated macrophages (Stumpo 2003). Of these genes several have angiogenic roles including hypoxia inducible elements and platelet activating factors (Stumpo 2003). IL-10 stimulated macrophages have been implicated in cancer progression and express VEGF (Riboldi 2005, Nardin 2008). Schistosome infection of IL-4R α ^{-/-} mice prevents AAM Φ development and induced exacerbated iNOS production around granulomas. IL-10 could not compensate for this loss of IL-4/IL-13 signalling and it is unclear whether in schistosome infection IL-10 can cause alternative activation of macrophages (Herbert 2004, Dewals 2010).

1.3.5.3 Dendritic cells

The main function of dendritic cells is to process antigens and present them to the cells of the immune system perpetuating an adaptive immune response (Cella 1997, Igyártó 2011). Dendritic cells can be distinctly pro or anti angiogenic depending on their activation status (Sozzani 2007). Activation in the presence of pro inflammatory conditions (e.g. LPS and TNF- α) produces an anti-angiogenic phenotype whilst, culture with prostaglandins will induce VEGF expression (Jonuleit 2005, Riboldi 2005, Banchereau 2000, Wollenberg 2002). Dendritic cells can also produce cytokines which increase endothelial sensitivity to angiogenic factors promoting angiogenesis (Dong 2009). In tumours, pro-angiogenic dendritic cells appear to accumulate in and around tumours expressing TNF α and IL-8 (Curiel 2004).

1.3.5.4 Eosinophils

Eosinophils control mechanisms associated with allergy (Efraim 2008) and are a hallmark of helminth infections (Ovington 2000, Behm 2000, Klion 2004). Eosinophils have also long been associated with allergy and also closely associated with fibrosis and tissue repair (Levi-Schaffer 2004, Williams 2004, Gharaee-Kermani 1998). Eosinophils can directly affect fibroblast properties increasing their production of ECM components modulating the process of tissue repair. This is suggested to be primarily through eosinophil expression of IL-4 and IL-13, and perhaps through release of stored TGF- β (Doucet 1998). Eosinophils also release MMPs, particularly MMP-9 (Schwingshacki 1999). These functions are all intrinsically wound healing linked but eosinophils may also have a role in angiogenesis. The major basic protein (MBP) of eosinophils can induce endothelial sprouting in a dose dependant manner and amplifies endothelial cell responses to VEGF (Puxeddu 2008) The granules of eosinophils also contain VEGF and PDGF which are bioactive when released. (Puxeddu 2005). Rat aorta sprouting models revealed that eosinophil sonicates can enhanced endothelial sprouting (Puxeddu 2003).

One disease in which eosinophils are unequivocally linked is asthma (Busse 1992, Jacobsen 2007, Wardlaw 2000, Humbles 2004). Characterised by tissue damage and remodelling, the eosinophil contributes by the production of destructive enzymes and the release of TGF β and MMP-9. However there is also considerable vascular remodelling in asthma and eosinophils are one of the main contributors of VEGF in asthma as well as producing FGF2 and IL-8 (Hoshino 2001). Schistosome infections show increased levels of eosinophils in granulomas and in the skin (Sabin 1996, Reiman 2006, Cook 2011). They can also drive recruitment of alternatively activated macrophages to tissue sites (Voehringer 2007).

1.3.5.5 Mast cells

Mast cells are resident in the tissue, and although mostly known for their role in allergic responses, they are also involved in wound healing and angiogenesis (Prussin 2003, Theoharades 2006). Mast cells produce inflammatory mediators and histamines which drive vessel dilation and promote the early stages of angiogenesis. They are also the source of significant levels of angiogenic growth factors, VEGF, FGF2, TGF β and IL-8 (Norrby 2002, Levi-Schaffer 2002,). Mast cells can also indirectly induce angiogenesis through protease degradation of the ECM releasing bound growth factors and through the recruitment of monocytes and lymphocytes which perpetuate the angiogenic response (Puxeddu 2005). Epithelial cancers can exploit the inflammatory mast cell response. De-granulating mast cells adjacent to the tumours inadvertently stimulate angiogenesis mainly through MMP induction, and the tumour cells then perpetuate this leading to highly vascularised tumours (Coussens 1999, Yano 1999, Tomita 2000).

1.4 Aim of this study

Previous studies in schistosomiasis have focused on the immune response in the skin to cercarial infection but little work has been done on the angiogenic response. It is known that the eggs of *S.mansoni* can induce angiogenesis but no evidence exists of cercarial induction of blood vessel growth. It is also known that multiple infections of mice with *S.mansoni* causes an up-regulation of Th2 cytokines in the skin and several factors closely linked to angiogenesis.

The main objective of this study is;

'To determine whether infection with S.mansoni induces angiogenesis in the skin and whether this is altered after multiple infections.'

If angiogenesis is induced following infection this could be by a combination of three different mechanisms; growth factor release in the skin, innate immune response or direct parasite antigen induction. The work presented here will address each of these mechanisms in turn:

Chapter 2: focuses on characterising the angiogenic response following single and multiple infections.

Chapter 3: attempts to determine whether the haematopoietic cells recruited to the dermis after infection contribute to angiogenesis.

Chapter 4: investigates the effect loss of IL-10 has on the innate immune cell response and the release of pro-angiogenic growth factors.

Chapter 5: aims to determine whether the cercarial secretions can directly induce angiogenesis.

Chapter 2: General Materials and Methods

2.1 General Materials and Methods

2.1.1 Parasite Maintenance

The schistosome parasite life cycle is maintained in house by routine passage of a Puerto Rican strain of *S. mansoni* through *Biomphalaria glabrata* snails and NMRI mice housed under specific pathogen free conditions. Parasites for infection were shed from snails by placing the snails in ~10ml of water and incubating under a bright light for 2 hours. Cercariae were then diluted in 'aged tap water' to the required concentration.

2.1.2 Infection Scheme

Female C57BL/6 mice weighing between 18 and 25 grams were used for all experiments unless otherwise stated. Mice were anaesthetised with 10% Sagatal in 10% ethanol (May & Baker, Dagenham UK) at a dose of 0.01ml/kg of body weight, and were then exposed to *S. mansoni* cercariae via each pinna. As described previously (Mountford et al 2001), pinnae were immersed in 1.3ml of water containing 150 cercariae and left submerged for 20 minutes before the mice were turned and the contralateral pinna infected in the same manner. The mice were then sacrificed at various time points post the final infection; days 1, 2, 4 and 8 were all used in this work (Figure 2.1). Multiply infected mice (4x) received one dose on the same day each week for four weeks in total (Cook et al. 2011). Single infection mice (1x) received just a single dose coinciding with the final dose for the 4x mice

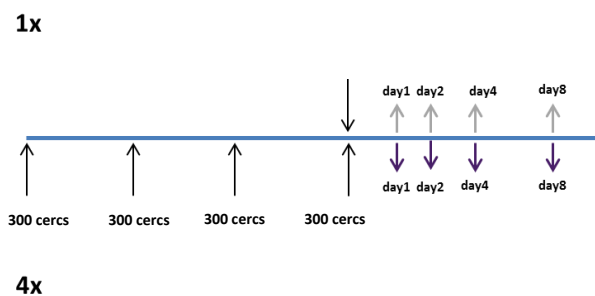


Figure 2.1 Timeline of infection

Mice were infected with 150 cercariae per pinnae (300 in total) on the same day for four weeks (4x) and once on the final day of the 4x infection (1x). Mice were sacrificed at one of four time points after the final infection

2.1.3 RNA Extraction

To analyse levels of mRNA transcript in the skin, pinnae were removed and immediately frozen in liquid nitrogen. Frozen whole pinnae were crushed using a micro dismembrator (B.Braun Biotech International), and the resulting powdered tissue re-suspended in 1ml Trizol (Invitrogen). RNA was extracted following the manufacturer's protocol using a phenol, chloroform extraction isopropanol precipitation. Pellets were washed in 70% ethanol and re-suspended in DEPC-treated water (Ambion). RNA concentrations were measured (Nano Drop 1000 Thermo Scientific) and adjusted to 0.5µg/10µl.

2.1.4 Reverse Transcription

RNA Samples were reverse transcribed following the manufacturer's protocol for Superscript II Reverse transcriptase (Invitrogen). Total RNA (10µl) at 0.5µg/10µl was added to 2µl of mix containing 1µl of OligodT (Invitrogen) and 1µl of 10mM dNTPs (Promega). The mix was heated for 5 minutes at 65°C then quickly chilled on ice before the addition of 7 µl of master mix (containing 4µl of 5x First strand buffer, 2 µl 0.1M DTT and 1 µl RNase OUT (Invitrogen)). The complete sample was heated at 42°C for 2 minutes prior to the addition of 1 µl Superscript II reverse transcriptase which was followed by incubation at 42°C for 50 minutes and at 70°C for a final 15minutes to yield cDNA.

2.1.5 Semi-quantitative Polymerase chain reaction (SQ-PCR)

The cDNA samples were each diluted with 30µl of DEPC water to produce cDNA at a concentration of between 5 and 20ng/ml. Each PCR reaction totalled 25 µl: 5 µl of cDNA and 20 µl of master mix. The mix contains 2 µl 10x Buffer, 1.5 µl MgCl₂, 0.5 µl 10mM dNTPS, 0.5 µl forward primer, 0.5 µl reverse primer, 0.2 µl Taq Polymerase and 14.9 µl DEPC water. The reaction followed the same cycle regime for each gene with alterations to the annealing temperature dependent on previous optimisation (Annealing temperatures, cycle numbers and primer sequences are provided in Appendix 1)

PCR Cycle:

- 1- 95°C for 3 Minutes
- 2- 95°C for 30 seconds
- 3- 60°C (or alternative) for 30 seconds
- 4- 72°C for 30 seconds
- 5- Repeat from 2-4 for the required number of cycles
- 6- 72°C for 5 minutes
- 7- End

PCR products were visualised on 2% agarose (Melford) gels in 250ml of 0.5% TAE buffer containing 5 µl of ethidium bromide. To each well, 5 µl of PCR product mixed with 1µl of 6x Green/orange loading dye (Fermentas) was loaded alongside 2µl of 100bp ladder (New England Biolabs) and run for ~20 minutes at 100V. The intensity of the bands was compared to the intensity of the house keeping gene GAPDH for each sample using (Alpha Imager, Alpha Innotech Corporation).

2.1.6 Real time Quantitative PCR (Q-PCR) of DEC

Real time PCR was used to detect expression levels of Arginase-1, Ym1, RELM α and iNOS. 5µl of diluted gene standard was added alongside 5µl of test cDNA, produced as described (3.2.9) and 20µl of PCR reaction mix (2.5µl 10x PCR Buffer, 2µl MgCl₂ [50mM], 0.25µl ROX reference dye, 0.1µl Platinum Taq DNA polymerase, 0.5µl dNTP, 1µl of both forward and reverse primers [10mM], 1.25µl TaqMan probe [0.5µM-0.05µM] and 11.4µl DEPC treated water) to each well of a 96-well optical reaction plate (Applied Biosystems). Samples were then run using the standard protocol;

PCR Cycle:

- 1- 95°C for 5 Minutes
- 2- 95°C for 30 seconds
- 3- 60°C for 1 minute
- 4- 72°C for 30 seconds
- 5- Repeat from 2-4 for 50 cycles
- 6- 72°C for 5 minutes
- 7- End

Results were analysed using ABI PRISM 7000, the cycle number at which the sample crossed the threshold was compared for each sample to the standard curve and from there the concentration of template calculated. For each sample the gene of interested was divided by GAPDH to normalise the expression and the ratio presented in arbitrary units.

2.1.7 In vitro cultured pinnae biopsies

To isolate the growth factors within the skin site of infection, whole pinnae were removed, dipped in 70% ethanol (to ensure sterility of the skin surface) and then split using forceps exposing the dermal surfaces. Each half was laid onto 500µl of complete media (RPMI1640, 10% Foetal Calf Serum, 1% Glutamine, 1% penicillin-Streptomycin) dermis side down and incubated at 37°C overnight. The culture supernatant was recovered and centrifuged to remove cells which had exuded from the pinnae overnight, and frozen at -80°C until analysis.

2.1.8 Enzyme linked immunosorbent assay (ELISA)

Culture supernatants obtained as above (2.2.12) were analysed for expression of VEGF using DuoSet ELISA kit (R&D Systems; VEGF – DY493, all concentrations were pre-determined by the manufacturer). Plates were coated with the required concentration of capture antibody diluted in PBS and left overnight at

4°C. Wells were aspirated twice with 400µl of PBS plus Tween (PBST = 0.05% Tween 20 in PBS) before blocking by the addition of 400µl of 1%BSA in PBS for 2hrs at room temperature. Standards were prepared as doubling dilutions in 1%BSA PBS to produce a standard curve of 11 points (Top standard was 1000pg/ml) Samples were incubated alongside the standard curve for 2hrs at room temperature. After washing 5x in PBST, the detection antibody was added for 2hrs at room temperature. Plates were washed again 5x in PBST and Streptavidin horseradish peroxidase added for 45 minutes at room temperature. Following 5x final washes, Sure Blue TMB Substrate (KPL, Gaithersburg MD, USA)was added and the plates left to develop at room temperature. Readings were taken at 650nm using a MRX II plate reader (Dynex Technologies Ltd, Worthing UK).

2.1.8 Statistical Analysis

Throughout the thesis the data is compared statistically using the students t-test. For each graph unless otherwise stated the groups being compared are the 1x with the 4x for each time point which is shown as stars on the graphs over the 4x time point. For most of the figures each of the infection time points is also compared to the naive and the results described in the text. The graphs show the mean value with the error bars representing the + standard error of the mean.

*p<0.05, **p<0.01 and ***p<0.001.

Chapter 3: Characterising the angiogenic response following single (1x) and multiple (4x) infections.

3.1 Introduction

The association between schistosomiasis and angiogenesis is not a new concept in respect to the interaction between the egg and the intestinal vessels (Loeffler 2002). However there is little evidence at present as to whether the cercariae also induce vessel growth and remodelling. The cercarial passage through the skin is likely to cause considerable damage to the skin and an intrinsic part of the wound healing response is the growth of new vessels to aid repair and production of new mature tissue (Tonnesen 2000). In addition to the eggs, the cercariae produce secretions thought to aid their passage through the skin and may be directly inducing angiogenesis.

Angiogenesis is a complex process involving several discrete steps which overlap temporally and spatially. As described (1.2.2) new vessel growth requires activation of the mature quiescent endothelium and signals to induce proliferation and migration of the endothelial cells. Initial loosening of the vessels is induced primarily by the balance of the angiopoietins (1.2.3.1) alongside a remodelling of the ECM by the MMPs (ref). The rate and manner of blood vessel growth following this depends on the type and level of the growth factors produced. VEGF has long been considered as essential in angiogenesis, indeed VEGF knockout mice die at embryonic day 11-12 (Carmeliet 1996). Alongside VEGF, PlGF is also widely described and considered to be primarily induced in pathological angiogenesis (1.2.3.3). Many additional growth factors including the fibroblast growth factor family and HGF have all been well documented as up regulated in angiogenesis and associated with several disease states (1.2.3.3).

Using both molecular and imaging techniques this chapter aims to determine whether after penetration of the skin the presence of the cercariae induces a change in the vasculature. Markers and features of angiogenesis will be monitored between days 1 and 8 after infection and will also compare between a single and a multiple infection with the cercariae using the model described in section 1.3.2 and method 2.2.2.

3.2 Materials and Methods

3.2.1 External imaging on the pinnae and vessel quantification

Mice were anaesthetised and the pinnae observed using a stereomicroscope (Carl Zeiss) at 18x magnification with down lighting. Multiple images were taken of the pinnae both loose and pressed between glass slides to produce a flat area to visualise. The vessel network and images were then analysed using Adobe Photoshop Cs3. In order to quantify the vascular network, a macro was devised to distinguish red vessels from the background tissue of the skin; naïve pinnae were used to set the baseline values and which was then applied to all images taken. Output is given as the density of the pixels identified by the software in the entire pinnae. (This method was devised and optimised by C.K. Saleh, University of York, Department of Biology).

3.2.2 Skin Histology

Groups of mice were infected either 1x or 4x via the pinnae as described in section 2.1.2. Pinnae thickness were measured at various times after the final infection using a dial gauge micrometer (Mitutoyo, Japan) and were then removed and fixed in 4% neutral-buffered formal saline (Sigma, UK). Tissues were wax-embedded, sectioned at 5µm and stained with Haematoxylin & Eosin (service provided by the Veterinary Pathology Department, University of Liverpool, UK.)

3.2.3 α CD31 and α CD105 vessel labelling

Pinnae from infected mice (2.1.2) were removed at selected time points post-infection (Days 1, 2, 4 & 8). In order to remove hair from the pinna surface, a depilating agent (SoftSheen-Carson, Magic shaving powder) was placed onto the pinnae and left for 2 minutes. Pinnae were then washed in PBS and split in two thereby exposing the internal dermal surfaces before fixing in 2% paraformaldehyde (Agar Scientific) for 10 minutes on ice. Pinnae were then

rinsed and placed in 0.5% saponin (Sigma Aldrich) containing 5% sheep serum (Sigma Aldrich) for 30 minutes at room temperature. Antibodies used to stain the vasculature were diluted to the required concentration (Rat anti Mouse CD31/PECAM conjugated to FITC – 1:100 (ebioscience clone # 390), rat anti Mouse CD105/Endoglin conjugated to pacific blue– 1:50 (ebioscience clone # MJ7/18) in the permeabilising mix. The pinnae were incubated with the antibodies at room temperature for one hour, and then washed thoroughly in PBS before being mounted in Vector shield (Vector Laboratories).

3.2.4 Visualisation and quantification of CD31+ and CD105+ vessels

Pinnae were imaged whole using a Zeiss LSM 510 meta (Carl Zeiss Ltd). All images were captured using identical laser settings at 488nm and 410nm excitation wavelengths and 520nm, or 455nm emission wavelengths. Levels of CD105 expression, as judged by staining with anti-CD105 antibody across pinnae samples, were quantified using Velocity software (Improvision®, UK), and determined as % expression within the fluorescent channel. The intensity was set to exclude the background and include only stained vessels. The total viewed area was then calculated for CD31 and CD105 separately. To normalise CD105 expression to the number of vessels present in an image, the area of the CD105 was divided by the area of CD31 expression and the ratio plotted.

3.2.5 Measurement of vascular leakage using the Modified Miles assay

Mice were placed at 40°C for 10minutes to dilate blood vessels, and then injected intravenously via the tail vein with 200µl of Evans blue dye(George.T.Gurr, London UK) (60mg/kg). Mice were left for 90 minutes to allow the dye to circulate around the body and then sacrificed. Pinnae were removed and weighed before imaging using a stereomicroscope under bright light.

After gross measurements, pinnae were split in half and placed in 600µl of formamide (Sigma Aldrich) and left rotating at 60°C for 18 hours. After incubation, the tissue extract was recovered leaving the tissue and plated in duplicate (50µl) into a 96 well tissue culture plate. A standard curve of Evans Blue diluted in formamide was prepared on the same plate (Top standard 1000µg/ml). The plate was read at 570nm using a MRXII plate reader (Dyner Technologies Ltd, Worthing UK) and the standard curve used to determine the concentration of dye within the test samples

3.2.6 Detection of active MMPs

The DQ-Gelatin Assay (Molecular Probes) was used to quantify active MMP expression in tissue samples. A vial of desiccated substrate was reconstituted in 1ml of dH₂O to prepare a 1.0mg/mL stock solution. Aliquots (20µl) of diluted substrate were added to wells of a black 96 well plate, supplemented by 80 µl of 1x reaction buffer (kit component) to produce a total volume of 100ul. Test samples (100 µl) were then added and incubated for 1hr at room temperature. Samples were the overnight culture supernatants obtained from skin biopsies (2.1.7) diluted 1:2 before addition. Resulting fluorescence of the substrate was measured using a fluorescent plate reader (BMG Labtech POLARstar OPTIMA).

To localise the MMP activation 50µl of reconstituted DQ-Gelatin substrate was mixed with 200µl of Cygel (Biostat) which is a thermo reversible gel. The Cygel and substrate mix was placed onto 10µm thick unfixed sections of pinnae and left to set and incubate at room temperature for 1hour. The sections were imaged using the Zeiss LSM 510 meta (Carl Zeiss Ltd). All images were captured using identical laser settings at 488nm excitation wavelengths and 520nm emission wavelengths.

3.3 Results

3.3.1 Vessels become more visible following infection

In un- infected pinnae, large central vessels were clearly visible from the exterior (Figure 3.1 A panel 1) and from these vessels there were commonly 2 to 3 visible branch points which lead to the smaller vessels throughout the dermis. After a single infection (1x), the skin became noticeably redder and the central vessels more visible (Figure 3.1 A panel 2). The vessels appeared wider and there was an increase in the number of branch points visible by eye: ~5 to 6 from the central vessel. After multiple infections (4x) this branching number increased again to approximately 7 to 8 branch points from the single source vessel (Figure 3.1 A panel 3). In addition, the vessels appeared wider than either naïve, or 1x infected pinnae, and pairs of vessels were clearly visible along the centre of the pinnae. Smaller vessels originating from the main trunk branches were also visible and can be identified at the terminal edge of the skin. In addition to an increase in the number of visible vessels, several have taken on an alternative structure, with deviations from the linear pattern to convoluted wavy vessels (Figure 3.1 A *).

The number of visible vessels was quantified to give a numerical readout for the area covered (Figure 3.1B). The vessels were identified using Photoshop® utilising a macro designed to identify the areas of 'red' in each image (3.2.1). By altering the higher and lower intensity parameters, this allowed the vessels to be identified from the background tissue. The number of red pixels in these layers equates to the area of vessels visible by eye in the image. Following both 1x and 4x infections, there was a significant increase in the area of visible vessels when compared with the naïve pinnae ($p < 0.001$ for all time points compared to naïve). At days 1, 2 and 4 post-infection there was an additional significant increase in the 4x pinnae compared to the 1x group ($P < 0.05$ and $P < 0.01$). Over the time course of infection, the vessels remained visible and the quantified increase did not return to naïve levels.

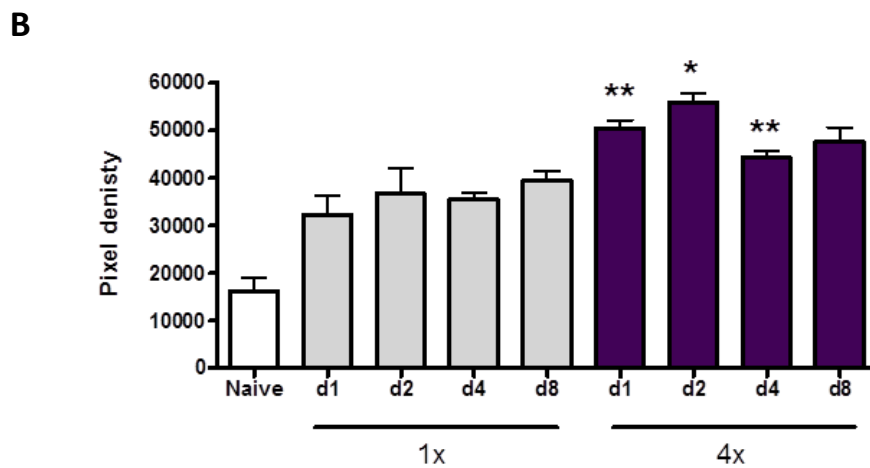
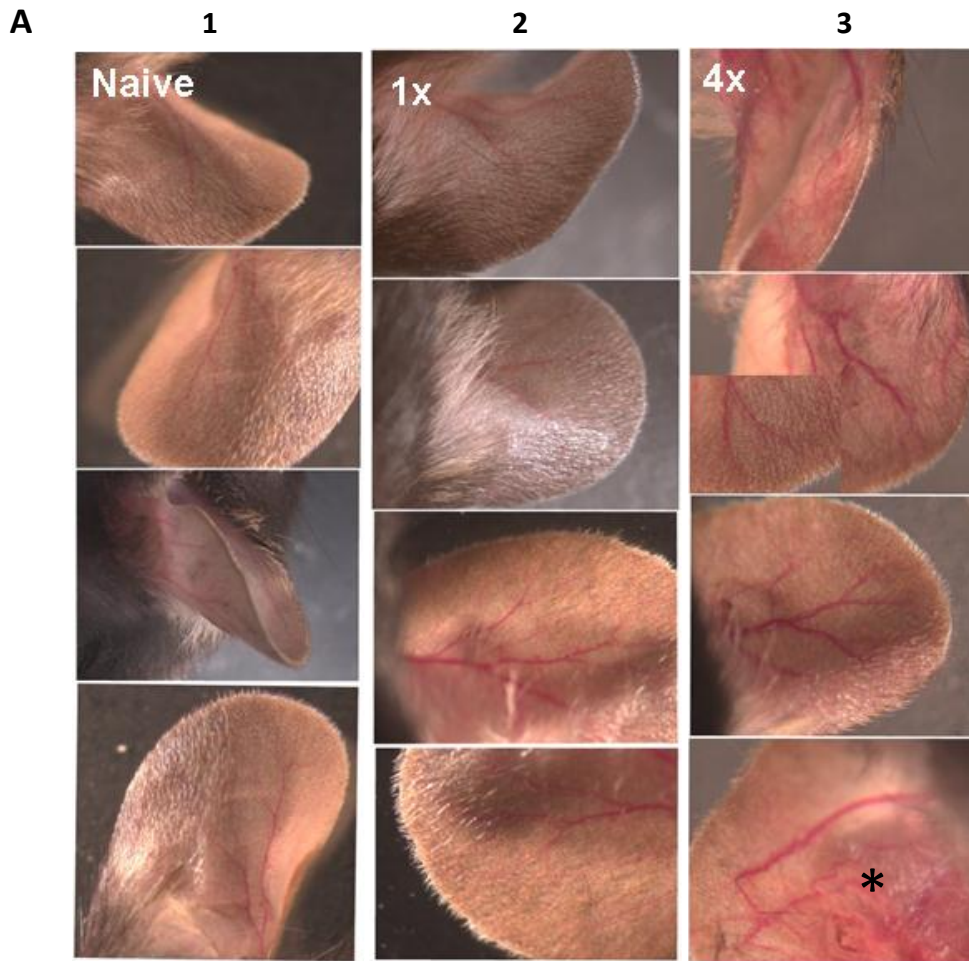


Figure 3.1 Imaging and quantification of blood vessels following infection

A: Images from naive and day 2 infected pinnae taken under 12x magnification from several orientations (panel 1 = Naive, panel 2= 1x, panel 3 = 4x) Several branches can be seen from the central vessels in all pinnae. * indicates vessels in the 4x which are no longer linear. **B:** Quantification of the visible vessels. Using Photoshop the visible vessels were identified based upon the intensity of the red. The number of individual pixels is proportional to the amount of vessels identified. All infected values versus the naive $p < 0.001$. Significant differences shown are 1x versus 4x $*p < 0.05$, $**p < 0.01$, (n=10 pinnae from 5 mice)

3.3.2 The epidermis and dermis are disrupted and thicken following infection

The thickness of infected pinnae was measured at days 1,2,4 and 8 post-infection and compared to naïve samples (Figure 3.2). The thickness of the pinnae did not increase significantly in the 1x mice compared to the naïve sample, although there was a slight increase in the average thickness at day 8. However, 4x pinnae increased in thickness significantly compared with both the naïve and 1x pinnae (all $p < 0.001$). This increase in thickness remained over the time course of infection and was still elevated at day 8 post infection.

Sections through the pinnae show that this increase in thickness occurs both in the dermis and epidermis (Figure 3.2 B). Within naïve skin, the dermis is organised and well-structured and the epidermis is thin consisting of 1-2 layers of cells. After 1x infection, the thickness of the epidermis appeared to increase to 2-3 cells particularly above areas where the dermis appears disturbed. Within the dermis there are several patches where haematopoietic cells have influxed though these are sparsely distributed throughout the dermis.

In 4x pinnae, the dermis is considerably thicker, predominantly to one side of the cartilage. The epidermis has thickened to 4-5 cells deep. The increased thickness in epidermis occurred throughout the pinna section. The structure of the dermis appeared damaged with pools of red blood cells detected along the section, perhaps indicative of vessel haemorrhaging. Blood vessels were also larger supporting the observations made in section 3.3.1, whilst immune cells were also visible within the vessels. Haematopoietic cells were apparent throughout the dermis and large groups were present under the epidermis particularly around areas of haemorrhaging. The H&E staining revealed that many of the cells within the focal influx have the morphology of eosinophils.

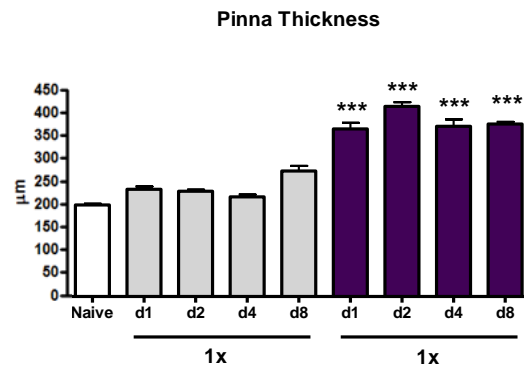
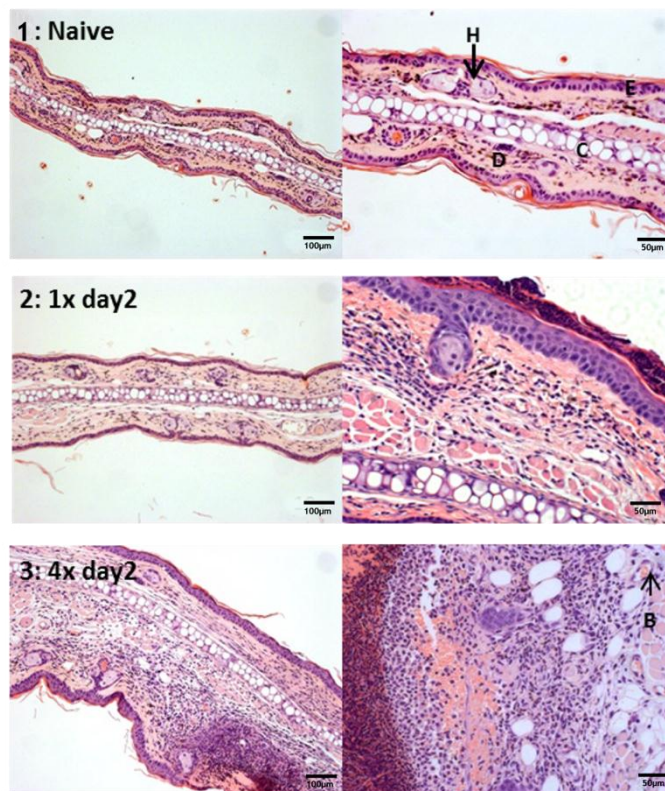
A**B**

Figure 3.2 Thickness and histology of pinnae

A: Measurement of the thickness of pinnae over the time course. Significance shown are the 4x time point compared with the equivalent 1x time point. All 4x groups were significantly increased compared with the naïve $p < 0.001$ however none of the 1x time points were significantly increased compared to the naïve. (n=40 pinnae measured from several experiments, Mean +SEM)

B1-B3: H&E stained sections of pinnae (panel 1 = Naïve, panel 2 = 1x day 2, panel 3 = 4x day 2). Sections show the cartilage central to the pinnae (C) with the epidermis stained darkly purple (E) and the dermis in pink (D). Hair follicles (H) and blood vessels (B) are also visible. After infection infiltrates of cells are visible in the dermis and blood vessels (arrowed). Sections were imaged under 10x - left panel and 20x - right panel, magnification. Images are shown of selected pinnae from 5 stained.

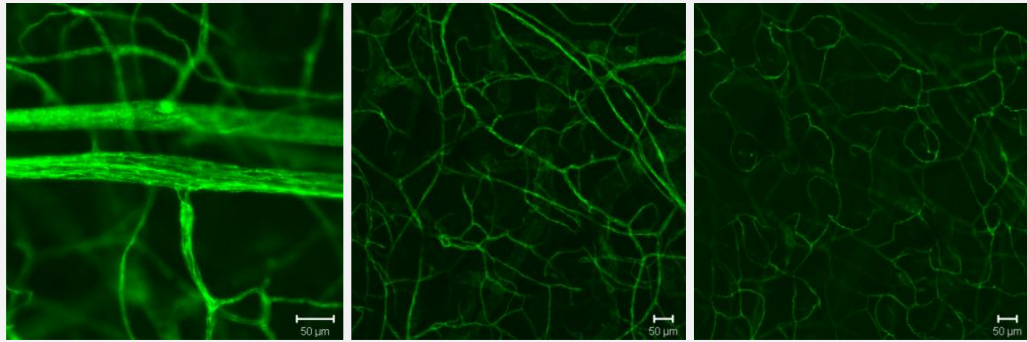
3.3.3 The vessels of 4x pinnae are thicker and more numerous than 1x and naïve

The vessels visible by eye on the surface of the pinnae are only a small proportion of the entire vasculature of the skin, a network of smaller capillaries and minor tributaries of the major vessels thread throughout the dermal layer of the skin. To visualise the entire vascular network, fluorescent microscopy was utilised (3.2.3) to detect vessels expressing platelet endothelial cell adhesion molecule 1 (PECAM1), otherwise known as CD31. This adhesion molecule is constitutively expressed on the vascular endothelium (Newman 1997). An antibody against CD31 (conjugated to FITC) was used to identify the vessels and images were taken throughout the entire depth of the skin to show that both the large arteries and veins, and the smaller vessels, have been stained throughout the dermis (Figure 3.3 A).

Images were taken over the entire area of several pinnae. Vessels in naïve pinnae appeared linear with regular branch points and become thinner as they branch towards the terminal ends (Figure 3.3 B Panel 1). Within 1x pinnae, there was an increase in the brightness of staining, and there were a greater number of vessels branching out from the large trunk vessels (Figure 3.3 B Panel 2 Δ). There was a similar density of small vessels at the terminal edge compared to naïve pinnae. In 4x pinnae, the vessels were also bright, with several branches and sprouts from the main vessels, as well as dense webs visible at the terminal ends (Figure 3.3 B Panel 3 O). Several of the main vessels exhibited a more convoluted construction, perhaps as a result of disruption to the integrity of the junctions between endothelial cells (Figure 3.3 B Panel 3 ◇).

Whole vessels were imaged in 1x and 4x pinnae by moving from the base of the pinna towards the very edge along a single vessel (Figure 3.3 C). In the 4x pinna, the main vessel is more convoluted than in the 1x pinna, and has small webs of vessels extending off. Some of the vessels do not appear properly formed, and at the edge of the 1x pinna the vessels form a neat network of fine capillaries, whilst in the 4x pinna they are more diffuse.

A



B

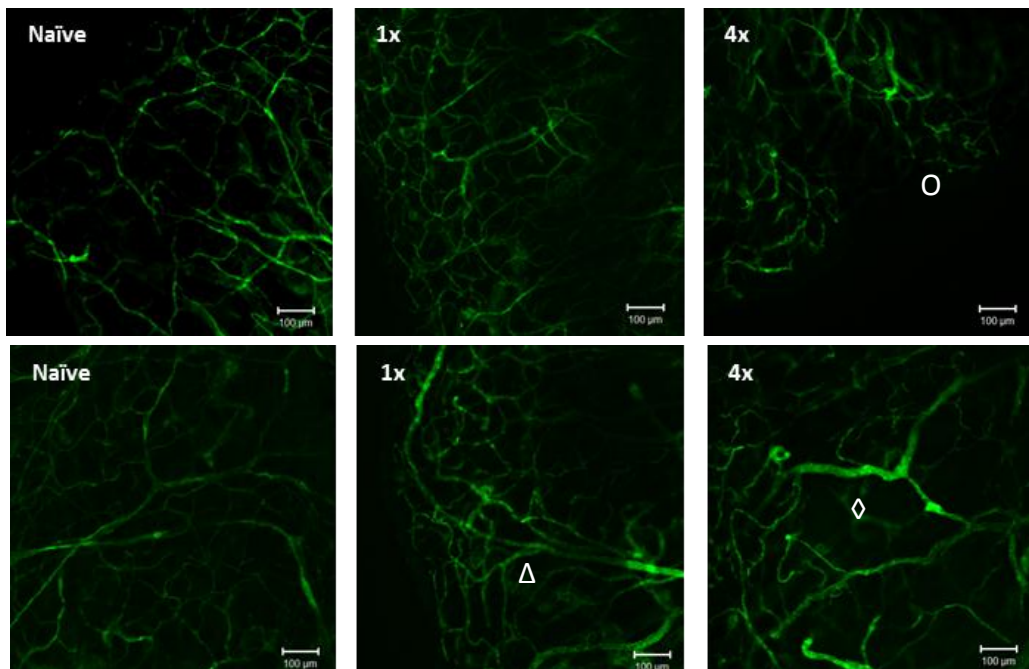


Figure 3.3 The vessels of the dermis in labelled with FITC conjugated anti CD31 mAb

A: Representative series of three images taken at different depths through similar zones of the pinnae. Left panel : main vessels at the base of the dermis. Middle panel; smaller vessels sprouting up along the larger main vessels. Right panel: fine capillaries near the epidermis of the skin. Images from naïve pinnae. Initial optimisation was completed on three naïve pinnae

B: Top panels show vessels at the edges of the pinnae. Bottom panels show vessels taken several frames in from the edge but do not include the large vessels visible by eye. O – Marks dense webs of vessels at the edge of 4x pinnae. Δ – Indicates multiple branches from the central vessels of 1x pinnae. ◊– Disruption of the linear structure of the 4x vessels. All infected images are day 2 post infection and are representative images from a group of 6 pinnae.

C

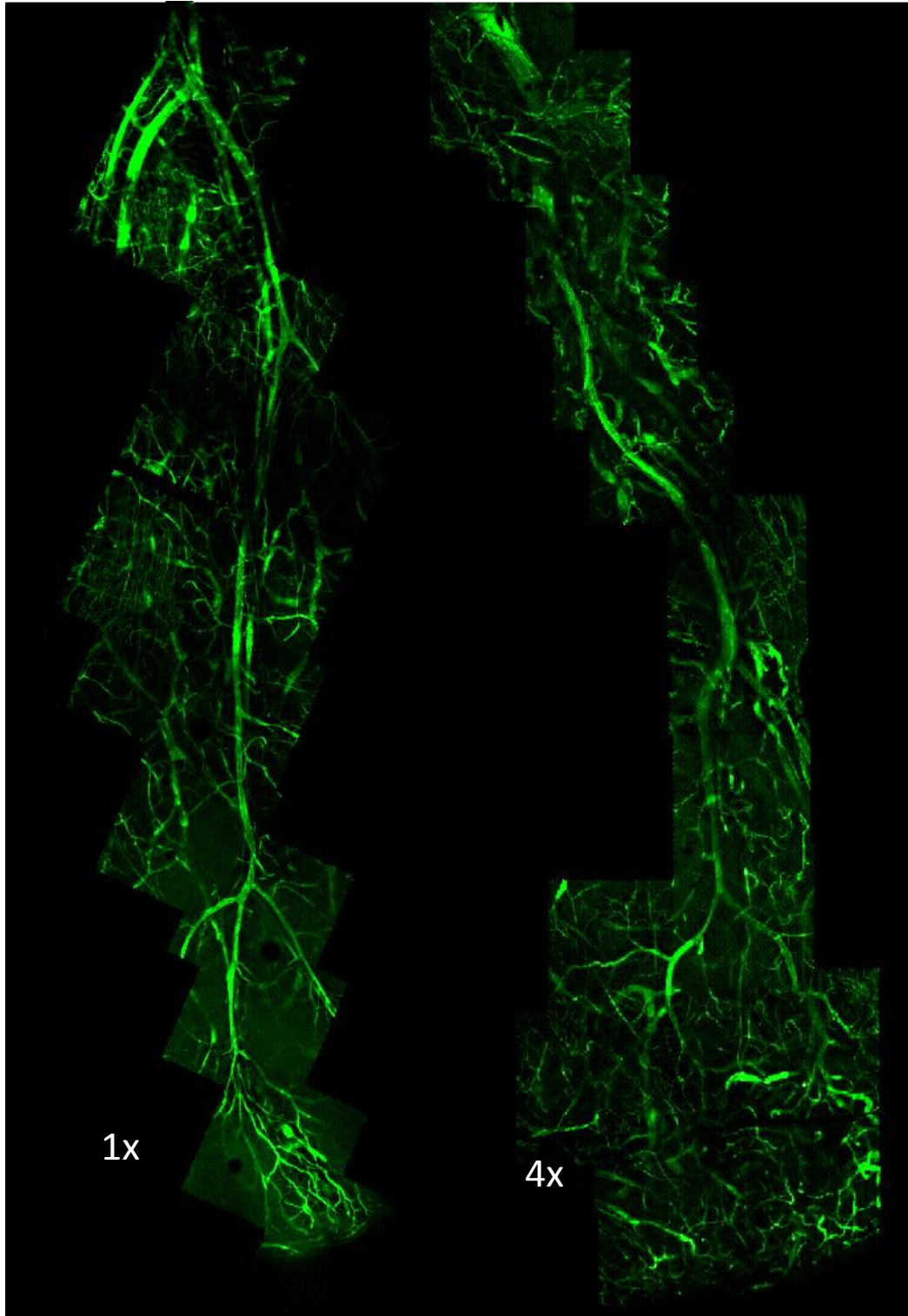


Figure 3.3 C Composites of the entire vessel network of 1x and 4x pinnae. Images follow one main vessel from the base of the pinnae to the very edge of the skin.

Expression of CD31 was quantified using Velocity imaging software (Improvision®, UK), and the total area of CD31⁺ vessels in each image calculated. Whilst CD31 is a widely used marker for blood vessels it is also expressed on lymphatic vessels, but to a lesser degree. In several of the images lymph vessels may be visible but the staining was fainter, and these faint vessels were excluded in the analysis. The average area of each 10x image taken at intervals over the entire area of several pinnae. This showed that both 1x and 4x infected pinnae had a significantly increased vessel area (Figure 3.4A) and this further increased in 4x compared to 1x pinnae (P<0.001). The vessels in infected mice were also wider, as the mean diameter increased significantly in both 1x and 4x compared to naïve pinnae (P<0.001; Figure 3.4B)

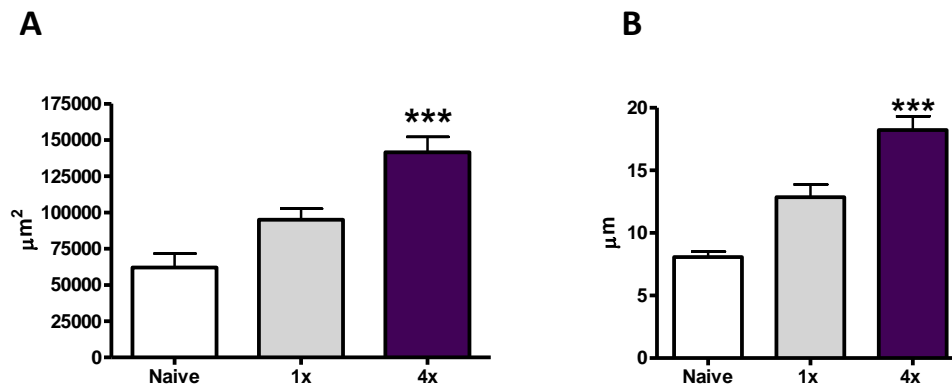


Figure 3.4 Quantification of CD31 positive vessels.

A: Total area in $920\mu\text{m} \times 920\mu\text{m}$ zones of the pinnae. 40 images were taken of each pinna; the mean values are areas from $n = 5$ mice \pm SEM in 1x vs naïve $p < 0.05$, and 4x vs naïve $p < 0.001$.

B: Diameters of CD31⁺ vessels measured from images chosen at random from all over the pinnae. 1x vs naïve $p < 0.001$, 4x vs naïve $p < 0.001$.

Significance shown in the figure are for 1x compared to 4x pinnae *** $p < 0.001$.

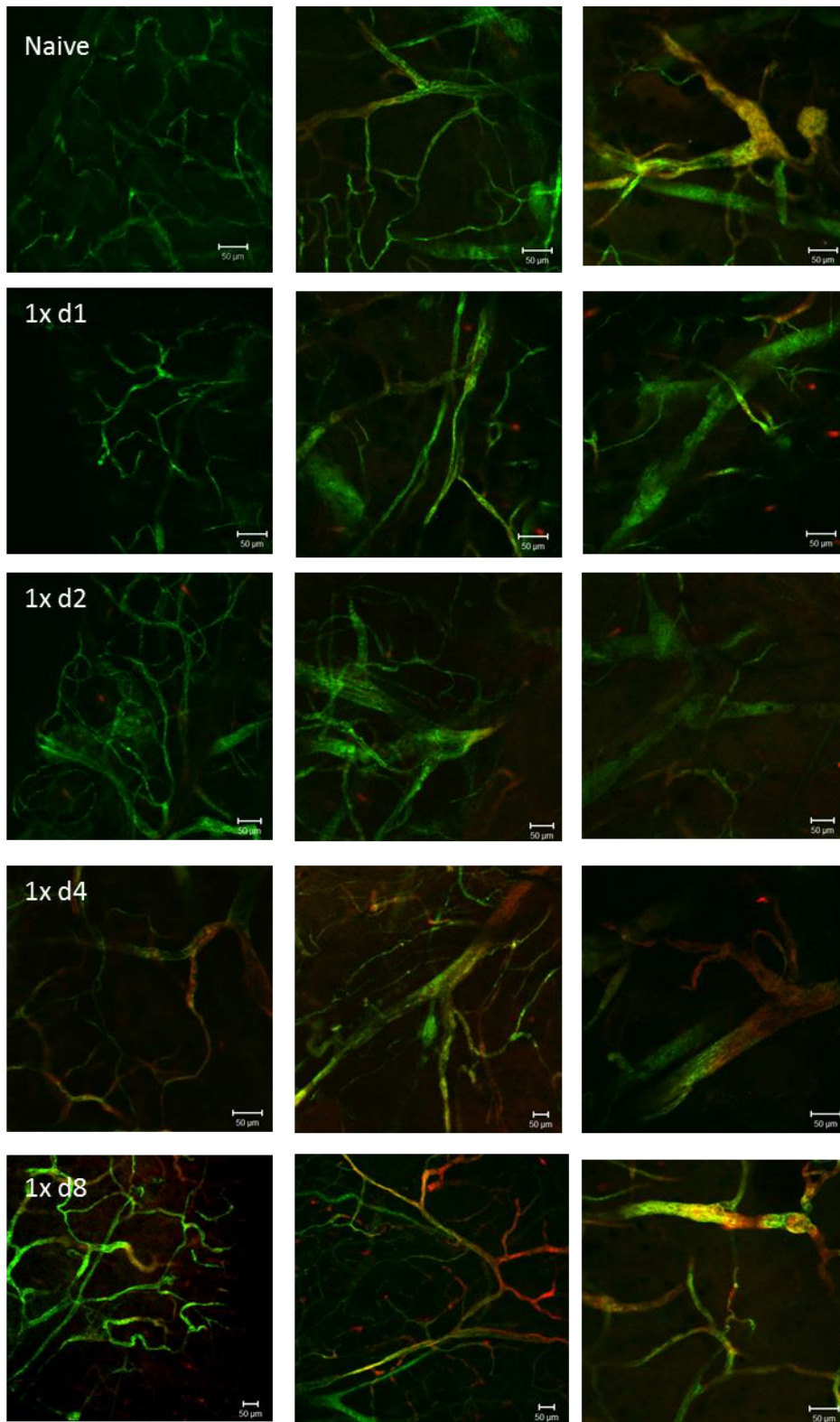
3.3.4 Vessel remodelling identified by labelling with α CD105

To better quantify the extent of vascular remodelling within the skin, pinnae were stained with anti-CD105 mAb, alongside anti-CD31 mAb. A member of the TGF β receptor family CD105 is up-regulated on remodelling vasculature and is expressed across metastatic vessels in tumours (Fonsatti 2003).

Whole pinnae were stained with both anti-CD105 and anti-CD31 mAbs and visualised by fluorescent microscopy (3.2.4). Images were taken from several regions of the pinnae: the trunk vessels at the base, the edges of the pinnae and vessels several frames from the edge. The three regions allow analysis of a range of different sized and shaped vessels throughout the pinnae.

CD105, in red, was present along the large trunk vessels of the pinnae, with similar expression in both naïve and 1x samples (Figure 3.5A). However in the 4x sample, the trunk vessels showed greater levels of red staining, than in the 1x and naïve pinnae, particularly at junctions (Figure 3.5B). At the edges of the naïve pinnae, CD105 expression was absent. CD105 was also not detected at the day 1 and 2 time points after 1x infection, although the small vessels at the edge and in the middle of the pinnae had up regulated CD105 expression by days 4 and 8. In contrast, the small edge vessels of the 4x group show elevated expression of CD105, compared with the naïve and 1x groups, immediately after the fourth infection (i.e. day 1) vessels express CD105 at all subsequent time points (Figure 3.5B). In the 4x group, consistently high expression of CD105 on the mid branches was detected, whilst naïve and 1x pinnae only expressed CD105 in small patches on the mid vessels (Figure 3.5A). Several of the vessels in 4x pinnae were predominantly red, and these might be entirely new vessels sprouting from the original CD31⁺ vessels. Intense CD105 staining is also seen around the junctions of vessels in several of the 4x pinnae.

A: Naïve and 1x infection samples



B: 4x infection samples

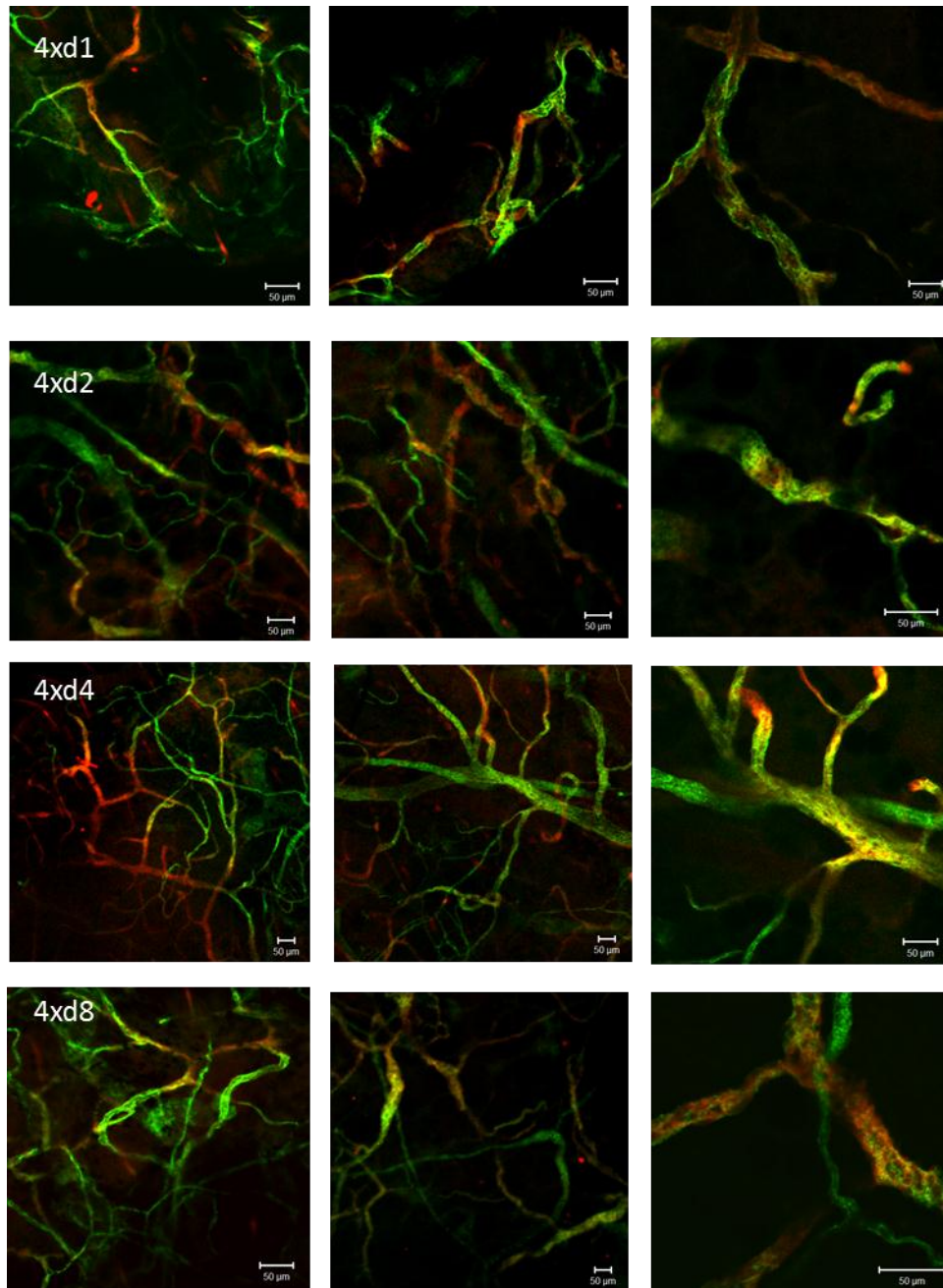


Figure 3.5 Identification of CD105 expression on pinnae vessels

A: Representative images of five naïve and five 1x pinnae. The 1st panel shows the vessels at the very edges of the pinna. The middle panel is a representative image several images from the edge and the final panel is the largest vessels found at the base. CD31 is shown in green and CD105 in red.

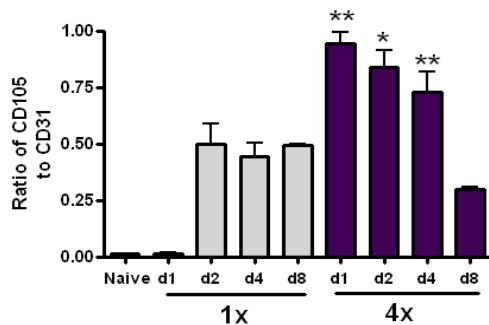
B: Same panels for 4x pinnae, images taken from five pinnae for each time point.

3.3.5 CD105 expression is up regulated on vessels in infected pinnae

In order to quantify the levels of CD105, the ratio of CD105 to CD31 in each image was calculated in many images taken from five biological replicates (3.2.4). Expression of CD105 on the vessels in both infection groups was detected at all of the time points (except 1x day 1 Figure 3.6A). The ratio of CD105 to CD31 in 4x pinnae was significantly higher compared with the equivalent 1x pinnae, apart from day 8 where expression in the 4x group is near 1x levels.

There was a slight increase in expression of CD105 mRNA in 1x pinnae but this was not significant compared to naïve levels (Figure 3.6 B). However, there was a significant increase in 4x pinnae on day 1, although the levels declined over the time course to resemble those in 1x and naïve pinnae. As CD105 expression was clearly detected by microscopy on days 4 and 8 in 4x mice, this could indicate that transcription occurs early after infection but that the receptor is maintained on the vessel surface until much later time points in the 4x infection group.

A: CD105 expression ratio



B: SQ-PCR of CD105 expression

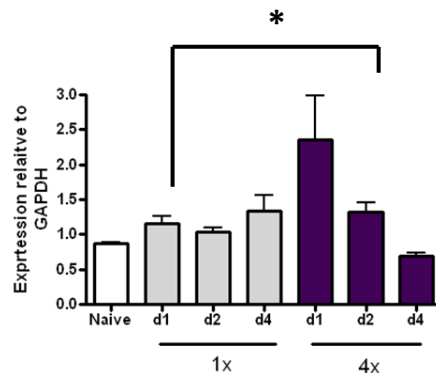


Figure 3.6 Analysis of CD105 expression

A: Ratio of CD105 to CD31 expression averaged across 5 pinnae. Sample size is 20-45 images per group taken from random fields of view over the total area of the 5 pinnae. Values are mean + SEM. Significance shown is each 1x and 4x time point compared, * $p < 0.05$, ** $p < 0.01$.

B: Transcript levels of CD105 quantified by SQ-PCR, expressed relative to the house keeping gene GAPDH; values are mean \pm SEM; sample size is 5 biological replicates per time point.

3.3.6 Increased vascular permeability following infection

In order to allow new vessels to sprout and existing ones to remodel, the junctions between endothelial cells must loosen (Aplin 2006). As such, one indicator of the induction of angiogenesis is increased permeability of the vasculature. The modified Miles assay (3.2.5) was used to determine vascular leakage by injecting Evans Blue dye into the vascular system of infected mice. The circulating dye extravasates into and is trapped in the tissue surrounding permeable vessels. This can then be extracted from the tissue and quantified. As an internal control for differences in the individual mouse, vasculature, and the administration of the dye, only one pinna from each mouse was infected.

External imaging of pinnae revealed that the dye was not detected in uninfected pinnae, whilst both 1x and 4x pinnae had regions of blue radiating predominantly from the midline of the pinna (Figure 3.7A). The dye was visible by eye in 1x pinnae on day 1, and faintly at day 2. In 4x pinnae, the dye was seen in the tissue on days 1, 2 and 4. The dye was extracted from the pinnae and the concentration analysed (Figure 3.7B). After infection there was an immediate increase in the levels of dye leaking into the tissue (day1) this was seen in both the 1x and 4x pinnae (Figure 3.7 B). However, the concentration within 4x pinnae was significantly higher at the early time points compared with 1x pinnae (d1 & 2). Furthermore, the levels of dye within the tissue remained greater for longer in 4x than 1x pinnae. Levels did not decrease to naive levels by day 8.

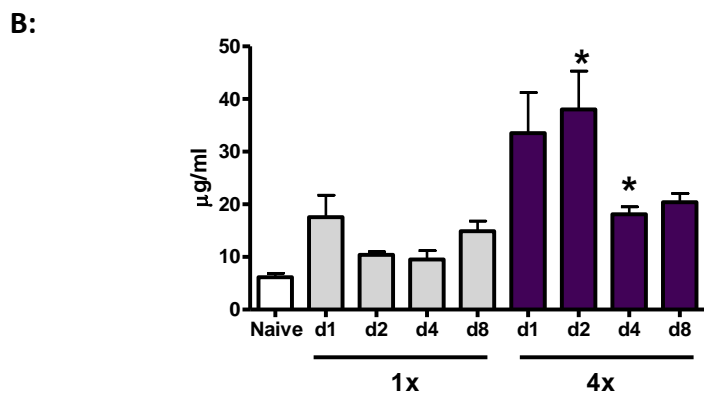
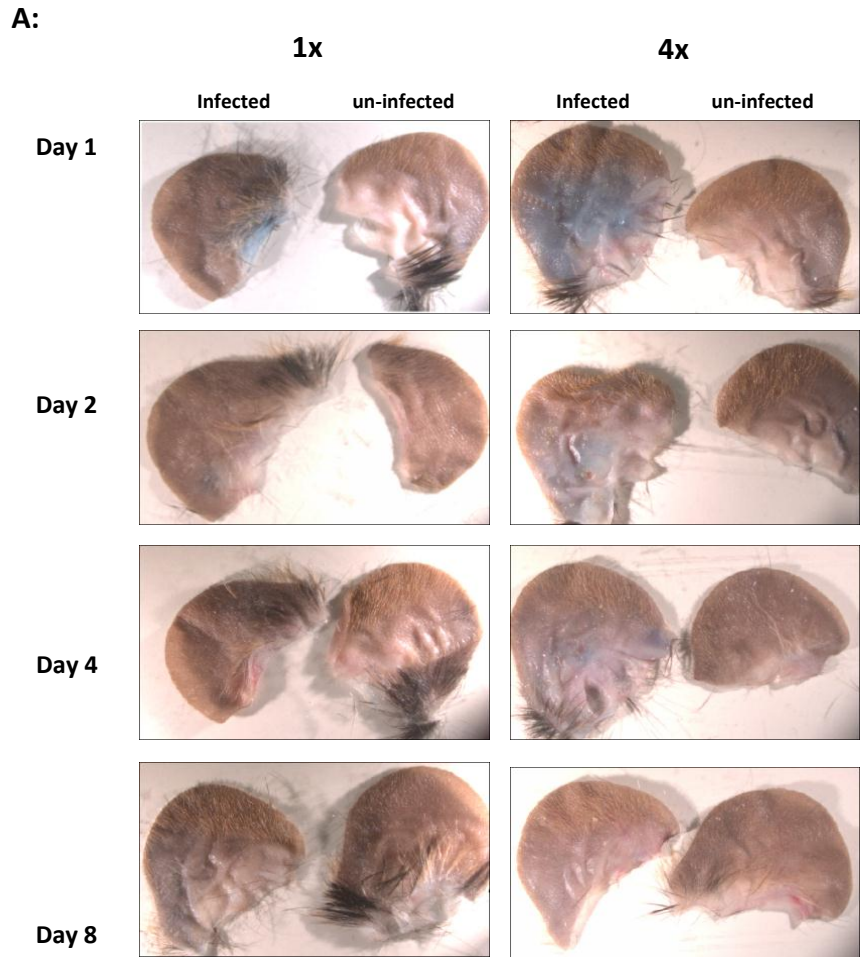


Figure 3.7 Vascular permeability following infection

A: Representative images of 1x (left) and 4x (right) pinnae 90minutes after Evans blue injection. In each image the un-infected pinnae is to the right and the infected pinnae from the same mouse on the left. Experiment completed once on three mice per timepoint.

B: Quantification of Evan's blue in the pinna extracts. Values are mean \pm SEM, n=3 All 4x values are significantly increased compared to naïve. Only day 8 of the 1x is significantly increased compared to the naïve p=0.05. Statistics shown are the 1x and 4x time points compared *p<0.05

3.3.7 Angiopoietin 2 is strongly induced in 4x pinnae

Vascular stability can be influenced by the levels of Angiopoietins 1 and 2 (Thurston 2000) and increased levels of Ang2 can compete with Ang1 to promote vessel permeability (Maisonpierre 1997). Transcript levels of Ang1 were analysed in whole pinnae between days 1 and 4 post infection (when the dye is still visible in the skin) and in 1x pinnae were observed to decrease between days 1 and 2 but increase again at day 4 (Figure 3.8). Ang 2 was detected at the same level as Ang 1 on day 1 but remained elevated over the time course. In 4x pinnae, levels of Ang1 remained relatively low, whereas Ang2 was significantly elevated ($p < 0.01$) compared to the equivalent 1x time points and remained elevated over the time course.

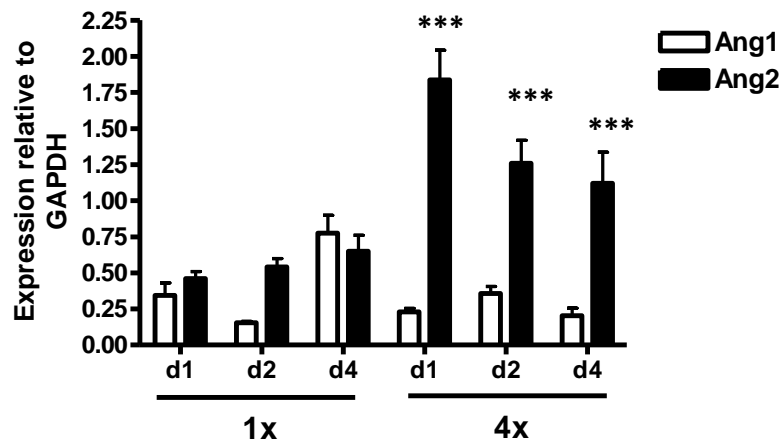


Figure 3.8 Angiopoietin 1 and 2 gene expression

Transcript levels of Ang 1 and Ang 2 were analysed at days 1, 2 and 4 after either 1x or 4x infection. Expression is shown relative to GAPDH. Values are mean \pm SEM; $n=5$. Statistics shown are Ang2 levels compared between the 1x and 4x for each time point, *** $p < 0.001$. Ang2 is also significantly increased in the 4x compared to Ang1 ($p < 0.001$)

3.3.8 4x pinnae show increased levels of active MMPs compared to 1x and naïve

Sprouting of new vessels requires the remodelling of areas of the ECM and the degradation of the vessel basement membrane. This is performed by the matrix metalloproteinases (Raza 2000). To analyse levels of active MMPs the DQ gelatin assay was used (3.2.6). This utilises a substrate which when cleaved, by MMPs of the collagenase and gelatinase families, becomes fluorescent. The levels of fluorescence are therefore proportional to the concentration of the MMPs within the sample. The levels of active MMP protein in the sample did not change between the naïve and 1x samples, however levels were significantly increased at days 2 and 4 in the 4x pinnae ($P < 0.05$ days 2 and 4; Figure 3.9A). Incorporating the DQ Gelatin into cygel (3.2.6) allows layering of the substrate over pinnae sections. The MMPs digest the substrate which remains trapped in the gel over the enzyme. Figure 3.9B shows that the MMP activation was within the dermis with the activation clustered around the cartilage in the middle of the pinnae where the larger vessels of the skin are located. Fluorescent patches are widespread in the 4x pinnae, whilst there are only a few in the 1x and absent in the naïve.

A:

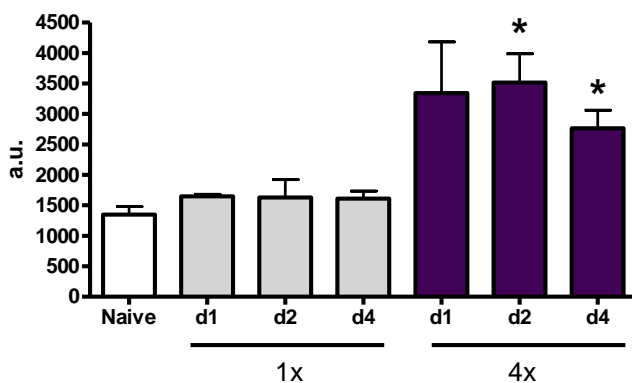
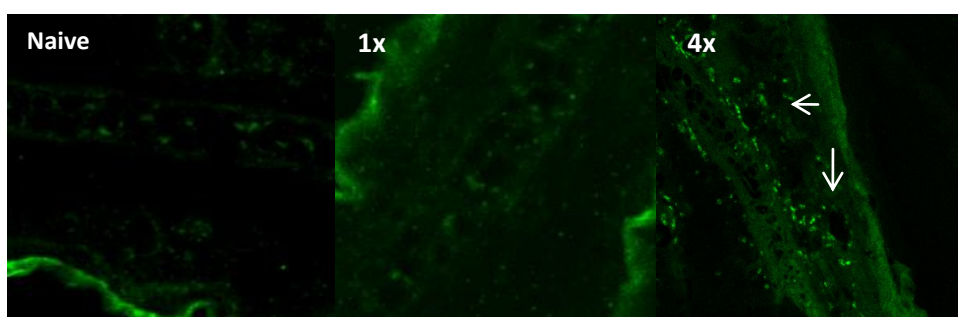


Figure 3.9 Levels of Collagenase and gelatinase MMPs in the skin.

A: Mean levels \pm SEM of fluorescence in supernatants collected from in vitro cultured skin biopsies; $n = 5$.

B: Representative overlays of substrate on pinnae sections; arrows in 4x pinnae indicate areas of high MMP activity. Infected pinnae are day 2 post infection.

B:



3.3.9 Transcript levels of MMP-9 and MMP-19 increased after infection

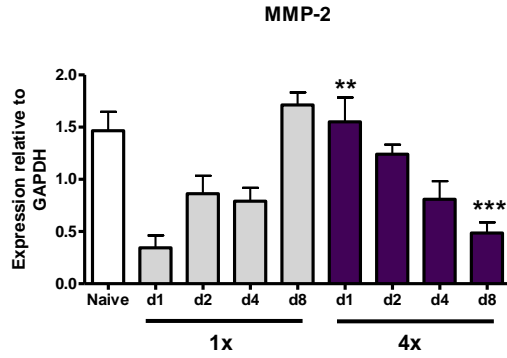
The DQ Gelatin assay identified increased levels of collagenase and gelatinase MMPs but does not quantify levels of each specific MMP. RNA from whole pinnae was reverse transcribed (2.1.4) and analysed by SQ-PCR (2.1.5) for expression of three MMPs commonly expressed in pathological angiogenesis particularly in the skin; namely MMP-2, 9 and 19 (Rundhaug 2005).

In both the 1x and 4x infection groups, transcripts for MMP-2 and 9 were identified (Figure 3.10 A & B). Analysis of MMP-2 identified an increase in transcript levels between days 1 and 8 in 1x pinnae, but a decrease over the same period in 4x pinnae. However, naïve levels of MMP-2 transcript were also high and at none of the time points in the infected samples was the expression significantly increased compared to the naïve.

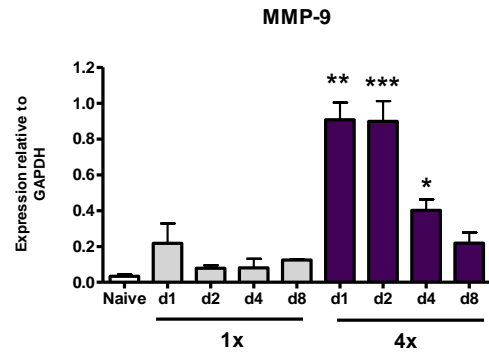
MMP-9 was significantly induced in 4x pinnae compared to the naïve and 1x groups at the earliest time points after infection ($P < 0.01$). After day 2, the expression of MMP-9 declined, though still remained greater than in naïve pinnae at day 8. 1x pinnae had a significant increase at day 1 compared to naïve ($p < 0.05$), although this returned to naïve levels by day 2 over the remainder of the time course.

MMP-19 was also up-regulated after infection and, similar to MMP-2, showed a late induction in 1x pinnae with a significant increase at day 8; in 4x pinnae there was a gradual decline in MMP expression. However, in contrast to MMP-2 there were still significantly higher levels of transcript at day 2 in the 4x

A:



B:



C:

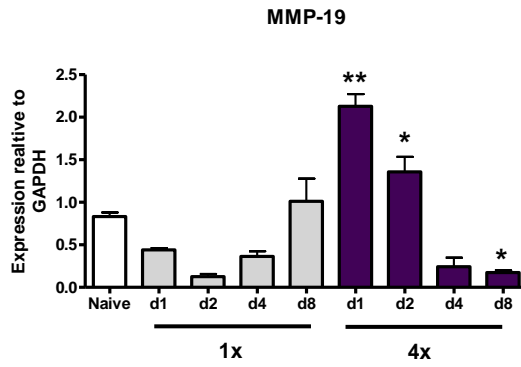


Figure 3.10 Transcript analysis of MMPs.

For all graphs the expression is shown relative to levels of GAPDH in the sample. Significance shown is student's t test on the corresponding time points for 1x versus 4x pinnae; n= 5. *p<0.05, **p<0.01, ***p<0.001

A: MMP-2, **B:** MMP-9 and **C:** MMP-19.

3.3.10 Two isoforms of VEGF are significantly up regulated after 4x infection

As discussed (1.2.3.3), VEGF is widely regarded as central to the angiogenic process (Ferrara 2003). Several isoforms of VEGF exist which have different phenotypic roles in the angiogenic process; VEGF₁₂₀ and VEGF₁₆₄ are soluble and partially soluble respectively, whilst VEGF₁₈₈ is membrane bound (Neufeld 1999). These three isoforms were identified during analysis of whole pinnae transcript following infection (Figure 3.11) and while expression of VEGF₁₂₀ was not significantly different between the infected and naïve groups, and did not alter over the time course of the infection (Figure 3.11 A), VEGF₁₆₄ was significantly up-regulated in the 4x groups compared to the naïve ($P < 0.05$), although no significant difference was observed between 1x and 4x pinnae (Figure 3.11 B). VEGF₁₈₈ was also significantly up regulated in 4x compared to 1x and naïve pinnae. There was no significant difference in the expression of VEGF₁₈₈ over the time course with levels remaining elevated until day 8 (Figure 3.11 C). The concentration of VEGF protein was also measured by ELISA. This measures only the concentration of the soluble isoforms VEGF₁₂₀ and VEGF₁₆₄ (Figure 3.11. D). There was a significant increase in the concentration of VEGF at 4x days 2-8 compared to the 1x time points but no significant difference at day 1 or between the naïve and 1x time points. 4x days 2 to 8 were also significantly increased compared to the naïve ($p < 0.001$ for all)

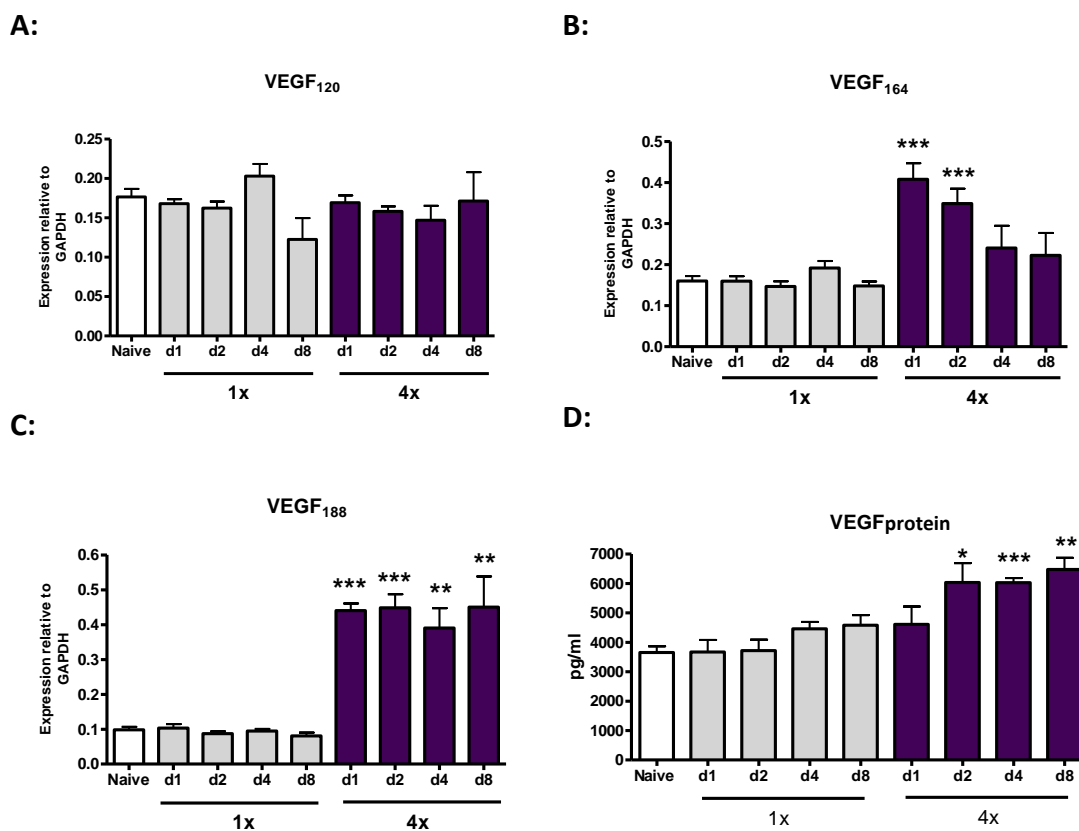


Figure 3.11 Transcript and protein levels of VEGF

A-C : Transcript analysis of the three individual isoforms of VEGF identified in the pinnae. **A** : VEGF₁₂₀ , **B** : VEGF₁₆₄ , **C** : VEGF₁₈₈. Values are means \pm S.E.M. Significance values are for 4x versus the 1x pinnae at respective time points (n = 5). *p<0.05, **p<0.01, ***p<0.001.

D: Protein levels of VEGF measured by ELISA. None of the single infection time points were significantly different to the naïve whilst days 2-8 of the 4x were significantly increased compared to naïve (day 2 p<0.05, day 4 and 8 p<0.01) n=10 supernatants from two experiments

3.3.11 Array analysis of angiogenic factors

To identify further angiogenic factors which may be induced by schistosome infection, a Q-PCR based array was utilised containing 84 genes for both pro and anti angiogenic factors. Five biological replicates were pooled for the 1x and 4x samples for each time point analysed.

Many of the genes showed little or no change in expression when infected time points were compared to the naïve as shown in Table 2.1. Several showed a small increase compared to the naïve which is likely not to be significant, as such genes which are up regulated at least two fold are identified in bold, and it is these genes that were selected for subsequent verification.

The majority of the genes on the array were growth factors and their receptors. Several of the genes were up regulated in both the 1x and 4x compared to naïve samples; Endothelial cell growth factor 1 (ECGF 1), Epidermal growth factor (EGF), fibroblast growth factors 1 and 6 (FGF1 & FGF6), all peaked in their expression on day 1 post infection in both the 1x and 4x groups. PDGF was expressed in both the naïve and infected pinnae but had an early peak of expression (day 1) in the 1x group, and a late peak in the 4x (day 4) group. Of note, the angiopoietin genes previously analysed (Figure 2.9) were up-regulated after infection. Ang2 in particular was up-regulated to a greater extent in 4x than in naïve or 1x pinnae. In addition, transcription of the angiopoietin receptor Tie2 was also up regulated in both infection groups.

Whilst many of the factors were present in both the 1x and 4x infection groups, several genes were up regulated only after 4x infection. FIGF and PlGF, and its receptor FMS-like tyrosine kinase 1 (Flt1), were all up regulated only in the 4x compared with naïve samples, but expression did not change in 1x compared with naïve pinnae. In addition to pro-angiogenic growth factors, the array analyses several anti angiogenic associated genes. Pro-collagen type 18 α 1, whose C terminal domain is cleaved to produce Endostatin (a potent angiogenesis inhibitor), was expressed in the 1x group at low levels and was absent in the 4x samples. In addition, the thrombospondins (1 and 2) which

inhibit the migration and proliferation of endothelial cells were down regulated in both the 1x and 4x groups compared to naïve. Transcription factors controlling growth and development of vessels were up regulated after infection; Heart and neural crest derivatives expressed transcript 2 (Hand2) and Hypoxia inducible factor 1 alpha (Hif1 α) were both up regulated in the 1x group after compared to the naïve but were further up regulated (over 2 fold) in the 4x compared to naïve. The T-box factors 1 and 4 were expressed only in the 4x group, although the increase was less than two fold compared to naïve.

Proteases and their inhibitors were detected in both the infection groups. The matrix metalloproteinases MMP-19 and 9 were up-regulated in both groups, although MMP-19 was expressed at higher levels in 4x compared to naïve pinnae. Tissue inhibitor of metalloproteinase 2 was down regulated in both infection groups whilst Tissue inhibitor of metalloproteinase 1 was up regulated.

In addition to the growth factors and signalling molecules associated primarily with angiogenesis, the levels of several angiogenesis associated chemokines and cytokines were analysed. All of the genes analysed were up regulated in both 1x and 4x infections compared to naïve. Many of the chemokines peaked at day 2 post infection in both 1x and 4x groups. However CCL2 was expressed more than 10 fold in 4x compared to 1x pinnae and peaked early at day 1 post infection. TNF and it's associated factors were up regulated to a greater extent in 4x compared to both naïve and 1x pinnae, and peaked late at day 4 post infection.

Growth Factors and Receptors	1x	4x	Adhesion molecules and matrix proteins	1x	4x
Angiopoietin 1	↑ 1	↑ 2	Cadherin 5	↑ 1	↑ 1
Angiopoietin 2	↑ 1	↑ 1	Pro collagen type IV alpha 3	↓	↑ 2
Connective tissue growth factor	x	↓	Coagulation factor 2	↑ 1	↑ 1
Endothelial cell growth factor 1	↑ 2	↑ 2	Integrin alpha V	↑ 1	x
Endothelial differentiation gene 1	x	↓	Integrin beta 3	↑ 4	↑ 1
Epidermal Growth factor	↑ 1	↑ 1	Laminin alpha 5	↓	x
Endoglin	↑ 1	↑ 1	Platelet/ Endothelial cell adhesion molecule 1	↑ 2	↑ 2
Eph receptor B4	↓	↓	Thrombospondin 1	x	↓
Epiregulin	x	↓	Thrombospondin 2	↓	↑ 2
Fibroblast growth factor 1	↑ 1	↑ 1	Transcription factors		
Fibroblast growth factor 2	x	↓	Ephrin A1	↑ 1	↑ 1
Fibroblast growth factor 6	↑ 2	↑ 2	Ephrin B2	x	↓
Fibroblast growth factor receptor 3	↑ 1	↓	Endothelial PAS domain protein 1	x	x
C-fos induced growth factor	x	↑ 2	Heart and neural crest derivatives expressed transcript 2	↑ 4	↑ 2
FMS-like tyrosine kinase 1	x	↑ 2	Hypoxia inducible factor 1α	↑ 2	↑ 2
Fizzled homolog 5	x	↑ 2	Mitogen activated protein kinase 14	↑ 4	↑ 1
Guanine nucleotide binding protein α13	↑ 2	↑ 2	Prostaglandin - endoperoxide synthase 1	↓	↓
Hepatocyte growth factor	↑ 2	↑ 2	MAD homolog 5	↑ 2	x
Insulin-like growth factor 1	↑ 4	x	Sphingosine kinase 1	↓	↓
Jagged 1	↓	↓	T-box 1	x	↑ 2
Kinase insert domain receptor	x	x	T-box 4	x	↑ 2
Leptin	↓	↓	Proteases and enzymes		
Midkine	↑ 4	↑ 1	Alanyl (membrane) aminopeptidase	↑ 1	↑ 1
Natriuretic peptide receptor 1	x	↑ 1	Matrix metalloproteinase 19	↑ 2	↑ 1
Neuropilin 1	↓	↑ 2	Matrix metalloproteinase 2	x	x
Neuropilin 2	x	↑ 2	Matrix metalloproteinase 9	↑ 2	↑ 2
Platelet derived growth factor alpha	↑ 1	↑ 4	Plasminogen activator urokinase	↑ 2	↑ 2
Placental Growth factor	x	↑ 1	Tissue inhibitor of metalloproteinase 1	↑ 4	↑ 4
Plexin domain containing 1	↑ 1	↑ 1	Tissue inhibitor of metalloproteinase 2	↓	↓
Tyrosine-protein kinase receptor	↑ 2	↑ 2	Trans-membrane serine protease 6	x	↑ 2
Transforming growth factor alpha	↑ 1	↑ 1	Serine (or cysteine) peptidase inhibitor, Clade F, member 1	↓	x
Transforming growth factor β1	x	↑ 2	Plasminogen	x	↑ 2
Transforming growth factor β2	↓	↓	Cytokines and Chemokines		
Transforming growth factor β3	↓	↓	CCL11	↑ 1	↑ 1
Transforming growth factor β1	↓	x	CCL2	↑ 2	↑ 1

Vascular growth factor A	x	x	Colony stimulating factor 3	↑ 2	↑ 2
Vascular growth factor B	x	x	CXCL1	↑ 2	↑ 2
Vascular growth factor C	x	↑ 2	CXCL2	↑ 2	↑ 2
Angiogenesis Inhibitors			CXCL5	↑ 2	↑ 2
Brain specific angiogenesis inhibitor 1	↑ 1	↑ 1	Interferon gamma	↑ 2	↑ 1
Pro-collagen type XVIII alpha 1	↑ 1	x	Interleukin 1 beta	↑ 2	↑ 2
Stabilin 1	↑ 2	↑ 2	Interleukin 6	↑ 2	↑ 2
Leukocyte cell derived chemotaxin 1	x	↓	Tumour necrosis factor α	↑ 2	↑ 4
Key ↑ - Up-regulated ↑ - Up-regulated > 2 fold ↓ - Down-regulated x - No change Numbers indicate peak day of expression post infection			Tumour necrosis factor α- induced protein 2	x	↑ 4
			Tumour necrosis factor (ligand) superfamily member 12	↑ 2	↑ 4

Table 3.1: Analysis of gene expression

Genes are grouped dependant on function and expression of the genes is identified as either up-regulated, up-regulated more than 2 fold (in bold), down-regulated or no change by comparing the infected time points to the naive. For each gene where up-regulation is identified the peak day of expression is noted to the right of the symbol.

3.3.12 Several pro-angiogenic growth factors were up regulated after infection

In addition to VEGF, five further growth factors were selected for verification based upon the results angiogenic growth factor array (Table 2.1). For PlGF there was no significant difference between 1x compared to naïve pinnae. However, in 4x pinnae there is a significant induction of PlGF at day 1 which decreased rapidly to naïve levels by day 2 (Figure 3.12 A).

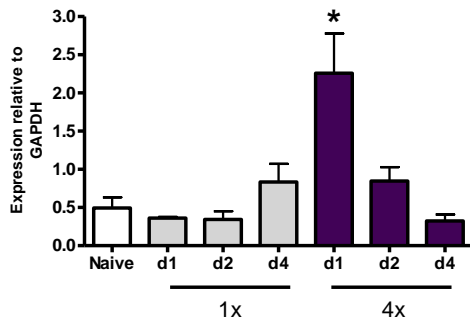
In contrast, ECGF was up-regulated in 1x and 4x pinnae compared to naïve samples but was not significantly different between the two infection groups. It was expressed from the earliest time point and remained elevated until day 8 when expression in 4x pinnae was significantly greater than in 1x pinnae ($P < 0.05$; Figure 3.12 B).

FGF1 was expressed in a similar profile to PlGF, peaking in 4x pinnae on day 1 and declining thereafter (Figure 3.12 C). However, in contrast to PlGF, FGF1 was still significantly up regulated at day 2 compared to the naïve levels. In 1x pinnae, the only value that was significantly greater than naïve levels was on day 4.

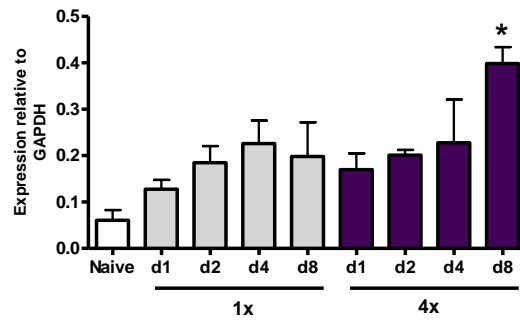
Expression of HGF was only significantly increased in 4x pinnae, whereas there was no difference between 1x and naïve pinnae (Figure 3.12 D). The mean level of expression fell slightly between days 1 and 8 but still remained elevated compared to either 1x or naïve values.

FIGF was also induced early in 4x pinnae but it was not significantly changed in 1x infected pinnae compared to naïve (Figure 3.12 E). Unlike the gradual decrease seen in FGF1, expression of FIGF in 4x pinnae dropped rapidly to naïve levels by day 4.

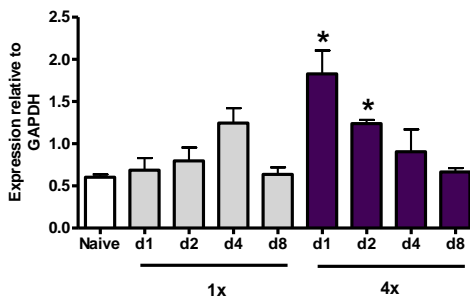
A Placental growth factor (PIGF)



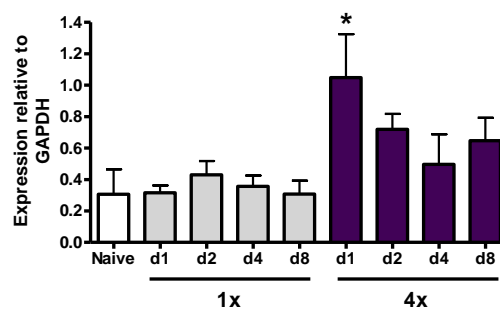
B Endothelial cell growth factor (ECGF)



C Fibroblast growth factor 1 (FGF1)



D Hepatocyte growth factor (HGF)



E C-fos induced growth factor (FIGF)

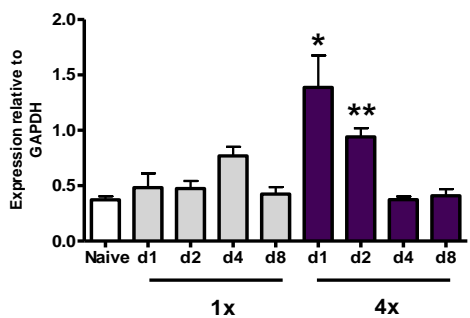


Figure 3.12 Levels of pro-angiogenic growth factor transcript from pinnae at days 1-8 after infection

Transcript levels of the growth factors were analysed from pinnae samples collected on days 1,2,4 and 8 after infection and compared to naïve. Values are mean \pm SEM; n=5. Significance is shown for 1x compared with 4x samples, at the corresponding time points. * $p < 0.05$, ** $p < 0.01$.

3.4 Discussion

3.4.1 Overview

The aim of this chapter was to determine whether angiogenesis is induced following schistosome infection and whether the process is enhanced following exposure to multiple infections. Utilising both visual and molecular techniques it was shown that the vasculature of the skin changes and levels of pro-angiogenic growth factors are significantly increased following infection. This was further amplified in 4x pinnae.

3.4.2 Pinnae vasculature changes after infection

Visible changes in the pinnae were monitored over the course of infection. Observations made many years previous to this research noted that the skin following *S.mansoni* infection becomes reddened and the vasculature more apparent (Pearce 1986). Within this study the skin infection site became markedly redder and the vessels more pronounced after cercarial exposure. Vessels also showed an alteration in structure with many no longer linear and a significant increase in their number in 4x compared to the naïve and 1x pinnae. This could be due to new vessels sprouting, or it could be dilation of existing vessels allowing smaller ones to be visible externally.

In order to determine the extent of vessel dilation which would lead to vascular leakage, the modified Miles assay was used to quantify plasma leakage into the surrounding tissues. Dye was only observed in infected pinnae (and not the contralateral uninfected control pinnae) indicating that the vascular dilation was not a systemic response. The early peak (day 1) of dye extravasation, is indicative of inflammatory vascular leakage which is likely to be controlled, at least in part by the increased levels of Ang2 expression (Roviezzo 2005), as observed after infection particularly in 4x pinnae. Ang 2 is only expressed at sites of remodelling and promotes destabilisation of the vessels and loosening of the connections between endothelial cells by signalling through Tie2 (Thurston 2000). Taken in

conjunction with evidence of dye leakage, the elevated expression of Ang2 transcript is strong evidence for remodelling of the endothelial cells in preparation for sprouting of new vessels.

Although external imaging of vessels and quantification of vascular leakage do not provide conclusive evidence of new vessel growth, expression of high levels of CD105 on new vessels or ones undergoing remodelling, provides additional evidence of angiogenesis. It was observed from images taken over a large area of the pinnae, that there are more vessels present after infection. Within each image there was a significant increase in the number of branches and area covered by the vessels; this was greater in 1x compared to naïve pinnae and was further increased in 4x mice. The diameter of the vessels also increased significantly thus corroborating data from the modified Miles assay. As the labelling procedure for CD31 and CD105 takes place on fixed tissue which is no longer under vascular pressure, the increase in vessel diameter is therefore a permanent change and not due to increased blood flow and pressure in the vascular circulation. Diameter increases were observed in 1x compared to naïve mice, and was further increased after multiple infections. The increased diameter of the vessels was sustained to day 8 when vasculature leakage had reduced indicating that this increase was a permanent feature of the vessels.

The shape of the vessels was also observed to change after multiple infections. Typically, vessels are linear and have several branch points along their length. The vessels in the 4x pinnae more closely resembled that of tumour vasculature. They were highly permeable and took on a convoluted appearance, are likely to be undergoing continuous remodelling and inflammation as seen around tumours (Seaman 2007). In 4x pinnae, there are several regions where the vessels are convoluted and small bundles of fine vessels have sprouted from larger vessels. This could be in regions where parasites have penetrated the skin. The parasites in the skin are approximately 50µm wide and as such will not penetrate through these small vessels (Crabtree 1980). However, the induction of high levels of pro-angiogenic growth factors in the skin around the parasite's point of entry may be inducing these bundles of neo vascular growth.

CD105 expression was up-regulated in 1x pinnae, although this was only detectable from day 2 while expression in 4x pinnae was increased from day 1. The ratio of CD105 to CD31 in the 4x skin is also significantly higher than in 1x pinnae and intense areas of labelling are apparent at junctions of vessels. This appearance and increase of CD105 staining after infection is, further evidence that the vessels are responding to cercariae and are remodelling and branching out to produce new vasculature.

3.4.3 MMPs are up-regulated in 4x pinnae

Essential to the process of angiogenesis is the clearance of the ECM around mature vessels. This allows the endothelial cells of mature vessels to proliferate and migrate and is controlled in part by MMPs (Stetler-Stevenson 1999). Degradation of the ECM also facilitates the influx of further inflammatory cells and perpetuates inflammation. Analysis of total active MMP levels in the pinnae using the DQ-gelatin assay indicated that a significant increase in activation was only present in 4x pinnae. However, the mechanical process of splitting the pinnae to obtain the supernatants may have activated latent MMPs in the skin, thus accounting for the high levels of fluorescence in naïve pinnae which may mask subtle differences in expression in 1x pinnae.

Whilst this assay measures active MMPs, it does not discriminate between the collagenases and gelatinases, of which there are two and four recognised members respectively (Nagase 1999). Analysis of selected skin and tumour angiogenesis associated MMP transcripts in the whole skin (i.e. MMP2, 9 and 19) revealed elevated levels of all three MMPs in 4x compared to 1x and naïve pinnae, and re-enforces the observation that MMPs were not greatly elevated after a single infection.

Up regulation of MMP-19 after multiple infections is indicative of significant remodelling in the epidermis of the skin. MMP-19 is not expressed in normal skin but is significantly produced by keratinocytes in inflammatory skin ulcers and psoriasis (Suomela 2003). High levels of MMP-19 in the 4x group could implicate

an exacerbated keratinocyte response which would correlate with the increase in epidermal thickness observed. MMP-9 has been identified in studies of angiogenesis in a wide range of models as essential for vascular production, and elevated levels of MMP-9 transcript were found in both infection groups. MMP-9 exposes the alpha 5 beta 3 integrin as it cleaves collagen, a process which is essential in pathological angiogenesis (Mahabeleshwar 2006). Higher levels of MMP-9 would expose more of the integrin and increase angiogenic potential in the skin. Observations of early skin wounds have identified that MMP-9 and MMP-2 levels can fluctuate significantly (Salo 1994). Additionally, knockout of MMP-2 does not affect the speed at which wounds heal (Frossing 2010). Combined, the results presented suggest that it is the Gelatinase B enzyme MMP-9, rather than the Gelatinase A MMP-2, which is responsible for the remodelling observed following both single and multiple infections, consistent with data from other skin wound healing models. One of the likely sources of increased MMP-9 transcript is the fibroblasts (Ravanti 2000), additionally the immune cells recruited to the skin following infection may also be a significant source (Chapter 4).

Transcript analysis of MMPs is only suggestive of the levels as MMPs must be proteolytically cleaved to become active. Therefore zymography would be a much better method to analyse the levels of specific MMPs. This technique utilises substrate specific gels to analyse levels of both pro and active MMPs based on their size. In addition to the three MMPs analysed there are many others which have been linked with pathological angiogenesis and more recently with schistosome infection. MMP-12 in particular is expressed at high levels in the liver and lung after infection with *S.mansoni* (Madala 2010). MMP-12, which is an elastase, is induced by IL-13 signalling and could potentially be driving and exacerbating the inflammation in the skin following 4x infection.

3.4.4 Infection induces the release of pro-angiogenic growth factors

Production of VEGF in schistosome infections has previously been studied in relation to the formation of granulomas to eggs in the intestines and liver (Baptista 2005). The data described in this chapter shows that VEGF expression is also induced in the skin in response to infective larvae.

Three isoforms of VEGF were identified in the 1x and 4x infections. The soluble isoform VEGF₁₂₀ is expressed at similar levels in all three groups of mice, whilst VEGF₁₆₄ was up regulated only after infection. This isoform is regarded as the isoform associated with pathological angiogenesis and is expressed at high levels in inflammatory conditions (Ishida 2003, Detmar 1998). However, the largest difference in VEGF expression was in VEGF₁₈₈. This isoform is matrix bound and promotes migration of endothelial cells by binding to the ECM to provide guidance cues (Robinson 2001). It is reportedly important in modulating the sprouting of new vessels. Several studies with single isoform expressing mice have suggested a model where different isoforms act as a gradient along which blood vessels elongate or branch (Poltorak 1997). The VEGF₁₈₈ isoform induces the endothelial cell branching. Over expression of the isoform produces thin highly branched vascular networks which may explain the pattern of branching seen in the 4x pinnae but absent in the 1x (Carmeliet 2000). The differential expression of the various isoforms in the skin after multiple infection, suggests that an amplified angiogenic response, or a more rapid response is occurring in the 4x pinnae.

To identify further angiogenic factors which may be acting following schistosome infection a gene array was utilised. This array identified several additional pro-angiogenic growth factors which were expressed after 1x or 4x infection and also several genes which were up regulated in only the 4x infected groups. Genes which were expressed either over the 2 fold limit in 1x and 4x pinnae, or expressed in 4x pinnae alone, were selected for verification by SQ-PCR. Unfortunately some of the results appeared un-reliable and several of the genes selected for verification by SQ- and Q-PCR showed remarkably different patterns

of expression to the array. This discrepancy in the array could have been due to some or all of the cDNA having been contaminated or degraded during the processing from RNA. DNA contamination would give false high readings whilst degradation of the samples would reduce the amount of transcript hypothesised to be seen. This may have been resolved by using biological replicates, unfortunately the cost of the arrays meant that pooled replicates had to be used. However the array did identify several genes which were up-regulated and identified HGF, PlGF, Flt-1 and VEGF as up-regulated only in the 4x group. PlGF is expressed only in pathological angiogenesis whilst HGF expression is primarily associated with invasive angiogenesis (Autiero 2003 and Rosen 1997). HGF stimulates cell migration, proliferation, and protease production to allow invasiveness of the endothelial cells through the ECM and formation into capillary-like tubes (Bussolino 1992) and it is overexpressed in several invasive cancers correlating with increased tumour angiogenesis. PlGF is associated with inflammatory lesions and neo vascularisation (Carmeliet 2001). Expression of both PlGF and HGF correlates with excessive inflammatory angiogenesis. The patterns of PlGF and HGF expression observed here, suggest that following multiple infections there is a significant increase in angiogenesis. In addition to HGF and PlGF, Flt-1 is also significantly expressed in 4x pinnae. Known as 'vascular endothelial growth factor D', this growth factor is active in both angiogenesis and lymphangiogenesis (Marconcini 1999). High levels in the present study could suggest that the lymphatics of the skin are also affected following multiple schistosome infection. Schistosome cercariae can reportedly extravasate from the skin through a lymphatic vessel (Curwen 2003) in addition to utilising blood vessels. Flt-1 activates VEGFR2, and can stimulate similar phenotypic changes as VEGFA by stimulating endothelial proliferation, branching of endothelial cells in vitro, and causing neovascularisation.

In addition to growth factors, the array identified the levels of several chemokines and cytokines which were all highly up-regulated after infection. In particular CCL11 (Eotaxin) , which recruits eosinophils, and CXCL1, a neutrophil chemo attractant, were both up-regulated more than 10 fold in the infected

groups compared to the naïve. Whilst both chemokines have immune functions they are also shown to have a direct effect on endothelial cells inducing micro vascularisation and migration of endothelial cells. (Salcedo 2001, Wang 2006)

The results from the array suggest an increase of pro-angiogenic factors following infection, and in addition different families of factors were up-regulated in the 4x compared to the 1x pinnae. However, several expression patterns of factors up regulated on the array were not replicated in the SQ-PCR verification. Hand2 and IFN γ which were both found on the array were undetectable by SQ-PCR. Therefore, verification of any of the genes is essential to be confident in the observed expression pattern, although the array was a useful indicator of which genes to study further.

Together, my data indicate an alternative, or amplified, series of angiogenic stimuli and pathways which are induced following multiple infections but are not induced by a single infection. This could be due to 'priming' of the ECM after a single infection with growth factors being sequestered which can then be released quickly after re-infection. However, as the growth factors induced differ between single and multiple infections, this appears unlikely. Instead, differences could be due to the cell types present and the cytokine environment of the skin after multiple infections. Cellular composition of the skin following infection is examined and discussed in the next chapter.

3.4.5 Summary

The results in this chapter show that angiogenesis is induced in the skin following exposure to infective schistosome larvae. The vessels of the skin become permeable and show increased levels of markers of remodelling. CD31 imaging reveals both an increase in the number and diameter of the vessels in the skin. High levels of matrix metalloproteinases following infection indicate the induction of the remodelling cascade preparing the ECM for the growth of new vessels. However, only total active collagenase and gelatinase levels were analysed, although individual MMPs were identified by transcript. Further work could utilise zymograms to determine the active levels of each MMP. Pro-angiogenic growth factors are induced by both single and multiple infections, however there is a difference in the predominant factors between the groups. This difference could be due to the immune response induced in the skin following infection. The next chapter will attempt to characterise the predominant immune response in the skin including characterisation of the phenotype of leukocytes recruited. In particular cells will be analysed for pro-angiogenic phenotypes.

Chapter 4: Determining the angiogenic phenotype of
the dermal innate immune response to infection

4.1 Introduction

The previous chapter has identified up regulation of pro-angiogenic growth factors following infection with schistosome cercariae. The entry of the cercariae into the skin involves penetration and transit through the epidermis to reach the blood vessel rich dermis (Haas 1997). This penetration will cause several reactions in the skin. Initially penetration will cause damage to the skin which would initiate the skin's wound healing mechanisms. This includes induction of the innate immune response (1.3.1). In addition during penetration the cercariae release secretions (termed 0-3hrRP) whose antigens are likely to be recognised by innate immune receptors such as TLRs which trigger innate immune responses. Activation of the immune system is highly interdependent with angiogenesis and therefore analysis of the dermal immune response and cell types recruited is essential in understanding the angiogenic process observed following infection.

Within mature resting tissue there are small numbers of residing leukocytes, however following tissue injury there is a significant influx of leukocytes to augment these residing cells (Neufeld 2006). These are essential in forming the granulation tissue and clearing both infectious agents and the debris produced from damage (Tsirogianni 2006). During this process blood vessels grow into the site to provide the cells and nutrients required for repair. Nearly all lineages of the immune system are involved in response to tissue damage and infection. Neutrophils followed later by macrophages are two of the main responders. Macrophages in particular are an important source of growth factors and cytokines and have long been known to play an important role in the regulation of wound repair and angiogenesis (Rappolee 1988)

Multiple infections with schistosome cercariae can alter the cytokine balance in the skin from predominantly Th1 to Th2. The cytokine production in a tissue site can have both a direct and indirect effect on angiogenesis. Many pro inflammatory cytokines including IL-6, IL-1 β and TNF α induce angiogenesis through release of growth factors or direct interaction with endothelial cells (Kim

2003, Margetts 2002). Additionally the release of cytokines determines the phenotype of cells recruited to the site of infection. The cytokine balance in the skin after 4x infections becomes predominately Th2 and as such may activate the leukocytes differently to the 1x and stimulate release of additional growth factors.

As described earlier in 1.3.4.2 & 1.3.4.3 cells are plastic in their phenotype, macrophages in particular are known to change significantly dependant on the cytokines produced at the site of infections. The broad classifications of classical and alternatively activated macrophages produce very different components and whilst classical macrophages have long been thought to be responsible for the clearance and microbial killing in wounds alternatively activated macrophages secrete components of the extracellular matrix and growth factors. Alternatively activated macrophages were initially described in helminth infections. They have been described in the intestinal granulomas of schistosome infected mice (Herbert 2004). More recently it has been suggested that AAMacs are in fact an innate and rapid response to tissue injury, macrophages are found in close association with vessels and produce VEGF (Allen 2011, Ausprunk 1977). Various phenotypes of macrophage are also found in and around vascularised tumours and depletion of monocytes leads to reduced vascularisation of the tumour (Sica 2002). The phenotype of the macrophages following multiple infection may change and contribute to the elevated levels of pro-angiogenic cytokines within the 4x pinnae.

In addition, helminth infections also lead to recruitment of mast cells, basophils and eosinophils. Eosinophils in particular are recruited to *S.mansoni* granulomas and are associated with several diseases which exhibit high levels of fibrosis and angiogenesis (Levi-Schaffer 1997). Eosinophils can directly affect fibroblast properties and modulate the process of tissue repair (Doucet 1998). They also store several pro-angiogenic growth factors within their granules; VEGF and FGF2 (Puxeddu 2005). Eosinophils have been shown to promote endothelial cell proliferation *in vitro* and induce new vessel formation in chick membrane model.

The type and phenotype of the cells recruited to the skin following cercarial infection could highly alter the angiogenic response. This chapter will determine the cytokine balance in the skin following both 1x and 4x infections and identify the types of cells recruited and their angiogenic phenotype. The difference in growth factor expression between 1x and 4x mice may be due to differing phenotypes in the immune cells.

4.2 Materials and Methods

4.2.1 Dermal Exudate Cell (DEC) retrieval and counts

In order to recover dermal exudate cells (DEC), pinnae were prepared as in section 2.2.12. During this overnight incubation, cells migrate out into the culture media and are then termed DEC comprising adherent and non-adherent cells. After recovery of the culture supernatants, they were spun (300 x g for 7 minutes) to pellet the non-adherent cells. To recover adherent cells, 500µl of ice cold PBS was added to the empty wells and incubated for 20 minutes at 37°C; the cells were re-suspended and added to the non-adherent cells previously collected. The total cell sample was then washed in PBS and either used for flow cytometric analysis (4.2.2), or frozen in Trizol for RNA extraction (2.1.3)

4.2.2 Labelling DEC with antibodies for flow cytometric analysis

DEC were re-suspended in PBS supplemented with 1% foetal calf serum (Biosera, UK), counted and aliquoted at 10^5 cells per tube in 100µl total volume. To each tube, 10µl of normal goat serum (Sigma-Aldrich) and 1µl of anti-CD16/32 mAb (BD Pharmingen) was added to block Fc receptors and incubated at 4°C for 30minutes. The following conjugated antibodies were added to the required tubes (Table 4.1).

Tubes were incubated with the required antibodies (as above) for 1hour at 4°C in the dark before being washed with 2ml of 1%FCS/PBS. Cells were then re-suspended in 500µl of 1%FCS/PBS and kept on ice until analysis using a CyAn ADP flow cytometer (DakoCytomation, Ely, UK) with 405nm, 485nm and 633nm lasers. The forward and side scatter properties of the cells were measured and the proportion of dead cells calculated using propidium iodide staining (PI) to gate out non-viable cells.

Antibody	Clone	Supplier	Isotype	Supplier
F4/80 FITC	BM8	eBioscience	Rat IgG2a	eBioscience
CD45 APC	30-F11	eBioscience	Rat IgG2bk	eBioscience
Ly6G PE	RB6-8C5	eBioscience	Rat IgG2bk	eBioscience
CD11b APC	M1/70	eBioscience	Rat IgG2bk	eBioscience
IA/IE Biotin	M5/114.15.2	eBioscience	Rat IgG2bk	eBioscience
CD11c FITC	N418	eBioscience	Armenian Hamster IgG	eBioscience
SiglecF PE	E50-2440	BD Pharmingen	Rat IgG2ak	BD Pharmingen
Streptavidin Pacific blue	Goat IgG	Invitrogen	-	-

Table 4.1 Antibodies used for DEC labelling

4.2.3 Cell sorting of DEC

DEC were obtained and labelled with antibodies to F4/80 (FITC conjugated) and MHCII (APC conjugated) (4.2.2). Cells were then separated using a MoFlo cell sorter (DakoCytomation) by Karen Hodgkinson of the Imaging and Cytometry Labs (University of York). Three populations were sorted; F4/80⁺MHCII⁻, F4/80⁺MHCII^{mid}, and MHCII^{hi}. Cells were collected into RPMI medium containing 10% FCS. After sorting, cells were washed, prepared for cytopspining, or re-suspended in 250µl of TRIZOL™ for RNA extraction.

4.2.4 Cytospins and DiffQuick staining

Cytospins of the sorted cell population were prepared to confirm cellular identity. Briefly, 2x10⁴ cells of each sample were spun for 3 minutes at 400g onto glass slides in a cytopspin (Cytospin 2, Shandon, UK) which were left to air dry before being stained with DiffQuick as per the manufacturer's protocol. Slides were then washed in pure water until all excess stain was removed; slides were then air dried and coverslips applied using DPX (BDH, UK).

4.2.5 Pinnae digest

The skin remaining after overnight culture for DEC was removed and placed into a solution of 50µg/ml Liberase. The pinnae sheets were incubated at 37°C/5%CO₂ for 30 minutes before being torn into smaller pieces. These were then incubated for a further 40minutes at 37°C shaking gently. After incubation the cell suspensions were strained and the cells pelleted. These were re-suspended in 1%FCS/PBS and labelled for flow cytometry using the same markers as the DEC (4.2.2)

4.2.6 Cytokine array kit

Skin biopsy culture supernatants from naïve, 1x day2 and 4x day 2 infected mice were collected (2.1.7) and analysed using the R&D Systems Proteome Profiler™ Array (Mouse Cytokine array panel A; ARY006 R&D Systems Europe, UK). The kit comprises a membrane spotted with 40 different cytokine antibodies in duplicate. The assay was performed following manufacturer's protocol. The final blot was detected using chemiluminescence kit (Promega). X-ray films were exposed for 20 sec. Results were analysed by densitometry of the spots (Alpha Imager)

3.2.7 Cytokine ELISAs

Skin biopsy culture supernatants (2.1.7) were analysed for levels of 7 different cytokines (Table 4.2):

Cytokine	Capture Antibody	Detection Antibody	Supplier	Standard top concentration	Supplier
IFN γ	R46A2	XMG1.2	BD Pharmingen	10ng/ml	Recombinant cell line 211A
IL-1 β	mAb-4a	BAF-401	BD Pharmingen	25ng/ml	R&D Systems
IL-4	BVD4-1D11	BVD6-24G2	BD Pharmingen	10ng/ml	R&D Systems
IL-5	TRFK-5	TRFK-4	BD Pharmingen	25ng/ml	R&D Systems
IL-10	Kit – DY417		R&D Systems	2ng/ml	R&D Systems
IL-12	Kit – DY499		R&D Systems	1ng/ml	R&D Systems
IL-13	Kit – DY413		R&D Systems	4ng/ml	R&D Systems
TNF α	Kit –CMC3013		Invitrogen	5ng/ml	Invitrogen

Table 4.2 Antibody pairs and kits for cytokine ELISAs

4.2.7.1 IFN γ , IL-1 β , IL-4, IL-5 (in house using paired antibodies from BD Pharmingen)

Plates were coated with the required concentration of antibody diluted in PBS (50 μ l per well) and left overnight at 4°C. After incubation, the plates were washed 2x in PBST (PBS and 0.05% Tween20) before blocking with 400 μ l of 10%FCS in PBS and incubated for a minimum of two hours at room temperature. The block was then expelled and the standards and samples added (50 μ l per well in duplicate); recombinant cytokine standards were prepared in doubling dilutions in 10%FCS/PBS and aliquoted to produce 11 dilutions. The plate was then incubated at 4°C overnight. The plates were washed 5x in PBST and incubated with the biotinylated detection antibody (50 μ l per well) at room temperature for 1-2 hours. Plates were then washed 5x and incubated with 50 μ l of streptavidin horseradish peroxidase (HPO) for 45 minutes (Section 4.2.7.3)

4.2.7.2 IL-10, IL-12p40, IL-13 (Duo kits from R&D Systems)

Plates were incubated with coating antibody in PBS (50µl per well) and left overnight at 4°C. Plates were then washed with 400µl of PBST and blocked with 400µl of 1%BSA PBS for 2hours at room temperature. After blocking, recombinant cytokine standards and test samples were added in duplicate (50µl per well) and left to incubate at room temperature for 2hours. Plates were then washed 5x in PBST and incubated with biotinylated detection antibody diluted in PBST (50µl per well) and incubated for 2hours at room temperature. Finally, plates were washed 5x in PBST and incubated with streptavidin HPO for 45 minutes (Section 4.2.7.3)

4.2.7.3 Addition of final substrate

For both plates after incubation with streptavidin HPO, plates were washed in PBST, and 50 µl Sure Blue TMB substrate (KPL Gaithersburg MD, USA) added to each well. The plates were left to develop colour at room temperature and readings taken using a MRXII plate reader (Dynex Technologies Ltd, Worthing UK) at 650nm every 5-10minutes .

4.2.8 Toluidine Blue staining of pinnae sections

Pinnae sections were prepared as previously (3.2.2) and stained with Toluidine Blue (service provided by the Veterinary Pathology Department, University of Liverpool, UK.)

4.3 Results

4.3.1 1x and 4x pinnae show varying levels of cytokines and chemokines

The cytokine and chemokine balance within the whole pinnae was established using array analysis of skin biopsy culture samples from pooled biological replicates (n=5) for day 2 only (Figure 4.1A).

4.3.1.1 Cytokines

There were several spots for different cytokines which were saturated in all three array blots and therefore comparisons between the 3 groups of mice are unreliable. These were the colony stimulating factors M-CSF, GM-CSF and G-CSF, and the pro-inflammatory cytokine IL-6. The concentration of these molecules appeared greater in the 1x and 4x than naïve groups, although there was little or no difference between the 1x and 4x samples (Figure 4.1B). The pro-inflammatory cytokines IL-1 β and IL-16 were expressed highly in 1x compared to naïve mice and increased further in the 4x group. The regulatory cytokine IL-10 followed a similar pattern of expression. IL-4 and IL-5 also increased after infection and were greater in 4x than 1x samples but both were expressed at much lower levels than IL-10. Of the other cytokines, only five were expressed in only 1x or 4x groups but not in both. The supernatant sample from 1x mice had much higher levels of IL-17 than the naïve sample, whilst the 4x group expressed similar levels to the naïve. IL-13, IL-27 and IFN γ were all up regulated only in the 4x group with no difference between the 1x and naïve. IL-3 also differed in the 4x group but was reduced in expression compared to the naïve.

4.3.1.2 Chemokines

In contrast to the pattern of cytokine expression, many of the chemokines showed no difference in expression between the three groups (Figure 4.1C). Six chemokines which did alter in expression were up regulated in both 1x and 4x samples compared to naïve, but there was no discernible difference between the 1x and 4x groups. These chemokines were; CCL1, CXCL9, CXCL13, MIP-1 α , MIP-2 and MCP-5. Both CXCL9 and CXCL13 were up regulated almost 2-fold compared to the naïve value, whilst the difference was not as great with the other four chemokines. In contrast, two chemokines, C5a and CCL11, which recruit neutrophils and eosinophils respectively, were up regulated after 1x infection but further up regulated in 4x infection. Two other chemokines, CXCL10 and MIP-1 β , were up regulated to a greater extent in the 1x group than either the naïve or 4x group. CCL5 was detected at similar levels in naïve and 1x samples but was lower in the 4x group.

A

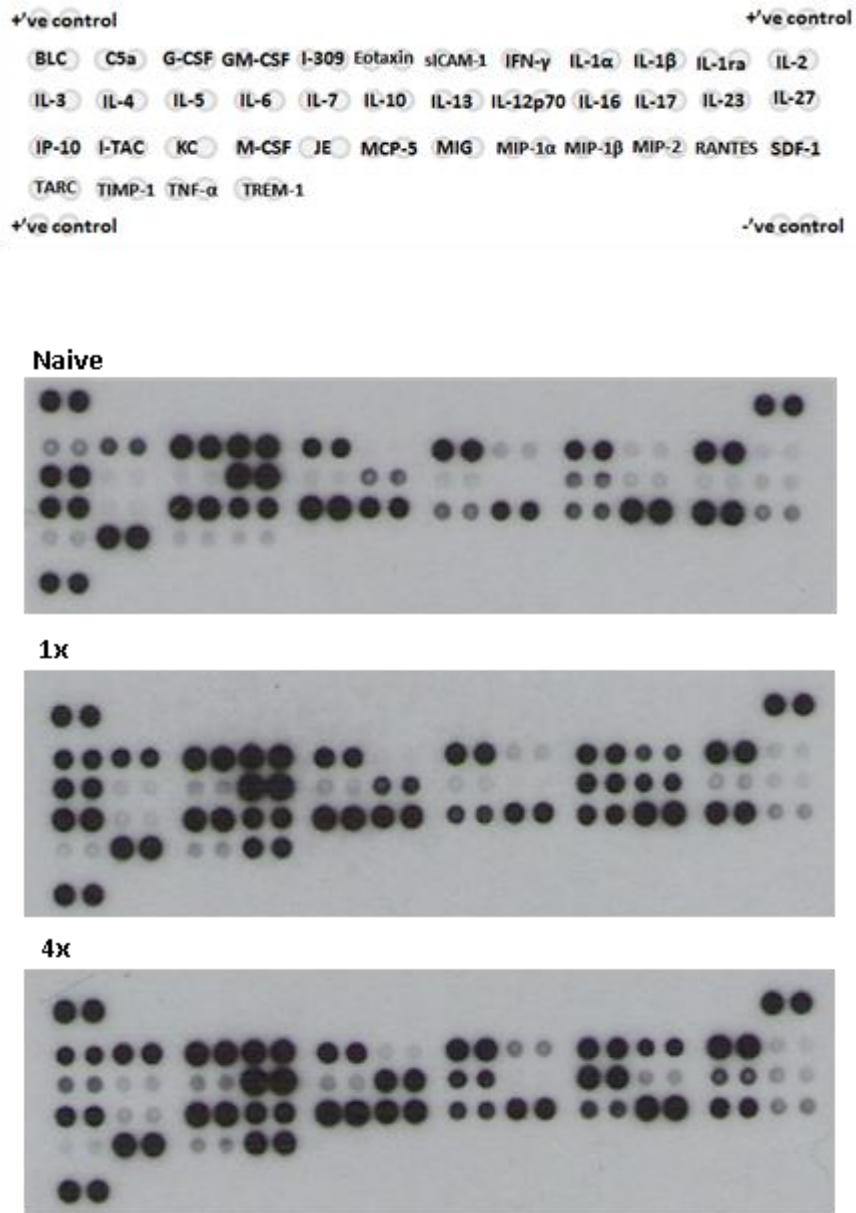
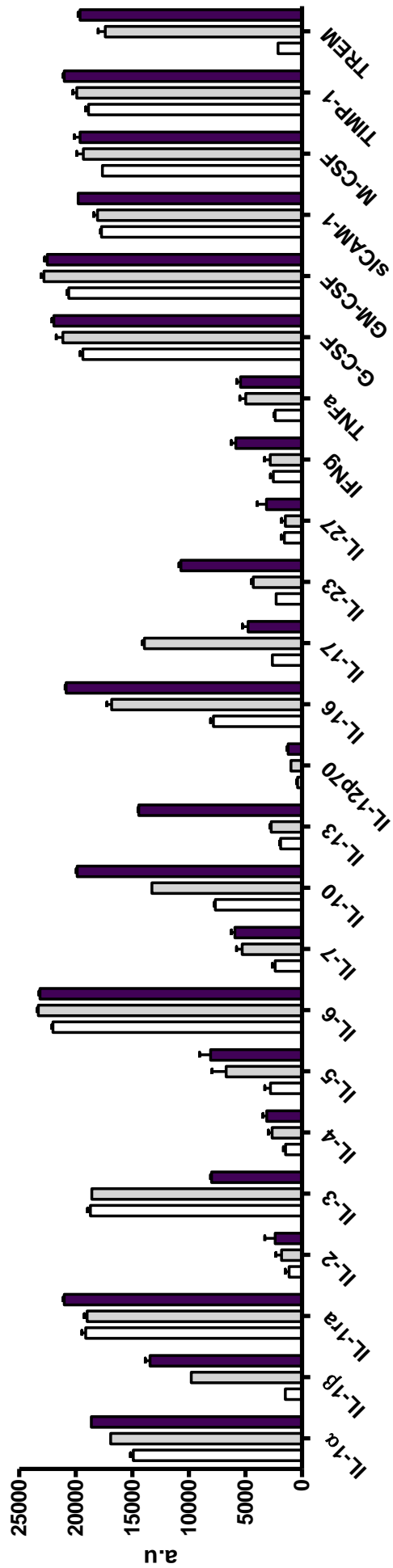
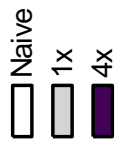


Figure 4.1 Images and graphical representation of the cytokine and chemokine array

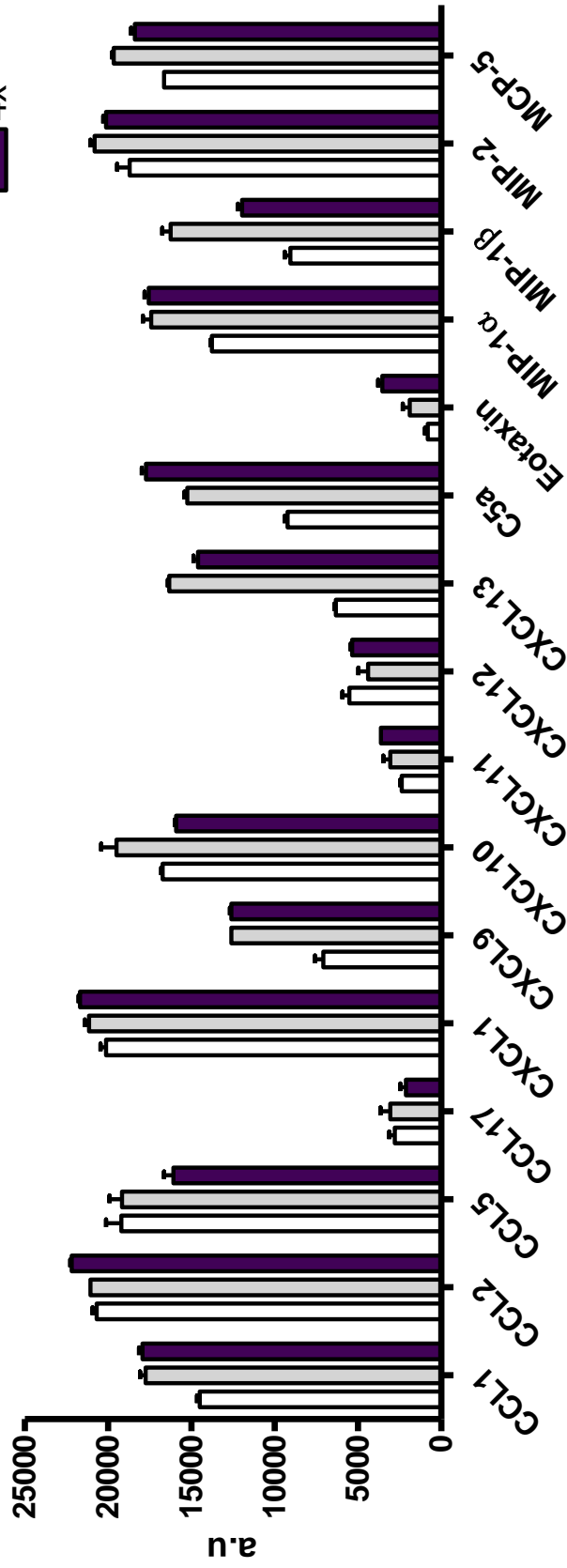
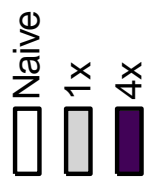
A: Proteome Profiler™ Array blots after 20 seconds of exposure. The plan of capture antibodies is shown in panel 1 with the results in panels 2-4. The positive controls are in the top corners and bottom left with the negative control in the bottom right. The samples were pooled biological replicates of 5 mice from day 2.

B & C: Graphical representation of the densitometry values of cytokine and chemokine spots. The intensity of each spot was calculated and the negative control deducted for each of the replicates and plotted as a mean of the 2 replicates \pm SD.

Cytokines



Chemokines



4.3.2 4x pinnae show significantly elevated levels of Th2 cytokines

Supernatants from skin biopsy cultures of pinnae from naïve mice, and from 1x and 4x mice collected on days 1, 2, 4 and 8 after the final infection were tested by cytokine specific ELISAs (Figure 4.2).

IL-1 β was expressed at high levels at the earliest time point (Day 1) in both infection groups and rapidly declined over the time course but no significant difference between the 1x and 4x groups was detected (Figure 4.2A). The expression of TNF α revealed a different profile showing a steady increase from naïve levels to a peak at day 4 post-infection followed by a decline back to naïve level at day 8 (Figure 4.2B). Again there was no significant difference between the 1x and 4x groups.

IL-12 was expressed by both infection groups at significantly higher levels than the naïve (Figure 4.2C). Expression of IL-12 remained steady over the time course of infection in 1x mice but in 4x mice levels were significantly elevated on day 2 and 4 compared to the 1x time points. In the 1x samples IL-10 was barely detectable over naïve levels until day 8 (Figure 4.2D). In contrast, in 4x mice IL-10 was expressed at high concentrations, ~1000pg/ml at its peak on day 2 before dropping at day 4 .

Of the Th2-type cytokines, IL-4 and IL-13 were both expressed at significantly higher concentrations in 4x compared to 1x pinnae (Figures 4.2E & F). For IL-4, the concentration of protein was relatively low compared to the other cytokines peaking at only ~60pg/ml at 4x day 4 before rapidly reducing over the time course, although levels of IL-4 remained significantly higher in 4x mice compared to either the 1x or naïve. In contrast to IL-4, IL-13 peaked at ~1500pg/ml at 4x day 2. The expression rapidly decreased by day 4 with 4x day 2 being the only significantly increased time point compared to 1x.

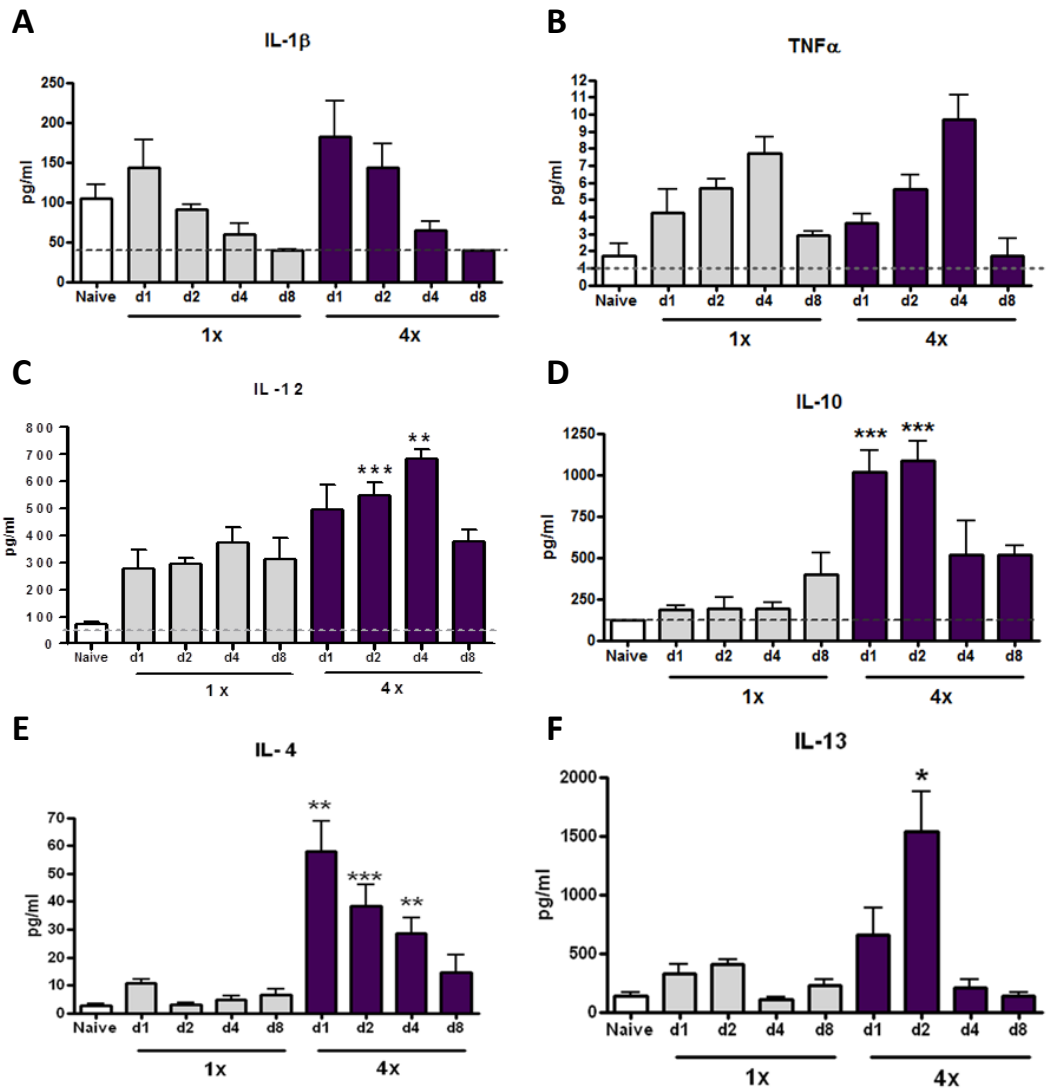


Figure 4.2 Cytokine ELISAs performed on skin biopsy supernatants

A: IL-1 β B, TNF α , C, IL-12p40, D, IL-10, E, IL-4, F, IL-13.

N= 5 biological replicates significance is given for 4x samples versus the equivalent 1x time point. Significance is the 1x versus 4x time points, *p<0.05, **p<0.01 and ***p<0.001. Dashed line indicates the minimum level of detection.

4.3.3 4x pinnae show a significant influx of DEC

After infection, there was a visible influx of cells in the dermis (Figure 3.2) and some of these were recovered as DEC. Both 1x and 4x pinnae compared to naïve tissues (Figure 4.3). In the 1x group, the cell number increased from day 1, peaked at day 2, and then fluctuated on days 4 and 8. The cell counts in 4x pinnae peaked earlier at day 1 and remained elevated on day 2 before declining to 1x levels by day 4. There were significantly more cells in the 1x compared to naïve at days 2-8 (day2 and 8 $p < 0.001$, day 4 $p < 0.05$). The 4x pinnae also had significantly higher numbers of DEC than naïve ($p < 0.001$ for all time points) and 1x pinnae on days 1 and 2 ($p < 0.001$).

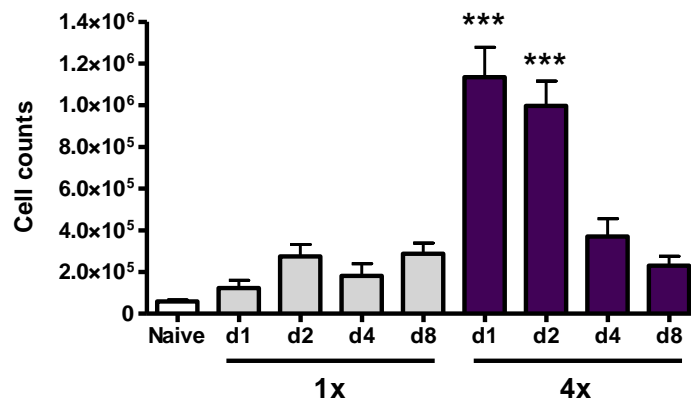


Figure 4.3 DEC counts

Total DEC counts from skin biopsies were calculated per pinnae and shown as mean + SEM ($n = 20$ samples from three experiments). Significance is shown for 4x values compared to the equivalent 1x time point. *** $p < 0.001$.

4.3.4 The majority of DEC are CD45⁺

To determine what proportion of these migratory cells were leukocytes, DEC were labelled with anti-CD45 mAb. Of the DEC recovered, approximately 80-90 % were CD45⁺ in all groups, at all time points (Figure 4.4). There was no significant difference in the percentage of CD45⁺ cells between time points over the infection time course and there were no significant differences between the 1x and 4x infection groups. The percentage of CD45⁺ cells reaches a maximum on day 2.

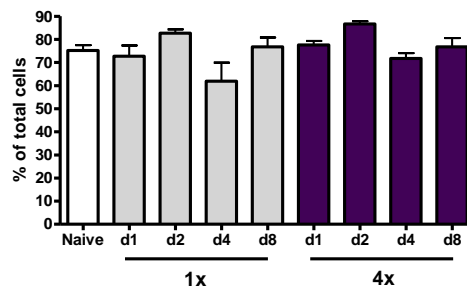


Figure 4.4 CD45⁺ cells in the DEC

The percentage of live CD45⁺ cells within the DEC obtained at different time points. Values are means + SEM for 5 DEC samples. There was no significant difference in or between infection and naïve groups.

4.3.5 Phenotypic characterisation of the DEC

DEC were labelled with a further panel of antibodies against various cell surface markers (Table 4.1) to distinguish various populations of hematopoietic cells, in particular those involved in angiogenesis (1.2.3). DEC recovered on days 1, 2 and 4 after infection were analysed to cover the early cell influx, peak and eventual reduction in cell number after infection. Various types of cells were identified based on their expression of different surface markers as shown in Table 4.3

Cell Type	Markers
Neutrophils	CD11b ⁺ , Gr1 ⁺ , F4/80 ⁻
Macrophages/Monocytes	CD11b ⁺ , MHCII ⁺ , F4/80 ⁺
Dendritic Cells	CD11c ⁺ , MHCII ^{hi} ,
Eosinophils	F4/80 ^{+mixed} , MHCII ⁻ , SiglecF ⁺

Table 4.3 Cell Identification through surface phenotype

4.3.5.1 Neutrophils

CD45⁺ cells were plotted according to their expression of F4/80 and Gr1 which revealed four populations (Figure 4.5B). The majority were F4/80⁺ and expressed varying levels of Gr1, however a separate population was Gr1⁺ but F4/80⁻ (shown as gated population). These cells were virtually undetectable in naïve pinnae (Figure 4.5A). F4/80⁻Gr1⁺ cells were 100% CD11b⁺ (Figure 4.5C) and thought to be neutrophils as confirmed by stained cytopins (Figure 4.5D). The percentage of DEC which were F4/80⁻Gr1⁺ and CD11b⁺ on days 1-4, peaked at day 1 in both 1x and 4x pinnae with an average of 12% and 14% respectively (Figure 4.5E). The percentage of these cells then decreased rapidly from day 1 to 2 and again at day 4.

4.3.5.2 Dendritic Cells

A scattered population of MHCII^{hi} and F4/80^{mixed} DEC was observed (Figure 4.6B). These were predominantly CD11c⁺ (80-90% of the MHCII^{hi} cells) and therefore thought to be dendritic cells (Figure 4.6C). These MHCII^{hi} and F4/80^{mixed} DEC were only a small percentage of the total in 4x mice and this percentage remained constant over the infection time course days 1-4 (Figure 4.6E). The highest percentage of dendritic cells within the DEC was in 1x mice at day 1 (~12%) which was significantly greater than in naïve or 4x groups.

4.3.5.3 Macrophages and monocytes

Both macrophages and monocytes express the myeloid markers CD11b and F4/80 but they express varying levels of MHCII (Figure 4.7). A mid to low MHCII expressing DEC population were also F4/80⁺ and CD11b^{hi}, peaking at ~15%, and were assumed to be macrophages. There was no difference in the percentage of these cells between the 1x and 4x groups over the time course (Figure 4.7E)

4.3.5.4 Eosinophils

A large proportion of the F4/80⁺ cells were MHCII⁻ and SiglecF⁺ which is a classic marker of eosinophils (Figure 4.8 B&C). After 1x infection there was an immediate increase in these F4/80⁺MHCII⁻SiglecF⁺ cells (up to ~15% of the DEC) but this declined slightly between days 1 and 2 to around 10%. F4/80⁺MHCII⁻SiglecF⁺ cells from 4x pinnae were more abundant peaking at ~45% on day 1 post infection and remaining elevated over the remaining time course. At all time points the proportion of these cells was significantly greater in infected pinnae compared to naïve (1x day 1 & 4 p<0.05, 1x day 2 and 4x days 1&2 p<0.01, 4x day 4 p<0.001). Additionally all 4x time points were significantly higher than the 1x equivalents (statistics shown in figure 4.8E)

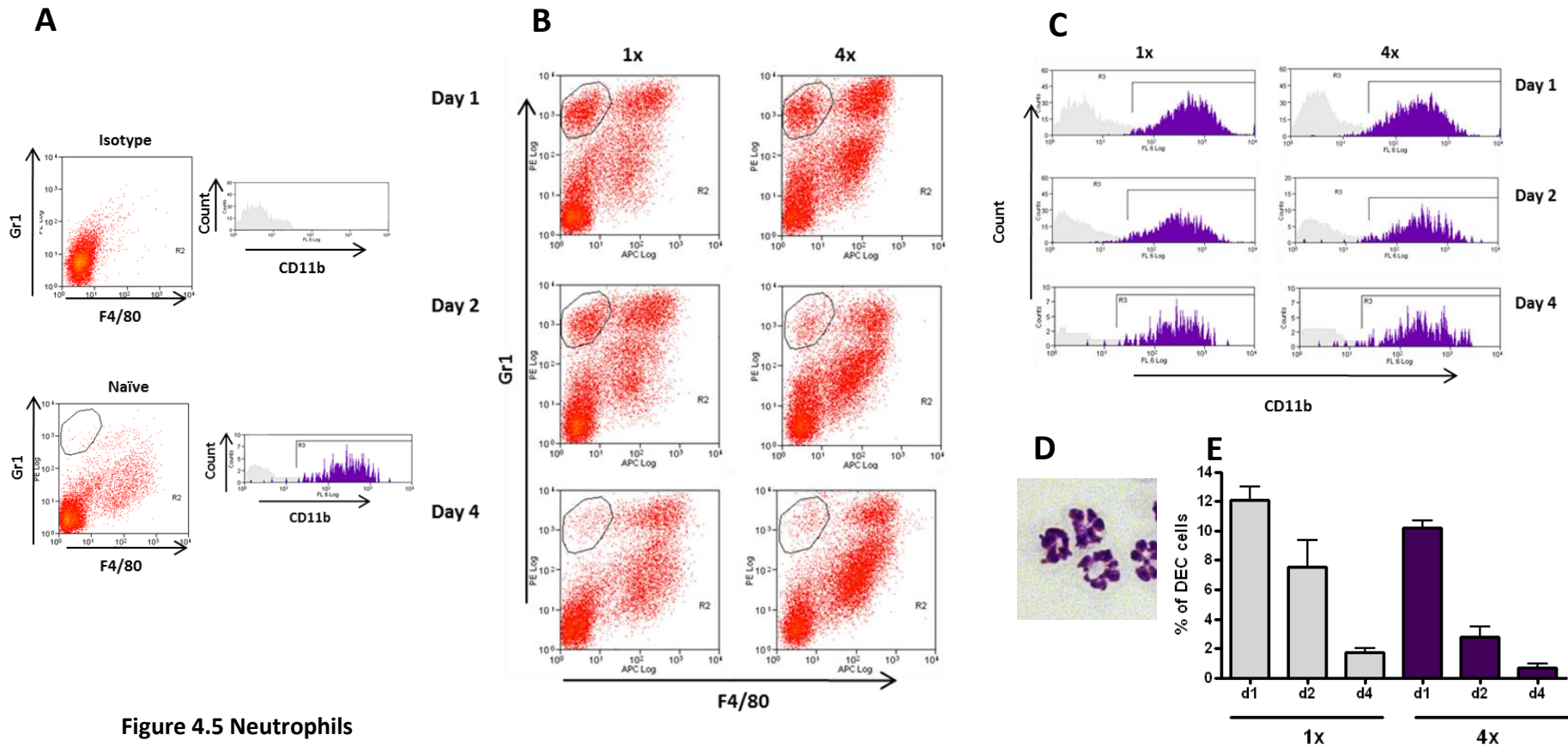


Figure 4.5 Neutrophils

A representative plot from 5 individual biological replicates is shown for all time points in panels B and C

A: Naïve and Isotype control. There was no nonspecific staining seen in the Isotype for the population selected. In the Naïve there is a small population of cells within the region marked which was selected based upon the infected sample. **B:** The infected samples from all 3 time points for 1x and 4x. The selected population is marked and used to gate on the plots shown in panel C for percentage CD11b+.

C: The % of CD11b shown as an overlay of selected cells (purple) over Isotype (grey). **D:** Cytopsin of the selected population showing neutrophil hology. **E:** The percentage of neutrophils within the entire DEC population. There is no significant difference between 1x and 4x time s however days 1 and 2 for both 1x and 4x are significantly increased compared to the naïve ($p < 0.001$ for all) statistics shown mean

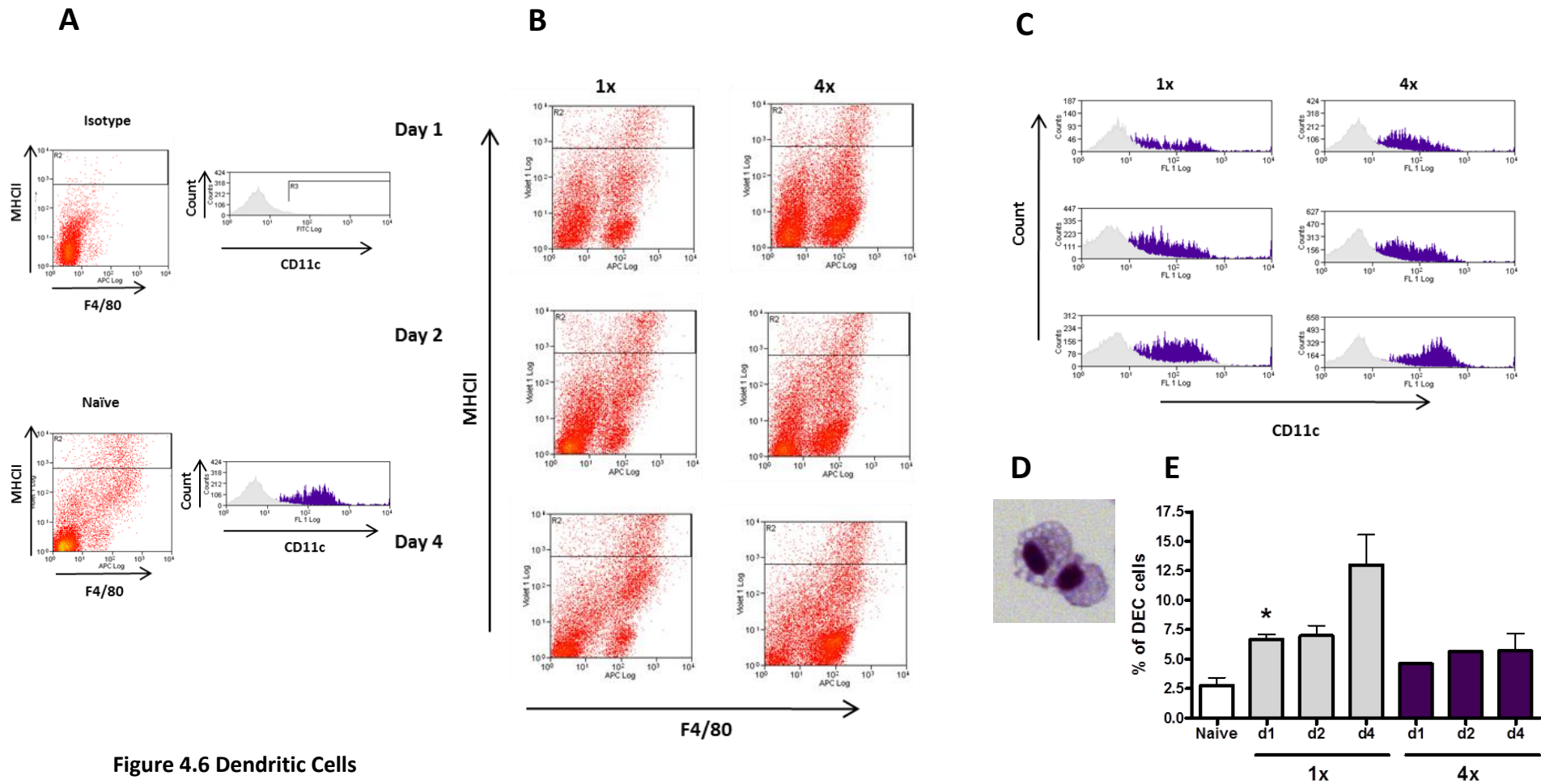


Figure 4.6 Dendritic Cells

A representative plot from 5 individual biological replicates is shown for all time points in panels B and C

A: Naïve and Isotype control. There was no nonspecific staining seen in the Isotype for the population selected. In the Naïve there was a reasonable proportion of the cells within the region marked which was selected based upon the infected sample. **B:** The infected samples from all 3 time points for 1x and 4x. The selected population is marked and used to gate on the plots shown in panel C for percentage CD11c. **C:** The % of CD11c shown as an overlay of selected cells (purple) over Isotype (grey). **D:** Cytopsin of the selected population showing morphology of the cells. **E:** The percentage of dendritic cells within the entire DEC population. There was a significant difference between 1x day 1 and 4x day 1 however there are significantly more dendritic cells in all 1x time points and at 4x day 2 compared to the naïve (p < 0.05) statistics shown mean + SEM

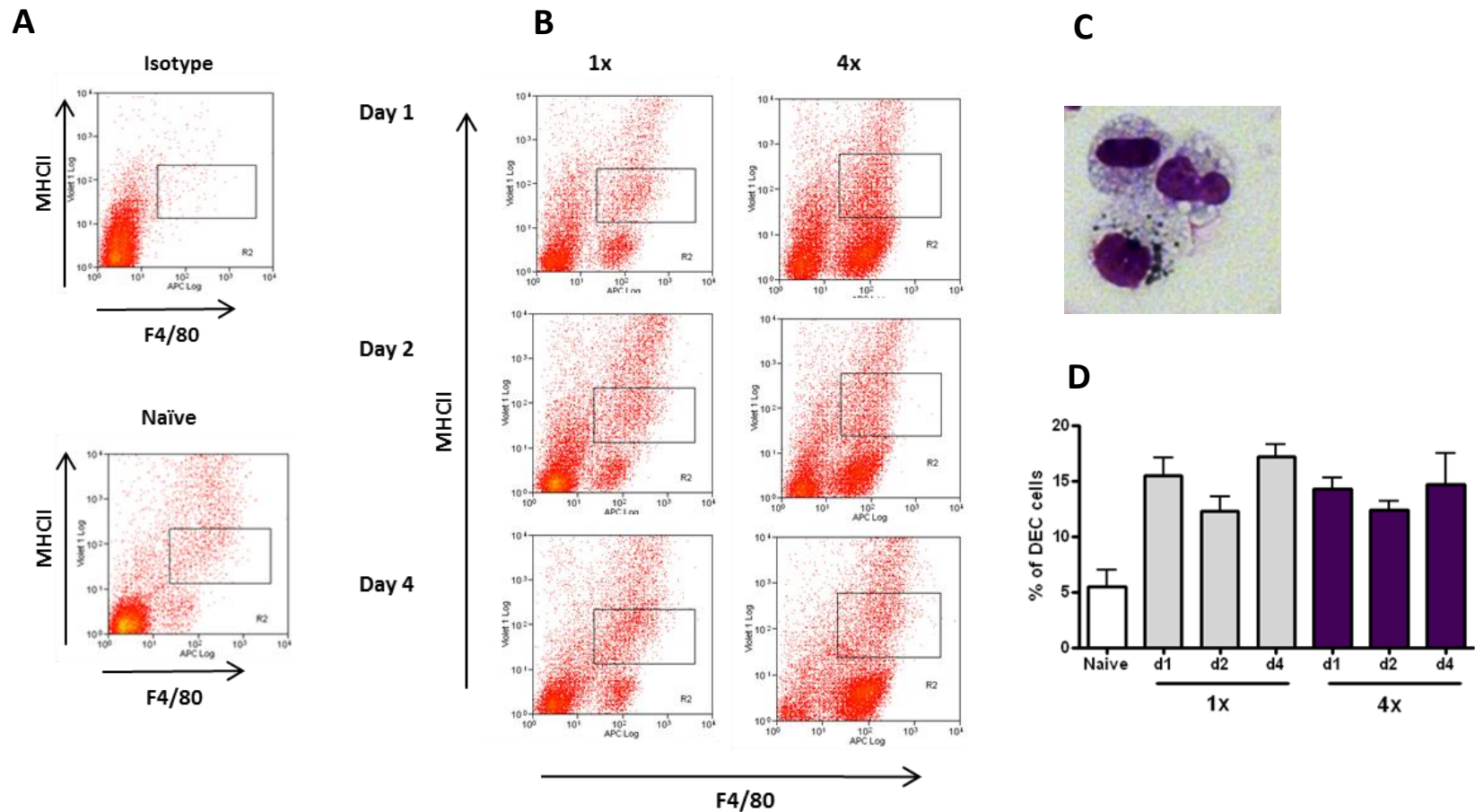


Figure 4.7 Macrophages

A representative plot from 5 individual biological replicates is shown for all time points in panel B

A: Naïve and Isotype control. There was only a small amount of nonspecific staining seen in the Isotype for the population selected (<1%). In the Naïve there was a reasonable proportion of the cells within the region marked which was selected based upon the infected sample. **B:** The infected samples from all 3 time points for 1x and 4x. The selected population is marked **C:** Cytopsin of the selected population showing morphology of the cells. **D:** The percentage of macrophages within the entire DEC population. There was no significant difference between 1x and 4x at any of the time points however all were significantly increased compared to naïve (1x and 4x days 1 and 2 $p < 0.01$, / 4 $p < 0.001$ and 4xday 4 $p < 0.05$) statistics shown mean +SEM

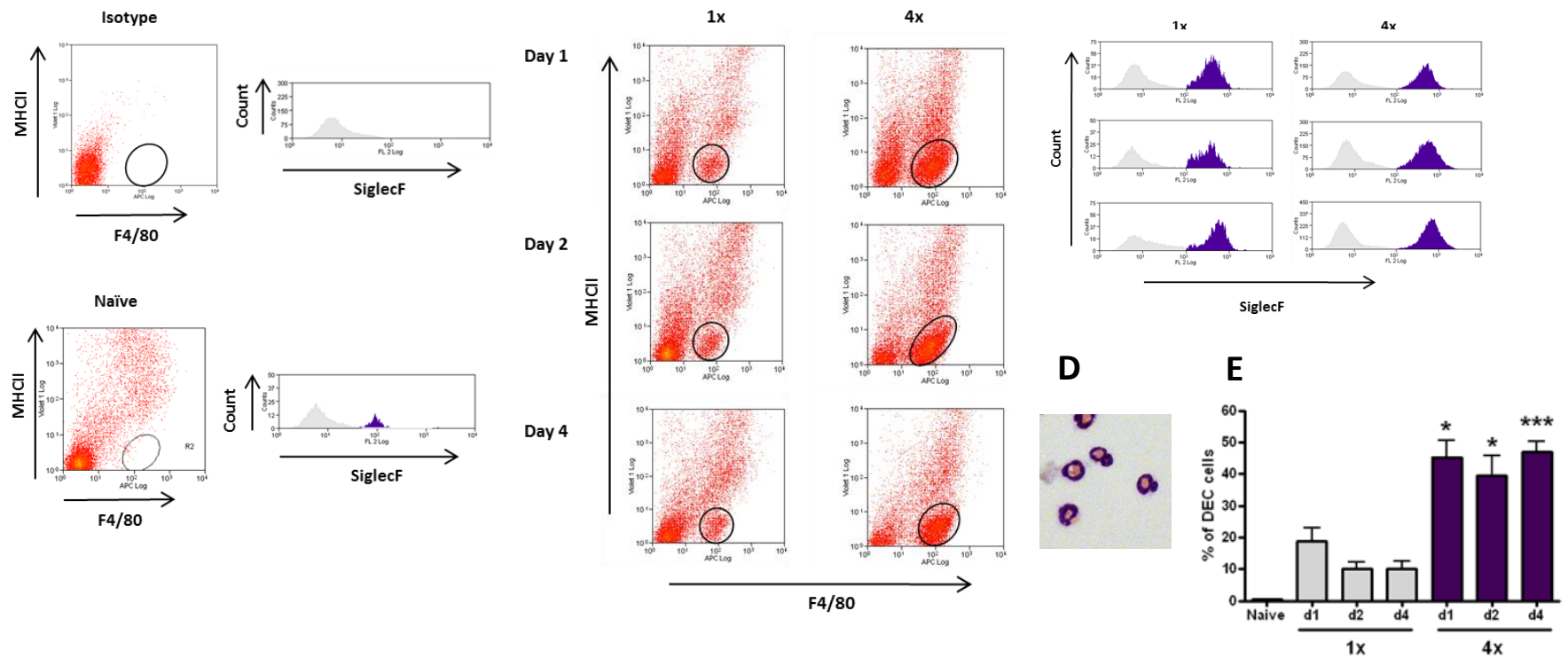


Figure 4.8 Eosinophils

A representative plot from 5 individual biological replicates is shown for all time points in panels B and C

A: Naïve and Isotype control. There was no nonspecific staining seen in the Isotype for the population selected. In the Naïve there was a very small percentage of cells (<2%) within the region marked which was selected based upon the infected sample. **B:** The infected samples from all 3 time points for 1x and 4x. The selected population is marked **C:** The % of SiglecF shown as an overlay of selected cells (purple) over Isotype (grey). **D:** Cytopsin of the selected population showing the morphology of the cells. **E:** The percentage of eosinophils within the entire DEC population. All 4x time points were significantly increased compared to the 1x (statistics shown mean +SEM). All infected samples re significantly increased compared to the naïve ($p < 0.001$)

4.3.6 Phenotypic characterisation of CD45⁺ cells remaining in the tissue

In order to establish the abundance of haematopoietic cells which did not emigrate as DEC, the pieces of skin remaining after overnight culture were digested with liberase and the single cell suspension subsequently analysed for the presence of CD45⁺ cells. As a proportion of the total digested skin cell population there were very few CD45⁺ cells remaining in the 1x pinnae, however there were significantly more in the 4x pinnae peaking at 30% of the total digested skin cells (Figure 4.9). These were subjected to the same analysis as the DEC for phenotypic markers of different populations. Gr-1⁺F4/80⁻ neutrophils were found in the remaining split pieces were significantly more in the infected groups than the naïve. There were also significantly more in the 4x compared to the 1x, perhaps indicating that in the 4x neutrophils are able to migrate further into the skin and remain after overnight culture (Figure 4.10).

Only a small percentage of cells were CD11c⁺ dendritic cells (2% at peak), and there was no significant difference between the naïve and infection groups (Figure 4.11). Flow cytometric analysis showed that F4/80^{mixed} MHCII^{hi} cells expressed low levels of CD11c compared to the DEC, suggesting they could be skin resident cells e.g. Langerhans cells. Macrophages showed a similar profile to the dendritic cells with similar numbers seen in all groups including the naïve group; there was no significant difference between the 1x and 4x groups (Figure 4.12). As in the DEC, a significant number of SiglecF⁺ eosinophils were observed in the 4x compared to the 1x group which were significantly more abundant than in the naïve group which had less than 0.5% eosinophil like cells (Figure 4.13).

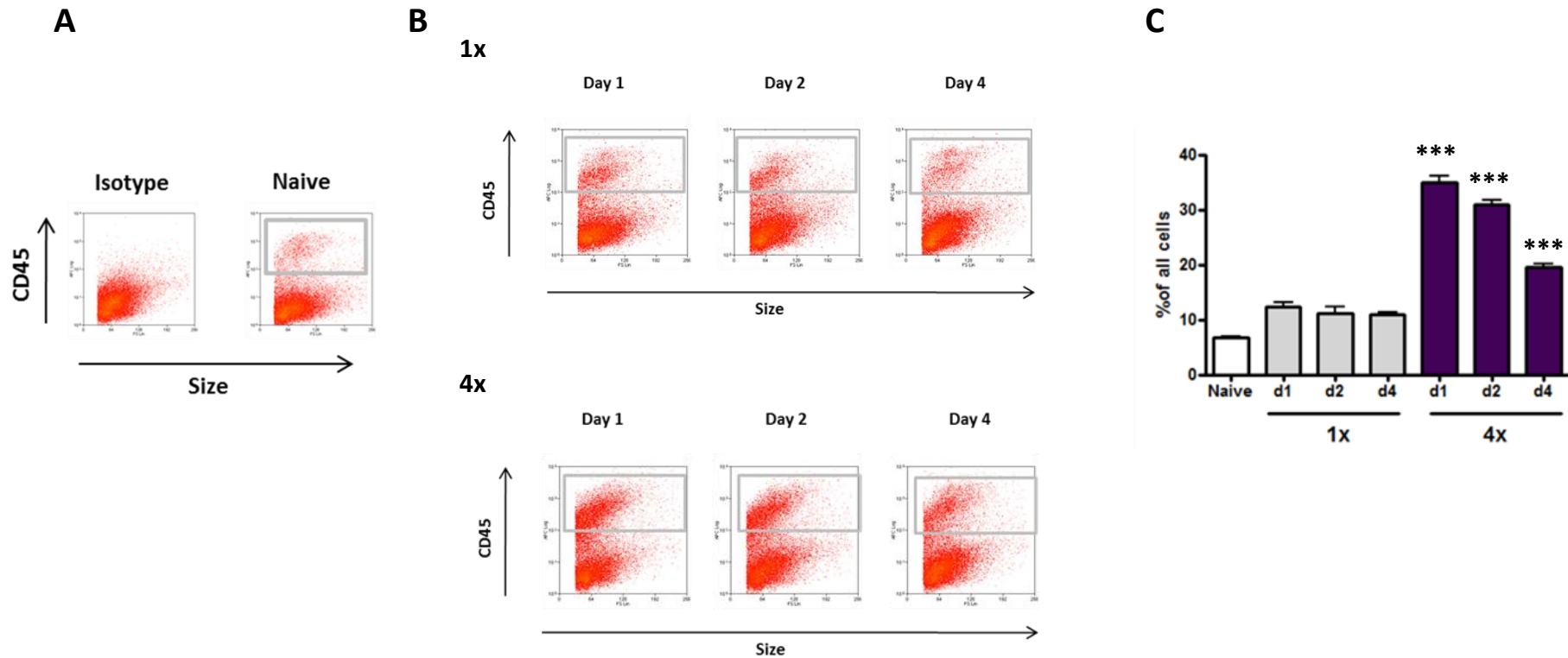


Figure 4.9 CD45+ cells in the skin

A representative plot from 5 individual biological replicates is shown for all time points in panels B and C

A: Naïve and Isotype control. There less than 0.5% nonspecific staining in the Isotype for the population selected. In the Naïve there were several CD45⁺ cells within the region marked. **B:** The infected samples from all 3 time points for 1x and 4x. The selected population is marked **C:** The percentage of CD45⁺ cells within the entire cell suspension after digest. All 4x time points were significantly increased compared to the 1x (statistics shown men +SEM). The 4x samples were significantly increased ($p < 0.001$) compared to the naïve as were days 1 and 2 of the 1x ($p < 0.05$) *** $p < 0.001$.

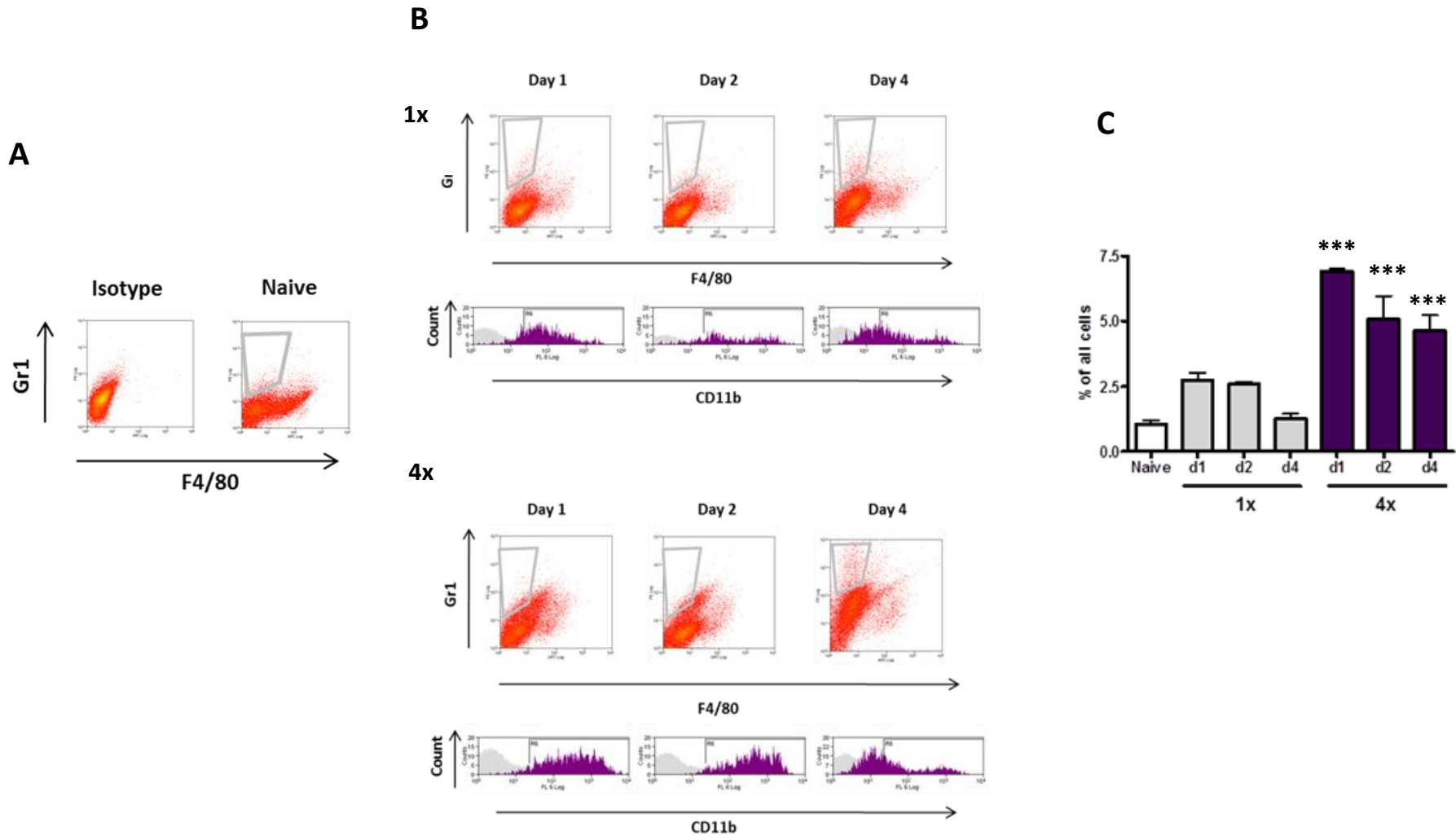


Figure 4.10 Neutrophils in the skin

A representative plot from 5 individual biological replicates is shown for all time points in panels B and C

A: Naïve and Isotype control. There less than 0.5% nonspecific staining in the Isotype for the population selected. In the Naïve there were several Gr1⁺/F4/80⁻ cells within the region marked. **B:** The infected samples from all 3 time points for 1x and 4x. The selected population is marked and analysed for CD11b expression below the plots **C:** The percentage of Gr1⁺/F4/80⁻ cells within the entire cell suspension after 1x time points were significantly increased compared to the 1x (statistics shown mean +SEM). The 4x samples were significantly p<0.001) compared to the naïve as were days 1 and 2 of the 1x (p<0.05) ***p<0.001

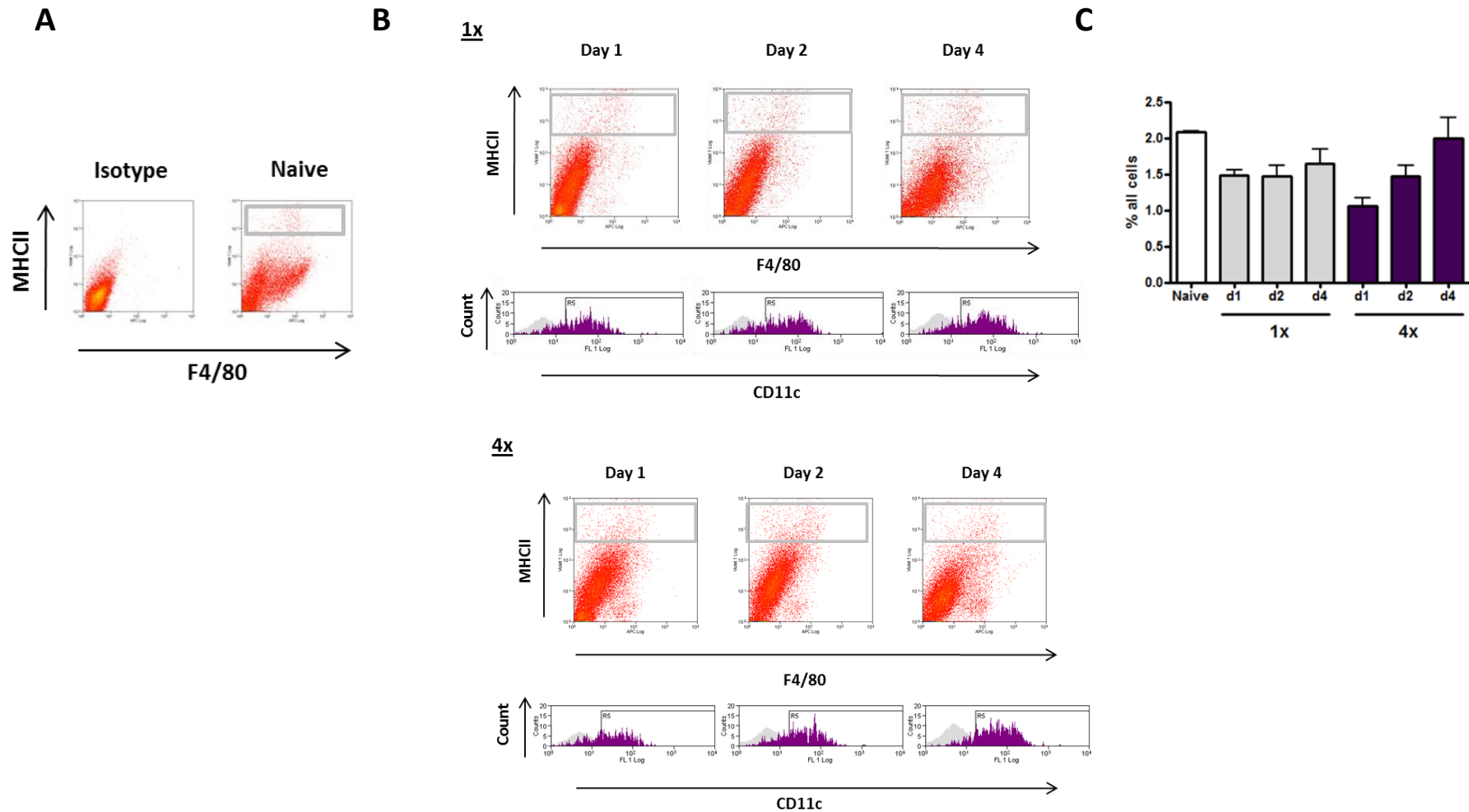


Figure 4.11 Dendritic cells in the skin

A representative plot from 5 individual biological replicates is shown for all time points in panels B and C

A: Naïve and Isotype control. There was no nonspecific staining in the Isotype for the population selected. In the Naïve there was a reasonably large percentage of cells within the region marked. **B:** The infected samples from all 3 time points for 1x and 4x. The selected is marked and analysed for CD11c expression below the plots **C:** The percentage of $F4/80^{\text{mxd}}/MHC^{\text{Hi}}/CD11c^+$ cells within the entire ision after digest. There was no significant difference between any of the groups, shown mean +SEM

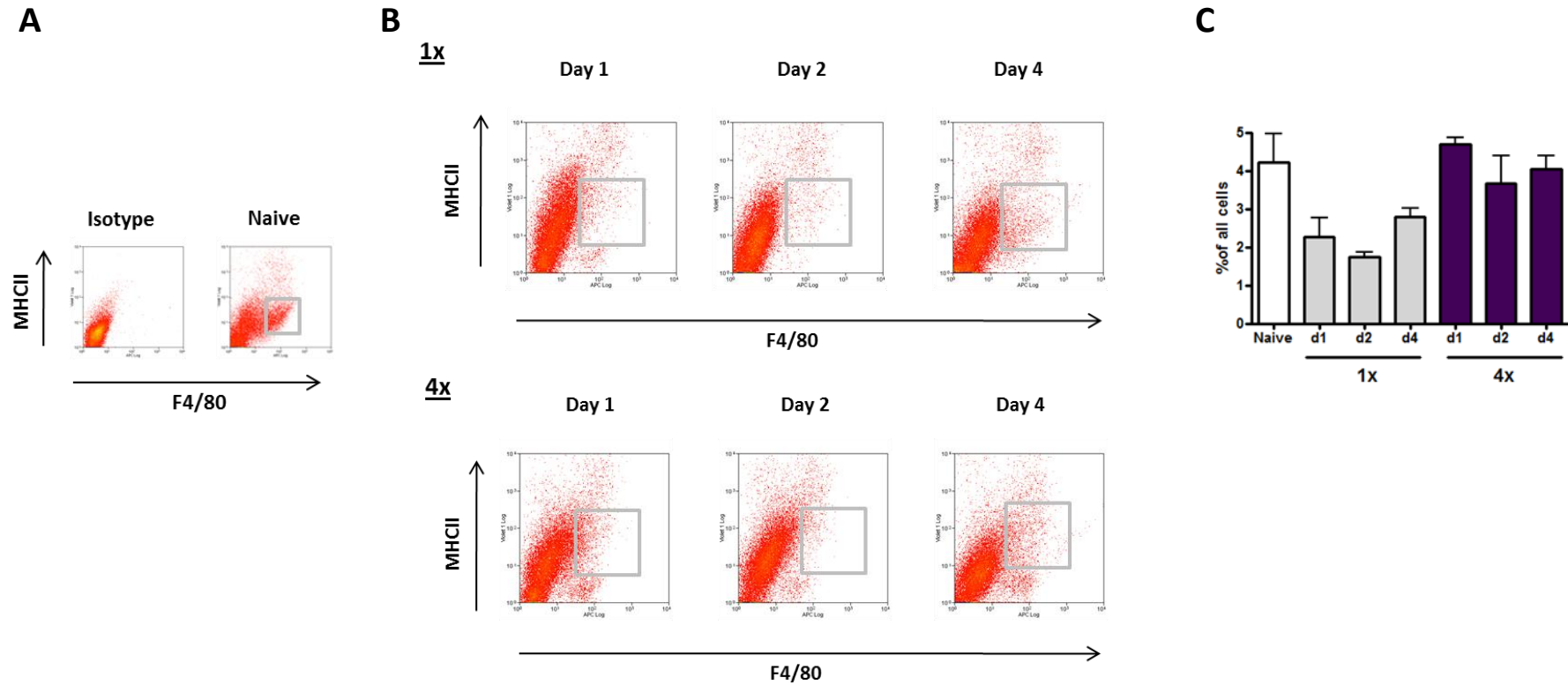


Figure 4.12 Macrophages in the skin

A representative plot from 5 individual biological replicates is shown for all time points in panels B and C

A: Naive and Isotype control. There was no nonspecific staining in the Isotype for the population selected. In the Naive there was a large percentage of cells within the region marked.

B: The infected samples from all 3 time points for 1x and 4x. The selected population is marked

C: The percentage of F4/80⁺/MHC^{Mid} cells within the entire cell suspension after digest. 1x day 2 is significantly reduced compared to the other groups ($p < 0.01$), but there was no significant difference between any of the other groups. shown mean +SEM

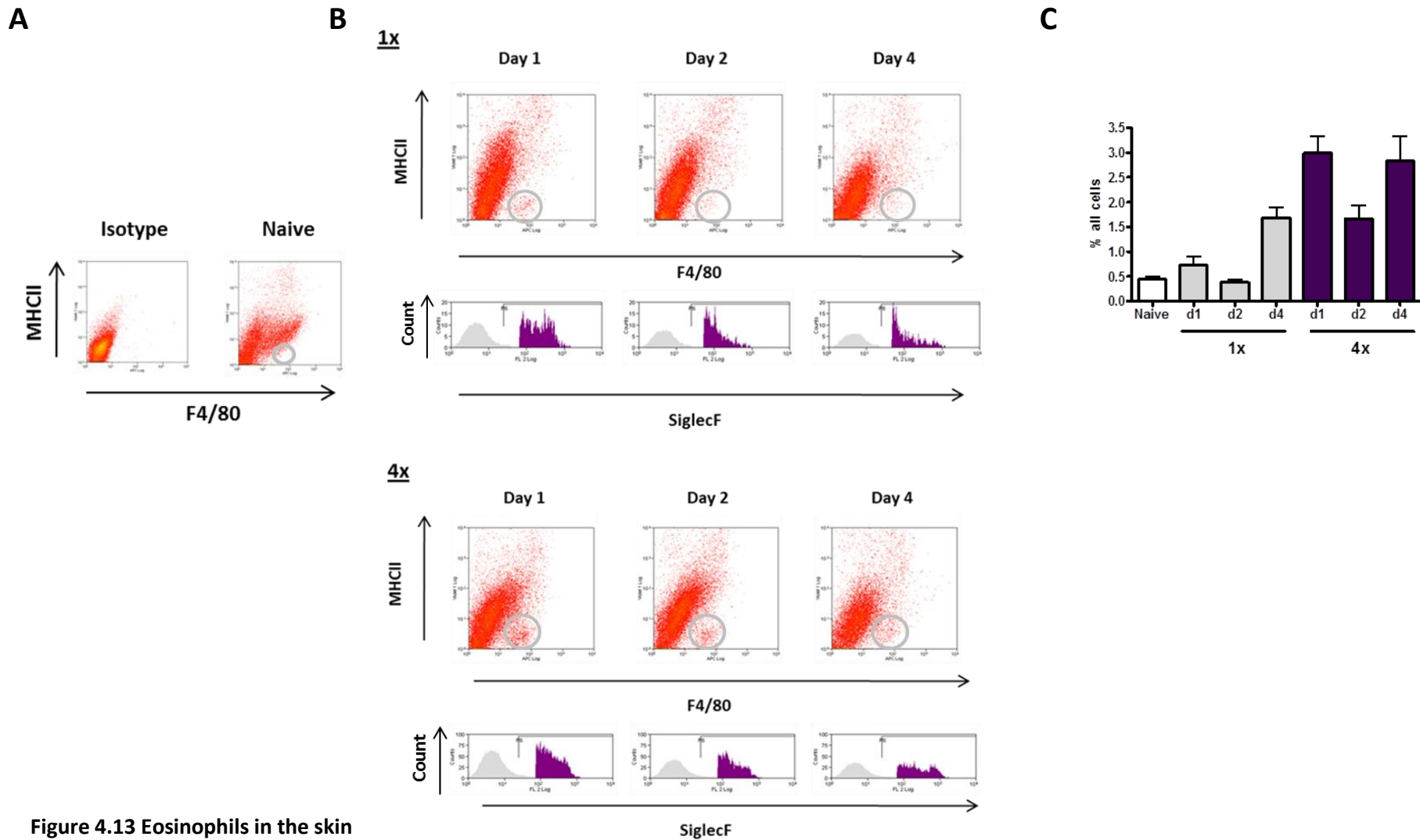


Figure 4.13 Eosinophils in the skin

A representative plot from 5 individual biological replicates is shown for all time points in panels B and C

A: Naïve and Isotype control. There was no nonspecific staining in the Isotype for the population selected. In the Naïve there were only a few cells in the region marked. **B:** The infected samples from all 3 time points for 1x and 4x. The selected population is marked and analysed for SiglecF expression below the plots **C:** The percentage of F4/80⁺/MHC/SiglecF⁺ cells within the entire cell suspension after digest. There were more cells in the 4x compared to the naïve and 1x time points ($p < 0.001$) and 1x day 4 was significantly increased compared to :0.01). statistics shown mean +SEM

4.3.7 More mast cells were presented in the dermis of 4x pinnae compared to 1x.

Mast cells can be found in connective tissue including the skin but are not thought to be present in DEC and can be detected by staining of pinnae sections with toluidine Blue (Figure 4.14A). Mast cells were seen in all groups and are distributed evenly throughout the skin. In naïve pinnae, 1-2 mast cells per field of view were detected whereas in the 1x pinnae a greater number were visible still within the dermal layer. In 4x pinnae the number increased further and were located amongst the cellular influxes under the epidermis. The number of cells per field of view from several pinnae sections were counted which showed there was a negligible increase in the number of mast cells in the 1x compared to the naïve group, however the number of mast cells increased significantly in the 4x pinnae compared to both 1x and naïve (Figure 4.14B).

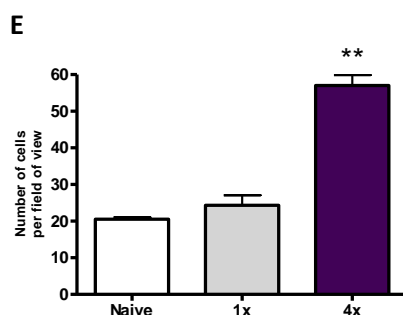
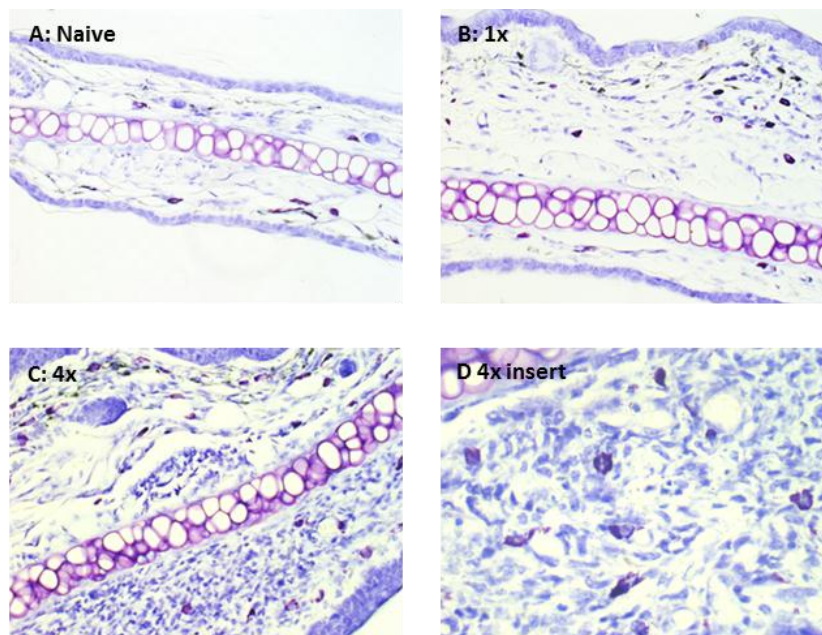


Figure 4.14 Mast cells in the dermis

A-D: Representative images of mast cells in the dermis, pinnae sections were stained with Toluidine blue (A-C 20x, D- 40x magnification)

E: Graphical representation of mast cell counts from day 2 pinnae. ** $p < 0.01$ 4x compared to 1x. 5 pinnae for each group were stained and counted.

4.3.8 4x DEC show increased expression of alternatively activated macrophage markers by PCR

As the majority of haematopoietic cells were found within the DEC, and because they were an easier population to handle, the DEC population was examined to determine whether alternatively-activated macrophages (implicated in angiogenesis) were present in the DEC. Cells were obtained on day 2 post-infection, as this is the peak of cell influx into the skin, and is when the highest levels of cytokines were produced. For all three genes identified as being markers of alternative activated macrophages; Arginase-1, Ym1 and RELM α , expression was most abundant and significantly greater in the 4x than in the naïve and 1x groups ($p < 0.001$) (Figure 4.15). There was a small and significant increase in expression of Ym1 in the 1x group compared to the naïve ($p < 0.05$). The 1x expressed significantly higher levels of transcript for the classical marker iNOS than either the 4x or naïve.

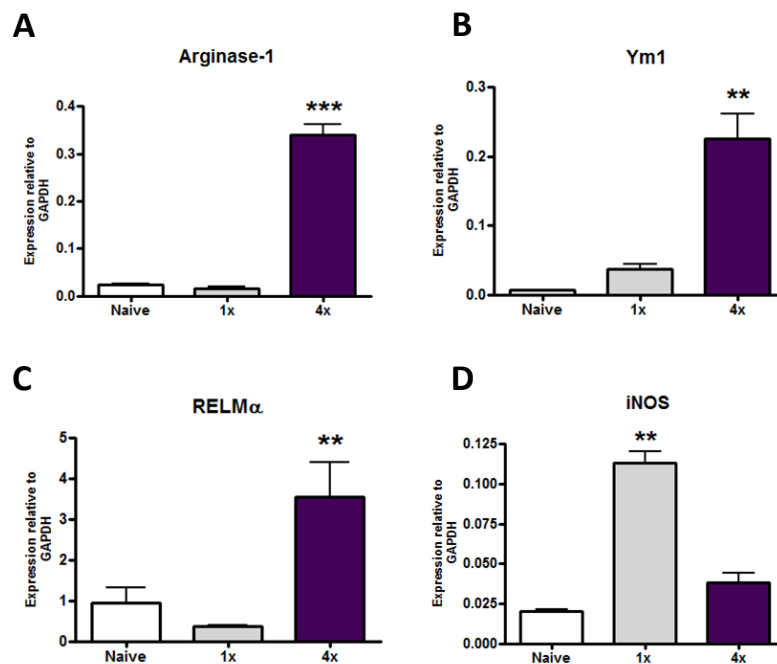


Figure 4.15 Expression by DEC of macrophage markers of activation.

A- Arginase-1 B – Ym1, C – RELM α , D – iNOS. Values are mean + SEM n = 5 biological replicates of DEC taken from day 2 for the infected samples. Expression is given relative to GAPDH ** $p < 0.01$, *** $p < 0.001$

4.3.9 DEC cell sorting into pure populations of Eosinophils, Macrophages and Dendritic Cells

To determine which of the three predominant leukocyte classes identified (Figures 4.6-4.9) – macrophages, dendritic cells and eosinophils, contribute to the angiogenic environment in the skin, samples of these cells were sorted from total DEC from 1x and 4x pinnae according to their expression of MHCII and F4/80 (Figure 4.16). Naive samples could not be sorted as not enough cells were attainable.

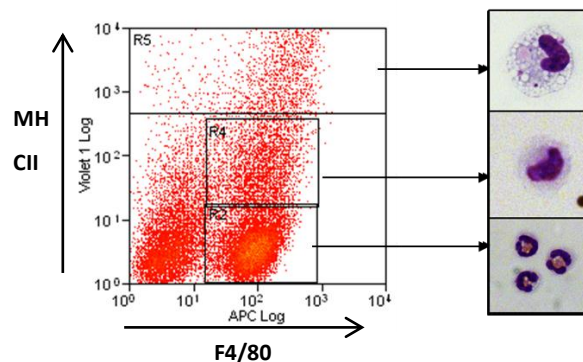


Figure 4.16 Representative graph of parameters for cell sorting.

Representative flow plot showing the gating strategy of cell sorting (Plot shown is 4x day 2) alongside representative images of cells from these sorted populations.

Previously, (P.C.Cook, PhD thesis), the sorted cell populations described above and denoted R2 (Eosinophils), R3 (Macrophages), and R4 (Dendritic cells) were analysed by real time PCR for different markers of alternative activation, and cytokine gene expression. This revealed the R3 population to express high levels of Arg-1 and Ym1 indicative of an alternative activated macrophage population whilst Relm α , IL-4, and IL-13 were most abundant in the eosinophil population (Figure 4.17A taken from Cook 2011). In addition for this study the cells were

analysed for their expression of COX2 (Figure 4.17B). COX 2 expression was detected in all three cell samples. In the macrophage and eosinophil samples expression was increased in the 4x compared to the 1x, significantly so for the macrophages ($p < 0.01$). Expression was reduced in the 4x dendritic cells compared to the 1x.

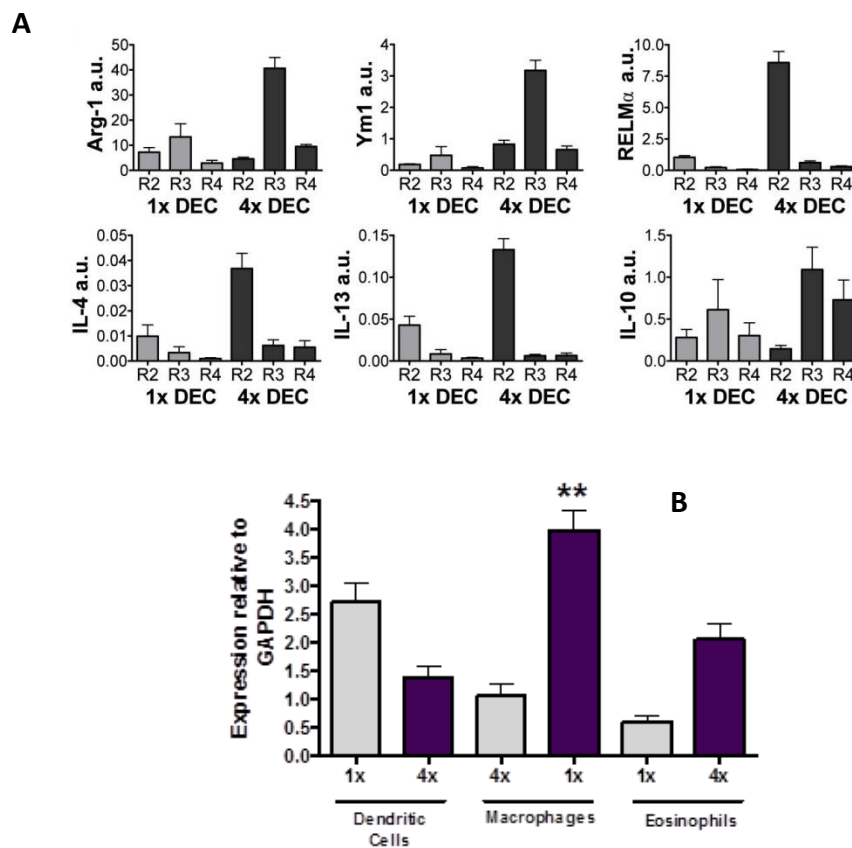


Figure 4.17 Analysis of markers of alternative activation and cytokine expression

A: Expression in sorted DEC samples. Figure is taken from Cook 2011. Sample size is $n=3-4$ separate experiments of 15 pooled biological replicates each. R2 = Eosinophils, R3 = Macrophages and R4 = Dendritic cells. **B:** COX2 expression analysed by SQ-PCR $n=3$ for each group. ** $p < 0.01$

4.3.10 DEC cells express transcript for selected growth factors and MMPs

The cDNA samples from the same cell sort were then tested for expression of VEGF, Flk-1(VEGF receptor 2), MMP-9, HGF and PlGF by SQ-PCR (Figure 4.18).

The two soluble isoforms of VEGF (VEGF₁₂₀ and VEGF₁₆₄) were identified in all of the cell samples but levels did not significantly differ between the 1x and 4x groups in either the eosinophil or macrophage samples. However, the dendritic cell sample expressed significantly higher levels of both VEGF₁₂₀ and VEGF₁₆₄ transcript in the 1x compared to the 4x group. The dendritic cell sample in the 1x group also contained significantly greater levels of transcript for the VEGF receptor, Flk1. Transcript for this receptor was also identified in both the macrophage and eosinophil samples of both groups of mice. In both the eosinophil and macrophage samples, the transcript was more abundant in the 4x group, although the difference was only significant in the macrophage population.

In the transcript analysis of whole pinnae (Section 3.3.12), HGF and PlGF were significantly up regulated only in the 4x group following infection. Here, transcript for HGF did not differ between the 1x and 4x groups in either the dendritic cell or the macrophage samples. However, expression was elevated 4-fold in the eosinophil sample from 4x mice, and was significantly greater than in the 1x group. Conversely, PlGF transcript was most abundant in the macrophage sample from 4x compared 1x mice. PlGF was undetectable in the dendritic cell and eosinophil samples from both 1x and 4x mice.

MMP-9 transcript was un-detected in all of the cell samples from 1x DEC but was found in all samples from 4x DEC, particularly the eosinophil sample which was significantly higher compared to the dendritic cell and macrophage samples from 4x mice ($p < 0.01$).

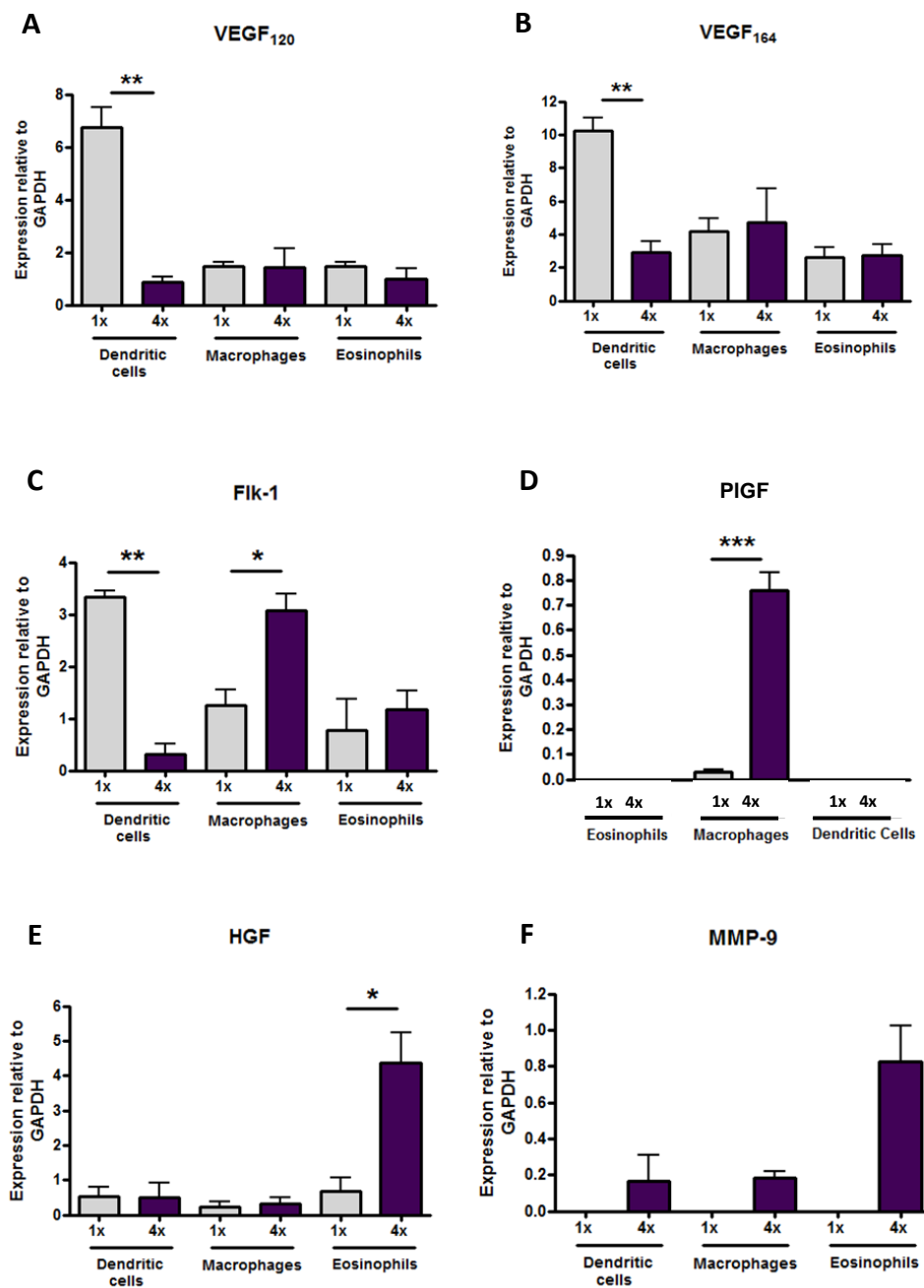


Figure 4.18 Analysis of growth factor and MMP9 expression by sorted DEC

A: VEGF₁₂₀, B: VEGF₁₆₄, C: Flk-1, D: PIGF, E: HGF, F: MMP-9. Transcript expression in the sorted DEC samples; 1x and 4x day 2 post infection. n=3 separate experiments each consisting of 15 biological replicates pooled for 1x and 4x. Statistics are the 4x and 1x groups compared for each cell type mean +SEM. *p<0.05, **p<0.01 and ***p<0.001.

4.4 Discussion

4.4.1 Overview

This chapter has shown that there is a difference in the predominant cytokines produced in the skin between 1x and 4x infections. The 4x pinnae contain elevated levels of IL-4, IL-13 and IL-10 compared to 1x. This coincides with an increase in the number of cells fluxing into the 4x pinnae with the majority of these being eosinophils. The macrophages and eosinophils of the 4x produce higher levels of transcript for the growth factors identified, although dendritic cells down regulated VEGF in the 4x pinnae and appeared less angiogenic.

As shown in Chapter 3, there were focal influxes of cells into the dermis of the pinnae following infection. Here, it was shown that there was a significant increase in the number haematopoietic cells recruited into the 4x compared to the 1x pinnae. The majority of these cells were recoverable as DEC, with only a few remaining in the skin tissue after overnight culture. The lineage and functional phenotype of the cells recruited can determine both the immune and angiogenic response to the infection.

4.4.2 Cytokine balance in the skin

Recruitment and persistence of leukocytes in tissue sites is dependent on the cytokine and chemokine release. It had already been established, that after multiple infections the initial skin response switches to a predominately Th2-type environment in the 4x pinnae characterised by high levels of IL-4, IL-10 and IL-13 (Cook 2011). The array and subsequent cytokine ELISAs performed in this chapter confirm this observation. The up-regulation of IL-4 and IL-13 are associated with fibrosis and IL-4 in particular can activate fibroblasts to produce collagen (Salmon-Her 2000). It is probable that the IL-4 and IL-13 produced are acting not only on the cells of the immune system but also on the cells of the skin. The pro-inflammatory cytokines such as IL-12, IL-1 β and TNF α were up regulated in both the 1x and 4x groups. All three are associated with wounding

and are typically produced early in response to damage (Hübner 1996). As there was no difference in the expression of either IL-1 β or TNF α between the infection groups, this suggests that the release of these cytokines is an immediate innate response to the damage to the cells of the skin; keratinocytes and fibroblasts (Albanesi 2005), and as such not influenced by the repeated exposure to the cercariae. One cytokine not analysed here is TGF β , which is expressed almost immediately upon wounding and has significant effects on the immune system. TGF β 1 induces re-epithelialisation and stimulates angiogenesis (Roberts 1986). Although not shown here a small experiment was done to test the levels of bioactive TGF β 1 within the skin 2 days post infection. The results of which showed a small increase between naïve and 1x and again between 1x and 4x although none of the differences were significant as only two samples were tested for each group.

In addition to the cytokines quantified by ELISA two additional factors were up regulated after infection, more in the 4x, CXCL13 and IL-16. Both of these are potent chemoattractants with CXCL13 being specific for B-cells whilst IL-16 recruits CD4+ cells including eosinophils. The increase of CXCL13 was surprising as no B-cells were detected in the skin in either the 1x or 4x. However CXCL13 has been significantly correlated with active cutaneous vasculitis and correlates with blood vessel damage and inflammation in Hepatitis C infected patients (Sansoono 2008). Within the schistosome model presented here CXCL13 may be acting in a similar way causing dis regulation of the blood vessel growth rather than B-cell recruitment. IL-16 can be released by the basal cells of the epidermis and throughout the dermis, and like CXCL13 can be up-regulated in inflammatory skin diseases (Lagerge 1998). There is evidence that IL-16 can promote IL-4 release from eosinophils (Bandeira-Melo 2002), which could present an earlier driver of the eosinophil recruitment and IL-4 release in the 4x pinnae in this model.

4.4.3 The neutrophil influx was not altered between 1x and 4x infections.

The initial cell type recruited to wounds is the neutrophil, here it functions to provide a first line of defence against micro-organisms entering the wound site (Kim 2008). In addition, neutrophils have also been proposed as potential initiators of the angiogenic cascade mainly through the release of preformed VEGF within their granules (Gaudry 1997), and the release of MMP-9 (Ardi 2007). Within this infection, the neutrophils were recruited to the same extent in both infections with a peak of recruitment at day 1 and declining over the time course. This suggests that following both 1x and 4x infection the initial penetration of the cercariae is stimulating the same wound healing mechanisms and is unaffected by the previous exposure to the cercariae. However the phenotype of the neutrophils was not analysed in this study and it was therefore not determined whether the neutrophils are a source of VEGF or other growth factors in this model. Recruitment and persistence of further leukocytes in tissue sites is dependent on the cytokine and chemokine release of which neutrophils are an important source. They predominantly release chemokines and cytokines which aid in the recruitment of monocytes and macrophages to the tissue site (Scapini 2000). CCL2 in particular can be produced by neutrophils in high concentrations. This was up-regulated only in the 4x. This could suggest that whilst the number of neutrophils does not change between 1x and 4x infections the milieu of chemokines they produce might, which could influence the further recruitment of the leukocytes.

4.4.4 4x macrophages express Arginase-1 and up-regulate PlGF compared to 1x

The predominance of cytokines within a tissue site can control the phenotypic differentiation of the cells recruited (1.3.4.2). As shown IL-4, IL-13 and IL-10 were all up-regulated in the 4x pinnae. These high levels of IL-4 and IL-13 would be expected to lead to alternative activation of the macrophages within the 4x pinnae. The alternative/ classical axis is almost certainly an over simplification of the activation of macrophages which as recently discussed (Mosser 2008) are more likely to be able to take on a range of intermediate phenotypes which cross

these standard boundaries. Early (within hours) after infection it is likely that there are mixed populations of macrophages in the skin which are then activated to an alternative phenotype by the increasing Th2 cytokines. Indeed the macrophages in this study did not express particularly high levels of RELM α which is considered to be marker of alternative activation by IL-4/IL-13. The macrophages did express Arginase-1 and Ym1 and were phenotypically pro-angiogenic in the 4x (Figure 4.18). Of the growth factors analysed the macrophages were the primary producers of PlGF in the 4x pinnae. PlGF can promote the survival of endothelial cells and tumour associated macrophages (Adini 2002). It is intrinsically linked with pathological angiogenesis and is expressed in inflammatory conditions in the adult body (Seaman 2007). PlGF was one of the growth factors significantly up regulated only in the 4x compared to the naïve. The data here suggests that this up-regulation could be partially if not solely due to the phenotype of the invading macrophages and resulting in inflamed and vigorous angiogenesis and perhaps the dysregulated branching seen in the 4x pinnae.

Interestingly, delivery of PlGF into skin causes severe inflammation and oedema (Carmeliet 2001). It is possible that PlGF in this model is either causing or exacerbating the oedema seen in the 4x pinnae and causing persistent inflammation through expression by the recruited macrophages whilst additionally activating the PlGF receptor Flt-1 on endothelial cells.

The macrophages also up regulated expression of the VEGF receptor; Flk-1. Whilst there was no difference in the expression of VEGF between the 1x macrophages and 4x macrophages the 4x pinnae are likely to be more responsive to the VEGF being produced by other cells in the skin. Flk-1 signalling can drive MMP production in macrophages and as seen MMP-9 is up regulated in the sorted macrophages of the 4x. COX 2, which drives the production of prostaglandins from arachadonic acid, is often up-regulated in inflamed tissues and is abundant in macrophages found in tumours and inflamed tissues (Nakao 2005). The macrophages in the 4x express significantly higher levels of COX2 enzyme consistent with the pro-inflammatory pro-angiogenic phenotype

hypothesised from the PIGF levels. Together these results suggest a more inflammatory macrophage phenotype expected with the high levels of MMP-9 and PIGF likely to cause extensive remodelling. The expression of these growth factors and phenotype may be dependent on one of several cytokines expressed in the skin. Knockout studies (See chapter 4 for IL-10^{-/-}) of cytokines would allow aid in determining the cytokine or combination of cytokines responsible for the angiogenic activation of the macrophages in the 4x. Additionally 4x infection in macrophage deficient mice would allow the functional consequences of the macrophage derived PIGF to be determined.

4.4.5 The majority of the 4x DEC are HGF expressing Eosinophils

Alongside the high levels of monocyte and macrophage chemoattractants there was a noticeable increase within the 4x group of the eosinophil chemoattractants CCL11 (Eotaxin-1) and C5a. These both drive eosinophil recruitment and rolling and C5a in particular aids attachment and transmigration of the eosinophils across endothelial cells (DiScipio 1999). In the 4x group, eosinophils are the vast majority of the cells recruited to the pinnae and comprise ~45% of the DEC.

The eosinophil has long been associated with helminth infections and varying opinions exist on the purpose and requirement of eosinophils for worm expulsion. Whilst it has been shown that eosinophils are responsible for the death of the larvae of *Onchocerca lienalis* (Folkard 1996) ablation of eosinophils in other infections have little or no effect on the pathology.

Indeed ablation of eosinophils does not affect any of the traditional measures of schistosomiasis pathology associated with the eggs (including granuloma size and worm burden) (Swartz 2006). But these studies did not look at the skin response or the effect of eosinophil loss on the levels of cytokines produced.

The eosinophils have been shown to produce IL-13 (Cook 2011) and, as such, may be a vital source of this cytokine in propagating further alternatively activated responses. This cytokine production by eosinophils is heavily linked to

fibrosis and angiogenesis in asthma. Within this study eosinophils appear to be a significant source of both HGF and MMP-9. Eosinophils can directly modulate ECM production through their release of MMPs. Expression of MMP-9 has been found to aid eosinophil migration through basement membrane proteins and the ECM (Okada 1997). Production of this could be beneficial for the eosinophil infiltration into the skin but may also have the side effect of releasing ECM sequestered growth factors and initiating the MMP cascade in the dermis. This could be exacerbating the remodelling and destruction of the ECM of the 4x skin.

Eosinophils are a significant source of angiogenic growth factors; VEGF, FGF2 and PDGF, have all been identified in the granules of the cells (Munitz 2004). They have been shown to promote endothelial cell proliferation *in vitro* and induce new vessel formation in chick membrane models. (Puxeddu 2005) Analysis of the growth factor expression revealed that the eosinophils produce HGF transcript and were the major contributors of HGF amongst the DEC cells. HGF mediates invasiveness and branching of the endothelial cells (Rosen 1997) and could be produced by the eosinophils to aid their own transit through the skin of the mice after 4x infections whilst inducing the angiogenic cascade as a by-product. HGF accelerates endothelial cell invasion and induces the cells to accumulate rapidly (Grant 1993). The immature larvae of the intravascular lung worm *Angiostrongylus cantonensis* reside in the vessels of the brain and in humans cause eosinophilic meningitis and up-regulation of VEGF, MMP-9 and HGF (Tsai 2009). All of these were found in this model and in other parasitic infections, including *Strongylus vulgaris*, indicating that induction of HGF and MMPs accompanied by eosinophil influxes may be a widespread phenomenon amongst vessel interacting parasites. As eosinophils comprise the majority of the cells in the 4x DEC the HGF they produce, if bioactive, could be cause of the dysregulated fine branching seen throughout the dermis of the 4x pinnae but not in the 1x.

4.4.6 Dendritic cells from 1x pinnae are more pro-angiogenic than those obtained from 4x pinnae.

The other antigen presenting cell identified in the skin was the dendritic cell. This is the primary APC and it has been shown that MHCII is down regulated on the DCs after multiple infections (Cook 2011). As a percentage of the total DEC there was a reduction in the numbers of DCs identified, although this was not significantly different to the naïve. Activated dermal DCs will contribute to the inflammatory response in the dermis and migrate to the skin draining lymph nodes to present antigen (Steinman 2006). Like macrophages, dendritic cells are proposed to have alternative activation states (1.3.4.3). Tumour models have shown that high levels of VEGF expressed by tumours can down regulate MHCII on the surface of DCs effectively halting their maturation as effective APCs and increasing the tumour's chance not to be detected (Gabrilovich 1998). In addition HGF also down-regulates MHCII on DCs and is protective in airway inflammation models (Rutella 2006). The increased expression of either VEGF or HGF or indeed both within the 4x whole pinnae could be down regulating the macrophage phenotype and may contribute to the down regulation of MHCII on DCs described in this model (Cook 2011).

The cytokines to which the dendritic cells are exposed can dramatically alter their angiogenic potential (Riboldi 2005). In comparison to the eosinophils and macrophages, the most pro-angiogenic DCs were found within the 1x DEC. These expressed high levels of VEGF and Flk-1 which was down regulated in the DCs obtained from 4x pinnae. VEGF expression in dendritic cells is induced by pro inflammatory cytokine whilst activation of DCs by IL-10 causes limited up-regulation of VEGF and up regulation of fibroblast growth factor antagonists (Riboldi 2005). The high concentration (~1000pg/ml) of IL-10 observed in the 4x pinnae may be causing this down regulation of VEGF expression. Conventional myeloid CD11c⁺ DCs express VEGF in the skin whilst plasmacytoid DCs fail to produce VEGF (Fiallo 2002). Within the DCs of the DEC there is a mixed population of CD11c^{+/hi} and CD11c^{-/low} these could represent two distinct populations in the skin. Further phenotyping of the cells may reveal a switch in

the predominance of the DC phenotype between 1x and 4x infections. Both growth factors produced by the skin cells and the cytokine balance appear to be affecting the activation of the DCs. While this appears unlikely to dramatically affect the angiogenesis seen following infection, it could have an impact on further downstream immune responses to the parasite something not explored in this thesis.

4.4.7 Summary

This chapter has confirmed that following multiple infections the cytokine balance in the skin switches to a predominantly Th2 phenotype with the up regulation of IL-4, IL-13 and IL-10. It is concluded that the differences in blood vessel growth after 4x infections as shown in chapter 2, are likely due to the Th2-type cytokine environment affecting the composition and phenotype of cells recruited to the infection site, and not a change in the initial intrinsic wound healing mechanisms. Pinnae from 4x mice showed a significant increase in eosinophils which had a pro angiogenic phenotype compared to pinnae from 1x mice. These p4x eosinophils produced higher levels of pro angiogenic growth factors and the remodelling protease MMP-9. Macrophages and dendritic cells also displayed different phenotypes between the 1x and 4 x infections. All three cell types produced the growth factors which differed between the 1x and 4x pinnae and as such could contribute to the differences in growth factors seen after each infection. In the next chapter, the role of IL-10 in determining phenotypic changes to these cells will be examined. There is mounting evidence that as well as influencing the levels of IL-4 and IL-13, IL-10 may directly induce a 'regulatory' macrophage phenotype (Mosser 2008)

**Chapter 5: Examining the influence of IL-10 in 4x
pinnae**

5.1 Introduction

The previous chapter characterised the immune cell influx into the pinnae following infection, and the growth factors expressed by these cells. It is apparent that following multiple infections the phenotype of the cells which influx into the skin changes. Particularly the eosinophils, macrophages and dendritic cells all showed a change in their growth factor expression (4.3.10). Phenotypic changes in leukocytes depend on the cytokines to which they are exposed. The now well documented alternative and classical axis of macrophages is a prime example of the relatively large change in function the exposure to cytokines has on cells (1.3.4.2).

Between the 1x and 4x infections it is the Th2 associated cytokines IL-13, IL-4 and IL-10 which change the most dramatically. IL-4 and IL-13 have close associations with alternative activation, particularly of macrophages (Gordon 2003). Whilst the function of IL-10 in repressing Th1 and promoting Th2 cytokine release is well known, it can also directly activate leukocytes (Dace 2008). There is mounting evidence of a 'regulatory' phenotype of macrophage induced by exposure to IL-10 (Mosser 2008). This phenotype does not produce ECM components but does express TGF β which has a functional role in angiogenesis and wound healing (Edwards 2006). IL-10 stimulated macrophages have been implicated in cancer progression and express several pro-angiogenic growth factors (Lin 2006). As such, within the 4x infection it is possible that the high levels of IL-10 induce the pro-angiogenic phenotype in both the macrophages. IL-10 may also influence the other major cell types in the DEC. Indeed IL-10 can conversely in dendritic cells suppressing expression of VEGF (Riboldi 2005).

IL-10 also has direct associations with wound healing and angiogenesis (Werner 2003). It is expressed early after wounding (within 60 minutes), and again several days later by keratinocytes and invading monocytes (Ohshima 1998). However excess levels of IL-10 can impair wound healing and cause chronic ulcers (Lundberg 1998). The balance of IL-10 following wounding is therefore important in regulating the response and resolution of wounds. The high levels of IL-10

within the 4x pinnae may be responsible for the excessive vessel branching and poor state of the skin following infection. As such this chapter will explore the role of IL-10 in the 4x infection, in relation to both growth factor expression by leukocytes and angiogenesis in the dermis.

To do this mice genetically deficient for Interleukin 10 (IL-10^{-/-}) will be infected either 1x or 4x. The resulting pinnae will be analysed for the same markers of angiogenesis identified in Chapter 2. Additionally the DEC in both 1x and 4x will be examined for activation status and growth factor expression.

5.2 Materials and Methods

5.2.1 IL-10 knock out mice

IL-10^{-/-} mice were kindly obtained from Dr M. Kullberg. These mice are backcrossed for 10 generations onto a C57BL/10 background and originally bred by W.Müller (Kühn 1993). Mice weighing approximately 20 grams and aged 7-9 weeks were infected as previously described (2.1.1). Wild type (WT) C57BL/6 controls were infected alongside the IL-10^{-/-} mice. Due to limited numbers of mice only days 2 and 4 post infection were analysed.

5.2.2 DEC retrieval and flow cytometry

DEC were retrieved from whole pinnae using the in vitro cultured pinnae biopsy method (2.1.7). DEC retrieval and staining was carried out as detailed in 4.2.1 and 4.2.2. In addition to the antibodies listed in table 4.1 the cells were labelled with α CD206/Mannose receptor (Alexa flour 647 conjugated # eBioRMUL.2)

5.2.3 Cell sorting

Pinnae were taken from 15 4x WT and 15 4x IL-10^{-/-} mice at day 2 post infection. The DEC were extracted and stained for cell sorting as detailed in Chapter 4 (4.2.1 & 4.2.3). Samples were analysed for cell surface expression of markers and by SQ-PCR for pro angiogenic growth factors.

5.3 Results

5.3.1 IL-10^{-/-} pinnae become inflamed and vessels more visible after infection

Analysis in this section focuses only on IL-10^{-/-} pinnae, the WT equivalents can be found in section 2.3.1. Naïve IL-10^{-/-} mice had clearly visible thin vessels throughout their pinnae (Figure 5.1). The large central vessels were visible with one or two branch points. In 1x mice two days post infection the large central vessels appeared slightly dilated. These vessels were more obvious than in the naïve with two or three branch points visible (Figure 5.1). This was accentuated at day 4 and some of the vessels appeared convoluted. Vessels were also clearly visible on the inner surface of the pinna, whilst these were faint in naïve pinnae.

In the 4x infected mice the vessels were considerably dilated and bright red (Figure 5.1). The surrounding tissue was red and scarred in several places. There were more branch points visible compared to the 1x. As with the WT mice (Figure 3.2) the 4x IL-10^{-/-} vessels were visible at the terminal edge of the pinnae. At day 4 the pinnae were still inflamed and the vessels red and visible. Several fine 'wispy' vessels were visible and the vessels of the outer surface of the pinnae were pronounced. There were several scars and scabbed regions which were surrounded by fine networks of vessels.

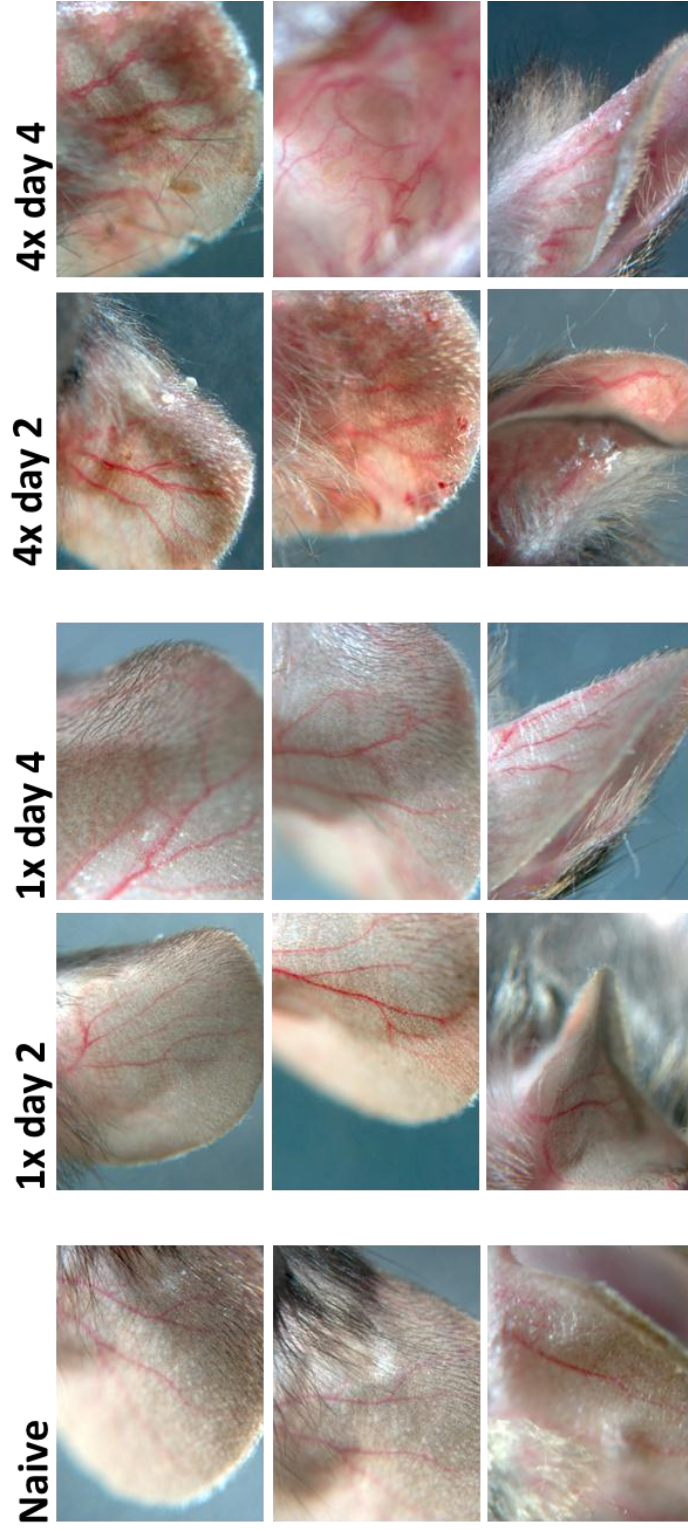


Figure 5.1 Images of IL-10KO pinnae after infection.

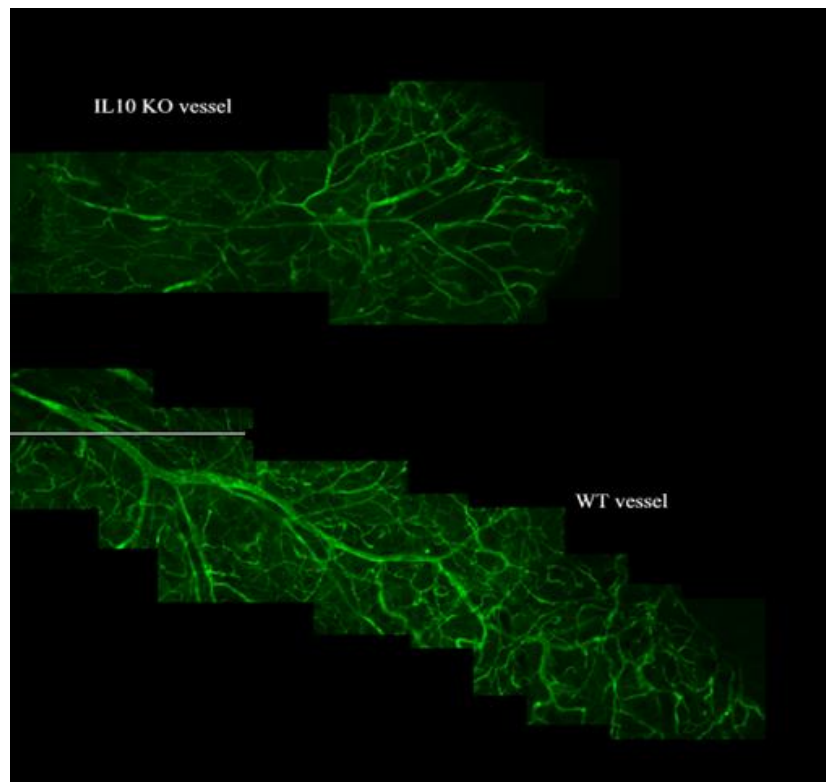
Images were taken of 1x and 4x and naïve IL-10^{-/-} pinnae. Images are a representative collection from 5 mice for each group.

5.3.2 The increases vasculature in 4x IL-10^{-/-} is more organised than in 4x WT

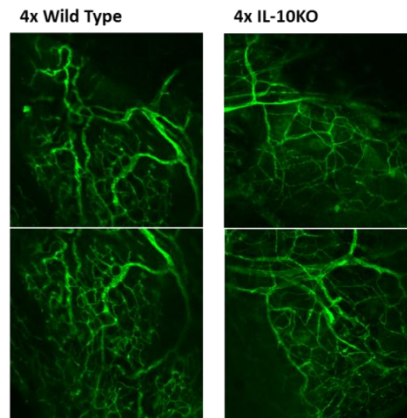
In WT mice the most obvious change to the naïve vasculature of the dermis was seen in the 4x mice (3.3.3). To determine whether the loss of IL-10 would affect the number and structure of the vessels, naïve and 4x IL-10^{-/-} pinnae were labelled with α CD31. The larger vessels of the pinnae were reasonably similar between WT and IL-10^{-/-}, although the trunk vessels of IL-10^{-/-} pinnae did not appear to be as wide as the WT (Figure 5.2A). Many of the vessels in 4x WT pinnae were distorted in shape, whereas in the 4x IL-10^{-/-} these branches were predominantly straight and even (Figure 5.2 A). In the IL-10^{-/-} there were bundles of small vessels, as seen in 4x WT (Figure 5.4), however these were not as numerous as in the WT (Figure 5.2 B).

An entire vessel was imaged from the base of the pinna to the fine branches at the edge for both 4x IL-10^{-/-} and 4x WT. In these images the irregular branching of the 4x WT was clear, with the smaller vessels highly distorted and tangled, whilst the 4x IL-10^{-/-} branches remained mostly regular. (Figure 5.2A). The vessel area in the 4x WT and 4x IL-10^{-/-} pinnae was quantified (Figure 5.2C). There was no significant difference in the total vessel area in the 4x IL-10^{-/-} pinnae compared to the 4xWT, however there was a significant increase in the vessel area in the 4x IL-10^{-/-} compared to the naïve IL-10^{-/-} pinnae.

A



B



C

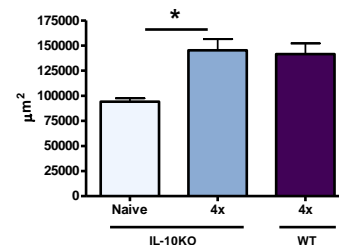


Figure 5.2 α CD31 labelled 4x IL-10^{-/-} and 4x WT pinnae

A: Composite images of whole vessels in both IL-10^{-/-} (top image) and WT (Bottom image) 4x pinnae 2 days after infection labelled with α CD31. **B:** Images from the edge (top panel) and mid (bottom panel) of 4x day 2 WT and IL-10^{-/-} pinnae. **C:** Analysis of the average area of α CD31 labelled vessels in each 920 μm x920 μm image. Each group is 35 images taken over 3 pinnae. Mean + SEM, there is no significant difference between the WT and IL-10^{-/-} 4x pinnae whilst both infected pinnae are significantly increased compared to the naïve ($p < 0.05$).

5.3.3 Pinnae from IL-10^{-/-} mice exhibit extensive cell influx and distortion after 4x infections

In this and the following four sections (5.3.4-5.3.7), analyses were performed on IL-10^{-/-} mice only, to focus on the responses in 1x compared to 4x infected mice sampled at day 2 and day 4 after infection. Results were viewed in light of data acquired for WT mice in chapter 4.

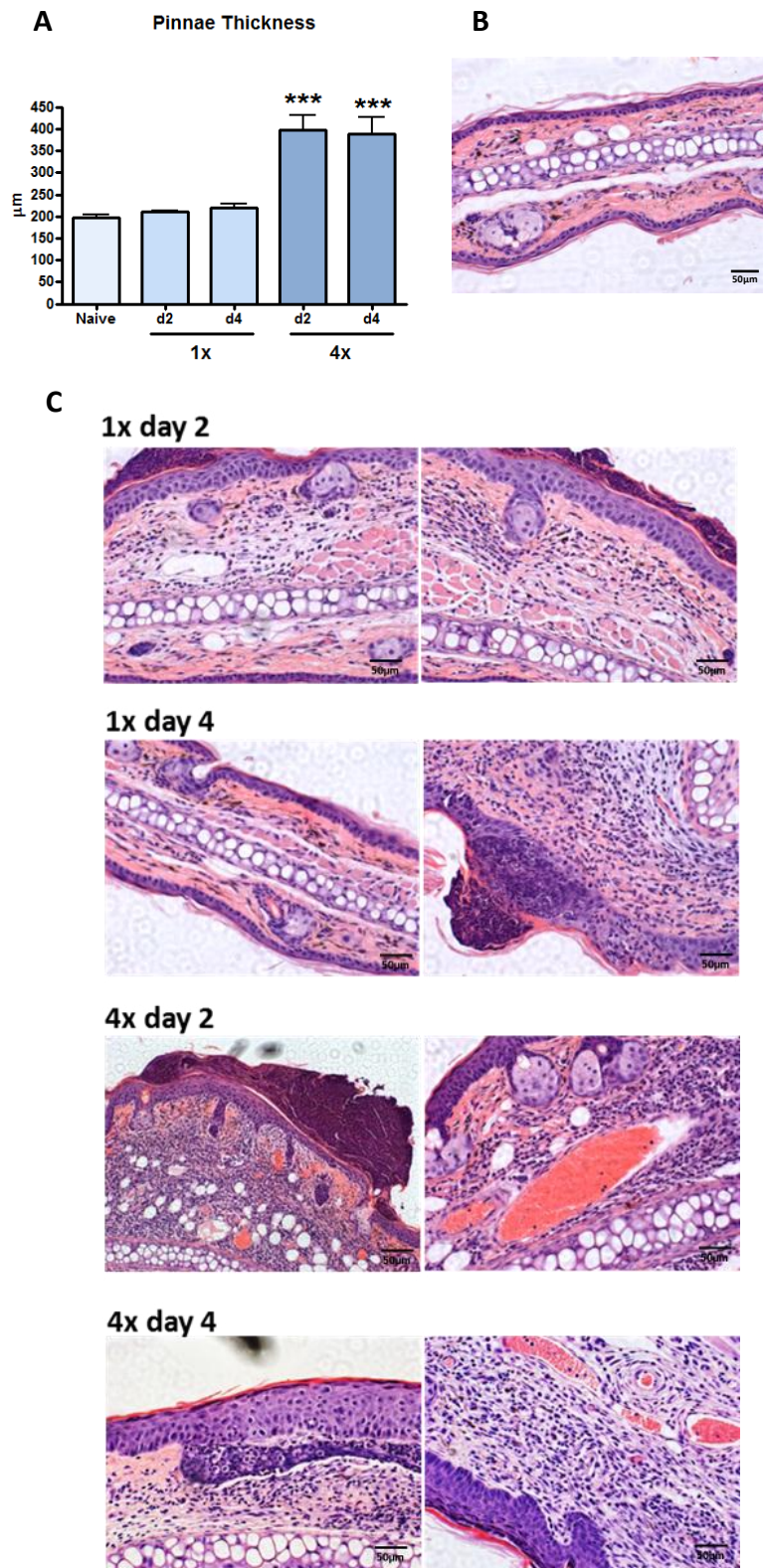
There was no significant increase in the thickness of the IL-10^{-/-} pinnae at the 1x time points compared to the naïve, however the thickness increased significantly after 4x infections, at both day 2 and day 4 post infection, compared to both naïve and 1x time points ($p < 0.001$). This was consistent with the observations made in the WT pinnae (Figure 3.3).

H&E stained sections showed that naïve IL-10^{-/-} pinnae are morphologically identical to WT naïve pinnae (Figure 3.3 B). With a thin epidermis and blood vessels spread evenly through an intact dermis. This confirmed that loss of IL-10 had no effect on the skin morphology before infection.

Within 1x pinnae there was an increase in the thickness of the dermis, particularly under regions where the epidermis was damaged (Figure 5.3C). There was a small increase in the thickness of the epidermis but only in patches along the pinnae. At day 2 after 1x infection there were clear cell infiltrates within the pinnae, these were spread throughout the dermis. There was also considerable scabbing on the outer edge of the epidermis. At day 4 these granulated areas were severe however the epidermis was already fully formed below the scabs visible.

Within the 4x pinnae, at day 2, there was an excessive influx of cells, which were densely packed under the epidermis and caused distortion of the dermis (Figure 5.3 C lower two panels). The epidermis had thickened across the entirety of the pinnae observed. Many of the blood vessels were visible and enlarged, with some signs of haemorrhaging in badly damaged areas of the tissue. At day 4 the epidermis appeared mostly repaired, although the cell influx had not reduced

and the dermis was still swollen and distorted. There were dense layers of granular cells packed under the epidermis lying along the basement membrane and within the scabs of the 4x pinnae.



5.3.4 Pro-angiogenic growth factors were up-regulated after infection in IL-10^{-/-} pinnae

The VEGF₁₂₀ and VEGF₁₆₄ isoforms of VEGFA were expressed in both the 1x and 4x groups although VEGF₁₈₈ was not detected (Figure 5.4 A&B). Infection induced a significant increase in both isoforms at day 4 post 1x and 4x infections compared to the naïve (1x d4 $p < 0.05$ and 4x d4 $p < 0.01$ for both VEGF₁₂₀ and VEGF₁₆₄). There was no significant difference in VEGF expression between the 1x and 4x groups and both showed an increase in VEGF between days 2 and 4.

In comparison to VEGF, HGF did show a difference between 1x and 4x at day 2. 4x IL-10^{-/-} pinnae 2 days post infection expressed significantly higher levels of HGF transcript compared to the equivalent 1x pinnae ($p < 0.05$) (Figure 5.4 C). All time points except day 2 of the 1x infection were significantly increased compared to the naïve ($p < 0.01$). FIGF was significantly up regulated only at day 4 post infection in both the 1x and 4x compared to naïve ($p < 0.01$) (Figure 5.4 D). There was no significant difference between the two infection groups at either day 2 or day 4 post infection.

MMP-9 showed a steady increase in expression between day 2 and day 4 in the 1x pinnae, and at day 2 this increase was significant compared to the naïve ($p < 0.001$) (Figure 5.4 E). The levels of MMP-9 transcript were further increased in the 4x. At day 2 and day 4 post infection expression of MMP-9 was significantly increased compared to the naïve (day 2 $p < 0.05$, day 4 $p < 0.001$). In addition the expression of MMP-9 in 4x pinnae 4 days post infection was significantly higher than in the same 1x time point ($p < 0.05$).

PIGF was significantly up-regulated compared to the naïve in all four of the infection time points (1x day 2 $p < 0.05$ 1x day 4, 4x day 2 and 4x day 4 $p < 0.001$) (Figure 5.4 F). Between the time points in each infection group there was little change in the expression of PIGF. However comparing each 1x and 4x time point there was significant up regulation of PIGF in the 4x at day 2 ($p < 0.05$).

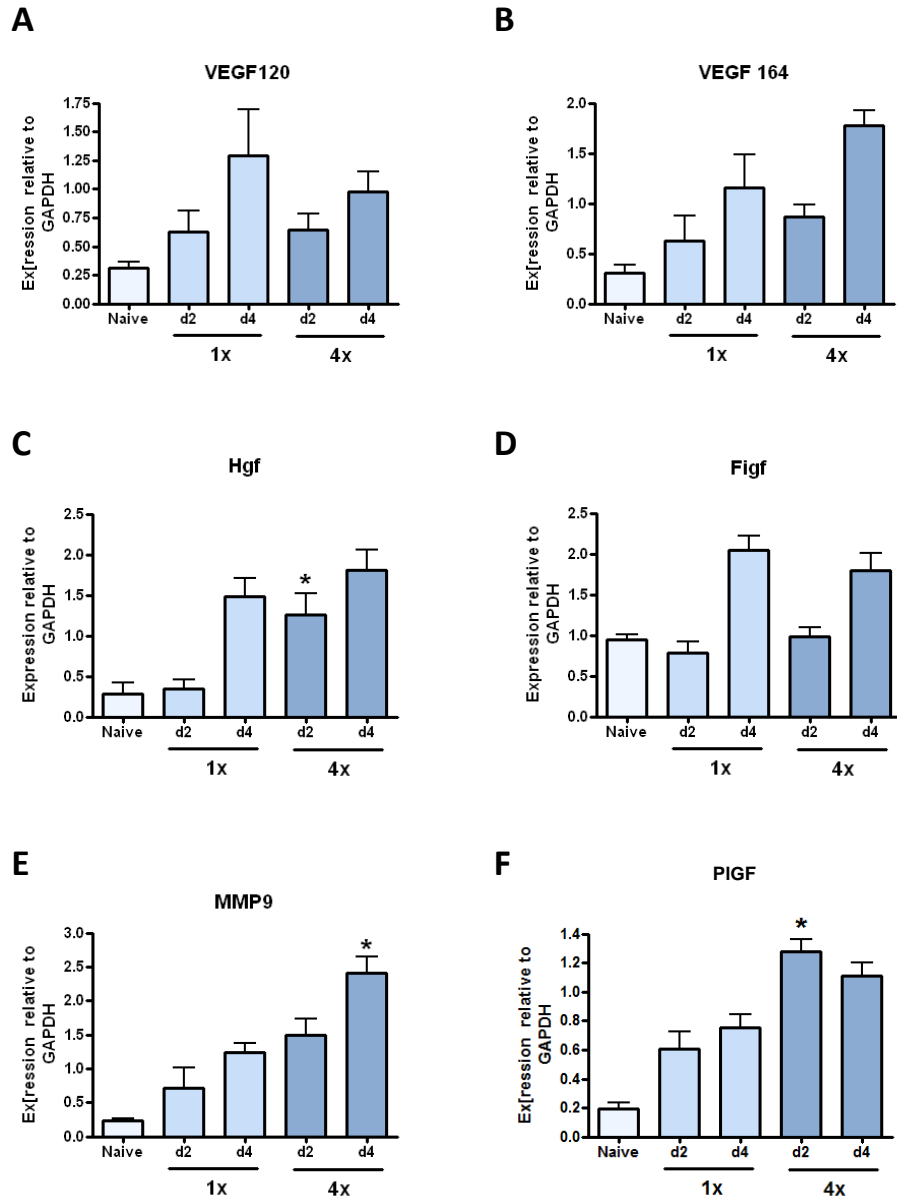


Figure 5.4 Pro-angiogenic growth factor expression in IL-10^{-/-} pinnae

cDNA from naïve, 1x day2 and 4 and 4x day 2 and 4 whole pinnae was analysed for each of the six growth factors below. The sample size for each group is 4 pinnae. Shown is the mean + SEM statistics are the 1x versus the 4x for each time point, *p<0.05. A: VEGF₁₂₀. B: VEGF₁₆₄. C: HGF. D: FIGF. E: MMP-9. F: PIGF.

5.3.5 Infection induces a significant influx of cells into the dermis

In both the 1x and 4x infections there are significantly more DEC when compared to the naïve (1x d2 and 4x d4 $p < 0.01$, 1xd4 and 4xd2 $p < 0.001$). There was no significant difference between the timepoints in either the 1x or 4x groups. This differs from the WT which showed a decrease of almost half between the day 2 and day 4 timepoints of the the 4x infection (4.3.3). There were however significantly more cells in the 4x groups at both timepoints compared to the 1x equivalent, consistent with wild type observations

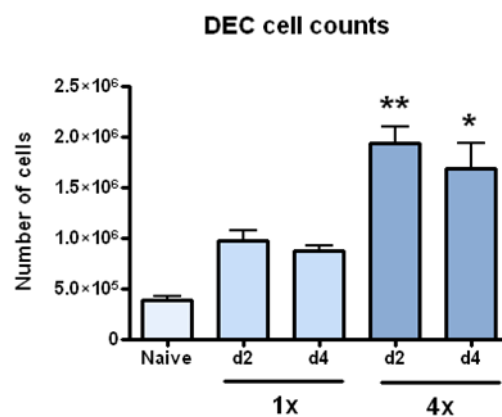


Figure 5.5 DEC cell counts from IL-10^{-/-} whole pinnae

DEC cell numbers were calculated per pinnae from 5 pinnae per group. Stats shown are the 1x and 4x time points compared. Mean +SEM * $p < 0.05$ and ** $p < 0.01$

5.3.6 4x IL-10^{-/-} DEC contains significantly more eosinophils than 1x

With limited mice available DEC analysis was restricted to the main cell types identified in the WT mice; eosinophils, macrophages/monocytes and dendritic cells. Similar to the WT (4.3.4) 80-90% of the DEC from the IL-10KO pinnae were CD45⁺ (Figure 5.6 A). There was no significant difference in the percentage of CD45⁺ cells between any of the groups.

Of these CD45⁺ cells the majority appeared to be macrophages and eosinophils. The percentage of macrophages in the DEC peaked at ~20% day2 after a single infection and was a similar percentage at day 4 (Figure 5.6C). This was a significant increase compared to the naïve at both day 2 and day 4 ($p < 0.001$). The percentage of macrophages in the 4x was also significantly increased compared to the naïve but only at day 2 ($p < 0.01$). By day 4 the percentage of macrophages had decreased.

The eosinophils were the majority of the DEC in the WT pinnae and similarly in the IL-10^{-/-} pinnae, ~30% of the DEC were eosinophils at day 4 after 4x infection (Figure 5.6D). There were significantly more eosinophils in the 4x compared to the naïve (day 4 $p < 0.001$, day 2 $p < 0.01$) and 1x (shown on graph Figure 5.6D). There were considerably fewer eosinophils in the 1x pinnae at days 2 and 4, although day 2 had a significantly higher percentage of eosinophils than the naïve ($p < 0.001$).

The dendritic cells, which made up a much smaller percentage of the wild type DEC, were again only a small proportion of the IL-10^{-/-} DEC. Only 1x DEC at day 4 showed a significant increase in the percentage of dendritic cells compared to the naïve ($p < 0.01$).

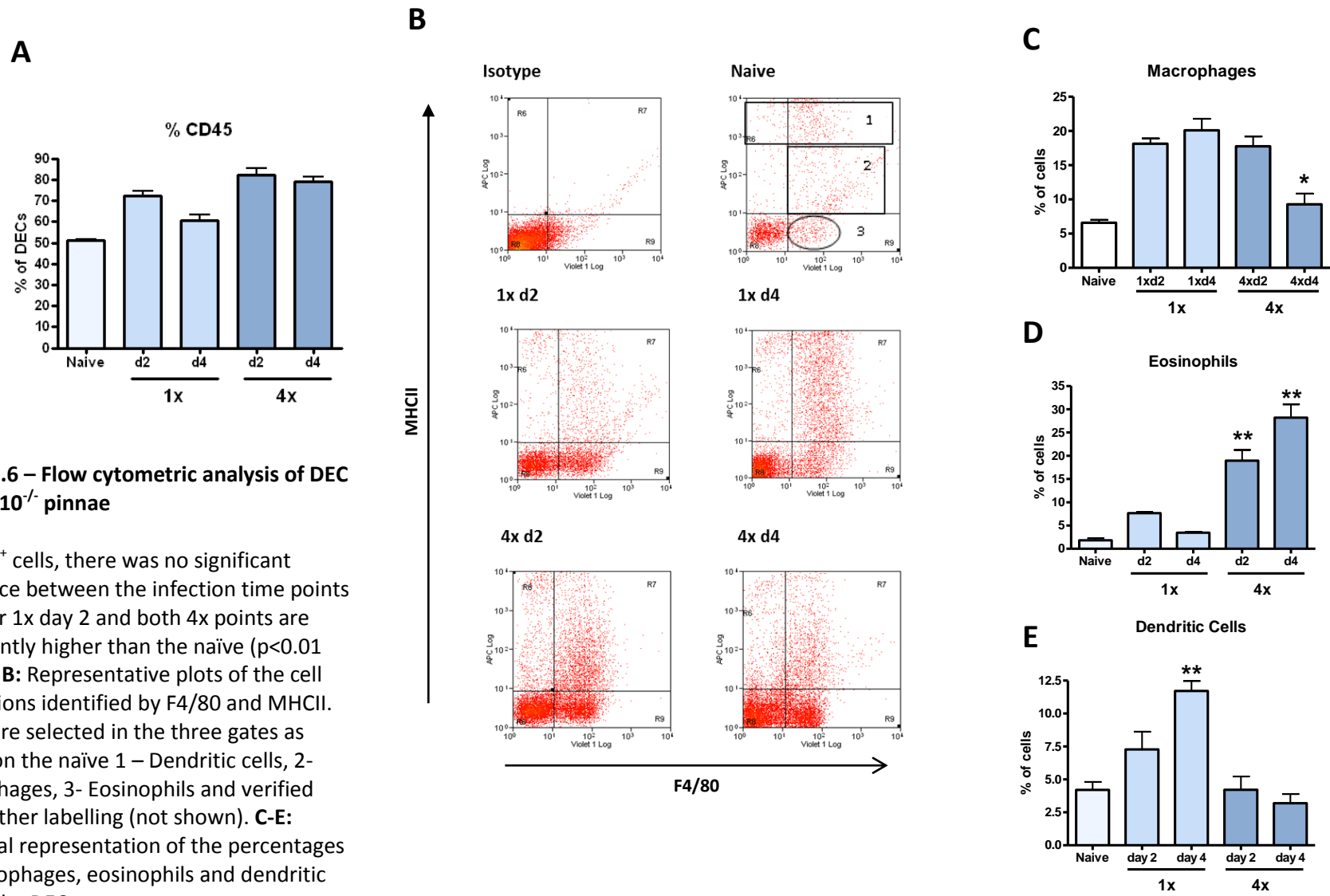


Figure 5.6 – Flow cytometric analysis of DEC from IL-10^{-/-} pinnae

A: CD45⁺ cells, there was no significant difference between the infection time points however 1x day 2 and both 4x points are significantly higher than the naïve ($p < 0.01$ for all). **B:** Representative plots of the cell populations identified by F4/80 and MHCII. Cells were selected in the three gates as shown on the naïve 1 – Dendritic cells, 2- Macrophages, 3- Eosinophils and verified with further labelling (not shown). **C-E:** Graphical representation of the percentages of macrophages, eosinophils and dendritic cells in the DEC.

5.3.8 Th2 cytokines are reduced in IL-10^{-/-} supernatants

Cytokine levels in the whole pinnae overnight culture supernatants were determined by ELISA, to ascertain the Th1/Th2 balance in the skin of IL-10^{-/-} mice (5.2.12). In contrast to the WT data in chapter four (4.3.2) several of the cytokines analysed here were undetectable in either one or more groups (Figure 4.7).

IL-4 expression was restricted to only the 4x samples and was below the level of detection in both the naïve and 1x pinnae (Figure 5.7 A). This expression was similar to the WT (4.3.2 Figure 4.2E), however some IL-4 was detected in the 1x infected WT mice whereas 1x IL-10^{-/-} supernatants contained no detectable IL-4. The concentration of IL-4 in the 4x was high at day 2 and decreased by ~50% by day 4

Whilst IL-4 expression was similar to the WT, IL-13 was undetectable in all but one of the IL-10^{-/-} groups (Figure 5.7 B). A small amount of IL-13 was detectable in the 4x pinnae at day 4, although this is only just above the minimum level of detection. In contrast IFN γ , which was undetectable in the WT mice, was expressed above the minimum level of detection in 4 of the 5 IL-10^{-/-} groups (Figure 5.7C). IFN γ was detected at day 4 in the 1x infection, whilst day 2 was below the level of detection. In the 4x however IFN γ was detectable at both day 2 and day 4 post infection and was significantly increased at day 2 compared to the 1x. Both time points were significantly increased compared to the naïve ($p < 0.05$).

IL-12 was detected in the 1x and absent in the 4x supernatants (Figure 5.7D). The 1x infected showed little difference compared to the naïve at day 2. However at day 4 the concentration was increased, although this was not quite significant compared to the naïve ($p = 0.061$). In comparison TNF α was detected in all infected groups and was expressed at significantly higher levels than the naïve (1x d2 and 4x d2 $p < 0.001$, 1x d4 $p < 0.05$ and 4x d2 $p < 0.01$) (Figure 5.7E). Between the time points in the 1x and 4x groups TNF α dropped slightly. There was significantly more TNF α in the 4x at day 2 compared to the 1x ($p < 0.01$).

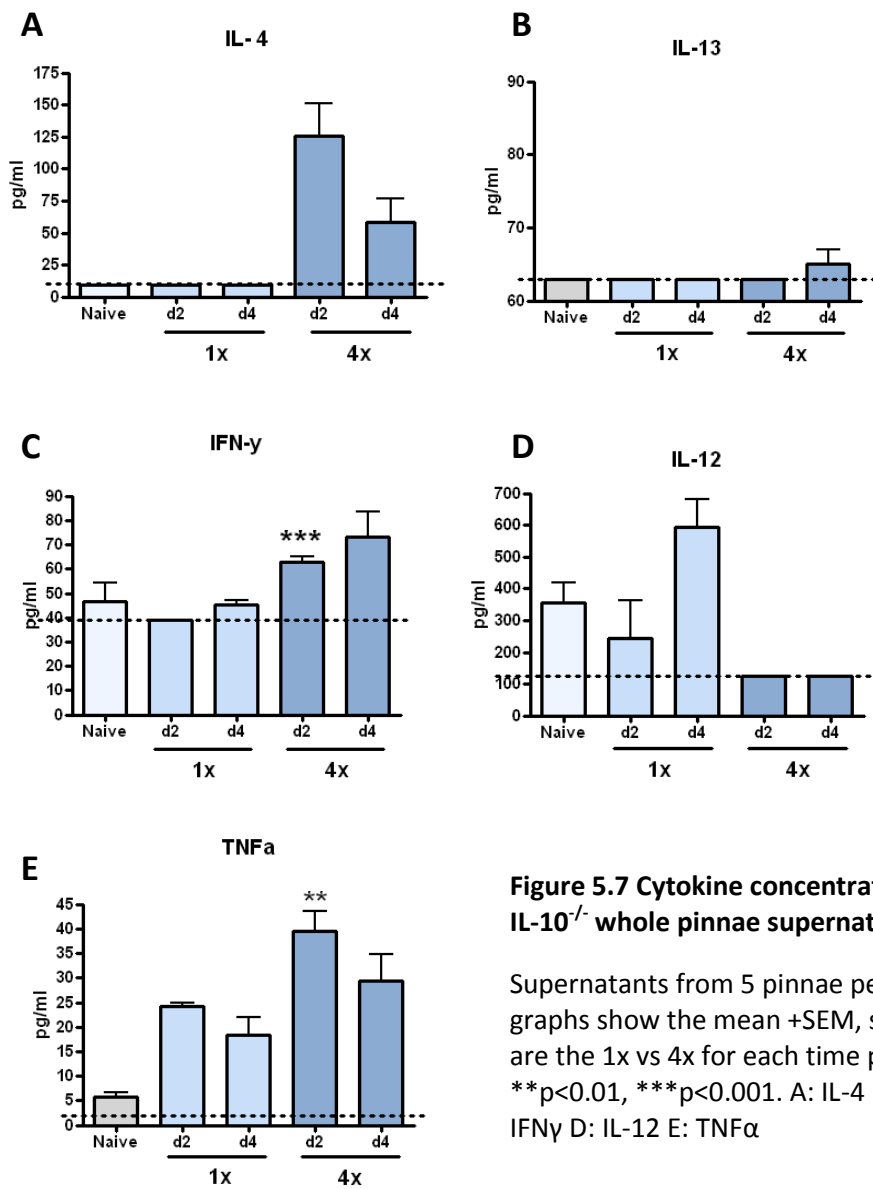


Figure 5.7 Cytokine concentrations in IL-10^{-/-} whole pinnae supernatants

Supernatants from 5 pinnae per group graphs show the mean +SEM, statistics are the 1x vs 4x for each time point.

p<0.01, *p<0.001. A: IL-4 B: IL-13 C: IFN γ D: IL-12 E: TNF α

5.3.8 4x IL-10^{-/-} pinnae contain increased levels of HGF and VEGF compared to WT

The WT 4x pinnae contained the most IL-10 and it is therefore within this group that IL-10 is likely to have the greatest effect. To more accurately determine the effect loss of IL-10 has in the pinnae, WT and IL-10^{-/-} pinnae were directly compared after 4x infection. Sections 5.3.8 - 5.3.12 contain results comparing growth factors and immune cell phenotype between 4x WT and 4x IL-10^{-/-} mice.

Expression levels of VEGF₁₂₀ and VEGF₁₆₄ were significantly increased in the IL-10^{-/-} compared to the WT at both day 2 and day 4 after infection (p<0.05) (Figure 5.8 A&B). The expression of both VEGF isoforms did not change significantly between the time points in either the IL-10^{-/-} or WT pinnae. In contrast levels of PlGF did differ between days 2 and 4 (Figure 5.8C). PlGF expression decreased significantly (p<0.05) at day 4 compared to day 2 in both the WT and IL-10^{-/-}. This trend is consistent with the data previously analysed of both the WT and IL-10^{-/-} time courses (3.3.12 & 5.3.4). There was no significant difference in expression of PlGF between the WT and IL-10^{-/-}.

HGF did differ between the IL-10^{-/-} and WT groups, but did not change over the time course (Figure 5.8D). Expression of HGF was significantly increased at both day 2 and 4 post infection in the IL-10^{-/-} pinnae compared to the WT (p<0.05). Comparison of the time points within the infection showed no change in HGF between day 2 and 4.

HGF and VEGF were also analysed by ELISA to determine protein levels of the genes (Figure 5.8 E&F). VEGF protein levels were significantly higher in the WT pinnae compared to the IL-10^{-/-} (Figure 5.8E). VEGF levels remained consistent between days 2 and 4 in both infection groups. This is in contrast to the transcript analysis which showed higher levels of both VEGF isoforms in the IL-10^{-/-}, although the difference between WT and IL-10^{-/-} in VEGF₁₂₀, the primary isoform the ELISA detects, was not as great as for VEGF₁₆₄.

As identified in the transcript, HGF was significantly up regulated in the IL-10^{-/-} group compared to the WT. Protein levels peaked at day 2 in both the WT and

the IL-10^{-/-} pinnae (Figure 5.8 F). There was significantly more HGF protein at IL-10^{-/-} day 2 than WT day 2, however there was no difference between the WT and IL-10^{-/-} at day 4.

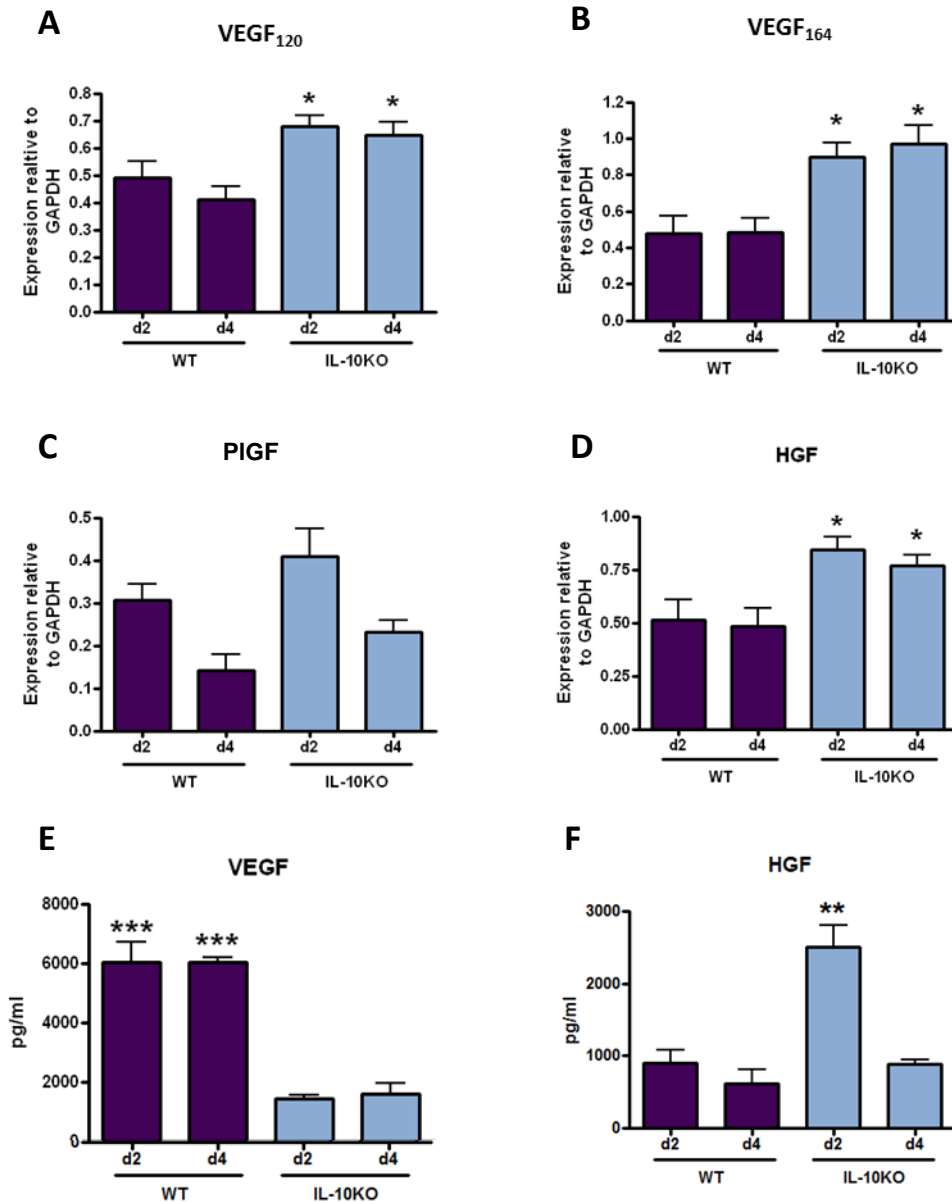


Figure 5.8 Comparison of growth factor expression between 4x WT and 4x IL-10^{-/-}

A-D Transcript analysis of four genes VEGF₁₂₀, VEGF₁₆₄, PIGF and HGF . E-F Protein analysis of HGF and VEGF. Sample size is 5 pinnae per group statistics shown are 1x vs 4x for each time point. Graphs are mean +SEM for both transcript and protein analysis *p<0.05, **p<0.01 and ***p<0.001.

5.3.10 IFN γ is up regulated in IL-10 $^{-/-}$ pinnae

Interleukins 4 and 13 and IFN γ varied the most between WT and IL-10 $^{-/-}$ pinnae therefore these three were chosen for direct comparison analysis.

The concentration of IL-4 in the IL-10 $^{-/-}$ and WT supernatants was almost identical at both days 2 and 4 (Figure 5.9 A). Both groups showed a peak of expression at day 2, which was reduced to approximately a fifth of the expression by day 4. Whilst the average concentration of IL-4 in the IL-10 $^{-/-}$ was slightly higher than the WT at day 4 this was not significant, neither was the concentration at day 2. In contrast IFN γ , which was previously shown to be undetectable in the WT (4.3.2) was significantly increased in the IL-10 $^{-/-}$ (Figure 5.9B). In the IL-10 $^{-/-}$ at both day 2 and day 4 the expression of IFN γ was significantly higher than in the WT.

The reverse was observed for IL-13, which was the predominant Th2 cytokine in the 4x wild type (Figure 5.2F). In the 4x IL-10 $^{-/-}$ IL-13 is undetectable at day 4 and barely detectable at day 2. The average levels are only just above the minimum level of detection (Average = 65pg/ml minimum level of detection = 60pg/ml).

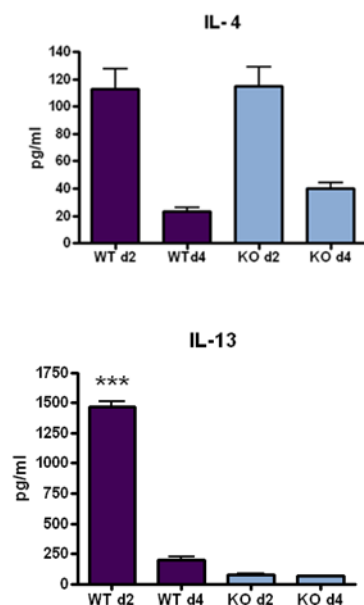


Figure 5.9 Comparison of IL-4, IL-13 and IFN γ concentrations between WT and IL-10 $^{-/-}$

A: IL-4, B: IFN γ , C: IL-13 Cytokine concentration determined by ELISA. Sample size is 5 pinnae per group shown is the mean +SEM. Statistics are 1x vs 4x for each time point *p<0.05 and ***p<0.001.

4.3.11 Macrophages and Eosinophils from IL-10^{-/-} DEC show reduced expression of Ym1 and RELM α respectively

In Chapter 3 the DEC was sorted to produce pure populations of macrophages, eosinophils and dendritic cells (4.3.9). Here DEC from 4x WT and 4x IL-10^{-/-} pinnae was sorted into the three cell populations. Due to limited numbers of mice only day 2 DEC was sorted, as after this time point the numbers of WT DEC decline (4.3.3). The sorted WT and KO cells were analysed by Q-PCR for expression of the three alternately activated macrophage associated markers; Ym1, RELM α , Arginase and classical marker iNOS (Figure 5.10)

In the IL-10^{-/-} macrophages there was a reduction in arginase expression compared to the WT by ~25% (Figure 5.10A). Expression remained the same in dendritic cells, however IL-10^{-/-} eosinophils showed a small increase in arginase expression compared to the WT. iNOS was reduced in the IL-10^{-/-} macrophages compared to WT whilst in contrast expression was up-regulated in IL-10^{-/-} dendritic cells (Figure 5.10B).

Ym1 is induced in WT macrophages whilst in the IL-10^{-/-} samples the level of Ym1 was severely decreased and expression was barely detectable (Figure 5.10C). Ym1 was also reduced in the IL-10^{-/-} eosinophils. RELM α , which is expressed by the eosinophils in the WT samples and at low levels by macrophages, was almost absent in IL-10^{-/-} eosinophils (Figure 5.10D). RELM α expression in IL-10^{-/-} macrophages was barely detectable.

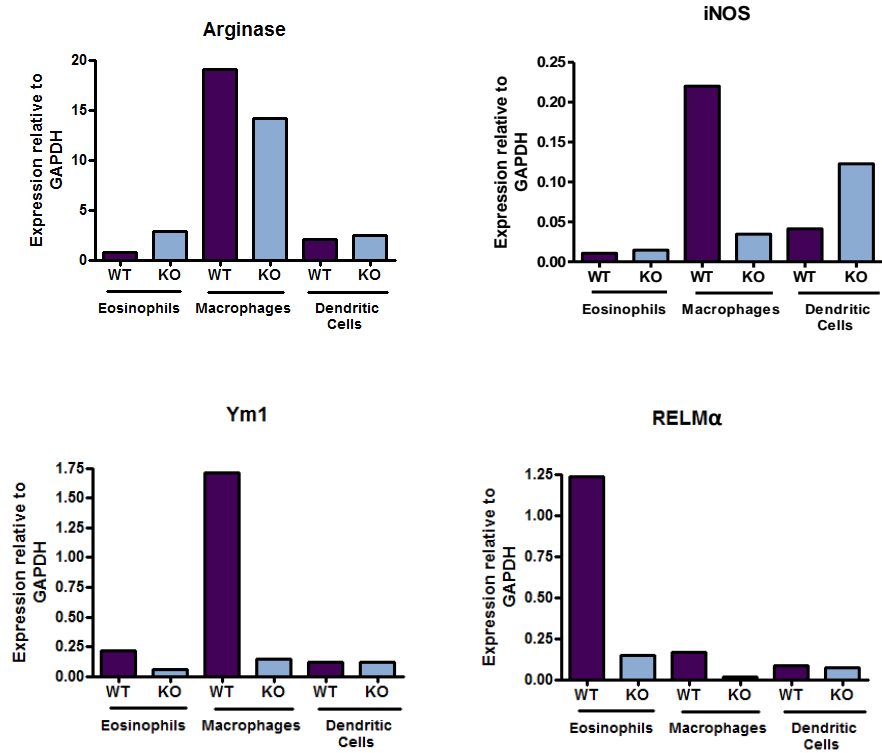


Figure 5.10 Alternatively activated macrophage markers in sorted IL-10^{-/-} DEC

Total DEC from 15 mice was pooled to produce enough cells to sort. A: Arginase-1, B: iNOS, C: Ym1 and D: RELMα

5.3.12 Macrophages and dendritic cells in IL-10^{-/-} DEC expressed more PlGF than WT.

To determine whether IL-10 signalling causes growth factor production by DEC, transcripts of the sorted cells were analysed for pro-angiogenic growth factors. VEGF₁₂₀ and VEGF₁₆₄ were detected in all three cell types, in both the WT and IL-10^{-/-} groups (Figure 5.11A&B). Expression of either VEGF isoform did not differ greatly between the WT and IL-10^{-/-} eosinophils. However VEGF expression by both macrophages and dendritic cells was up regulated in the IL-10^{-/-} compared to the WT. Within the IL-10^{-/-} samples the macrophages expressed the highest levels of both VEGF₁₂₀ and VEGF₁₆₄.

Two MMPs were also analysed; MMP-9 and 19 (Figure 5.11 C&D). MMP-9 expression was increased slightly in IL-10^{-/-} eosinophils and macrophages, compared to their WT counterparts, whilst levels did not change in the dendritic cells. Macrophages produced much higher levels of MMP-9 transcript than either the eosinophils or dendritic cells in both WT and IL-10^{-/-}. MMP-19 expression was similar, however unlike MMP-9 there was an increase in MMP-19 in the IL-10^{-/-} dendritic cells compared to the WT. In addition MMP-19 was slightly down regulated in the IL-10^{-/-} eosinophils compared to WT.

HGF expression, in contrast, was increased in IL-10^{-/-} eosinophils compared to WT. In IL-10^{-/-} macrophages and dendritic cells HGF expression was down regulated slightly (Figure 5.11E). PlGF, which was previously detected only in WT macrophages, was detected in the IL-10^{-/-} macrophages but also in IL-10^{-/-} dendritic cells (Figure 5.11 F). Expression of PlGF increased substantially in the IL-10^{-/-} macrophages compared to the WT.

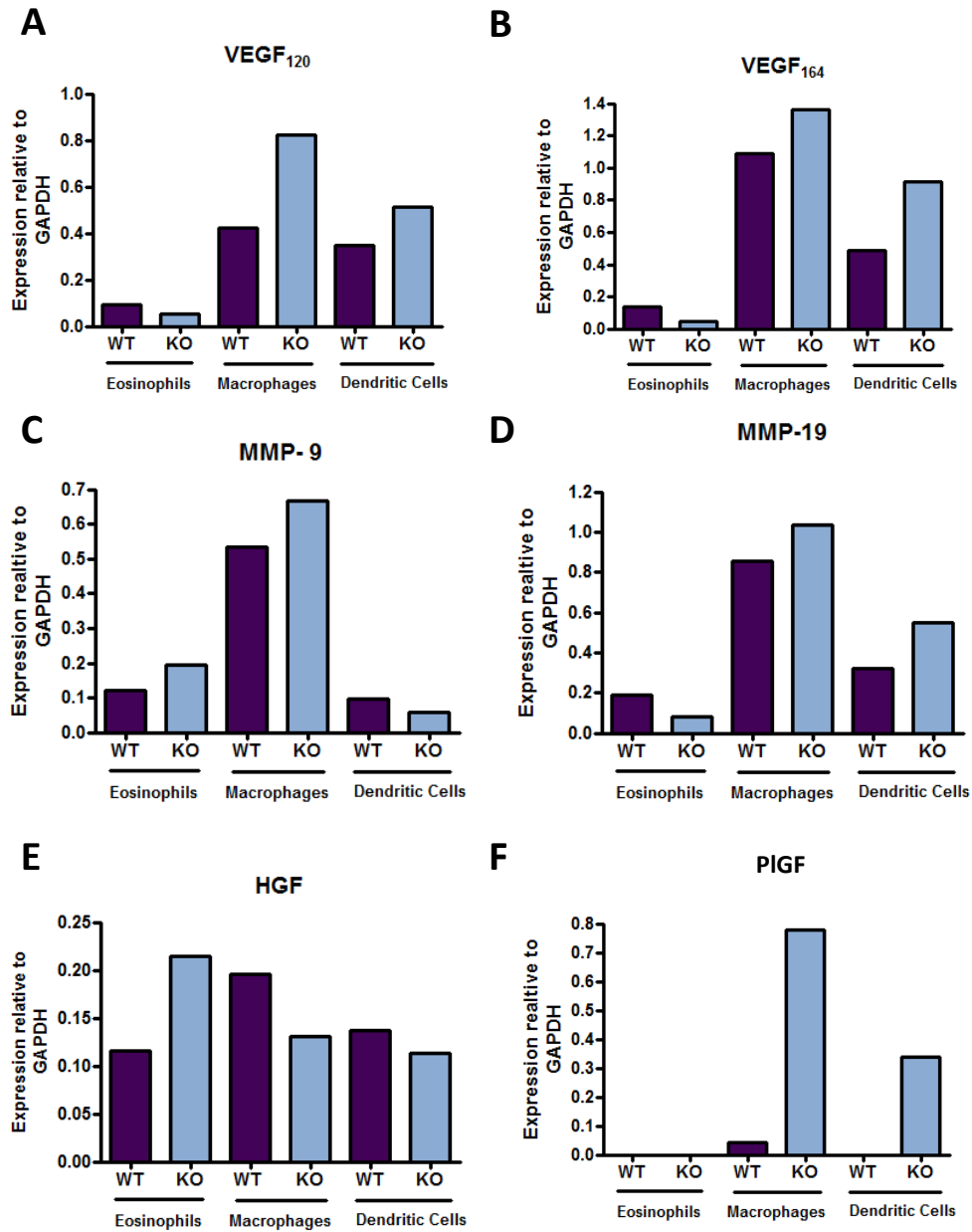


Figure 5.11 Pro-angiogenic growth factor and MMP expression by sorted KO and WT DEC

A: VEGF₁₂₀, B: VEGF₁₆₄, C: MMP-9, D: MMP-19, E: HGF and F: PIGF. Samples are from sorted DEC of 15 pooled biological replicates. SQ-PCR was used to determine the expression of the genes.

5.4 Discussion

5.4.1 Overview

In this chapter it was shown that loss of IL-10 leads to the increased production of various angiogenic growth factors after a single infection and that after multiple infection the pinnae of 4x IL-10^{-/-} mice had significantly enhanced levels of both VEGF and HGF. There was also a significant increase in the cell influx into the pinnae of 4x IL-10^{-/-} mice which was composed mainly of neutrophils. It was also found that eosinophils and macrophages from these mice expressed increased levels of pro-angiogenic growth factors, whilst dendritic cells began expressing VEGF and PlGF.

5.4.2 The vasculature in IL-10^{-/-} pinnae was increased, but displayed a more organised morphology.

The outward appearance of pinnae in IL-10^{-/-} mice was similar to that of WT mice, with no discernible difference between naïve and 1x pinnae. After a single infection the vessels were more visible, consistent with observation of 1x WT pinnae and the vessels remained organised with no excessive scabbing or distortion. After multiple infections the vessels became more visible and appeared thicker, similar to pinnae in 4x WT mice. However unlike the WT skin, shown in chapter 2, there was more scarring and scabbing discernible in the IL-10^{-/-} pinnae. IL-10 is expressed rapidly in wounds, and transcript for IL-10 is up-regulated within 60 minutes (Ohshima 1998). IL-10 has been suggested as a marker for wound vitality and can be detected as late as 10 days after wounding (Sato 1999). Here, loss of IL-10 in the 4x pinnae appears to result in reduced maturation and remodelling of the wounds leading to the distinctive scarring seen externally.

Anti CD31 labelling revealed that, as in WT pinnae, there was an increase in the area of the vessels in infected IL-10^{-/-} mice compared with naïve cohorts. However compared to the WT pinnae, the vessels remained 'neat' and not

distorted. In fact, the increase in vasculature in 4x IL-10^{-/-} pinnae was more organised and controlled, perhaps indicating that in 4x WT pinnae one of the up regulated growth factors, identified in chapter 2, causes excessive growth and vessel distortion. One candidate growth factor may be VEGF₁₈₈ which ordinarily controls directional growth of new vessels (Ruhrberg 2002) and which in IL-10^{-/-} pinnae is absent. Thus in 4x WT mice, where an abundance of this factor is observed, this may be the cause of the tangled excessive growth.

5.4.3 Expression of pro-angiogenic growth factors in whole IL-10^{-/-} pinnae

Analysis of the whole pinna ensures that the entire composite cell population, such as keratinocytes and fibroblasts as well as in fluxing haematopoietic immune cells, were included during sampling. The levels of pro angiogenic growth factors in the 4x IL-10^{-/-} pinnae peaked later than in 4x WT pinnae and, with regards to HGF and VEGF, the transcript was more abundant. To better elucidate the dynamics of growth factor expression, a longer time course would be essential but not feasible within this project. In addition, analysis of the angiopoietin expression (Ang1, Ang2) and measurement of vascular leakage as determined in Chapter 2, would also be essential to determine the speed of maturing vasculature. Unfortunately, limited numbers of IL-10^{-/-} mice made performing such assays impossible in this study.

Infected 1x IL-10^{-/-} pinnae exhibited a significant increase in the expression of several growth factors identified in WT pinnae compared to naïve samples, most noticeably HGF which was not up-regulated in 1x WT pinnae. Since IL-10 was not produced in abundance in 1x WT pinnae, its absence in 1x IL-10^{-/-} pinnae was not expected to affect the growth factor levels. However, it would appear that either IL-10 directly, or a downstream gene activated by IL-10, restricts growth factor expression in WT mice. Indeed, since keratinocytes produce IL-10 at wound edges to promote the resolution and maturation of wounds, loss of this function may increase the release of growth factors and induction of angiogenesis by the fibroblasts (Sato 1999).

Direct comparison between the 4x WT and 4x IL-10^{-/-} tissue samples demonstrated that the cytokine deficient mice produced more VEGF and HGF transcript but similar levels of PlGF. This suggests that IL-10 does not affect all angiogenic pathways activated in the schistosome infected pinnae. As HGF was up-regulated in 4x WT pinnae where IL-10 was abundant, one hypothesis might be that loss of IL-10 could reduce HGF expression. However, the opposite situation was observed.

The loss of IL-10 could affect skin resident cell populations. Digest and analysis of the epidermal and dermal layers without the DEC would be needed to determine the relative contribution of fibroblasts and/or keratinocytes to the change in growth factors.

5.4.4 Changes in the cytokine profile of IL-10^{-/-} pinnae

The profile of cytokine production in the absence of IL-10 was similar to that detected in WT pinnae apart from with respect to IL-13 and IFN- γ . After 4x infections, IL-4 remained elevated, although IL-13 was undetectable and IFN γ was detectable. Regulation of IFN- γ has been shown to be dependent on IL-10 in *S.mansoni* infections, particularly at the granuloma stage (Gazzinelli 1992). IL-10 inhibits the expression of IFN- γ by T-cells and subsequently prevents its activation of macrophages. The increased levels of IFN- γ could be altering the activation status of the macrophages and explain the reduced Ym-1 expression seen in the IL-10^{-/-} DEC. Although it is unknown which cell type is now producing the IFN- γ it could be the small population of CD4⁺ lymphocytes detected in the DEC (not shown). One of the main sources of IL-13 in the WT 4x pinnae is the eosinophil (Chapter 4). Loss of IL-10 may have directly affected the eosinophil phenotype or the IL-13 expression of skin resident cells including mast cells (Gessner 2005). Unfortunately mast cell levels were not determined in this chapter due to limited availability of IL-10^{-/-} tissue. Analysis of WT and IL-10^{-/-} skin after the removal of DEC would aid to determine the source of these cytokines.

5.4.5 Changes in cell recruitment in IL-10^{-/-} pinnae

Cell recruitment to skin sites of inflammation in IL-10^{-/-} mice appears to be associated with accelerated wound healing and is characterised by rapid re-epithelisation and high infiltrates of cells into the skin (Eming 2007). The pinnae of IL-10^{-/-} mice infected with RA cercariae exhibit increased cell influx compared to WT mice and elevated levels of IL-12 and IFN γ (Hogg 2003 (b)). The data presented here shows that infected IL-10^{-/-} mice had significantly higher numbers of DEC than WT mice, and these persist at a high level to day 4.

The proportions of different types of leukocytes present in DEC from IL-10^{-/-} mice was markedly different from WT mice. The number of eosinophils and dendritic cells were reduced in IL-10^{-/-} mice whilst neutrophils were significantly more abundant. The available evidence demonstrating that IL-10 controls cell recruitment by IL-10 is conflicting. For example, using IL-10^{-/-} mice in models of asthma, the absence of IL-10 was reported to increase IFN γ expression and reduce levels of IL-5 and eosinophilia but without effecting levels of IL-4 (Yang 2000). In contrast, over expression of IL-10 in a different asthma model, lead to reduced eosinophilia and IL-4 (van Scott 1999). The data shown here is more in agreement with the IL-10^{-/-} model of asthma.

Neutrophil numbers were significantly increased in IL-10^{-/-} compared to WT mice. Experimental administration of exogenous IL-10 to cutaneous wounds inhibits the infiltration of both neutrophils and macrophages to the wound site (Sato 1999). Therefore loss of IL-10 in the multiple schistosome infection model may release this control allowing excessive neutrophil influx. However, an increase in the numbers of macrophage was not observed in the present study.

5.4.6 Phenotypic changes in IL-10^{-/-} DEC

IL-10 directly influences VEGF expression by macrophages, particularly in hypoxic conditions (Dace 2008). In ischemia induced angiogenesis in rat corneas there was excessive vessel growth which was induced by VEGF positive macrophages. In the absence of IL-10 these macrophages did not promote excessive vessel growth and did not up regulate VEGF (Dace 2008). However, according to the data shown in this chapter, macrophages worked in the opposite way, with higher levels of PlGF and VEGF transcript in 4x IL-10^{-/-} macrophages.

The activation of macrophages is particularly plastic and can be influenced by the balance of a number of cytokines (1.3.4.2). Recent reviews have suggested IL-10 may directly induce a “regulatory” phenotype or up-regulate IL-4/13 which in turn induces an alternative phenotype (Mosser 2008). To elucidate which cytokines drive the alternative activation phenotype in the 4x WT pinnae the three AAmac markers - Arginase, Ym1 and RELM α and also the classical marker iNOS were analysed in the sorted DEC populations. Arginase expression in infected IL-10^{-/-} macrophages was only reduced by ~25% compared to WT pinnae, although iNOS and Ym1 expression were almost completely ablated. This differential patterns of expression of arginase and Ym1, which would conventionally be expected to be co-expressed, may suggest that arginase-1 expression is controlled by IL-4 mediated activation, whilst IL-10 or IL-13 are responsible for the stimulation of Ym1 expression.

Macrophages from the pinnae of IL-10^{-/-} mice produced slightly elevated levels of growth factors which is contrary to the hypothesis that IL-10 induces a more pro-angiogenic phenotype. It would appear that the up regulation of IL-4, IL-13 or IL-10 in the 4x WT mice, induces up regulated levels of transcript for pro-angiogenic growth factors in DEC but loss of IL-10 does not completely ablate this phenotype. This would suggest that IL-4 is the primary cytokine involved in controlling the up-regulation of pro-angiogenic factors in macrophages. Multiple infections of IL-4R α ^{-/-} mice have shown that arginase-1 expression in 4x

macrophages is reduced to 1x levels (Cook 2011) and analysis of these cells for angiogenic mediators may show more of a reduction in growth factor expression than in IL-10^{-/-} mice. Loss of IL-10 however did affect the levels of PlGF which was up-regulated considerably more in the 4x IL-10^{-/-} compared to WT macrophages. As PlGF is primarily induced in inflammatory conditions, it is possible that loss of IL-10 and the subsequent up regulation of IFN γ or TNF α , induces expression of PlGF by macrophages.

RELM α which was largely expressed by eosinophils, was also much reduced in the IL-10^{-/-} compared to WT mice. The transcript levels in eosinophils of the growth factors analysed did not change dramatically with the exception of HGF which was increased by 50%. This indicates that eosinophils recruited in the presence of IL-10, or a downstream IL-10 effector molecule, can alter the phenotype of eosinophils either before or upon entry into the skin. Eosinophils cultured in cytokines and chemokines derived from macrophages induced growth factor expression and it was shown that IL-10 can up-regulate HGF expression in eosinophils (Kobayashi 2009).

Dendritic cells were more pro angiogenic in IL-10^{-/-} than WT mice consistent with the hypothesis that IL-10 activation of dendritic cells in the 4x pinnae inhibits their maturation and VEGF expression. Dendritic cells from IL-10^{-/-} mice expressed slightly higher levels of VEGF and transcript for PlGF. The pro-angiogenic potential of dendritic cells is conflicting. The exact contribution of these PlGF expression dendritic cells was not investigated in this work but several studies have implicated them in exacerbating tumour growth and becoming part of new blood vessels (Fainaru 2010, Conejo-Garcia 2005).

5.4.7 Summary

The results in this chapter highlight the complex nature of cytokine interaction and composition of leukocytes in and the skin cell response. Vessel growth was affected by the loss of IL-10 but not through a reduction in vessels. Instead the number of vessels was increased but appeared more organised and mature than in 4x WT pinnae. The angiogenic phenotypes of all three major constituent cell populations comprising DEC were affected by the loss of IL-10. However, IL-10 does not appear to be the major stimulator of angiogenic factors in macrophages as initially thought, IL-4 expression was unaffected by the loss of IL-10 indicating it is probably produced by a cell of the skin, for example mast cells or keratinocytes (Enk 1992), which is unaffected by the presence of IL-10. In addition to cytokine environment of the skin, uptake of the parasite antigens may influence the phenotype of constituent cells. In the next chapter, the direct effect of larval parasite secretions on leukocytes and vascular endothelial cells will be determined, and will be related to the development of an angiogenic phenotype and *de novo* vessel growth.

**Chapter 6: Investigating the pro angiogenic potential
of cercarial secretions (0-3hRP)**

6.1 Introduction

The majority of this thesis has focused on characterising the angiogenic response following either a single or multiple infection through examination of both the vessels in the skin, and the influx of haematopoietic cells. This final chapter will focus on determining whether the cercarial secretions themselves induce angiogenesis.

Upon penetration of the skin, cercariae release the contents of their acetabular glands. These are thought to aid the transit of the schistosome larvae through the skin, and perhaps its entry into the vasculature (McKerrow 2002). These secretions, within the first 3 hours after transformation, can be collected and are termed the 0-3 hour released preparation (0-3hRP). They consist primarily of proteases but also several glycans and other protein and carbohydrate components (Curwen 2006). This chapter aims to determine if these secretions also contain component(s) which induce angiogenesis.

There is emerging evidence for the involvement of angiogenesis in the survival of several parasitic infections, including species which either dwell in, or utilise, the skin as a point of entry to the body. The migration of mature *O. volvulus* from the skin is suggested to be aided by the release of secretions by the parasites which promote tissue degradation and angiogenesis (Higazi 2003). Current hypotheses propose that release of an angiogenic growth factor by various parasites may be essential for their transit or development in the host organism (Dennis 2011)

Angiogenesis induction by schistosome eggs has been long established. The livers of infected mice exhibit increased vasculature induced by either host-derived growth factors stimulated by the passage of eggs, or an egg-derived factor. (Freedman 1988). Indeed, egg secretions and live eggs both induce endothelial cell proliferation (Shariati 2011). The schistome eggs secrete a component, which induces changes in mature vasculature and appears to induce the process of angiogenesis. Many of these studies, also compared responses with sonicated cercarial extracts which did not induce angiogenic responses (Kanse 2005,

Shariati 2011), but no work to date has examined the effect of cercarial secretions in their native state. As shown with schistosome eggs, cercarial secretions may directly induce angiogenic factors, or interact receptors on the blood vessels. This chapter will utilise both *in vitro* and *in vivo* assays to determine the angiogenic potential of cercarial secretions in the form of purified O-3hRP.

Finally, it was shown in chapter 4 that after multiple exposures to schistosome larvae, macrophages in the skin displayed a pro angiogenic phenotype (4.3.10). Whilst this may be due to changes in cytokine environment, it may also be the result of direct uptake of parasite antigen by these cells. Therefore, the angiogenic phenotype of phagocytic cells in the skin could be due to both the uptake of antigen and the influence of the cytokine environment. This chapter will address whether cercarial secretions directly influence phagocytic cells and promote the secretion of angiogenic factors.

6.2 Materials and Methods

6.2.1 Collection of 0-3hRP

Cercariae were shed from snails in 'aged tap water' placed under a 200 W lamp for 2 hours. The cercariae were washed by gentle centrifugation in aged tap water and placed in serum free RPMI 1640 medium containing 200U/ml of penicillin and 100ug/ml streptomycin (Pen-strep RPMI 1640). Cercariae were mechanically transformed by vortexing for 3 bursts of 30 seconds to separate heads from tails, and were then incubated in serum free Pen-strep RPMI 1640 at 37°C and 5% CO₂ for 3 hours. The supernatant (parasite free) was then collected and concentrated in Vivaspin 15 tubes (Sartorius Stedim Ltd, Epsom, UK) with a 5kDa membrane. (Jenkins 2005). The protein concentration of the final 0-3hRP was determined using a Coomassie plus-200 assay (Perbio Science Ltd. UK).

6.2.2 L929 fibroblast culture and production of conditioned media

L929 fibroblasts (from Professor P. Kaye, University of York) were cultured in 75cm² flasks on DMEM with 10% FCS, 2mM L-glutamine, 200U ml⁻¹ penicillin and 100µg ml⁻¹ streptomycin, 50µM 2-mecaptoethanol at 37°C/5% CO₂ for 5-7 days. The culture supernatant was then harvested, filter sterilised (0.22µM), and frozen at -80°C.

6.2.3 Bone marrow cell extraction and differentiation

The femurs, tibia and fibula of 8 week old C57BL/6 mice were removed and cleaned of tissue. Bones were briefly sterilised in 70% ethanol and rinsed twice in 1% Pen-strep PBS. Bone marrow was removed by flushing the bones with 1% Pen-strep PBS. Cells were dissociated with gentle pipetting and spun at 900rpm for 7 minutes. Cell pellets were re suspended in ACK buffer for 5 minutes at room temperature to lyse red blood cells, before being washed in an excess of 1% Pen-strep PBS.

6.2.3.1 Bone marrow derived macrophages

Bone marrow cells were re-suspended in culture media (DMEM supplemented with 10% heat-inactivated low endotoxin foetal bovine serum, 2mM L-glutamine, 200U ml⁻¹ penicillin and 100µg ml⁻¹ streptomycin, 50µM 2-mercaptoethanol and 20% L929 cell-conditioned medium (containing M-CSF). Cells were plated at a density of 2.5x10⁶ cells per well in 24 well plates and incubated 37°C/5%CO₂ for 7 days.

6.2.3.2 Bone marrow derived dendritic cells

Bone marrow cells were re suspended in DMEM containing 10% FCS 2mM L-glutamine, 200U ml⁻¹ penicillin and 100µg ml⁻¹ streptomycin, 50µM 2-mercaptoethanol and 20ng/ml GM-CSF (Peprotech, London UK), plated at 2.5x10⁶ cells per well in 24 well plates, and incubated 37°C/5%CO₂ for 4 days. Fresh culture media containing 40ng/ml of fresh GM-CSF was added on day 4 and the cells cultured for a further 2 days.

6.2.4 Bone marrow derived cell culture with 0-3hRP

After culture of bone marrow cells to facilitate differentiation into macrophages or dendritic cells, the cells were removed using cold shock treatment described in 4.2.1. Cells were counted and re plated at 5.0x10⁴ cells per well, and stimulated with fresh culture media containing no stimulant, 0-3hRP (10µg/ml) or LPS and cultured for 18hrs. Cells were removed after culture and a sample labelled for flow cytometry to confirm cell identity using the antibodies listed below (Table 6.1) (Paveley 2009).

Antibody	Clone	Supplier	Isotype	Supplier
F4/80 FITC	BM8	eBioscience	Rat IgG2a	eBioscience
CD11b APC	M1/70	eBioscience	Rat IgG2bk	eBioscience
IA/IE Biotin	M5/114.15.2	eBioscience	Rat IgG2bk	ebioscience
CD11c FITC	N418	eBioscience	Armenian Hamster IgG	ebioscience
Streptavidin Pacific blue	Goat IgG	Invitrogen	-	-

Table 6.1 Antibodies used for bone marrow derived cell staining.

6.2.5 Transcript analysis from bone marrow derived cells

Samples of cells after stimulation were collected and placed in 250µl of TRIZOL™ before RNA was extracted and cDNA produced (as described for the DEC 3.2.9). SQ-PCR was performed using primers for VEGF, HGF and PIGF (3.2.10 , Primer sequences in appendix 1)

6.2.6 Wound Healing Assay

L929 Fibroblasts were cultured as before (6.2.2) and harvested when confluent. After washing in fresh media, cells were plated at 5×10^4 per well of a 24 well plate in 'Fibroblast media' (DMEM with 10% FCS, 2mM L-glutamine, 200U ml⁻¹ penicillin and 100µg ml⁻¹ streptomycin) and allowed to adhere and proliferate overnight at 37°C/5%CO₂. The cell monolayers were scratched with a P1000 pipette tip to remove a strip of cells and gently washed to remove debris. Growth factors or stimulants were added in fibroblast media to each well; VEGF 10ng/ml (Peprotech,USA), 0-3hRP 10µg/ml, SEA 10µg/ml or media alone. Cells were imaged immediately after addition of stimulants, and again at 24 hours and 36 hours using a Zeiss inverted microscope under bright light.

6.2.7 Culture of Human Umbilical Vein Endothelial Cells (HUVECs)

HUVECs (Promocell, UK) were cultured in endothelial cell growth medium with supplement mix containing foetal calf serum, endothelial cell growth supplement, epidermal growth factor, basic fibroblast growth factor, heparin and hydrocortisone (PromoCell). HUVECs used in this study were no older than passage number five and were grown to confluence in complete HUVEC media at 37°C/ 5% CO₂. Cells were recovered following aspiration of culture medium and addition of Trypsin/EDTA. Cells were incubated for 2 minutes at 37°C until they had rounded up and released into suspension. PBS was then added to quench the trypsin. The cell suspensions were centrifuged at 900rpm for 7 minutes, and then re suspended in fresh medium and then plated out at the required density.

6.2.8 HUVEC proliferation Assay

HUVECs were cultured as described in section 6.2.7. At a concentration of 2.5×10^4 per well of a 96-well plate in 100ul of complete endothelial cell media. Aliquots of 100µl of soluble egg antigen (5, 10 or 50µg/ml) 0-3hRP (5, 10 or 50µg/ml), VEGF (5, 10 or 50ng/ml) (Peprotech, USA), or media alone were added at the desired final concentration. HUVECs were incubated at 37°C/5%CO₂ overnight, prior to removal of 120µl of culture media, and replacement of 20µl fresh medium containing 18.5kBq of radioactive thymidine (methyl- ³H) (GE Healthcare Life Sciences, UK). Cells were incubated for a further 18hrs before harvesting using Filter-Mate Harvester onto UniFilter-96 GF/C plates. After the filter had completely dried, 20ul of Microscint-20 was added to each well and sealed with film. The plates were analysed using a TopCount scintillation counter (PerkinElmer Beconsfield UK)

6.2.9 Proliferation assay with protease inhibition

Cells were cultured and plated as described (6.2.8) but to 50ug/ml 0-3hRP a protease inhibitor cocktail (Halt Protease Inhibitor Cocktail Kit #78410, Pierce) was added in decreasing concentrations. To control for cell death due to the inhibitor, cells in media alone plus inhibitor were used as a control. As above, cells plates were incubated overnight at 37°C/5%CO₂ prior to assay for proliferation activity (6.2.8).

6.2.10 Branching Assay

The wells of a 24 well culture plate were coated with 300µl of BD Growth factor reduced Matrigel (BD Biosciences) which was allowed to set for 30mins at room temperature. BD Matrigel is a mix of proteins used as an ECM substitute in cell culture. It is liquid between 4°C and 10°C at which point test stimulants can be mixed in. Above 10°C the Matrigel sets into a solid plug. HUVECs (5.0x10⁴) were plated on top of Matrigel in 500µl of endothelial cell growth media containing either SEA, 0-3hRP (both 10ug/ml), VEGF (10ng/ml; Peprotech, USA) or media alone. The plate was then incubated overnight at 37°C/5%CO₂. After incubation the plates were imaged under transmitted light.

6.2.11 Staining of HUVECs with phalloidin and DAPI

HUVECs were cultured (6.2.7) and plated at a density of 5x10⁴ per well onto coverslips in a 24 well plate,. The plate was then incubated overnight at 37°C/5%CO₂. Test substances were then added at a final concentration of; SEA, 0-3hRP (both 10ug/ml) VEGF (10ng/ml) prior to incubation for a further 24hrs. Coverslips were removed from the wells, and adherent cells fixed in BD Fix/Perm (BD Biosciences) for 15mins at 4°C. After rinsing in PBS, 50µl of Perm/Wash buffer (BD Biosciences) containing 10% normal rabbit serum (NRS) was added for 20minutes at room temperature. Phalloidin (AF488 conjugated, Invitrogen) and DAPI (Invitrogen) were diluted in Perm/Wash buffer containing 10%NRS and added to the coverslips for 30minutes at room temperature. Slides were rinsed

in PBS before being mounted in Vecta shield (Vector Laboratories UK) on a microscope slide. Slides were imaged using a Zeiss LSM 510 meta (Carl Zeiss Ltd).

6.2.12 Matrigel Plug assay

BD Matrigel was thawed on ice and mixed with the test reagents, SEA (50µg/ml), O-3hRP (50µg/ml), VEGF (400ng/ml), or PBS. Solutions were mixed in a ratio of 100µl of test substance to 400µl of Matrigel to keep the protein concentration of the Matrigel high enough to set. Aliquots of 500µl were injected into the ventral side of the groin area close to the dorsal midline of anaesthetised mice using chilled needles. The mice were sacrificed at day 4 post injection and the plugs excised. The plugs were imaged using a stereomicroscope at 18x magnification (Carl Zeiss)

6.3 Results

6.3.1 PIGF expression is induced in bone marrow derived macrophages and dendritic cells after culture with 0-3hRP

6.3.1.1 Bone marrow-derived macrophages

For the three predominant growth factors identified in the previous chapters, VEGF₁₂₀, PIGF and HGF there was no significant difference between the transcript expression profile between blank (medium only) and LPS stimulated cells (Figure 6.1). For VEGF₁₂₀ and HGF, there was also no difference between the blank and 0-3hRP stimulated cells. However, 0-3hRP induced a significant increase in PIGF transcript compared to cells cultured in medium only and those stimulated with LPS.

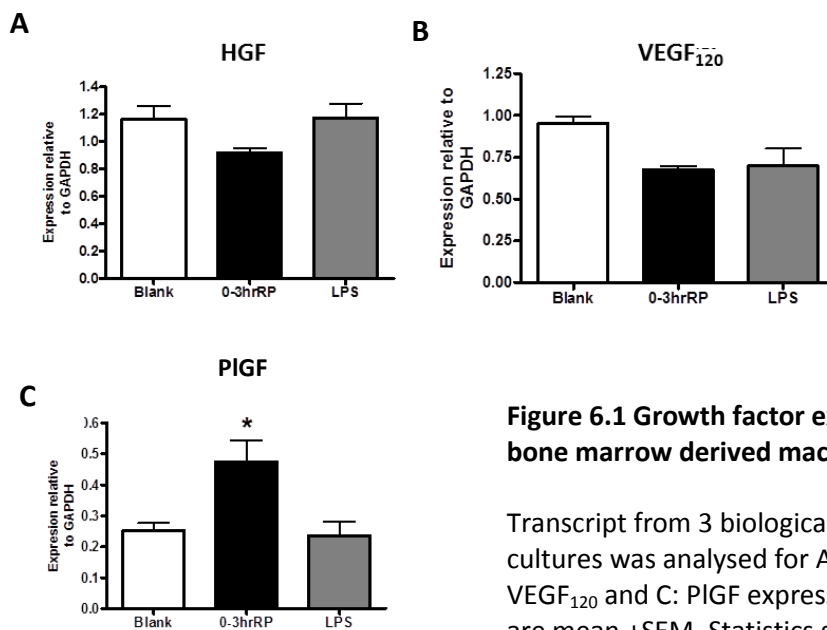


Figure 6.1 Growth factor expression by bone marrow derived macrophages.

Transcript from 3 biological replicate cultures was analysed for A: HGF, B: VEGF₁₂₀ and C: PIGF expression. Graphs are mean +SEM. Statistics shown are for 0-3hRP vs Blank *p<0.05

6.3.1.2 Bone marrow-derived dendritic cells

Dendritic cells stimulated with LPS or 0-3hRP expressed significantly less HGF than the un-stimulated cultures ($p < 0.05$ for both) and there was no significant difference in the expression of HGF between the LPS and 0-3hRP stimulated cells (Fig 6.2). In contrast, VEGF₁₂₀ expression did not differ between any of the three groups of cells, although the relative levels of VEGF₁₂₀ were much lower in dendritic cells than macrophages. In contrast, there was a small increase in transcript levels for PIGF cells stimulated with 0-3hRP compared to medium and LPS, although this was not statistically significant.

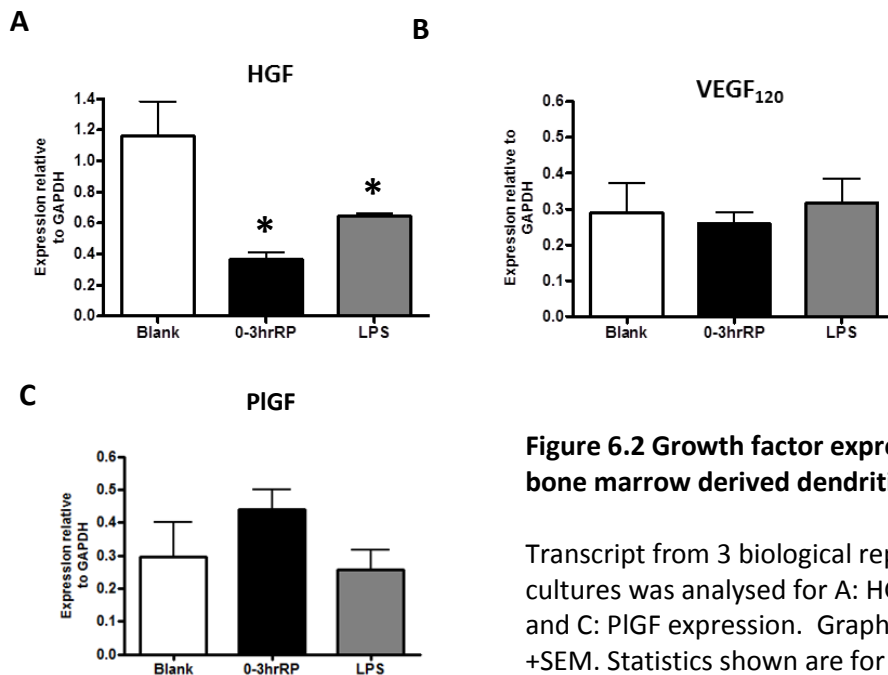


Figure 6.2 Growth factor expression by bone marrow derived dendritic cells.

Transcript from 3 biological replicate cultures was analysed for A: HGF, B: VEGF and C: PIGF expression. Graphs are mean +SEM. Statistics shown are for 0-3hRP and LPS vs Blank * $p < 0.05$

6.3.2 Parasite antigens induce fibroblast migration

One of the main components of the dermis are fibroblasts (Smith 1982). They are important in the remodelling and release of angiogenic factors in the skin and the recruitment of leukocytes (Smith 1997). To determine whether 0-3hRP can directly activate fibroblasts and enhance their migration, an *in vitro* wound assay was performed (6.2.6). This assay is commonly used to indicate the wound healing potential of a substance but is only a suggestive *in vitro* model.

VEGF is not reported to enhance fibroblast migration and as such serves as a further negative control, along with media alone, in this assay. The fibroblasts at the leading edges of the 0-3hRP and SEA treated wounds became elongated and moved to cover the scratch in the plate (Figure 6.3A). Fibroblasts along the leading edges of the VEGF and media alone wells (blank) were slower to elongate and more remained rounded early after scratching. At 24hrs, the fibroblasts in the 0-3hRP treated wounds almost covered the scratch, although sparsely distributed, whereas relatively large cell free are discernible in the VEGF and Blank cultures.

The width of the wound was measured at the start and 24hrs after culture and the distance the leading edge of fibroblasts had moved expressed as a percentage of wound closure (Figure 6.3B). There was no significant difference between VEGF-treated and un-treated wells. However, there was a significant increase in wound closure in response to SEA and 0-3hRP compared to medium (SEA $p < 0.01$, 0-3hRP $p < 0.05$).

A

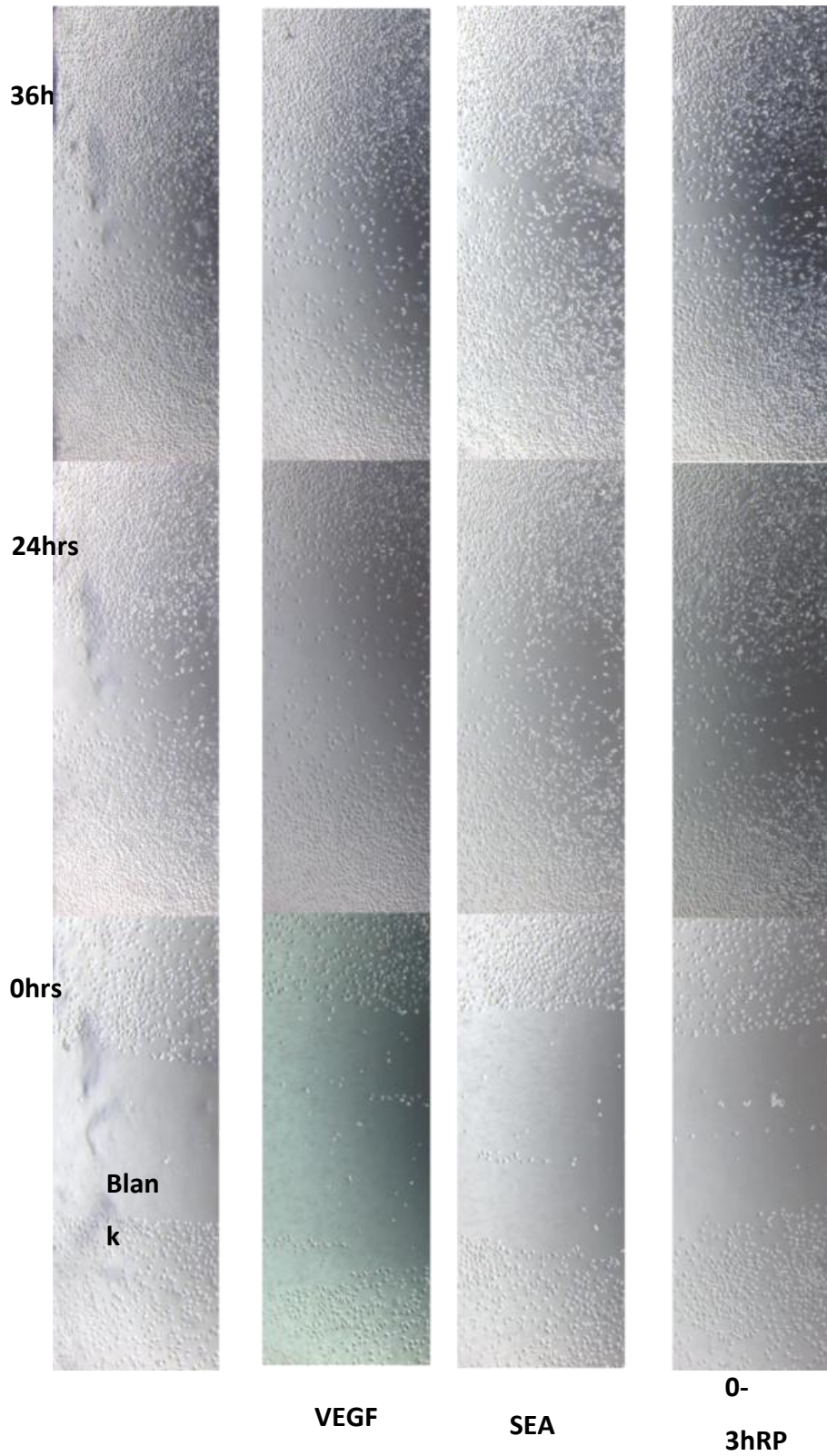


Figure 6.3 Fibroblast migration in the presence of parasite antigens

A: Representative images from three wells for each condition. The same area of plate is shown for each time point

B

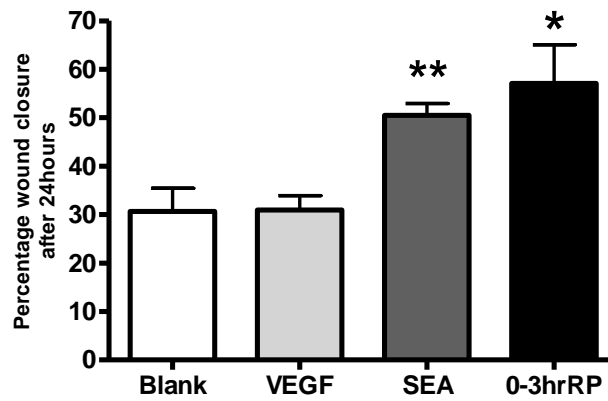


Figure 6.3B Fibroblast migration in the presence of parasite antigens

B: Fibroblast migration shown as a percentage of the initial scratch now covered. Data is 12 measurements over the three wells for each condition. Mean +SEM. Statistics are for 0-3hrRP and SEA vs Blank * $p < 0.05$ and ** $p < 0.01$

6.3.3 0-3hrRP induces endothelial cell proliferation

In order to form new vessels, the endothelial cells of existing vessels must proliferate (Carmeliet 2000). Therefore one of the more commonly used *in vitro* models for angiogenic potential is the ability of the test substance to induce increased endothelial cell proliferation. It has been shown previously that SEA will induce endothelial proliferation (Loeffler2002) and SEA was used as a positive control alongside VEGF.

HUVECs cultured in media alone proliferated and incorporated H^3 -thymidine into their DNA (Figure 6.4). However, VEGF induced significantly greater levels of proliferation compared to the blank ($p < 0.01$). This appeared to be a dose-dependent trend, although there was no significant difference between the different concentrations. Addition of SEA induced also significantly increased levels of proliferation; however unlike VEGF this was not dose-dependent, and

there was no significant difference in the level of proliferation between the different doses. Proliferation induced by SEA was only slightly lower than that induced by VEGF and not significantly different. 0-3hrRP induced significant proliferation compared to the blank at 5µg/ml, but at greater concentrations the level of proliferation induced by 0-3hrRP showed an inverse relationship, and proliferation appeared to be inhibited at 50µg/ml.

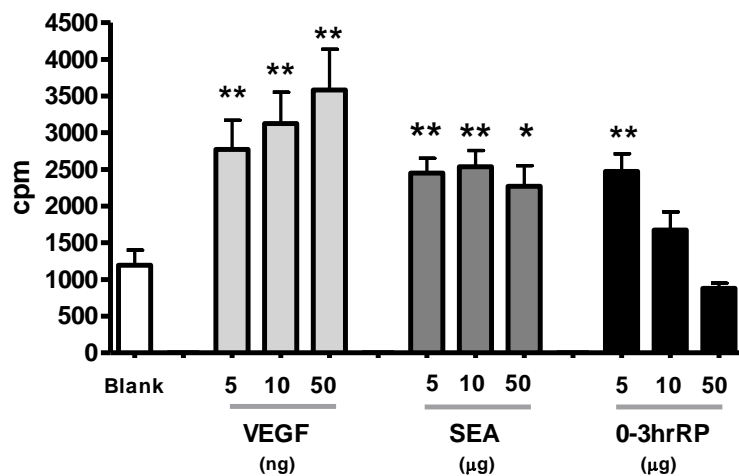


Figure 6.4 HUVEC proliferation following 24hrs culture

Data is from 3 replicate wells for each condition. Cells were cultured with either media alone (blank) or increasing concentrations of VEGF (ng), SEA (µg) or 0-3hrRP (µg). Cells were cultured with radioactive thymidine (methyl- ³H) and the counts analysed. Statistics shown are test substances compared to blank; Mean cpm + SEM *p<0.05 and **p<0.01.

6.3.4 Protease inhibition restores 0-3hRP induced proliferation

At high concentrations of 0-3hRP (50µg/ml) proliferation appeared to be inhibited (Figure 6.4) and as 0-3hRP contains high levels of proteases it was hypothesised that they may inhibit the proliferation of the cells HUVECs, or decrease cell viability as the concentration of 0-3hRP increased.

Culture of HUVECs in media alone induced proliferation, whilst addition of 5µg/ml of 0-3hRP induced significant up regulation of proliferation (Figure 6.5). Cell cultures containing 50µg/ml of 0-3hRP again inhibited proliferation as previously shown (Figure 6.4). At the highest concentrations of protease inhibitor (1:400) proliferation increased but was not significantly higher than cells cultured with media alone, and was significantly lower than cells in 5µg/ml of 0-3hRP. However, as the concentration of inhibitor decreased, cell proliferation was restored to levels higher than the blank ($p < 0.01$ and $p < 0.001$), and were similar to levels induced by 5µg/ml 0-3hRP.

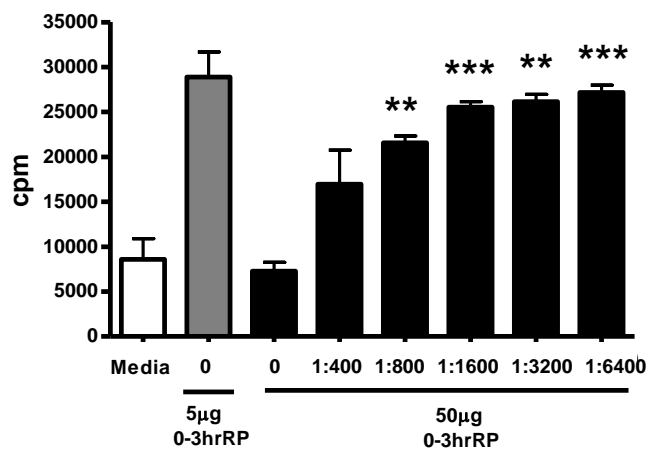


Figure 6.5 HUVEC proliferation in the presence of a protease inhibitor

Data is from 3 replicate wells for each condition. Cells were cultured with either media alone (blank) or 0-3hRP in the presence of increasing concentrations of protease inhibitor. Significance shown is each sample containing protease inhibitor compared to the 50µg/ml of 0-3hRP without inhibitor. Mean +SEM ** $p < 0.01$ and *** $p < 0.001$.

6.3.5 HUVECS form primitive branch-like structures in response to 0-3hRP

After proliferation, endothelial cells ordinarily migrate into primitive tubes (Carmeliet 2000). In order to determine whether this occurs in response to 0-3hRP, HUVECs were grown on Matrigel coated plates in the presence of 0-3hRP, VEGF, SEA or media alone for 24hours. HUVECs cultured in media alone survived and remained evenly distributed across the plate with no cell to cell interactions observed (Figure 6.6D). Culture with VEGF induced the cells to form branch structures across the plate with multiple branching points from the cells and webs of branches apparent (Figure 6.6A). SEA induced similar branch patterns with webs of primitive tubes (Figure 6.6C), however it additionally induced high levels of proliferation of the HUVECs with a large 'pool' of endothelial cells feeding into the branching network. Finally, cells stimulated with 0-3hRP exhibited primitive branching with 2-3 junctions (Figure 6.6B). Cells did not form webbed networks but were spaced across the plate in small groups of branches.

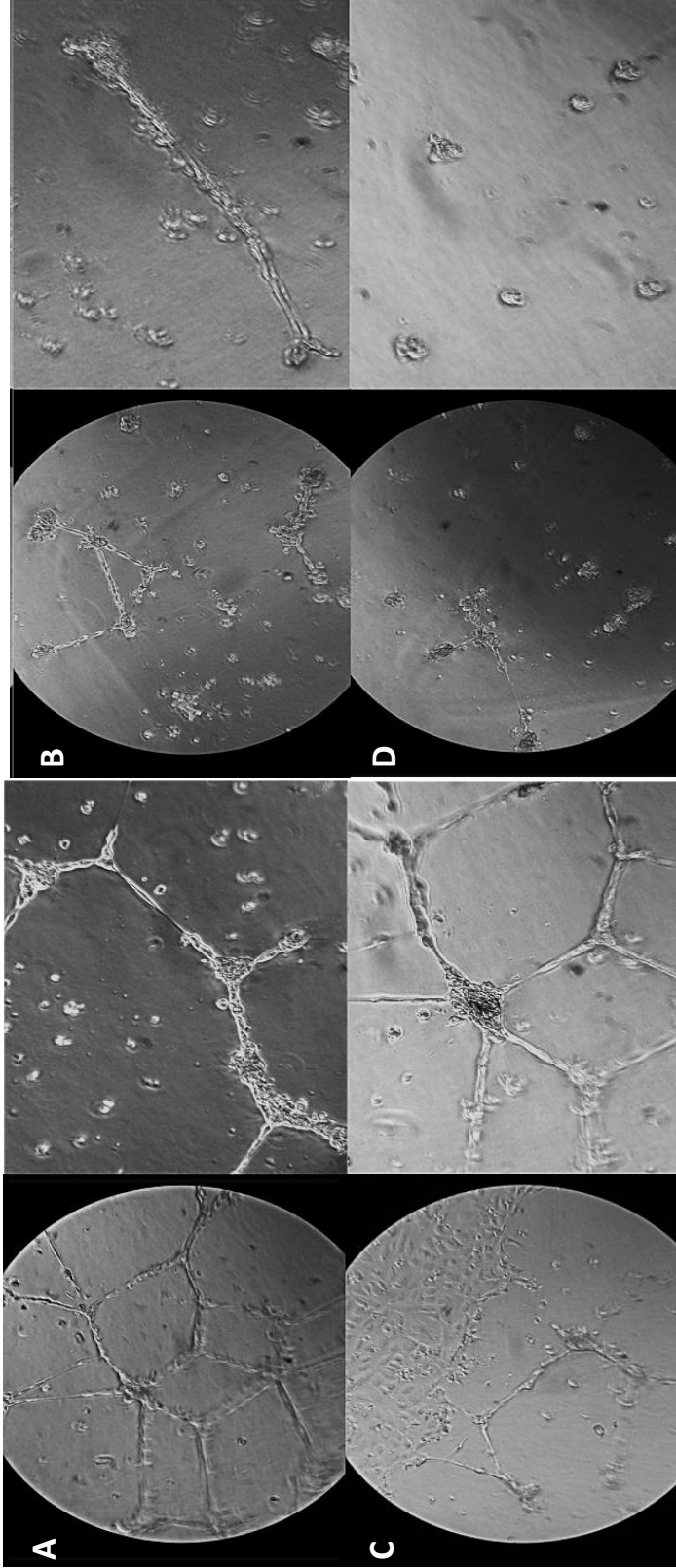


Figure 6.6 HUVEC branching after 24hr culture
 Representative images from 3 replicate wells of cells per treatment. HUVECs were cultured with either **A: VEGF**, **B: 0-3hRP**, **C: SEA** and **D: Media alone**

6.3.6 HUVECs extend filopodia and align after culture with 0-3hRP

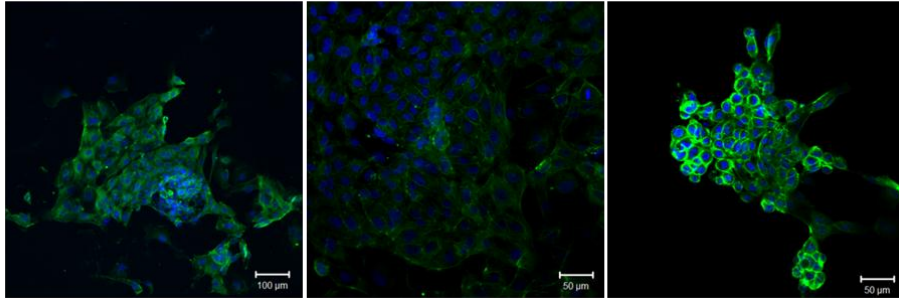
To determine the morphological changes to the HUVECs, cells were stained with phalloidin and DAPI after culture and imaged (Figure 6.7). Cells grown in only basal endothelial cell media, without any additional growth factors, grew in neat sheets of cells which were grouped together sporadically over the plate (Figure 6.7A). The cells were predominately round with a cobblestone morphology and fit closely together. Closer examination of the cells showed organised actin and a small cytoplasm.

Addition of VEGF to the culture media dramatically altered the morphology of the HUVECs (Figure 6.7B). Examination of single cells revealed that they had a much larger cytoplasm than the cells cultured in media alone. Several had long actin filaments reaching out to contact other cells in the surrounding area. Over the entire surface of the plate, the cells were elongated with actin filaments stretched across the length of the cells. The cells had an oblong morphology and lined up into strings of cells. In several regions, these tubes of cells were stretched thin and aligned into circles of interacting cells.

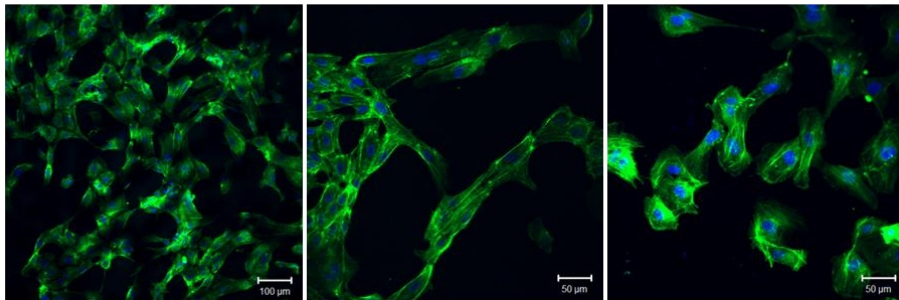
HUVECs cultured with SEA showed a similar morphology to the VEGF stimulated cells, with cells grouping and stretching across the plate in a web formation (Figure 6.7C). Many of the cells were stretched thinner than the VEGF cultured cells with long reaching filopodia contacting between cells. Like VEGF treated cells, those cultured with SEA had a larger cytoplasm than the cells in only media.

0-3hRP treated HUVECs had a similar morphology to the VEGF and SEA cells. However unlike cells in these conditions, they 0-3hRP HUVECs were spread out thinly across the plate with large gaps between the strings of cells. They did not produce the dense circles of 3 or 4 cells as seen in the VEGF and SEA treatments, and there did not appear to be as much proliferation. As with the other stimulants, 0-3hRP-stimulated HUVECs had a large cytoplasm and several extensions of the cytoplasm making contacts between the cells. They also elongated and formed into primitive vessel like cords of endothelial cells.

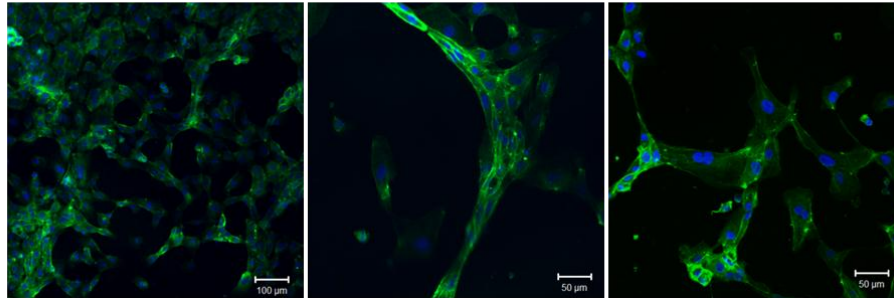
A: Blank



B: VEGF



C: SEA



D: 0-3hrRP

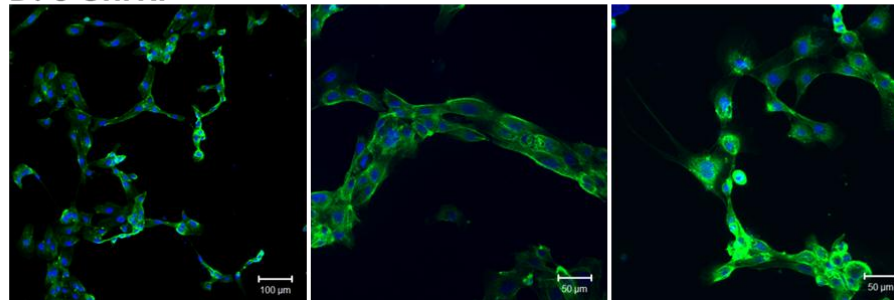


Figure 6.7 Actin filament staining of HUVECs after 24hr culture

Representative images from 3 replicate wells of cells. HUVECs were cultured in 24 well plates on coverslips for 24hrs before being removed and stained with DAPI (blue) and Phalloidin (Green). **A: Blank, B: VEGF, C:SEA and D: 0-3hrP.** 1st panel is taken under 20x magnification the 2nd and 3rd panels are 10x magnification under invert confocal.

6.3.7 0-3hRP induces blood vessel growth into Matrigel plugs *in vivo*

0-3hRP was integrated into the synthetic extracellular matrix – Matrigel, to determine whether it induces blood vessel growth *in vivo*. Matrigel combined with different stimulants was injected subcutaneously into the lower abdomen of mice to produce a solid plug (6.2.12), which were excised 4 days post implantation. Matrigel was removed in tact with no signs of absorption into the body.

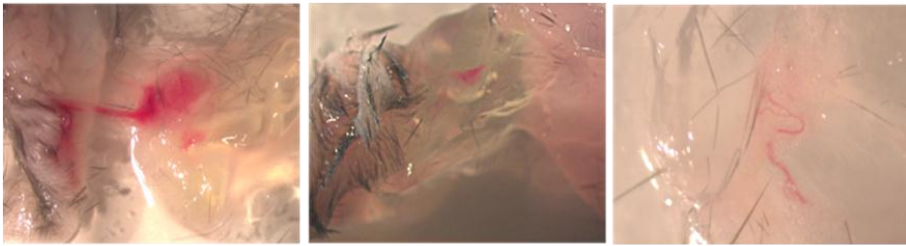
Matrigel containing only PBS, showed no vessel growth into, or within the plugs (Figure 6.8; top). Vessels within the peritoneum and dermis adjacent to the plug also showed no dilation or branching. Plugs incorporating VEGF, exhibited vessels growing into the plug from both the peritoneal and dermal sides (Figure 6.8; second top). Vessels were present in the centre of the plug and the larger vessels showed one or two branches. Existing vessels of the body adjacent to the plug were dilated and branched from the surrounding tissue into the plug. Areas of vessels appeared burst with blood extravasated into the surrounding tissue.

Plugs incorporating SEA showed a similar level of blood vessel growth to VEGF plugs but without the dilation of the surrounding vessels (Figure 5.8; second from base). Vessels were long and they penetrated from the dermal and peritoneal sides into the entire plug with several showing small branches (Figure 6.8 third panel →). Plugs with 0-3hRP also exhibited many branching vessels (Figure 6.8; base *). The majority of these appeared to be growing from the dermal side over and into the plug (Figure 6.8 base →). The mature surrounding vessels of the body branched into the plug but again did not exhibit vessel dilation and blood extravasation as seen with VEGF plugs.

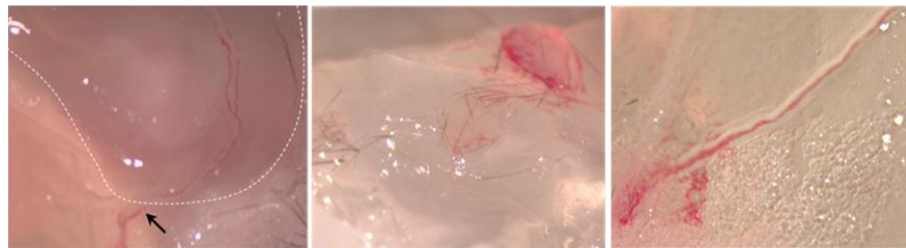
Blank



VEGF



SEA



0-3hrRP

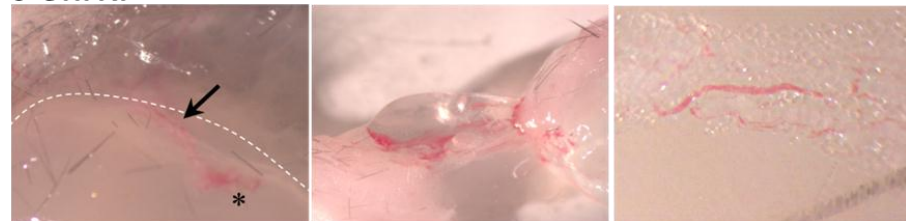


Figure 6.8 Matrigel plugs 4 days after implantation

Representative images of plugs excised 4 days after implantation. There were a total of 4 plugs for each test substance. Left panel shows the plugs in situ with the edges marked in white where not clear. The mid and right panels show part and fully excised plugs A: PBS B: VEGF C: SEA D: 0-3hrRP Vessels grew into the plug (arrowed) and were seen clearly throughout the plug. * indicates a small network of fine vessels within the plug.

6.4 Discussion

6.4.1 Overview

This chapter revealed that angiogenic responses were induced directly by cercarial secretions. Bone marrow-derived dendritic cells and macrophages stimulated with 0-3hRP resulted in up regulation of PlGF expression without additional cytokine stimulus. The cercarial secretions appear to contain a pro-angiogenic growth factor which is not a protease and can induce both endothelial cell proliferation and organisation into new vessels.

6.4.2 0-3hRP induced PlGF expression in bone marrow derived macrophages

The three growth factors up regulated in the DEC; VEGF, HGF and PlGF were all analysed in directly stimulated macrophages and dendritic cells. However, the only factor to be enhanced by 0-3hRP was PlGF. This indicates that differences in HGF and VEGF expression detected in samples collected *ex vivo* after infection, are likely to be due to the cytokine environment in the whole pinnae not direct antigen recognition. However, the increase in PlGF in dendritic cells was not significant, and PlGF expression was only detected in *ex vivo* dendritic cells from the DEC of 4x IL-10^{-/-} mice (4.3.12) whilst it was absent in the WT group (3.3.10). In the presence of IL-10, MHCII expression on dendritic cells can be down-regulated (Laxmanan 2005), so perhaps the high levels of IL-10 in 4x WT mice, also prevents the recognition of 0-3hRP by dendritic cells and inhibiting expression of PlGF. The macrophages significantly increased expression of PlGF. Further analysis of receptors on the macrophages and dendritic cells which could be inducing PlGF may elucidate a pathway by which cercariae are directly inducing the leukocytes to produce inflammatory angiogenic genes.

It was planned to use bone marrow-derived cells (stimulated with 0-3hRP) in co-culture experiments with murine endothelial cells to determine whether they directly interact with and stimulate the endothelial cells. Several attempts were

made to extract vascular endothelial cells *ex vivo* from mouse pinnae by adapting several methods employing various enzymes (trypsin, liberase, dispase and collagenase) in combination with differential centrifugation, or fluorescent cell sorting (van Beijnum 2008, Tae Cha 2005, Marelli-Berg 2000, Normand 1995). Unfortunately, no endothelial cells were gained using differential centrifugation, and only a small number of cells (31% purity) were extracted using anti CD31 cell sorting, which did not survive to culture. More work is needed to refine the techniques. Therefore, for the remainder of the cell experiments with 0-3hRP, HUVECs were used as a substitute as they are robust and easy to culture.

6.4.3 0-3hRP stimulates fibroblast migration

As discussed the cercariae will cause considerable damage to the structure of the skin (1.1.2). The dermis of 4x pinnae thickens and there is up-regulation of MMPs and growth factors (Chapter 3), to restore the pinnae structure the damage must be healed. An essential step in wound healing is the deposition of ECM by fibroblasts (Eckes 2000). It has been shown that T-cells cultured with SEA can induce fibroblast migration and proliferation. This is due to the release of a fibroblast activating protein by the stimulated T-cells (Lammie 1986).

To determine whether 0-3hRP can directly induce fibroblast activation an *in vitro* wound assay was utilised. Although this is only a basic *in vitro* model of wound healing it is a useful tool in first assessing the potential of a test substance (Rodriguez 2005). Addition of 0-3hRP to scratched fibroblast monolayers caused the cells to proliferate and migrate across the wound quicker than in media alone. This suggests that 0-3hRP may contain a factor which directly stimulates the fibroblasts, inducing either proliferation alone or proliferation and migration.

Transcript analysis of 0-3hRP stimulated fibroblasts could be undertaken to determine whether they up-regulate the expression of growth factors or cytokines, which may contribute to the environment seen in the skin following infection. An additional further experiment would be to determine if 0-3hRP

could affect the speed of wound healing *in vivo* by the addition of 0-3hRP to incisional wounds in mice. These experiments were planned but due to availability and time restraints were unable to be performed within this project and the *in vitro* assay serves only as a basic model hypothesising some fibroblast simulation by the 0-3hRP.

6.4.4 0-3hRP induces cell endothelial proliferation and branching

Angiogenesis requires mature vessels to become permeable and for the endothelial cells to proliferate and form into new tubes which eventually develop a lumen and mature (Carmeliet 2000). Co culture of HUVECs and 0-3hRP was undertaken to determine if 0-3hRP could induce endothelial cell proliferation or branching. Both branching and proliferation assays are commonly used as *in vitro* markers of angiogenic processes although they do not conclusively prove a substance can induce angiogenesis *in vivo* (Auerbach 2000). Culture with both SEA and 0-3hRP induced cell proliferation, although at higher concentrations of 0-3hRP proliferation was inhibited. As 0-3hRP contains a high level of proteases it was hypothesised that at higher concentrations the proteases may be damaging the cells. This appeared to be true as proliferation was restored by including a protease inhibitor in the culture.

This appears to be in contrast to research on the pro-angiogenic abilities of egg secretions. In previous studies, SEA induced proliferation was ablated after the antigen was pre boiled or incubated with proteinase K (El-Awady 2001), suggesting it to be a protein. A later study however identified a factor which was heat and protease resistant and produced by live eggs in culture stimulating vessel proliferation (Kanse 2005). The results here suggest that 0-3hRP induces proliferation of endothelial cells using a different mechanism than the eggs and is likely to be a growth factor homolog as opposed to a protease. *Caenorhabditis elegans* produces a PDGF/VEGF like ligand which is biologically active (Tarsitano 2006). In addition to growth factor homologs *Onchocerca* venom like antigens

induce an angiogenic response when injected into the cornea of mice. (Tawe 2000). Within the cercarial secretions are a series of venom allergen like genes which may be the factors promoting the endothelial cell proliferation (Chalmers 2008, Curwen 2006).

HUVECs were also cultured in plates coated with Matrigel to determine whether 0-3hRP can induce vessel branching. Endothelial cells respond to guidance cues to direct them to line up into tubes of cells connected to each other with vascular adhesion molecules including PECAM1 and VE-cadherin (Carmeliet 2000). Culture of the HUVECs with 0-3hRP induced small branches to form over the plate as seen with VEGF and SEA stimulated cells. Directional growth and the assembly of endothelial cells into vessels could potentially benefit the cercariae by increasing their chances of finding a vessel to extravasate through.

Several parasites require blood vessel growth, during the life cycle of *Trichinella spiralis* the larvae transform into a nurse cell-parasite complex contained in a collagenous capsule, which requires a continuous supply of nutrients in order to survive (Baruch 1991). Vessels are stimulated to grow into and surround the capsule through the secretion of an angiogenic factor by the nurse cell and stimulates the release of angiogenic factors from macrophages (Shariati 2009). Schistosome eggs induce vessel growth through up-regulation of endothelial cell produced VEGF (Loeffler 2002). Granulomas were considered to be avascular however many early granulomas are vascularised with the vessels regressing during maturation (Baptista 2005).

Closer examination of the endothelial cells after culture revealed structural changes in the cytoskeleton of the cells, and close association between individual cells. In cells cultured in media alone remained rounded with a small cytoplasm. After culture with stimulants the size of the endothelial cells increased and the cytoplasm swelled. This is characteristic of activated endothelial cells which have been stimulated by either a growth factor or cytokine (Cheville 1994). In addition, cells cultured with SEA and 0-3hRP developed long filopodia extensions.

These are a hallmark of activation and serve to contact endothelial cells to each other and follow guidance cues (De Smet 2009).

Vascular endothelium develops with a leading tip cell, these up-regulate expression of Notch1 and direct migration in response to VEGF and other growth factors (Hellström 2007). Additional labelling of the HUVEC cultures with antibodies to adhesion molecules would reveal whether the parasite secretions are inducing a tip cell morphology, as well as activating an angiogenic pathway. The cells in the stimulated cultures became long and thin increasing their contact surface area to each other and potentially developing cell to cell tight junctions, close electron microscopy would help to confirm this. The general morphology and change in the shape of the cells after culture with 0-3hRP is indicative of endothelial cell activation and branching, showing that cercarial secretions can induce blood vessel organisation into branches and strongly implies that the secretions can induce new vessel growth by direct interaction with the endothelial cells of the blood vessel.

6.4.5 0-3hRP induces blood vessel growth *in vivo*

The proliferation and branching assays are both *in vitro* models. To determine whether cercarial secretions can induce vessel growth within a mammal host, the Matrigel plug assay was used. This gelatinous protein mix is analogous to ECM, but can be kept liquid to allow growth factors to be integrated into it before setting into a solid plug. It has been widely used in tumour models and to test the angiogenic potential of known and hypothesised growth factors (Akhtar 2002, Cattaneo 2009, Murayama 2002).

Plugs containing just PBS showed no vessel growth, and did not affect the vessels of the body surrounding the plugs. As the plugs were introduced by injection there was minimal damage to the skin and no disturbance noticeable to the vessels of the skin or peritoneum. VEGF induced considerable growth into the Matrigel and also caused noticeable haemorrhaging around the plug. As VEGF

induces vessel permeability (Weis 2005) this is likely due to the continuous presence of VEGF from the plug next to the mature vessels of the skin and peritoneum. Both the SEA and 0-3hRP plugs also induced vessel growth into the plugs but without the noticeable vessel dilation seen in VEGF plugs. This suggests that the growth factor produced by the parasite is likely to not induce excessive vascular permeability and does not work in the same pathway as VEGF. 0-3hRP induced deep vessel growth into the plug confirming the hypothesis that the factor in the cercarial secretions could be acting as a guidance cue for the vessel growth.

Vessel growth in the plugs was rapid (plugs were excised at day 4 and day 7) indicating that the parasite secretions are acting quickly on the vessels. To determine whether the secretions could act in the time frame that the cercariae are within the skin further time points would need to be analysed. Additionally different concentrations of the cercarial 0-3hRP should be tested to determine if vessel growth can occur at lower concentrations or if the growth is an artefact of the concentration used in this assay.

The aim of the cercariae is to penetrate and progress out through into a blood vessel as quickly as possible. Whilst the cercariae could rely entirely on physical movement the production of a growth factor, and the proteases within the secretions, may aid the parasites passage through the skin and increase its chances of exit and survival into the blood stream. Release of proteases in the 0-3hRP is likely to degrade the ECM and release sequestered growth factors. But as the HUVEC cultures were completed without an ECM or additional growth factors than those found in the media, this data shows that the cercariae also produce a growth factor like molecule. This may activate the endothelial cells of the blood vessels prior to the cercariae reaching them aiding their transition into the vessel.

Endothelial cells can express Protease activated receptors (PARs) which are activated by extracellular proteases (Brass 1997). These may be activated by the

cercarial proteases and stimulate the endothelial cells. Further to this work PAR reporter cell lines could be tested with O-3hRP to determine if it activates the receptor, perhaps revealing an additional method of endothelial cell activation.

6.4.6 Summary

This chapter has shown that macrophages and dendritic cells primed with O-3hRP up regulate some angiogenic growth factors. Additional experiments using murine endothelial cells and O-3hRP primed macrophages will determine whether the immune cells, after exposure to parasite antigen, can directly interact with and induce angiogenic processes in the endothelial cells. In addition, the work here has shown that the cercariae directly induce endothelial cell activation and new vessel growth *in vitro* and *in vivo*. This appears to be through the production of a growth factor and not solely due to the proteases in the O-3hRP. Early studies with schistosome eggs have proposed a mechanism by which the eggs interact with the endothelial cells causing proliferation and migration of the cells over the surface of the egg, subsequently aiding in egg progression through the vessel wall (File 1995). It has also been observed that the vessels in which eggs are residing become dilated and torturous in chronic infections, due to continual stimulation and remodelling of the vessels (Nagy 1981, Freedman 1988). These morphological changes were also seen in the pinnae of mice in this study (Chapter 3) and the endothelial cell proliferation and migration data, although only a superficially model, presented in this chapter appears to suggest a similar mechanism.

Very little parasite and blood vessel interaction work has been done in recent years, as *S.mansoni* is a vessel dwelling parasite better understanding of its entry and exit from vessels would be beneficial to identifying life cycle stage targets for therapy. If cercariae and eggs are utilising similar methods to enter and exit vessels this provides a potential mechanism to target which could affect more than one stage during infection. In addition the lung stage somules are in close association with vasculature while they progress through the lung capillaries.

This is a tight space for the somules to navigate and whilst the presiding theory has been that the parasite pushes through using mechanical means they may produce a vessel-dilating factor or induce the expression of growth factors and cytokines in the lungs. Indeed it has been shown that induction of IL-13 by the lung somules increased fibrosis and lung vessel remodelling (Graham 2010). More work is needed to determine the exact mechanisms and the component of the O-3hRP responsible for the vessel growth and comparisons between gene expression during different life cycle stages may identify a common factor or family of factors responsible for vessel interactions.

Chapter 7: General Discussion

7.1 General Discussion

7.1.1 Overview

This study has shown visually and quantifiably that after infection with cercariae there is an up regulation of pro-angiogenic growth factors in skin. After multiple infections, growth factor levels were elevated and the predominant factors changed (Figure 7.1). Three growth factors were up regulated predominantly in the multiply infected skin; HGF, VEGF and PlGF. These are all angiogenic factors with wide ranging roles, HGF and PlGF are particularly associated with pathological angiogenesis (Seaman 2007, Bussolino 1992). The difference in growth factors appeared to be mainly due to the changes in the phenotype of leukocytes infiltrating into the dermis. Macrophages were a rich source of PlGF and eosinophils, the primary cell type in the 4x, expressed HGF (Figure 7.1). The appearance and structure of the blood vessels following 4x infection closely resembled that of tumour vasculature. Many of the vessels were dilated and twisted as is commonly seen with new vessels around tumours. As these vessels are continuously exposed to high levels of vasodilators and growth factors the tumour vasculature never fully matures and remains leaky (Carmeliet 2000). The morphology of the 4x vessels appears to be remarkably similar to that of tumour vasculature. The increased levels of growth factors, persisting to day 8 after infection, may present a similar situation in the 4x infected pinnae as that observed around tumours. To determine this, imaging with markers for pericytes and smooth muscle actin would help to determine the maturity state of the vessels.

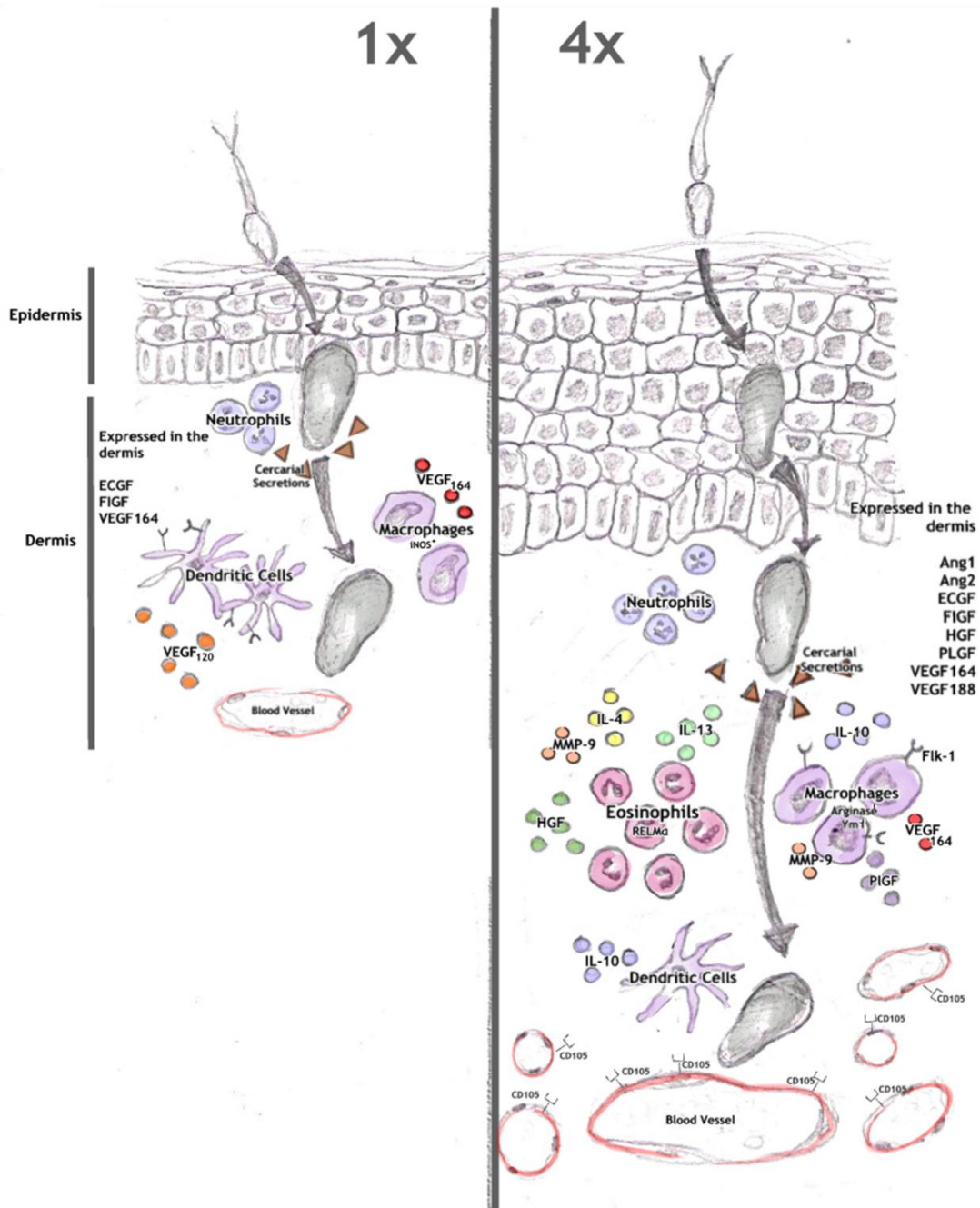


Figure 7.1: Overview of experimental model

Cercariae attach to the skin and penetrate into the epidermis, at this point the tail detaches. The somule migrates throughout the epidermis and release the contents of its acetabular glands. Early upon entry to the dermis neutrophils respond releasing pro-inflammatory cytokines. As the somule migrates macrophages and dendritic cells are recruited as well as eosinophils in the 4x pinnae. These cells express predominantly Th2 cytokines in the 4x and high levels of PIGF and HGF. The dermis of the 4x pinnae has increased dermal vasculature which is positive for the remodelling marker CD105.

Loss of IL-10 in the pinnae affected the structure of the 4x vessels unlike in the WT, vessels in the knock out were more organised and less distorted. There was also reduced eosinophil recruitment but up regulated the expression of HGF and PlGF, consistent with observations that these growth factors are up regulated in a pro inflammatory environment. In addition, it was shown that cercarial secretions can induce angiogenic phenotypes in the phagocytic leukocytes, macrophages and dendritic cells, through up regulation of PlGF. Finally, it was shown that the O-3hRP can directly activate endothelial cells. *In vitro* it was observed that O-3hRP induces endothelial cell proliferation and migration into tubes. *In vivo* new vessels grew into completely a vascular Matrigel plugs containing O-3hRP.

7.1.2 Pro-angiogenic growth factors in the skin following *S.mansoni* infection

Previous to this research, angiogenesis had only been associated with the egg stage of infection (Loeffler 2002, Freedman 1988). Indeed, previous studies using sonicated cercariae had shown little or no angiogenic potential (Kanse 2005). Combined with more recent data from this lab showing that cytokines associated with wound healing and angiogenesis were up regulated in the skin, particularly after 4x infection, it was hypothesised that angiogenesis could be occurring in response to the cercariae. The data presented within chapter 3 has confirmed this hypothesis and shown that pro-angiogenic genes are up-regulated in the skin following infection and in addition the vasculature of the pinnae visibly increases. This increase and the levels of growth factors were exacerbated after multiple infections.

Utilising imaging techniques widely used in cancer angiogenesis (Levashova 2010, Seshadri 2007) the vasculature was successfully labelled with a CD31mAb and imaged (Figure 3.4). This revealed an increase in the diameter and area of the vessels in the pinnae which was not due to increased vascular pressure. Increased vessel diameter could aid the schistosome egress from the skin. As schistosomula are approximately 50µm in diameter they can only exit via larger

vessels (Crabtree 1982). If vessel dilation and diameter increase are induced by the parasite antigens this could represent a way in which the schistosomes aid their own exit from the dermis into the blood vessel. This could be true for other stages in the life cycle, in particular maturation in the lung capillaries. Within the lungs the capillaries are difficult for the schistosomes to pass through. They reside here for a number of days and during this time may activate endothelial cells and induce vessel dilation to aid their passage. If this is true the parasitic factor which interacts with the vessels in the skin may be conserved across the life cycle stages.

Whilst images of the dermal vasculature were clear and relatively easier to produce, no images of the parasite and the vessels were successfully taken. Antibody labelling of the parasite was accomplished (Figure 7.2) but no clear picture was obtained with the confocal techniques available. A better technique using would be Optical projection tomography producing a 3D reconstruction of the entire vasculature of the pinnae (Oldham 2006).

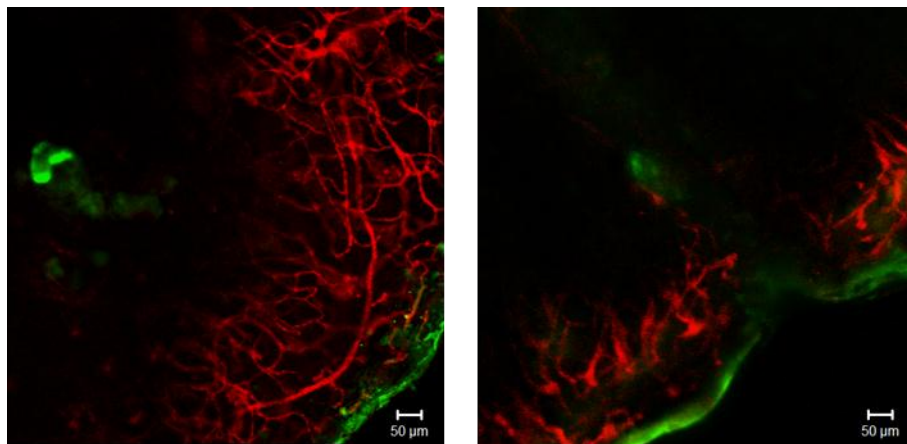


Figure 7.2 Parasite and Blood vessel imaging

Pinnae were labelled with α CD31-APC (Red) and serum antibodies to cercariae and a secondary antibody conjugated to AF488 (Green). Images were taken using a confocal microscope using the same method for α CD31 labelling (Chapter 2).

Reconstruction of entire pinnae, with both vessels and parasites labelled, may help to determine which vessels the parasite interacts with and whether the small fine bundles of vessels are surrounding a parasite in the skin. Trapped parasites may release secretions to encourage vessels growth towards their position in the skin in a similar way to *Onchocerca volvulus* whose larvae are deposited in the skin where they undergo developmental stages and actively encourage new vessels growth towards the developing larvae to help provide the nutrients for development (Higazi 2003).

Angiogenesis is influenced by a wide array of growth factors with several families showing overlapping functions. To narrow down the gene families activated after infection a Q-PCR based gene array was utilised. Whilst several of the results were unreliable, the array did give a general impression that pro-angiogenic growth factors were induced following infection with many of these peaking earlier in the 4x pinnae when compare to 1x pinnae. PlGF and HGF were up-regulated significantly in only the 4x pinnae and both are strongly associated with pathological angiogenesis and inflammation (Seaman 2007, Xin 2001). They are often up regulated in fibrotic conditions, e.g. asthma and may be the driving factors in the considerable thickness seen in the skin. They are likely to influence the considerable scarring and damage to the external layers of the skin observed in whole pinnae imaging. HGF in particular promotes the growth of scar tissue and can be found in Keloid scars (Mukhopadhyay 2010).

This increase in scarring and thickness was one of the most noticeable differences between the 1x and 4x pinnae. The thickness could also be from excessive collagen deposition as MMP-9 persisted at an increased level compared to the naïve until day 8. This suggests continual remodelling of the collagen. Pinnae sections were analysed following trichrome staining (which marks collagen in blue), unfortunately as the skin is very collagen dense it was hard to discern any differences.

The increase in the number and width of the dermal vessels could aid the parasites escape from the skin. To determine the functional effect of

angiogenesis following infection, manipulation of the angiogenic pathways would be necessary. Attempts to inhibit angiogenesis in the skin during infection were made using endostatin (data not shown). Unfortunately, insufficient endostatin could be purchased for a full scale experiment within the constraints of this project and delivery into the skin was difficult. Specific antibody blocking of VEGF receptors and Met (the HGF receptor) would help to determine the phenotypic changes each of these growth factors is responsible for in the 4x pinnae. Blocking of angiogenesis, and in particular the vascular leakage, could affect the migration of the schistosome larvae through the host. Infection in Ang1 overexpressing mice which have leakage resistant vasculature (Thurston 1999) may result in significant numbers of the cercariae being trapped in the skin.

7.1.3 Pro-angiogenic leukocyte influx

The differences in the growth factor expression between 1x and 4x were at least partly due to changes in the DEC phenotype. As previously described after multiple infections with RA cercariae and the bird schistosome *T.regenti* there was an increase in Th2 cytokines (IL-4, IL-13 and IL-10) in 4x pinnae. This was accompanied by a significant increase in dermal leukocytes, containing predominately eosinophils (Chapter 4), these were the main source of the HGF. The combination of cytokines and eosinophils gives the 4x pinnae an asthma type phenotype. Asthma is a condition characterised by excessive tissue damage and exaggerated repair in the lungs during which there is an increase in the number and size of bronchial blood vessels. Lung tissue contains high levels of IL-4, IL-13, MMPs and VEGF alongside significant eosinophil influx. The 4x skin shows a very similar profile of cells and cytokines. The eosinophil influx may be the cause of much of the excessive damage to the skin and the persistence of both HGF and MMPs. 4x infection in an eosinophil knockout would be an ideal method to test how much of the angiogenesis in 4x pinnae is due to the eosinophil influx. As the eosinophils are the main producers of the HGF and IL-13 it would be predicted that the tissue damage and remodelling would be decreased.

The 4x macrophages are the source of PlGF in the DEC. Infections in IL-10^{-/-} mice showed a loss of Ym1 and a significant increase in PlGF. This could indicate that the IL-10 in the multiple infection is regulating the expression of PlGF by the macrophages reducing their inflammatory ability. The loss of IL-10 did not affect IL-4 levels but did result in the complete loss of IL-13. This indicates that the Ym1 expression in the macrophages was not IL-4 dependant but instead could be IL-10 or IL-13 induced. IL-4 itself is widely regarded as anti angiogenic but does induce angiogenic phenotypes in several cells (Mantovani 2002). The 1x/4x infection model was tested in IL-4Rα^{-/-} mice whilst this research was on going (Cook 2011). The pinnae of IL-4Rα^{-/-} mice had reduced eosinophilia and significantly reduced expression of alternatively activated macrophage markers, Arginase-1 and Ym-1. As the IL-4Rα^{-/-} mice will be unable to respond to both IL-13 and IL-4 these studies did not conclude whether Ym-1 expression is IL-4 or IL-13 controlled. In the future IL-4^{-/-} and/or IL-4Rα^{-/-} mice could be subjected to the multiple infection model and the growth factor levels analysed within the whole pinnae and DEC. Loss of IL-4 may reduce the expression of pro-angiogenic genes from the DEC, in particular the macrophages (Gordon 2003).

One cytokine not analysed within this study was TGFβ, as it is only active after a series of cleavage steps, PCR is not an accurate way to measure levels. A TGFβ reporter cell line was utilised to measure bioactive levels of the cytokine however only a small number of supernatants were tested (data not shown). This revealed a slight increase between naïve and 1x and 1x and 4x, although due to the small sample size this was not significant. A more thorough study of TGFβ would be prudent in the future as it has significant angiogenic abilities (Pepper 1997, Viñals 2001, Wakefield 2002) and could also compensate for the loss of IL-10 in the 4x resulting in the less severe phenotype seen than expected.

One cell type not thoroughly explored in this study was the neutrophil. Although not as well associated with angiogenesis as macrophages or eosinophils, neutrophils are an emerging cell type in the initiation and control of angiogenesis

(Gaudry 1997, Ardi 2007, Piccard 2011). Like macrophages, neutrophils have recently been proposed to have several alternative activation states – N1 and N2 in addition to tumour associated neutrophils (TAN). TGF β is proposed to induce a pro-tumoral phenotype in neutrophils by up-regulating Arginase, VEGF and MMP-9 whilst down regulating TNF- α expression; N2 neutrophils. In contrast neutrophils activated with Interferon beta (IFN β) express TNF- α and no pro-angiogenic growth factors (Piccard 2011). This is currently a simplified explanation of neutrophil polarisation and IL-10 has also been instigated as a mediator of this phenotypic switch (Moore 2001). Neutrophils are recruited early after cercarial penetration and infiltrate into both the dermis and epidermis (Iceni 1984, Hogg 2003). The angiogenic phenotype of these cells may be different between 1x and 4x pinnae and could either directly induce early vessel branching and/or activate further angiogenic pathways up-regulating angiogenesis. Analysis of cDNA from sorted neutrophils could be used to determine the pro-angiogenic phenotype and any differences between the 1x and 4x pinnae.

7.1.4 0-3hRP induced angiogenesis

Coinciding with the culmination of this research, several reviews on angiogenesis in parasite infections have hypothesised that parasites may induce this neovascularisation for their own benefit (Dennis 2011).

Chapter 6 tested the angiogenic potential of 0-3hrRP in several well described angiogenic assays (Akhtar 2002, Poulaki 2011). Endothelial cells cultured with 0-3hRP became activated, both proliferating and migrating into vessel structures.

The working hypothesis for this chapter was that the increase in pro-angiogenic growth factors in the skin was due to 0-3hRP degradation of the ECM releasing bound growth factors. This is likely to be one mechanism by which the growth factor levels are increased *in vivo* after schistosome penetration. The physical movement of the parasite may also induce activation of the MMP pathways. However, the assays used in this chapter indicated that the secretions alone

without the presence of ECM could induce angiogenesis. Endothelial cell proliferation assays in the presence of the inhibitor revealed that 0-3hRP contains a factor other than a protease which can activate the endothelial cells. To determine whether 0-3hRP has homology to a known growth factor, and signals through known receptors, the growth factor pathways activated in the endothelial cells must be identified. Unfortunately these experiments could not be completed with murine dermal endothelial cells as extraction of the cells from the pinnae was relatively unsuccessful. Only a 30% pure population was achieved through cell sorting and these did not survive subsequent cells culture. Endothelial cells can vary widely in their phenotype between tissue sites (Jackson 1997, Chi 2003). As such HUVECs may have a different panel of receptors expressed compared to murine dermal endothelial cells (mdECs). Therefore, some of the features seen after HUVEC culture with 0-3hRP may not be induced in mdECs, conversely mdECs may be more responsive to 0-3hRP than HUVECs.

Administration of 0-3hRP directly into the skin of mice would show whether the secretions alone can induce all or some of the pro-angiogenic factors detected in the dermis following infection. However the method of administration would have to be simple and cause as little wounding as possible, as growth factors would be released upon damage to the skin and may cloud any observations. A less invasive technique could be the use of micro needles (Prausnitz 2004, Henry 2000, Gill 2006). Needles coated in 0-3hRP would deliver the secretion thoroughly through the skin and cause limited damage. A negative control, e.g. PBS, would have to be administered to a second set of mice to control for any damage following the infection.

Within this study however an alternative method was used to determine whether 0-3hrRP induces *de novo* vessel growth although this was not within the skin. Matrigel plugs containing 0-3hrRP were implanted into mice using a single fine needle and no surgery thereby limiting the damage caused. These showed vessel growth into the plugs which was absent in the PBS only plugs. VEGF and SEA plugs also induced vessel growth. This *in vivo* experiment was strong

evidence of a molecule within the 0-3hRP and SEA which can induce directional growth of new vessels into an avascular region.

The up-regulation of growth factors and matrix metalloproteinases alongside direct induction of endothelial cells suggests that 0-3hRP could be useful in inducing wound healing mechanisms. 0-3hRP was added to fibroblasts after the monolayer had been scratched. This increased the migration of the fibroblasts and closed the wound in the monolayer more rapidly than those cultured in media alone. To determine more accurately whether 0-3hRP can induce wound healing it would be applied to incisional wounds in murine skin. The speed of wound closure and histological analysis of the wounds would reveal whether 0-3hRP was accelerating the process. If it does increase fibroblast activation it or the component which induces this within the secretions could have potentially used as a therapeutic to aid in non healing wounds.

7.1.5 Summary

In conclusion, work in the thesis has shown that the passage of the cercariae through the skin does induce new vessel growth. This could be by one or more of three potentially overlapping mechanisms: Wound healing, innate immunity induction or direct endothelial activation by parasite secretions. The hypothesis prior to the beginning of this work was that the cercariae would cause considerable damage during penetration of the skin and with this induce wound healing responses. This appears to be true, but additionally after multiple infections, it was shown that the angiogenic response in the skin changed. This was because of an increase in a different profile of growth factors which seems to be due in part by a change in the immune cells recruited to the dermis. The final part of this thesis showed that the cercariae themselves can induce new vessel growth. More work is needed to determine what the factor within the 0-3hRP is which induces the growth and if possible to purify a sample to test in further assays. Overall, multiple infections with cercariae provide an interesting model to study angiogenesis induction following parasite infection. Interestingly,

0-3hRP may present a novel substrate which could induce angiogenesis and wound healing. If the precise component of the 0-3hrRP which induces angiogenesis and fibroblast proliferation could be isolated it may present a possible therapeutic in the treatment of slow and non-healing wounds and could have clinical applications.

Appendix

Section 1 - Primer Pairs, cycle numbers and annealing temperatures

Gene	Forward Sequence	Reverse Sequence
Ang 1	GATCTTACACGGTGCCGATT	TTAGATTGGAAGGGCCACAG
Ang 2	CTTAAGCCTGCACCGCTAAC	CTGAACTCCCACGGAACATT
CD105	GCTGAAGACACTGACGACCA	CCATGTCGATGCACTGTACC
ECGF1	CCTTCGCTGAACTTGTCTC	CCCTAGAGCCAGTAGCATCG
Flk-1		
Figf	CTGAACAACAGATCCGAGCA	TGCTGAGCGTGAGTCCATAC
FGF 1	TTCATTCATGAGGCCTTCC	ATGCAGTACCCCTGGAGTTG
FGF 2	AGCGGCTCTACTGCAAGAAC	TATGAAGGAAGATGGACGGC
FGF 6	GGCCCTGTGCATAAGAAAAA	CAATCCTGCTGACTCGACAA
HGF	TCCCAGCTGGTCTATGGTC	TGGTGCTGACTGCATTTCTC
MMP-2	AACTGGGACCTGTCACTCC	TGCTACTGTCCGCCAAATAA
MMP-9	CCCAGAGGTAACCCACGTCA	CACACGCCAGAAGAATTTGC
MMP-19	TGAGGAGGAAGAGACCGAGA	CCAAAGGGCAGATATTTGGA
PIGF	TGCTGGTCATGAAGCTGTTC	ACCCACACTTCGTTGAAAG
Tie 2	AAGCATGCCATCTGGTTAC	GTAGGTAGTGGCCACCCAGA
VEGF	CAGGCTGCTGTAACGATGAA	CTTGGCGATTTAGCAGCAGA
COX2	AGAAGGAAATGGCTGCAGAA	CCCCAAAGATAGCATCTGGA
Arginase-1	TCACCTGAGCTTTGATGTCG	CTGAAAGGAGCCCTGTCTTG
	Probe	TTCTGGGAGGCCTATCTTACAGAGAAGGTCTCTAC
RELM α	TGCTGGGATGACTGCTACTG	CTGGGTTCTCCACCTCTTCA
	Probe	CAAGATCCACAGGCAAAGCCACAA
Ym1	CTCAATATACACAGTCAAGTTG	TGGGATTCAATTTAGGAAAGTTCA
	Probe	TCCACAGTGCATTCTGCATCATGCT
iNOS	CTGCATGGACCAGTATAAGG	CTAAGCATGAACAGAGATTTCTTC
	Probe	AGTCTGCCATTGCTG
GAPDH	CCATGTTTGTGATGGGTGTG	CCTTCCACAATGCCAAAGTT
	Probe	CATCCTGCACCACCAACTGCTTAGC

Gene	Cycle number	Annealing Temperature °C
Ang 1	32	60
Ang 2	32	60
CD105	30	60
ECGF1	30	60
Flk-1	32	63
Figf	30	60
FGF 1	30	60
FGF 2	30	60
FGF 6	30	60
HGF	30	60
MMP-2	30	60
MMP-9	28	60
MMP-19	30	60
PIGF	30	61
Tie 2	30	60
VEGF	29	60
COX2	30	60
Arginase-1	50	60
RELM α	50	60
Ym1	50	60
iNOS	50	60
GAPDH	26(SQ-PCR)/50 (Q-PCR)	60

Section 2 - Raw data from array analysis

The numbers shown are the relative quantification compared to naïve (Naïve was set to 1)

Gene	d1	d2	d4	d1	d2	d4
Alanyl (membrane) aminopeptidase	4.31	1.39	2.49	1.02	2.17	0.40
Angiopoietin 1	1.43	0.89	0.67	2.59	1.81	1.20
Angiopoietin 2	2.01	0.70	0.57	2.65	1.57	1.37
Brain specific angiogenesis inhibitor 1	2.70	0.62	2.59	5.86	1.84	8.28
Cadherin 5	3.13	0.99	2.40	5.49	3.08	1.82
CCL11	X	14.05	10.71	19.26	1.00	0.85
CCL2	1.86	1.10	1.27	1.95	1.15	0.73
C-fos induced growth factor	1.20	1.07	1.24	1.07	0.99	0.63
Coagulation factor 2	0.11	0.67	0.47	0.99	1.21	0.25
Colony stimulating factor 3	0.05	1.37	0.14	0.10	3.21	0.01
Connective tissue growth factor	0.02	0.82	0.12	0.07	0.68	0.00
CXCL1	0.69	25.40	0.30	0.32	13.27	0.07
CXCL2	1.26	56.72	1.43	6.44	134.29	0.13
CXCL5	0.03	9.08	0.50	3.42	43.67	0.01
Endoglin	0.13	1.28	0.90	3.56	3.67	1.00
Endothelial cell growth factor 1	0.01	0.96	0.09	0.03	0.82	0.01
Endothelial differentiation gene 1	2.15	0.71	1.21	1.34	0.47	1.71
Endothelial PAS domain protein 1	0.06	1.10	0.00	0.14	0.62	0.01
Eph receptor B4	3.33	0.96	2.49	4.66	1.34	5.01
Ephrin A1	1.15	1.11	0.86	2.71	1.40	0.47
Ephrin B2	0.80	0.69	0.32	0.87	0.46	0.21
Epidermal Growth factor	0.04	0.80	0.01	0.06	0.73	0.00
Epiregulin	0.01	1.03	0.00	0.03	0.62	0.00
Fibroblast growth factor 1	1.75	0.97	1.74	5.96	2.47	5.70
Fibroblast growth factor 2	4.27	1.06	1.46	1.33	1.14	0.97
Fibroblast growth factor 6	1.45	0.98	0.90	0.67	0.64	0.44
Fibroblast growth factor receptor 3	0.58	1.43	0.49	1.01	3.54	0.47

Fizzled homolog 5	1.60	0.83	0.83	0.47	0.35	0.27
FMS-like tyrosine kinase 1	0.14	0.85	0.16	0.12	2.26	0.02
Guanine nucleotide binding protein α 13	0.10	1.04	0.19	0.09	1.47	0.03
Heart and neural crest derivatives expressed transcript 2	0.17	1.09	1.00	0.37	1.26	0.12
Hepatocyte growth factor	0.27	1.18	0.35	0.21	1.30	0.05
Hypoxia inducible factor 1 α	0.63	0.85	1.56	1.39	2.76	1.92
Insulin-like growth factor 1	0.03	1.30	0.18	0.23	4.54	0.04
Integrin alpha V	0.00	1.51	0.02	0.00	2.16	0.00
Integrin beta 3	1.61	2.29	2.07	5.80	5.40	5.30
Interferon gamma	0.75	0.69	1.34	0.73	1.06	0.67
Interleukin 1 beta	1.82	22.60	1.55	7.86	66.03	0.80
Interleukin 6	0.03	1.89	0.19	0.12	8.80	0.02
Jagged 1	1.43	0.68	1.41	1.11	0.43	0.82
Kinase insert domain receptor	1.80	0.87	2.44	5.94	1.48	3.40
Laminin alpha 5	0.17	0.75	0.50	0.37	0.49	0.19
Leptin	0.16	0.87	0.99	0.89	0.97	0.21
Leukocyte cell derived chemotaxin 1	0.21	0.78	0.34	0.25	0.96	0.21
MAD homolog 5	0.05	0.82	0.23	0.05	0.40	0.01
Matrix metalloproteinase 19	0.01	0.59	0.14	0.04	0.28	0.01
Matrix metalloproteinase 2	1.07	0.77	1.79	1.92	0.68	1.26
Matrix metalloproteinase 9	0.87	1.01	1.71	1.32	1.19	0.72
Midkine	0.62	1.68	0.64	4.88	3.80	2.08
Mitogen activated protein kinase 14	0.03	0.84	0.05	0.04	0.94	0.05
Natriuretic peptide receptor 1	0.61	2.50	0.18	1.04	10.28	0.96
Neuropilin 1	0.94	0.83	1.22	2.16	0.92	1.48
Neuropilin 2	0.43	0.74	0.47	0.76	1.22	0.68
Placental Growth factor	0.01	1.08	0.02	0.03	1.73	0.01
Plasminogen	2.19	0.73	1.65	1.68	0.54	2.09
Plasminogen activator urokinase	0.02	2.14	0.05	0.07	7.56	0.02
Platelet/ Endothelial cell adhesion molecule 1	1.08	0.66	1.06	3.11	1.66	2.34
Platelet derived growth factor alpha	X	1.35	0.00	0.00	2.20	0.00

Plexin domain containing 1	X	1.04	0.02	0.03	3.33	0.08
Pro collagen type IV alpha 3	1.12	0.82	1.20	1.28	0.60	1.99
Pro-collagen type XVIII alpha 1	0.11	0.83	0.24	0.12	0.45	0.01
Prostaglandin - endoperoxide synthase 1	0.00	0.27	0.00	0.00	0.96	0.00
Serine (or cysteine) peptidase inhibitor, Clade F, member 1	0.03	1.14	0.13	0.13	0.96	0.09
Sphingosine kinase 1	0.00	0.79	0.02	0.00	0.47	0.00
Stabilin 1	0.53	1.08	0.48	0.70	11.62	0.03
T-box 1	0.00	0.98	0.00	0.00	1.21	0.00
T-box 4	0.00	1.47	0.00	0.01	2.54	0.00
Thrombospondin 1	2.07	0.78	1.33	1.38	0.60	1.66
Thrombospondin 2	0.00	1.07	0.04	0.02	3.41	0.04
Tissue inhibitor of metalloproteinase 1	0.13	0.57	0.19	0.09	0.35	0.16
Tissue inhibitor of metalloproteinase 2	0.32	0.57	0.58	0.29	0.31	0.37
Transforming growth factor alpha	0.53	0.67	0.66	0.50	0.78	0.92
Transforming growth factor β 1	0.00	0.86	0.00	0.00	0.55	0.01
Transforming growth factor β 2	0.05	0.72	0.01	0.07	1.29	0.45
Transforming growth factor β 3	1.47	1.09	1.64	3.66	1.71	3.90
Transforming growth factor β 1	0.25	0.89	0.60	1.00	1.81	1.40
Trans-membrane serine protease 6	1.91	1.52	1.35	2.82	2.31	3.23
Tumour necrosis factor (ligand) superfamily member 12	1.08	1.11	1.10	2.10	1.49	2.40
Tumour necrosis factor α	0.01	0.70	0.04	0.02	0.63	0.26
Tumour necrosis factor α - induced protein 2	1.33	0.83	0.91	1.42	1.43	2.05
Tyrosine-protein kinase receptor	0.01	0.90	0.01	0.01	0.85	0.00
Vascular growth factor A	0.07	0.71	0.08	0.02	0.83	0.56
Vascular growth factor B	0.00	1.00	0.02	0.01	1.42	0.12
Vascular growth factor C	0.06	0.88	0.20	0.10	1.75	0.22

Abbreviations

0-3hRP	0-3 hour released preparation
AAM ϕ	Alternatively activated macrophage
Ang1	Angiopoetin 1
Ang2	Angiopoetin 2
APC	Allophycocyanin
Arg-1	Arginase-1
BSA	Bovine serum albumin
CCL	Chemokine (C-C) motif ligand
COX2	cyclooxygenase isoenzyme
CXCL	Chemokine (C-X-C) motif ligand
DEC	Dermal exudate cell
DEPC	Diethylpyrocarbonate
DMEM	Dulbecco's modified Eagle's medium
DNA	deoxyribonucleic acid
EC	Endothelial cell
ECM	Extracellular Matrix
ELISA	Enzyme linked immunosorbent assay
FGF	Fibroblast growth factor
FIGF	c-fos inducible growth factor
FITC	Fluorescein isothiocyanate
Flk-1	Foetal liver kinase 1
Flt-1	fms-related tyrosine kinase 1
Flt-4	fms-related tyrosine kinase 4
GM-CSF	Granulocyte-macrophage colony-stimulating factor
H&E	hematoxylin and eosin
Hand2	Heart and neural crest derivatives
HGF	Hepatocyte growth factor
HIF-1	Hypoxia inducible factor 1
HRP	Horseradish peroxidase
HUVEC	Human umbilical vein endothelial cells
IFN γ	Interferon gamma
IgG1	Immunoglobulin G1
IL-10 ^{-/-}	Interleukin 10 deficient mice
IL-X	Interleukin- X
iNOS	inducible nitric oxide synthase
L-Glut	L-Glutamine
LPS	Lipopolysaccharide
MIP1 α	Macrophage inflammatory protein 1 alpha
MMP-X	Matrix Metalloproteinase -X
MR	Mannose receptor
PAF	Platelet-activating factor
PBMC	Peripheral blood mononuclear cells
PBS	Phosphate buffered saline

PBST	Phosphate buffered saline + TWEEN20
PCR	Polymerase chain reaction
PDGF	Platelet derived growth factor
PE	Phycoerythrin
PECAM-1	Platelet endothelial cell adhesion molecule -1
Pen/Strep	Penicillin/Streptomycin
PIGF	Placental growth factor
Q-PCR	Quantitative polymerase chain reaction
RA	Radiation attenuated
RELM α	Resistin like molecule alpha
RNA	Ribonucleic acid
RPMI	Roswell Park Memorial Institute medium
SEA	Soluble egg antigen
SMC	Smooth muscle cell
SQ-PCR	Semi quantitative polymerase chain reaction
TGF β	Transforming growth factor beta
Th	T helper cell type
Tie2	Tyrosine-protein kinase receptor 2
TLR	Toll like receptor
TMB	3,3',5,5'-Tetramethylbenzidine
TNF- α	Tumour necrosis factor - α
VE-Cadherin	Vascular endothelial cadherin 1
VECAM-1	Vascular endothelial cell adhesion protein 1
VEGF	Vascular endothelial growth factor
WT	Wild Type

References

- Adini, A. et al. 2002. Placental growth factor is a survival factor for tumour endothelial cells and macrophages. *Cancer Research*. **62**: 2749
- Aghajanian, A. et al. 2008. Endothelial cell junctions and the regulation of vascular permeability and leukocyte transmigration. *Journal of Thrombosis and Hemostasis*. **6**:1453
- Aihua, L. et al. 2003. IL-8 Directly Enhanced Endothelial Cell Survival, Proliferation, and Matrix Metalloproteinases Production and Regulated Angiogenesis. *The Journal of Immunology*. **170**:3369
- Akhtar, N. et al. 2002. The sponge/Matrigel angiogenesis assay. *Angiogenesis*. **5**:75
- Albanesi, C. et al. 2005. Keratinocytes in inflammatory skin diseases. *Current Drug Targets – Inflammation & Allergy*. **4** :329
- Allen, J.E. and T.A, Wynn. 2011. Evolution of Th2 immunity: A rapid repair response to tissue destructive pathogens. *PLoS Pathogens*. **7**:e1002003
- Angeli, V., et al. 2001. Role of parasite-derived prostaglandin D2 in the inhibition of epidermal Langerhans cell migration during Schistosomiasis infection. *The Journal of Experimental Medicine*. **193**:1135
- Anthony, R.M. 2006. Memory Th2 cells induce alternatively activated macrophages to mediate protection against nematode parasites. *Nature Medicine*. **12**:955
- Aplin, A.C. et al. (2006) Angiopoietin-1 and vascular endothelial growth factor induce expression of inflammatory cytokines before angiogenesis. *Physiological Genomics* **27**:20
- Ardi, V.C. et al. 2007. Human neutrophils uniquely release TIMP-free MMP-9 to provide a potent catalytic stimulator of angiogenesis. *Proceedings of the National Academy of Sciences*. **104**:20262
- Assoian, R.K. et al. 1987. Expression and secretion of type beta transforming growth factor by activated human macrophages. *Proceedings of the National Academy of Sciences*. **84**:6020
- Auerbach, R. et al. 2000. Angiogenesis assays: Problems and pitfalls. *Cancer and Metastasis Reviews*. **19**:167

Ausprunk, D.H and J, Folkman. 1977. Migration and proliferation of endothelial cells in preformed and newly formed blood vessels during tumour angiogenesis. *Microvascular Research*. **14**:53

Autiero, M. et al. 2003. Placental growth factor and its receptor, vascular endothelial growth factor receptor-1: novel targets for stimulation of ischemic tissue revascularization and inhibition of angiogenic and inflammatory disorders. *The Journal of Thrombosis and Haemostasis*. **1**:1356

Banchereau, J. et al. 2000. Immunobiology of dendritic cells. *Annual review of Immunology*. **18**:767

Bandeira-Melo, C. et al. 2002. IL-16 promotes leukotriene C(4) and IL-4 release from human eosinophils via CD4- and autocrine CCR3-chemokine-mediated signalling. *The Journal of Immunology*. **168**: 4756

Baptista, A.P. and Z.A, Andrade. 2005. Angiogenesis and schistosomal granuloma formation. *Memórias do Instituto Oswaldo Cruz*. **100**:183

Barleon, B. et al. 1996. Migration of human monocytes in response to vascular endothelial growth factor (VEGF) is mediated via the VEGF receptor flt-1. *Blood*. **87**:3336

Baruch, A.M. and D.D. Despommier. 1991. Blood vessels in *Trichinella spiralis* infections: a study using vascular casts. *The Journal of Parasitology*. **77**:99

Behm, C.A. and K.S. Ovington. 2000. The role of eosinophils in parasitic helminth infections: insights from genetically modified mice. *Parasitology Today*. **16**:202

Bos, J.D, et al. 2005. Psoriasis: Dysregulation of innate immunity. *British journal of Dermatology*. **152**:1098

Bottaro, D.P. et al. 1991. Identification of the Hepatocyte Growth Factor Receptor as the *c-met* proto-oncogene product. *Science*. **251**:802

Bottomley, M.J, et al. 1999. Peripheral blood mononuclear cells from patients with rheumatoid arthritis spontaneously secrete vascular endothelial growth factor (VEGF): specific up-regulation by tumour necrosis factor-alpha (TNF- α) in synovial fluid. *Clinical and Experimental Immunology*. **117**:171

Brass, L.F. and M. Molino. 1997. Protease-activated G protein-coupled receptors on human platelets and endothelial cells. *Journal of Thrombosis and Haemostasis*. **78**:234

- Brindle, N.P.J, et al. 2006. Signalling and functions of Angiopoetin-1 in vascular protection. *Circulation Research*. **98**:1014
- Brogi, E.T, et al. 1994. Indirect angiogenic cytokines up regulate VEGF and bFGF gene expression in vascular smooth muscle cells, whereas hypoxia up regulates VEGF expression only. *Circulation*. **90**:649
- Busse, W.W. and J.B. Sedgwick. 1992. Eosinophils in asthma. *Annals of Allergy, Asthma & Immunology*. **68**:286
- Bussolino F, et al. 1992. Hepatocyte growth factor is a potent angiogenic factor which stimulates endothelial cell motility and growth. *The Journal of Cell Biology*. **19**:629
- Byzova, V. et al. 2002. Adenovirus encoding vascular endothelial growth factor-D induces tissue-specific vascular patterns in vivo. *Blood*. **99**:4434
- Caldas. I.R, et al. 2000. Susceptibility and resistance to *Schistosoma mansoni* reinfection: parallel cellular and isotypic immunologic assessment. *The American Journal of Tropical Medicine and Hygiene*. **62**:57
- Camussi, G. et al. 1997. Angiogenesis induced in vivo by hepatocyte growth factor is mediated by platelet-activating factor synthesis from macrophages. *The Journal of Immunology*. **158**:1302
- Carmeliet, P. et al. 1996. Abnormal blood vessel development and lethality in embryos lacking a single vascular endothelial growth factor allele. *Nature*. **380**:435
- Carmeliet, P. 2000. Mechanisms of angiogenesis and arteriogenesis. *Nature Medicine*. **6**:389
- Carmeliet, P and R.K, Jain. 2000. Angiogenesis in cancer and other diseases. *Nature*. **407**:249
- Carmeliet, P. et al .2001. Synergism between vascular endothelial growth factor and placental growth factor contributes to angiogenesis and plasma extravasation in pathological conditions. *Nature Medicine*. **7**:575
- Carmeliet, P. 2003. Angiogenesis in health and disease. *Nature Medicine*. **9**:653
- Carmeliet, P. 2005. VEGF as a key mediator of angiogenesis in cancer. *Oncology*. **69**:s3
- Caulada-Benedetti, Z. et al. 1991. Comparison of Th1- and Th2-associated immune reactivities stimulated by single versus multiple vaccination of mice with irradiated *Schistosoma mansoni* cercariae. *The Journal of Immunology*. **146**:1655

- Cella, M. et al. 1997. Origin, maturation and antigen presenting function of dendritic cells. *Current Opinion in Immunology*. **9**:10
- Ch'ang, L. Y. and D.G, Colley. 1986. Cutaneous sensitivity induced by immunization with irradiated *Schistosoma mansoni* cercariae. II. Autoimmunoregulation of cell-mediated cutaneous sensitivity and its reversal. *Cellular Immunology*. **100**: 129
- Chalmers, I.W. et al. 2008. Developmentally regulated expression, alternative splicing and distinct sub-groupings in members of the *Schistosoma mansoni* venom allergen-like (SmVAL) gene family. *BMC genomics*. **9**:89
- Cheville, N.F. 1994. Ultrastructural Pathology: An Introduction to interpretation. Chapter 8 – Vascular tissue. Wiley-Blackwell. 337
- Chi, J.T. et al. 2003. Endothelial cell diversity revealed by global expression profiling. *PNAS*. **100**:10623
- Chitsulo, L. et al. 2000. The global status of Schistosomiasis and its control. *Acta Tropica*. **77**:41
- Chiquet, M. et al. 2003. How do fibroblasts translate mechanical signals into changes in extracellular matrix production? *Matrix Biology*. **22**:73
- Conejo-Garcia, J.R. et al. 2005. Vascular leukocytes contribute to tumour vascularization. *Blood*. **105**:679
- Cook, P.C. et al. 2011. Multiple helminth infection of the skin causes lymphocyte hypo-responsiveness mediated by Th2 condition of Dermal Myeloid cells. *PLoS Pathogens*. **7**:1
- Coulson, P. S. and R.A. Wilson. 1989. Portal shunting and resistance to *Schistosoma mansoni* in 129 strain mice. *Parasitology*. **99**: 383
- Coussens, L.M. et al. 1999. Inflammatory mast cells up-regulate angiogenesis during squamous epithelial carcinogenesis. *Genes & Development*. **13**:1382
- Coussens, L.M. and Z.Werb. 2002. Inflammation and cancer. *Nature*. **420**:860
- Crabtree JE, and R.A. Wilson. 1980. *Schistosoma mansoni*: a scanning electron microscope study of the developing schistosomulum. *Parasitology*. **81**: 553
- Crabtree, J. E. 1982. An ultrastructural study of migrating schistosomulum of *Schistosoma mansoni* *Biology*. Ph.D thesis, University of York, York

Crabtree, J. E. and R.A. Wilson. 1985. *Schistosoma mansoni*: an ultrastructural examination of skin migration in the hamster cheek pouch. *Parasitology*. **91**: 111

Cozzani, E. et al. 2001. Adhesion molecules in keratinocyte. *Clinics in Dermatology*. **19**:544

Cross, M.J. and L.Claesson-Welsh. 2001. FGF and VEGF function in angiogenesis: signalling pathways, biological responses and therapeutic inhibition. *Trends in Pharmacological Sciences*. **22**:201

Crowther, M. et al. 2001. Microenvironmental influence on macrophage regulation of angiogenesis in wounds and malignant tumours. *Journal of Leukocyte Biology*. **70**:478

Curiel, T.J. et al. 2004. Dendritic cell subsets differentially regulate angiogenesis in human ovarian cancer. *Cancer Research*. **64**:5535

Curwen, R.S and R.A. Wilson. 2003. Invasion of skin by schistosome cercariae: some neglected facts. *Trends in Parasitology*. **19**:63

Curwen, R.S, et al. 2006. Identification of novel proteases and immunomodulators in the secretion of schistosome cercariae that facilitate host entry. *Molecular & Cellular Proteomics*. **5**:835

Dace, D.S. et al. 2008. Interleukin-10 promotes pathological angiogenesis by regulating macrophage response to hypoxia during development. *PLoS ONE*. **3**:e33881

Dean, D. A. et al. 1984. Comparison of *Schistosoma mansoni* migration patterns in normal and irradiated cercaria-immunized mice by means of autoradiographic analysis. Evidence that worm elimination occurs after the skin phase in immunized mice. *The American Journal of Tropical Medicine and Hygiene*. **33**: 89.

Delavary, B.M. 2011. Macrophages in skin injury and repair. *Immunobiology*. **216**:753

Dennis, R.D. et al. 2011. Angiogenesis and parasitic helminth-associated neovascularization. *Parasitology*. **138**:426

Detmar, M. et al. 1997. Hypoxia Regulates the Expression of Vascular Permeability Factor/Vascular Endothelial Growth Factor (VPF/VEGF) and its Receptors in Human Skin. *Journal of Investigative Dermatology*. **108**:263

Detmar M, et al. 1998. Increased microvascular density and enhanced leukocyte rolling and adhesion in the skin of VEGF transgenic mice. *Journal of Investigative Dermatology*. **111**:1

De Smet, F., et al. 2009. Mechanisms of Vessel Branching. Filopodia on endothelial tip cells lead the way. *Arteriosclerosis, Thrombosis and Vascular Biology*. **29**: 639

Dewals, B.G, et al. 2010. IL-4R α -independent expression of mannose receptor and Ym1 by macrophages depends on their IL-10 responsiveness. *PLoS Neglected Tropical Diseases*. **18**:e689

Dewals, B.G. et al. 2010. Control of *Schistosoma mansoni* egg-induced inflammation by IL-4-responsive CD4(+)CD25(-)CD103(+)Foxp3(-) cells is IL-10-dependent. *European Journal of Immunology*. **40**:2837

Ding, Y-B. et al. 2003. Association of VCAM-1 overexpression with oncogenesis, tumour angiogenesis and metastasis of gastric carcinoma. *World Journal of Gastroenterology*. **9**:1409

Dirix, L.Y. et al. 2010. Bevacizumab in the treatment of patients with advanced breast cancer: where have we landed? *Therapeutic advances in medical oncology*. **2**:331

DiScipio, R.G. et al. 1999. A Comparison of C3a and C5a-Mediated Stable Adhesion of Rolling Eosinophils in Postcapillary Venules and Transendothelial Migration In Vitro and In Vivo. *The Journal of Immunology*. **162**:1127

Doenhoff, M.J. et al. 1985. Does the immunopathology induced by schistosome eggs potentiate parasite survival? *Immunology Today*. **6**:203

Dong, G. et al. 2001. Hepatocyte Growth Factor/Scatter Factor-induced Activation of MEK and PI3K Signal Pathways Contributes to Expression of Proangiogenic Cytokines Interleukin-8 and Vascular Endothelial Growth Factor in Head and Neck Squamous Cell Carcinoma. *Cancer Research*. **61**:5911

Dong, D.Z.M. et al. 2009. Regulation of angiogenesis by macrophages, dendritic cells, and circulating myelomonocytic cells. *Current Pharmaceutical Design*. **15**:365

Dorsey, C.H. et al. 2002. Ultrastructure of the *Schistosoma mansoni* cercaria. *Micron*. **33**:279

Douchet, C. et al. 1998. Interleukin (IL) 4 and IL-13 act on human lung fibroblasts: implication in asthma. *The Journal of Clinical Investigation*. **101**:2129

- Dovi, J.V. et al. 2004. Neutrophil function in the healing wound: adding insult to injury. *Journal of Thrombosis and Haemostasis*. **92**:275
- Eckes, B. et al. 2000. Fibroblast-matrix interactions in wound-healing and fibrosis. *Matrix Biology*. **19**:325
- Edwards, J.P. et al. 2006. Biochemical and functional characterisation of three activated macrophage populations. *Journal of Leukocyte Biology* **80**:1298
- Efraim, A.H. and F. Levi-Schaffer. 2008. Tissue remodelling and angiogenesis in asthma: the role of the eosinophil. *Therapeutic Advances in Respiratory Disease*. **2**:163
- El-Awady, M.K. et al. 2001. *Schistosoma hematobium* soluble egg antigens induce proliferation of urothelial and endothelial cells. *World Journal of Urology*. **19**:263
- Eliceiri, B.P. et al. 1999. Selective requirement for Src kinases during VEGF-induced angiogenesis and vascular permeability. *Molecular Cell*. **4**:915
- Elsaghier, A. A. and D.J. McLaren. 1989. *Schistosoma mansoni*: influence of immunization and challenge schedules on the sites and mechanisms of resistance in CBA/Ca mice vaccinated with highly irradiated cercariae. *Journal of Helminthology*. **63**: 173
- Eming, S.A. et al. 2007. Accelerated wound closure in mice deficient for Interleukin-10. *The American Journal of Pathology*. **170**:188
- Emoto, N. et al. 1998. Fibroblast growth factor-2 free from extracellular matrix is increased in papillary thyroid carcinomas and Graves' thyroids. *Thyroid*. **8**:491
- Enk, A.H. and S.I. Katz. 1992. Identification and induction of keratinocyte – derived IL-10. *The Journal of Immunology*. **149**:92
- Erwig, L.P. and P.M Henson. 2007. Immunological consequences of apoptotic cell phagocytosis. *The American Journal of Pathology*. **171**:2
- Fainaru, O. et al. 2010, Tumour growth and angiogenesis are dependent on the presence of immature dendritic cells. *Federation of American Societies for Experimental Biology*. **24**:1411
- Fallon, P.G and D.W. Dunne. 1999. Tolerisation of mice to *Schistosoma mansoni* egg antigens causes elevated type 1 and diminished type 2 cytokine responses and increased mortality in acute infection. *The Journal of immunology*. **162**:4122.
- Farah, I.O. et al. 2000. Repeated exposure induces periportal fibrosis in *Schistosoma mansoni*-infected baboons: role of TGF-beta and IL-4. *The Journal of immunology*. **164**:5337

- Feldmann, M. et al. 1996. Role of cytokine in rheumatoid arthritis. *Annual Review of Immunology*. **14**:397
- Ferrara, N. 2002. Role of vascular endothelial growth factor in physiologic and pathologic angiogenesis: Therapeutic implications. *Seminars in Oncology*. **29**:10
- Ferrara N, et al. 2003. The biology of VEGF and its receptors. *Nature Medicine*. **9**:669
- Fichtner-Feigl, S. et al. 2005. IL-13 signalling through the IL-13 receptor is involved in induction of TGF-1 production and fibrosis. *Nature Medicine*. **12**:99
- File, S. 1995. Interaction of Schistosome eggs with vascular endothelium. *The Journal of Parasitology*. **81**: 234
- Files, V.S. and E.B, Cram. 1949. A study on the comparative susceptibility of snail vectors to strains of *Schistosoma mansoni*. *The Journal of Parasitology*. **35**:555
- Fiorentino, D.F. et al. 1991. IL-10 acts on the antigen-presenting cell to inhibit cytokine production by Th1 cells. *The Journal of Immunology*. **146**:3444
- Firestein, G.S. 2003. Evolving concepts of rheumatoid arthritis. *Nature*. **423**:356
- Folkard, S.G. 1996. Eosinophils are the major effector cells of immunity to microfilariae in a mouse model of onchocerciasis. *Parasitology*. **112**:323
- Fonsatti, E. et al. 2003. Endoglin (CD105): a powerful therapeutic target on tumour-associated angiogenetic blood vessels. *Oncogene*. **22**:6557
- Frantz, S. et al. 2005. Innate immunity and angiogenesis. *Circulation Research*. **96**:15
- Freedman, D.O. and E.A. Ottesen. 1988. Eggs of *Schistosoma mansoni* stimulate endothelial cell proliferation in vitro. *Journal of Infectious Diseases*. **158**:556
- Frelin, C. et al. 2000. Vascular endothelial growth factors and angiogenesis. *Annales D'endocrinologie*. **61**:70
- Frossing S, et al. 2010. Skin wound healing in MMP2-deficient and MMP2/Plasminogen double-deficient mice. *Experimental Dermatology*. **19**:234
- Fukumura, D. et al. 2001. Predominant role of endothelial nitric oxide synthase in vascular endothelial growth factor- induced angiogenesis and vascular permeability. *Proceedings of the National Academy of Sciences*. **98**:2604

Fukushi, J. et al. 1998. Novel biological functions of Interleukin-4: Formation of tube-like structures by vascular endothelial cells *in vitro* and angiogenesis *in vivo*. *Biochemical and Biophysical Research Communications*. **250**:444

Fukushi, J. 2000. The activity of soluble VCAM-1 in angiogenesis stimulated by IL-4 and IL-13. *The Journal of Immunology*. **165**:2818

Fulgham, D. L. et al. 1999. FGF-2 dependant angiogenesis is a latent phenotype in basic fibroblast growth factor transgenic mice. *Endothelium*. **6**:185

Gabrilovich, D. et al. 1998. Vascular Endothelial Growth Factor Inhibits the Development of Dendritic Cells and Dramatically Affects the Differentiation of Multiple Hematopoietic Lineages In Vivo. *Blood*. **92**:4150

Gamble, J.R, et al. 2000. Angiopoetin-1 is an ant permeability and anti-inflammatory agent *in vitro* and targets cell junctions. *Circulation Research*. **87**:603

Gaudry, M. et al. 1997. Intracellular pool of vascular endothelial growth factor in human neutrophils. *Blood*. **15**:4153

Gazzinelli, R.T. et al. 1992. IL-10 inhibits parasite killing and nitrogen oxide production by IFN- gamma- activated macrophages. *The Journal of Immunology*. **148**:1792

Gerber, H.P. et al. 1998. Vascular endothelial growth factor induces expression of the antiapoptotic proteins Bcl-2 and A1 in vascular endothelial cells. *The Journal of Biological Chemistry*. **273**:13313

Gessner, A. et al. 2005. Mast cells, basophils and eosinophils acquire constitutive IL-4 and IL-13 transcripts during lineage differentiation that are sufficient for rapid cytokine production. *The Journal of Immunology*. **174**:1063

Gharaee-Kermani, M. and S.H, Phan. 1998. The role of eosinophils in pulmonary fibrosis. *International Journal of Molecular Medicine*. **1**:43

Gill, H.S. and M.R, Prausnitz. 2006. Coated microneedles for transdermal delivery. *Journal of Controlled Release*. **117**:227

Gleissner, C.A. et al. 2008. Platelet chemokines in vascular disease. *Arteriosclerosis, Thrombosis and Vascular Biology*. **28**:1920

Gordan, J.D. and M.C. Simon. 2007. Hypoxia-inducible factors: central regulators of the tumor phenotype. *Current Opinion in Genetics & Development*. **17**: 71

- Gordon, S. 2003. Alternative activation of macrophages. *Nature Reviews Immunology*. **3**:23
- Goumans, M.J. et al. 2003. Controlling the Angiogenic Switch: A Balance between Two Distinct TGF- β Receptor Signaling Pathways. *Trends in Cardiovascular Medicine*. **13**:301
- Graham, B.B. et al. 2010. Schistosomiasis-Induced Experimental Pulmonary Hypertension: Role of interleukin-13 signalling. *The American Journal of Pathology*. **177**:1549
- Grant, D.S., et al. 1993. Scatter factor induces blood vessel formation in vivo. *Proceedings of the National Academy of Sciences*. **90**:1937
- Grimstad, O. et al. 2011. Cellular sources and inducers of cytokines present in acute wound fluid. *Wound Repair and Regeneration*. **19**:337
- Grinnell, F. 1992. Wound repair, keratinocyte activation and integrin modulation. *Journal of Cell Science*. **101**:1
- Gryseels, B. et al. 2006. Human Schistosomiasis. *Lancet*. **368**:1106
- Haas, W.D. et al. 1994. Schistosoma haematobium cercarial host-finding and host-recognition differs from that of S.mansoni. *The Journal of Parasitology*. **80**:345
- Hass, W.D. et al. 1997. Schistosoma mansoni cercariae: stimulation of acetabular gland secretion is adapted to the chemical composition of mammalian skin. *The Journal of Parasitology*. **86**:1079
- He, Y.X., et al. 2002. Schistosoma mansoni, S.Haematobium and S.japonicum; early events associated with penetration and migration of schistosomula through human skin. *Exp Parasitol*. **102**:99
- He, Y.X, et al. 2005. Comparison of skin invasion among three major species of Schistosoma. *Trends in Parasitology*. **21**:201
- Heidenreich, R. et al. 2009. Angiogenesis drives psoriasis pathogenesis. *International Journal of Experimental Pathology*. **90**:232
- Hellström, M. et al. 2007. Dll4 signalling through Notch1 regulated formation of tip cells during angiogenesis. *Nature*. **445**:776

- Henry, S. et al. 2000. Microfabricated microneedles: A novel approach to transdermal drug delivery. *Journal of Pharmaceutical Sciences*. **87**:922
- Herbert, DBR. et al. 2004. Alternative Macrophage Activation Is Essential for Survival during Schistosomiasis and Downmodulates T Helper 1 Responses and Immunopathology. *Immunity*. **20**:623
- Hewitson, J.P. et al 2005. Immunity induced by the radiation-attenuated schistosome vaccine. *Parasite Immunology*. **27**:271
- Higazi, T.B. et al. 2003. Angiogenic activity of an *Onchocerca volvulus* *Ancylostoma* secreted protein homologue. *Molecular and Biochemical Parasitology*. **129**:61
- Hirani, N. et al. 2001. The regulation of interleukin-8 by hypoxia in human macrophages--a potential role in the pathogenesis of the acute respiratory distress syndrome (ARDS). *Molecular Medicine*. **7**:685
- Hiratsuka, S. et al. 2001. Involvement of Flt-1 tyrosine kinase (vascular endothelial growth factor receptor-1) in pathological angiogenesis. *Cancer Research*. **61**:1207
- Hoffman, K.F. et al. 2000. IL-10 and the dangers of immune polarization: Excessive type 1 and Type 2 cytokine responses induce distinct forms of lethal immunopathology in Murine Schistosomiasis. *The Journal of Immunology*. **164**:6406
- (a) Hogg, K.G. et al. 2003. Interleukin-12p40 secretion by cutaneous CD11c+ and F4/80+ cells is a major feature of the innate immune response in mice that develop Th1-mediated protective immunity to *Schistosoma mansoni*. *Infection and Immunity*. **71**:3563.
- (b) Hogg, K.G. et al. 2003. IL-10 regulates early IL-12 mediated immune responses induced by the radiation-attenuated schistosome vaccine. *International Immunology*. **15**:1451
- Holt, P.G. and D.H. Strickland. 2010. Interactions between innate and adaptive immunity in asthma pathogenesis: New perspectives from studies on acute exacerbations. *Journal of Allergy and Clinical Immunology*. **125**:963
- Horak, P. et al. 2002. Biology of the schistosome genus *Trichobilharzia*. *Advances in Parasitology*. **52**:155
- Hoshino, M. et al. 2001. Expression of vascular endothelial growth factor, basic fibroblast growth factor and angiogenin immunoreactivity in asthmatic airways and its relationship to angiogenesis. *The Journal of Allergy and Clinical Immunology*. **107**:295

Hübner, G. et al. 1996. Differential regulation of pro-inflammatory cytokines during wound healing in normal and glucocorticoid-treated mice. *Cytokine*. **8**:548

Humbles, A.A. et al. 2004. A critical role for eosinophils in allergic airways remodelling. *Science*. **305**:1776

Icani, R.N and D.J.McLaren. 1984. Histopathological and ultrastructural studies of cutaneous reactions elicited in naïve and chronically infected mice by invading schistosomula of *Schistosoma mansoni*. *International Journal for Parasitology*. **14**:259.

Igyártó, B.Z. et al. 2011. Skin-Resident Murine Dendritic Cell Subsets Promote Distinct and Opposing Antigen-Specific T Helper Cell Responses. *Immunity*. Electronic ahead of print

Ishida S, et al. 2003. VEGF164-mediated inflammation is required for pathological, but not physiological, ischemia-induced retinal neovascularization. *The Journal of Experimental medicine*. **198**:483

Itoh, T. et al. 1998. Reduced angiogenesis and tumour progression in gelatinase A- deficient mice. *Cancer Research*. **58**:1048

Jackson, C.J. and M. Nquyen. 1997. Human micro vascular endothelial cells differ from micro vascular endothelial cells in their expression of matrix metalloproteinases. *The International Journal of Biochemistry & Cell Biology*. **29**:1167

Jackson, J.R. et al. 1997. The codependance of angiogenesis and chronic inflammation. *Federation of American Societies for Experimental Biology*. **11**:457

Jacobsen, E.A. et al. 2007. Eosinophils and asthma. *Current Allergy and Asthma Reports*. **7**:s11882

Jenkins, S.J. and A.P. Mountford. 2005. Dendritic cells activated with products released by schistosome larvae drive Th2-type immune responses, which can be inhibited by manipulation of CD40 co stimulation. *Infection and Immunity*. **73**:395

Jonuleit, H. et al. 2005. Pro-inflammatory cytokines and prostaglandins induce maturation of potent immunostimulatory dendritic cells under foetal calf serum-free conditions. *European Journal of Immunology*. **27**:3135

Kabaterein, N.B, et al. 2002. Epidemiology and geography of *Schistosoma mansoni* in Uganda: implications for planning control. *Tropical Medicine and International Health*. **9**:372

- Kanse, S.M., O.Liang et al 2005. Characterisation and partial purification of *Schistosoma mansoni* egg-derived pro-angiogenic factor. *Molecular & Biochemical Parasitology*. **144**:76
- Kaviratne, M. et al. 2004 IL-13 activates a mechanism of tissue fibrosis that is completely TGF-beta independent. *The Journal of Immunology*. **173**:4020
- Keene, W. E et al. 1983. Degradation of extracellular matrix by larvae of *Schistosoma mansoni*. II. Degradation by newly transformed and developing schistosomula. *Laboratory Investigation*. **49**: 201
- Kim, I. et al. 2000. Angiopoetin-2 at high concentration can enhance endothelial cell survival through phosphatidylinositol3'-kinase/Akt signal transduction pathway. *Oncogene*. **19**:4549
- Kim, H.K. et al. 2003. Elevated levels of circulating platelet micro particles, VEGF, IL-6 and RANTES in patients with gastric cancer: possible role of a metastasis predictor. *European Journal of Cancer*. **39**:184
- Kim, M.H. et al. 2008. Dynamics of Neutrophil Infiltration during Cutaneous Wound Healing and Infection Using Fluorescence Imaging. *Journal of Investigative Dermatology*. **128**:1812.
- Kinne,, R.W. et al. 2007. Cells of the synovium in rheumatoid arthritis: Macrophages. *Arthritis Research & Therapy*. **9**: 224
- Klion, A.D. and T.B, Nutman. 2004. The role of eosinophils in host defence against helminth parasites. *Journal of Allergy and Clinical Immunology*. **113**:30
- Kobayashi, N. et al. 2009. Activation of eosinophils by Lipopolysaccharide-Induced-Monocyte-Derived Cytokines. *Allergology International*. **58**:103
- Kono, H. and K.L. Rock. 2008. How dying cells alert the immune system to danger. *Nature reviews Immunology*, **8**:279
- Kouřilová, P. et al. 2004. Cercarial dermatitis caused by bird schistosomes comprises both immediate and late phase cutaneous hypersensitivity reactions. *The Journal of Immunology*. **172**:3766
- Krilleke, D. et al. 2007. Molecular mapping and functional characterisation of the VEGF164 heparin-binding domain. *The Journal of Biological Chemistry*. **282**:28045
- Kühn, R. et al. 1993. Interleukin-10-deficient Mice Develop Chronic Enterocolitis. *Cell*. **75**:263

Laberge, S. et al. 1998. Association of increased CD4+ T-cell infiltration with increased IL-16 expression in atopic dermatitis. *The Journal of Allergy and Clinical Immunology*. **102**: 645

Lammie, P.J. et al. 1986. Production of a fibroblast-stimulating factor by *Schistosoma mansoni* antigen-reactive T cell clones. *The Journal of Immunology*. **136**:1100

Lanone, S. et al. 2002. Overlapping and enzyme specific contributions of matrix metalloproteinases-9 and -12 in IL-13 induced inflammation and remodelling. *The Journal of Clinical Investigation*. **110**:463

Lathbury, L.J. and L.A, Salamonsen. In vitro studies of the potential role of neutrophils in the process of menstruation. *Molecular Human Reproduction*. **6**:899

Laxmanan, S. et al. 2005. Vascular endothelial growth factor impairs the functional ability of dendritic cells through Id pathways. *Biochemical and Biophysical Research Communications*. **334**:193

LeBrasseur, N. 2002. ECM communicates with MMP. *The Journal of Cell Biology*. **159**:388

Levashova, Z. et al. 2010. Molecular Imaging of Changes in the Prevalence of Vascular Endothelial Growth Factor Receptor in Sunitinib-Treated Murine Mammary Tumors. *Journal of Nuclear Medicine*. **51**:959

Levi-Schaffer F. and V.B. Weg. 1997. Mast cells, eosinophils and fibrosis. *Clinical & Experimental Allergy*. **27**:64

Levi-Schaffer, F. and J. Pe'Er. 2002. Mast cells and angiogenesis. *Clinical & Experimental Allergy*. **31**:521

Levi-Schaffer, F and A, Munitz. 2004. Eosinophils: 'new' roles for 'old' cells. *Allergy*. **59**:268

Lewis C.E. and J.W, Pollard. 2006. Distinct role of macrophages in different tumour microenvironments. *Cancer Research*. **66**:605

Ligresti, G. et al. 2011. Macrophage-derived tumour necrosis factor-alpha is an early component of the molecular cascade leading to angiogenesis in response to aortic injury. *Arteriosclerosis, Thrombosis and Vascular Biology*. **31**:1151

Lin. E.Y. et al. 2006. Macrophages Regulate the Angiogenic Switch in a Mouse Model of Breast Cancer. *Cancer Research*. **66**:11238

- Liu, Y. et al. 1995. Hypoxia regulates vascular endothelial growth factor gene expression in endothelial cells. *Circulation Research*. **77**:638-643
- Liu, A. et al. 2005. Fibroblast growth factors in development. *eLS*.
- Loeffler, D.A., et al. 2002. Soluble egg antigens from *Schistosoma mansoni* induce angiogenesis- related processes by up-regulating vascular endothelial growth factor in human endothelial cells. *Journal of infectious diseases*. **185**:1650
- Loke, P. et al. 2007. Alternative activation is an innate response to injury that requires CD4⁺ T cells to be sustained during chronic infection. *The Journal of Immunology*. **179**:3926
- Lucas T. et al. 2010. Differential roles of macrophages in diverse phases of skin repair. *The Journal of Immunology*. **184**:3964
- Lundberg, J.E., et al. 1998. Comparison of IL-10 levels in chronic venous insufficiency ulcers and autologous donor tissue. *Archives of Dermatological Research*. **290**:669
- MacDonald, A.S., et al. 2001. CD8- dendritic cell activation status plays an integral role in influencing Th2 response development. *The Journal of Immunology*. **167**:1982
- Madala, S.K., et al. 2010. Matrix Metalloproteinase 12-deficiency augments extracellular matrix degrading metalloproteinases and attenuates IL-13-dependent fibrosis. *The Journal of Immunology*. **184**. 3955
- Mahabeleshwar, G.H. et al. 2006. Integrin signalling is critical for pathological angiogenesis. *The Journal of Experimental Medicine*. **203**:2495
- Maisonpierre, P.C. et al. 1997. Angiopoietin-2, a natural antagonist for Tie2 that disrupts in vivo angiogenesis. *Science*. **277**:55
- Mannaioni, P.F., et al. 2004. Platelets and inflammation: role of platelet-derived growth factor, adhesion molecules and histamine. *Inflammation Research*. **46**:4
- Mantovani, A. et al. 2002. Macrophage polarization: tumour-associated macrophages as a paradigm for polarized M2 mononuclear phagocytes. *Trends in Immunology*. **23**:549
- Mantovani, A. et al. 2004. The chemokine system in diverse forms of macrophage activation and polarization. *Trends in Immunology*. **25**:677
- Marconcini L, et al .1999. c-fos- induced growth factor/vascular endothelial growth factor D induces angiogenesis *in vivo* and *in vitro*. *Proceedings of the National Academy of Sciences*. **96**:9671

- Marelli-Berg, F, et al. 2000. Isolation of endothelial cells from murine tissue. *Journal of Immunological Methods*. **244**:205
- Margetts, P.J. et al. 2002. Inflammatory cytokines, angiogenesis, and fibrosis in the rat peritoneum. *The American Journal of Pathology*. **160**:2285
- Martinez, F.O. et al. 2008. Macrophage activation and polarization. *Frontiers in Bioscience*. **13**:453
- Maruoka Y, et al. 1998. Comparison of the expression of three highly related genes, *Fgf8*, *Fgf17* and *Fgf18*, in the mouse embryo. *Mechanisms of Development*. **74**:175
- Mastin, A.J. et al. 1983. *Schistosoma mansoni*: migration and attrition of irradiated and challenge schistosomula in the mouse. *Parasitology*. **87**:87
- Matsumoto, K and T. Nakamura. 1992. Hepatocyte growth factor: molecular structure, roles in liver regeneration, and other biological functions. *Critical Reviews in Oncogenesis*. **3**:27
- McColl, B.K. 2004. Molecular regulation of the VEGF family- inducers of angiogenesis and lymphangiogenesis. *Acta Pathologica, Microbiologica et Immunologica Scandinavica*. **112**:463
- McCourt, M. et al. 1999. Pro-inflammatory mediators stimulate neutrophil-directed angiogenesis. *Archives of Surgery*. **134**:1325
- McKerrow, J.H. et al. 1983. Degradation of extracellular matrix by larvae of *Schistosoma mansoni*. I. Degradation by cercariae as a model for initial parasite invasion of host. *Laboratory Investigation*. **49**:195
- McKerrow, J.H and J. Salter. 2002. Invasion of the skin by *Schistosoma* cercariae. *Trends in Parasitology*. **18**:193
- McKerrow, J.H. 2003. Invasion of the skin by schistosome cercariae: some neglected facts. *Trends in Parasitology*. **19**:66
- McLaren, D. J. 1990. The cutaneous inflammatory immune response to parasite infestation. In Behnke, J. M. (Ed.) *Parasites, immunity and pathology: the consequences of parasitic infection in mammals*. Taylor & Francis, London, pp 168-200
- Miller, P. and R.A, Wilson 1980. Migration of the schistosomula of *Schistosoma mansoni* from the lungs to the hepatic portal system. *Parasitology*. **80**: 267
- Menon, G.K. 2002. New insights into skin structure: scratching the surface. *Advanced Drug delivery reviews*. **54**:3

Montesano, R. et al. 1986. Basic fibroblast growth factor induces angiogenesis in vitro. *Proceedings of the National Academy of Sciences*. **83**:7297

Moore, K.W. et al. 2001. Interleukin-10 and the interleukin-10 receptor. *Annual Review of Immunology*. **19**:683

Morishita, R. et al. 1999. Therapeutic Angiogenesis Induced by Human Recombinant Hepatocyte Growth Factor in Rabbit Hind Limb Ischemia Model as Cytokine Supplement Therapy. *Hypertension*. **33**:1379

Moses, M.A. and R, Langer. 1991. Inhibitors of angiogenesis. *Nature Biotechnology*. **9**:630

Mosser, D.M. 2003. The many faces of macrophage activation. *Journal of Leukocyte Biology*. **73**:209

Mosser, D.M and J.P. Edwards. 2008. Exploring the full spectrum of macrophage activation. *Nature Reviews Immunology*. **8**:958

Mountford, A.P. et al. 1988. Antigen localisation and the induction of resistance in mice vaccinated with irradiated cercariae of *Schistosoma mansoni*, *Parasitology* **97**: 11

Mukhopadhyay, A. et al. 2010. The Role of Hepatocyte Growth Factor/c-Met System in Keloid Pathogenesis. *The Journal of Trauma*. **69**:1457

Munitz, A. and F. Levi-Schaffer. 2004. Eosinophils: 'new' roles for 'old' cells. *Allergy*. **59**:268

Munitz A. et al. 2008. Distinct roles for IL-13 and IL-4 via IL-13 receptor alpha1 and the type II IL-4 receptor in asthma pathogenesis. *Proceedings of the National Academy of Sciences*. **105**:7240

Nagase H and Woessner JF. 1999. Matrix Metalloproteinases. *The Journal of Biological Chemistry*. **274**:21491

Naggy, B.A. e al. 1981. Changes in the enteric vasculature of mice infected with *Schistosoma mansoni*. *American Journal of Tropical Medicine and Hygiene*. **301**: 999

Naginei, C.N. et al. 2003. Transforming growth factor- β induces expression of vascular endothelial growth factor in human retinal pigment epithelial cells: Involvement of mitogen-activated protein kinases. *Journal of Cellular Physiology*. **197**:453

Nakamura, T, et al. 1989. Molecular cloning and expression of hepatocyte growth factor. *Nature*. **342**:440

- Nakao, S. et al. 2005. Infiltration of COX-2–expressing macrophages is a prerequisite for IL-1 β –induced neovascularization and tumour growth. *Journal of Clinical Investigation*. **115**:2979
- Nardin, A. and J.P., Abastado. 2008. Macrophages and cancer. *Frontiers in Bioscience*. **13**:3494
- Nathan, C.F. et al. 1984. Activation of human macrophages. Comparison of other cytokine with interferon-gamma. *The Journal of Experimental Medicine*. **160**:600
- Neufeld G, et al. 1999. Vascular endothelial growth factor (VEGF) and its receptors. *Federation of American Societies for Experimental Biology*. **13**:9
- Neufeld, G and O. Kessler. 2006. Pro-angiogenic cytokines and their role in tumour angiogenesis. *Cancer Metastasis Review*. **25**:373
- Newman, P.J. 1997. The Biology of PECAM1. *The Journal of Clinical Investigation*. **99**: 3
- Newport, G. R. et al. 1988. Cloning of the proteinase that facilitates infection by schistosome parasites. *The Journal of Biological Chemistry*. **263**: 13179
- Ng, L.G. et al. 2011. Visualizing the Neutrophil Response to Sterile Tissue Injury in Mouse Dermis Reveals a Three-Phase Cascade of Events. *Journal of Investigative Dermatology*. *Ahead of print*
- Nishimura, Y. et al. 2008. IL-13 attenuates vascular tube formation via JAK2-STAT6 pathway. *Circulation Journal*. **72**:469
- Noël, W. et al. 2004. Alternatively activated macrophages during parasite infections. *Trends in Parasitology*. **20**:126
- Normand, J. and M.A. Karasek. 1995. A method for the isolation and serial propagation of keratinocytes, endothelial cells and fibroblasts from a single punch biopsy of human skin. *In Vitro Cellular & Developmental Biology*. **34**:447
- Norrby, K. et al. 2002. Mast cells and angiogenesis. *Acta Pathologica, Microbiologica et Immunologica Scandinavica*. **110**:355
- Nozawa, H. et al. 2006. Infiltrating neutrophils mediate the initial angiogenic switch in a mouse model of multistage carcinogenesis. *Proceedings of the National Academy of Sciences*. **103**:12493
- Nurden, A. 2011. Platelets, inflammation and tissue regeneration. *Thrombosis and Haemostasis*. **105**:s13

- Nyindo, M. et al. 1999. Role of adult worm-specific immunoglobulin E in acquired immunity to *Schistosoma mansoni* infection in baboons. *Infection and Immunity*. **67**:636
- Odorisio, T., et al. 2002. Mice overexpressing placenta growth factor exhibit increased vascularization and vessel permeability. *Journal of Cell Science*. **115**:2559
- Ohshima, T. and Y. Sato. 1998. Time-dependent expression of interleukin-10 (IL-10) mRNA during the early phase of skin wound healing as a possible indicator of wound vitality. *International Journal of Legal Medicine*. **111**:251
- Okada, S. et al. 1997. Migration of eosinophils through basement membrane components in vitro: role of matrix metalloproteinase-9. *American Journal of Respiratory Cell and Molecular Biology*. **17**:519
- Oldham, M et al. 2006. Three-dimensional imaging of xenograft tumours using optical computed and emission tomography. *Medical Physics*. **33**:3193
- Ornitz, D.M and N. Itoh. 2001. Fibroblast growth factors. *Genome Biology*. **2**: 3005.1
- Ortega, S et al. 1998. Neuronal defects and delayed wound healing in mice lacking fibroblast growth factor. *Proceedings of the National Academy of Sciences*. **95**:5672
- Otrock, Z.K. et al. 2007. Vascular endothelial growth factor family of ligands and receptors: Review. *Blood Cells, Molecules and Diseases*. **38**:258
- Ovington, K.S. and C.A. Behm. 2000. The role of Eosinophils in parasitic helminth infections: insights from genetically modified mice. *Parasitology Today*. **16**:202
- Patan, S. 2000. Vasculogenesis and angiogenesis as mechanisms of vascular network formation, growth and remodelling. *Journal of Neuro-oncology*. **50**:1
- Paveley, R. et al. 2009. Fluorescent imaging of antigen released by a skin-invading helminth reveals differential uptake and activation profiles by antigen presenting cells. *PLoS Neglected Tropical Diseases*. **3**:e528
- Pearce EJ and McLaren DJ. 1986. *Schistosoma mansoni*: The cutaneous response to cercarial challenge in naive guinea pigs and guinea pigs vaccinated with highly irradiated cercariae. *International Journal for Parasitology*. **16**:491
- Pearce, E.J., 1991. Down-regulation of Th1 cytokine production accompanies induction of th2 responses by a parasitic helminth, *Schistosoma mansoni*. *The Journal of Experimental Medicine*. **173**:159

- Pearce, E.J and A.S. MacDonald. 2002. The Immunobiology of Schistosomiasis. *Nature Reviews*. **2**:499
- Pepper, M.S. 1997. Transforming growth factor-beta: vasculogenesis, angiogenesis, and vessel wall integrity. *Cytokine & Growth Factor Reviews*. **8**:21
- Peranteau, W.H. 2008. IL-10 overexpression decreases inflammatory mediators and promotes regenerative healing in an adult model of scar formation. *Journal of Investigative Dermatology*. **128**:1852
- Piccard, H et al. 2011. On the dual role and polarized phenotypes of neutrophils in tumour development and progression. *Critical reviews in Oncology/Haematology*. Article in press at this time
- Pflieger, D. et al. 2006. Comparative proteomic analysis of extracellular matrix proteins secreted by two types of skin fibroblasts. *Proteomics*. **6**:5868
- Poltorak, Z. et al. 1997. VEGF₁₄₅ a secreted Vascular Endothelial Growth Factor isoform that binds to the extracellular matrix. *The Journal of Biological Chemistry*. **272**:7151
- Poulaki, V. 2011. Angiogenesis assays. *Methods mol Biol*. **731**:345
- Prausnitz, M.R. 2004. Microneedles for transdermal drug delivery. *Advanced Drug Delivery Reviews*. **56**:581
- Puzeddu, I. et al. 2003. Modulatory role of human blood eosinophils in angiogenesis: ex vivo and in vitro studies. *Journal of Allergy and Clinical Immunology*. **111**:S211
- Puxeddu, I. et al. 2005. Human peripheral blood eosinophils induce angiogenesis. *The International Journal of Biochemistry and Cell Biology*. **37**:628
- Puxeddu, I. et al. 2005. Mast cells and eosinophils: a novel link between inflammation and angiogenesis in allergic diseases. *Journal of Allergy and Clinical Immunology*. **116**:531
- Puxeddu, I. et al. 2008. The role of major basic protein in angiogenesis. *Allergy*. **64**:368
- Prussin, C. and D.D. Metcalfe. et al. 2003. IgE, mast cells, basophils, and eosinophils. *Journal of Allergy and Clinical Immunology*. **111**:S486
- Ramaswamy, K. et al. 2000. A role for parasite-induced PGE₂ in IL-10 mediated host immunoregulation by skin stage schistosomula of *Schistosoma mansoni*. *Journal of Immunology*. **165**:4567

- Rappolee, D.A. et al. 1988. Wound macrophages express TGF-alpha and other growth factors in vivo: analysis by mRNA phenotyping. *Science*. **241**:708
- Ravanti, L and V.M. Kähäri. 2000. Matrix metalloproteinases in wound repair. *International Journal of Molecular Medicine*. **6**: 391
- Raza SL and Cornelius LA. 2000. Matrix Metalloproteinases: Pro- and Anti-Angiogenic Activities. *Journal of Investigative Dermatology Symposium Proceedings*. **5**:47
- Reiman, R.M. et al. 2006. Interleukin-5 augments the progression of liver fibrosis by regulating IL-13 activity. *Infection and Immunity*. **74**:1471
- Riboldi, E. et al. 2005. Cutting edge: pro-angiogenic properties of alternatively activated dendritic cells. *The Journal of Immunology*. **175**:2788
- Riengrojpitak, S. 1998. Induction of immunity to *Schistosoma mansoni*: interaction of schistosomula with accessory leucocytes in murine skin and draining lymph nodes. *Parasitology*. **117**:301
- Roberts, A.B. et al 1986. Transforming growth factor beta: rapid induction of fibrosis and angiogenesis in vivo and stimulation of collagen formation in vitro. *Proceedings of the National Academy of Sciences*. **83**:4167
- Robinson CJ and S.E. Stringer. 2001. The splice variants of vascular endothelial growth factor (VEGF) and their receptors. *Journal of Cell Science*. **114**:853
- Rodriguez-Sosa, M. 2002. Chronic Helminth Infection Induces Alternatively Activated Macrophages Expressing High Levels of CCR5 with Low Interleukin-12 Production and Th2-Biasing Ability. *Infection and Immunity*. **70**:3656
- Rodriguez, L.G. et al. 2005. Wound Healing Assay. *Cell Migration : Methods in Molecular Biology*. **294**: 23
- Rosen EM, et al .1997. HGF/SF in angiogenesis. *Ciba Found Symp*. **212**:215
- Roviezzo, F. et al. 2005. Angiopoietin-2 causes inflammation *in vivo* by promoting vascular leakage. *Journal of Pharmacology and Experimental Therapeutics*. **314**:738
- Rudolph, E.H. and J.M. Woods. 2005. Chemokine expression and regulation of angiogenesis in rheumatoid arthritis. *Current Pharmaceutical Design*. **11**:613

Ruhrberg, C. et al. 2002. Spatially restricted patterning cues provided by heparin-binding VEGF-A control blood vessel branching and morphogenesis. *Genes and Development*. **16**:2684

Rundhaug, J.E. 2005. Matrix metalloproteinases and angiogenesis. *Journal of Cellular and Molecular Medicine*. **9**: 267

Russel, R.E.K. et al. 2002. Alveolar macrophage-mediated elastolysis: roles of matrix metalloproteinases, cysteine, and serine proteases. *Lung Cellular and Molecular Physiology*. **283**:867

Rutella, S. et al. 2006. Hepatocyte growth factor favours monocyte differentiation into regulatory interleukin (IL)-10⁺IL-12^{low/neg} accessory cells with dendritic-cell features. *Blood*. **108**:218

Sabin, E.A. et al. 1996. *Schistosoma mansoni* egg-induced early IL-4 Production is dependent upon IL-5 and eosinophils. *The Journal of Experimental Medicine*. **184**:1871

Sadler, C.H, et al. 2003. IL-10 is crucial for the transition from acute to chronic disease state during infection of mice with *Schistosoma mansoni*. *European Journal of Immunology*. **33**.880.

Sadowski, T. et al. 2003. Matrix metalloproteinase-19 expression in normal and diseased skin: Dysregulation by epidermal proliferation. *Journal of Investigative Dermatology*. **121**:989

Saharinen, P. et al. 2004. Lymphatic vasculature: development, molecular regulation and role in tumour metastasis and inflammation. *Trends in Immunology*. **25**:387

Salcedo R, et al. 2001. Eotaxin (CCL11) Induces In Vivo Angiogenic Responses by Human CCR3 Endothelial Cells. *The Journal of Immunology*. **166**:7571

Salgado, R. et al. 1999. Platelet number and interleukin-6 correlate with VEGF but not bFGF serum levels of advanced cancer in patients. *British Journal of Cancer*. **80**:892

Salmon-Her, V., et al. 2000. Implication of Interleukin-4 in Wound Healing. *Laboratory Investigation*. **80**:1337

Salo T, et al. 1994. Expression of matrix metalloproteinase-2 and -9 during early human wound healing. *Laboratory Investigation*. **70**:176

Sansonno, D. et al. 2008. Increased serum levels of the chemokine CXCL13 and up-regulation of its gene expression are distinctive features of HCV-related cryoglobulinemia and correlate with active cutaneous vasculitis. *Blood*. **112**: 1620

Sato, Y. et al. 1999. Regulatory Role of Endogenous Interleukin-10 in Cutaneous Inflammatory Response of Murine Wound Healing. *Biochemical and Biophysical Research Communications*. **265**:194

Scapini, P. et al. 2000. The neutrophil as a cellular source of chemokines. *Immunological reviews*. **177**:195

Scheingshackl, A. et al. 1999. Human eosinophils release matrix metalloproteinase-9 on stimulation with TNF-alpha. *Journal of Allergy and Clinical Immunology*. **104**:983

Schermuly, R.T. et al. 2011. Mechanisms of disease: pulmonary arterial hypertension. *Nature Reviews Cardiology*. **8**:443

Seaman, S., et al. 2007. Genes that distinguish Physiological and Pathological Angiogenesis. *Cancer Cell*. **11**:539

Seshadri, M. et al. 2007. Visualizing the acute effects of vascular-targeted therapy in vivo using intravital microscopy and magnetic resonance imaging: correlation with endothelial apoptosis, cytokine induction, and treatment outcome. *Neoplasia*. **9**:128

Shariati, F., et al. 2009. *Trichinella*: differential expression of angiogenic factors in macrophages stimulated with antigens from encapsulated and non-encapsulated species. *Experimental Parasitology*. **123**:347

Shariati, F. et al. 2011. Evaluation of the role of angiogenic factors in the pathogenesis of schistosomiasis. *Experimental Parasitology*. **128**: 44

Shibuya, M. 2001. Structure and function of VEGF/VEGF- receptor system involved in angiogenesis. *Cell Structure and Function*. **26**:22

Sica, A. et al. 2002. Tumour associated macrophages: a molecular perspective. *International Immunopharmacology*. **2**:1045

Silvestre J-S., et al. 2000. Antiangiogenic effect of Interleukin-10 in Ischemia induced angiogenesis in mice hind limb. *Circulation Research*. **87**:448

Skjøt-Arkil, H. et al. 2010. Macrophage-mediated proteolytic remodelling of the extracellular matrix in atherosclerosis results in neoepitopes: a potential new class of biochemical markers. *Assay and Drug Developmental Technologies*. **8**:542

- Smeets, T.J.M. et al. 2003. Analysis of the cell infiltrate and expression of proinflammatory cytokines and matrix metalloproteinases in arthroscopic synovial biopsies: comparison with synovial samples from patients with end stage, destructive rheumatoid arthritis. *Annals of the Rheumatic Diseases*. **62**:635
- Smith, L.T. et al. 1982. Structure of the dermal matrix during development and in the adult. *Journal of Investigative Dermatology*. **79**:93
- Smith, R.S. et al. 1997. Fibroblasts as sentinel cells. Synthesis or chemokines and regulation of inflammation. *The American Journal of Pathology*. **151**:317
- Smith, S.K. 2001. Regulation of angiogenesis in the endometrium. *Trends in Endocrinology & Metabolism*. **12**: 147
- Sozzani, S. et al. 2007. Dendritic cell-endothelial cell cross-talk in angiogenesis. *Trends in Immunology*. **28**:385
- Stacker, S.A. et al. 1999. Biosynthesis of vascular endothelial growth factor-D involves proteolytic processing which generates non-covalent homodimers. *The Journal of Biological Chemistry*. **274**:32127
- Steinman, R. and H. Hemmi. 2006. Dendritic cells: Translating innate to adaptive immunity. *Current topics in Microbiology and Immunology*. **311**:17
- Stetler-Stevenson WG. (1999) Matrix metalloproteinases in angiogenesis: a moving target for therapeutic intervention. *The Journal of Clinical Investigation*. **103**:1297
- Stoeltzing, O. et al. 2003. Angiostatin-1 inhibits vascular permeability, angiogenesis, and growth of hepatic colon cancer tumours. *Cancer Research*. **63**:33707
- Stumpo, R. et al. 2003. IL-10 induces gene expression in macrophages: partial overlap with IL-5 but not with IL-4 induced genes. *Cytokine*. **24**:46
- Sunderkötter, C. et al. 1991. Macrophage-derived angiogenic factors. *Pharmacology & Therapeutics*. **51**:195
- Sunderkötter, C. et al. 1994. Macrophages and angiogenesis. *Journal of Leukocyte Biology*. **55**:410
- Suomela, S. et al. 2003. Matrix metalloproteinase-19 is expressed by keratinocytes in psoriasis. *Acta Derm Venereol*. **83**:108
- Swartz, J.M. et al. 2006. *Schistosoma mansoni* infection in eosinophil-lineage-ablated mice. *Blood*. **108**:2420

- Tae Cha, S. et al. 2005. A method of isolation and culture of microvascular endothelial cells from mouse skin. *Microvascular Research*. **70**:198
- Tamm, M. et al. 1998. Hypoxia-induced interleukin-6 and interleukin-8 production is mediated by platelet-activating factor and platelet-derived growth factor in primary human lung cells. *American Journal of Respiratory Cell and Molecular Biology*. **19**:653
- Tarsitano, M., et al. 2006. The *C.elegans* pvf-1 gene encodes a PDGF/VEGF-like factor able to bind mammalian VEGF receptors and to induce angiogenesis. *Federation of American Societies for Experimental Biology*. **20**:227
- Tawe, W., et al. 2000. Angiogenic activity of *Onchocerca volvulus* recombinant proteins similar to vespid venom antigen 5. *Molecular and Biochemical Parasitology*. **109**:91
- Taylor, A.P. et al. 2010. Placental growth factor (PlGF) enhances breast cancer cell motility by mobilising ERK1/2 phosphorylation and cytoskeletal rearrangement. *British Journal of Cancer*. **103**:82
- Theoharades, T. C. and D. Kalogeromitros. 2006, The Critical Role of Mast Cells in Allergy and Inflammation. *Annals of the New York Academy of Sciences*. **1088**: 78
- Thurston, G. et al. 1999. Leakage-resistant blood vessels in mice transgenically overexpressing angiopoietin-1. *Science*. **286**:2511
- Thurston G, et al. 2000. Angiopoietin-1 protects the adult vasculature against plasma leakage. *Nature Medicine*. **6**:460
- Tischer, E. et al. 1991. The human gene for vascular endothelial growth factor. Multiple protein forms are encoded through alternative exon splicing. *The Journal of Biochemical Chemistry*. **266**:11947
- Tomita, M. et al. 2000. Effect of mast cells on tumour angiogenesis in lung cancer. *The Annals of Thoracic Surgery*. **69**:1686
- Tonnesen, M.G. et al. 2000. Angiogenesis in wound healing. *Journal of Investigative Dermatology Symposium Proceedings*. **5**:40
- Tsai, H.C. et al. 2009. Dynamic changes of hepatocyte growth factor in eosinophilic meningitis caused by *Angiostrongylus cantonensis* infection. *American Journal of Tropical Medicine and Hygiene*. **80**:980
- Tsirogianni, A.K. et al. 2006. Wound healing: Immunological aspects. *Injury*. **37**:s5
- van Beijnum, J.R., et al. 2008. Isolation of endothelial cells from fresh tissues. *Nature Protocols*. **3**:1085

- Van der Biggelaar, A.H. et al. 2000. Decreased atropy in children infected with *Schistosoma haematobium*: a role for parasite- induced interleukin-10. *Lancet*. **356**:1723.
- Van der Werf, M.J., et al. 2003. Quantification of clinical morbidity associated with schistosome infection in sub-Saharan Africa. *Acta Tropica*. **86**:125
- Van Hinsbergh, et al. 2006. Pericellular proteases in angiogenesis and vasculogenesis. *Arteriosclerosis, Thrombosis and Vascular*. **26**:716
- Van Scott, M.R., et al. 1999. IL-10 reduces Th2 cytokine production and eosinophilia but augments airway reactivity in allergic mice. *Lung Cellular and Molecular Physiology*. **278**: L667
- Vaupel, P. 2004. The role of Hypoxia-Induced Factors in Tumor Progression. *The Oncologist*. **9**:10
- Viñals, F and J. Pouyssegur. 2001. Transforming Growth Factor 1 (TGF-1) Promotes Endothelial Cell Survival during In Vitro Angiogenesis via an Autocrine Mechanism Implicating TGF-Signalling. *Molecular and Cellular Biology*. **21**:7218
- Voehringer, D. et al. 2007. Eosinophils develop in distinct stages and are recruited to peripheral sites by alternatively activated macrophages. *Journal of Leukocyte Biology*. **81**:1434
- Volpert, O.V. et al. 1998. Inhibition of angiogenesis by interleukin 4. *The Journal of Experimental Medicine*. **188**:1039
- Wakefield, L.M. and A.B. Roberts. 2002. TGF- β signalling: positive and negative effects on tumorigenesis. *Current Opinion in Genetics and Development*. **12**:22
- Wakisaka, S. et al. 1998. Modulation by pro-inflammatory cytokines of Fas/Fas ligand-mediated apoptotic cell death of synovial cells in patients with rheumatoid arthritis (RA). *The Journal of Translational Immunology*. **114**:119
- Walsh, D.A. and C.L. Pearson. 2001. Angiogenesis in the pathogenesis of inflammatory joint and lung diseases. *Arthritis Research*. **3**:147
- Wang, H. and J.A. Keiser. 1998. Vascular Endothelial Growth Factor up regulates the expression of matrix metalloproteinases in vascular smooth muscle cells: Role of flt-1. *Circulation Research*. **83**:832
- Wang D, et al. 2006. CXCL1 induced by prostaglandin E2 promotes angiogenesis in colorectal cancer. *Journal of Experimental Medicine*. **203**:941

- Ward, R. E. and D.J. McLaren. 1988. *Schistosoma mansoni*: evidence that eosinophils and/or macrophages contribute to skin-phase challenge attrition in vaccinated CBA/Ca mice. *Parasitology*. **96**: 63
- Wardlow, A.J. et al. 2000. Eosinophils in asthma and other allergic diseases. *British Medical Bulletin*. **56**: 985
- Weidner, K.M. et al. 1993. The Met receptor tyrosine kinase transduces motility, proliferation and morphogenic signals of scatter factor/hepatocyte growth factor in epithelial cells. *The Journal of Cell Biology*. **121**:145
- Werner, S. and R. Grose. 2003. Regulation of wound healing by growth factors and cytokines. *Physiological Reviews*. **83**:835
- Weiss, S.J. 1989. Tissue destruction by neutrophils. *The New England Journal of Medicine*. **320**:365
- Weis, S.M. and D.A. Cheresh. 2005. Pathophysiological consequences of VEGF-induced vascular permeability. *Nature*. **437**:497
- Wheater, P. R. and R.A. Wilson. 1979. *Schistosoma mansoni*: a histological study of migration in the laboratory mouse. *Parasitology*. **79**: 49
- Whitfield, P.J. et al. 2003. Invasion by schistosome cercariae: studies with human skin explants. *Trends in Parasitology*. **19**:339
- Willet, C.G. et al. 2004. Direct evidence that the VEGF-specific antibody bevacizumab has anti vascular effects in human rectal cancer. *Nature Medicine*. **10**:145
- Williams, T.J. 2004. The eosinophil enigma. *Journal of Clinical Investigation*. **113**:507
- Wilson R.A. and J.R. Lawson. 1980. An examination of the skin phase of schistosome migration using a hamster cheek pouch preparation. *Parasitology*. **80**:257
- Wilson. R.A and P.S.Coulson. 1986. *Schistosoma mansoni*: dynamics of migration through the vascular system of the mouse. *Parasitology*. **92**: 83
- Wilson, R. A., 1987. Cercariae to liver worms: development and migration in the mammalian host. In Rollinson, R. and Simpson, A.J.G. (Eds.) *The biology of schistosomes: From genes to Latrines*. Academic Press, London, pp115
- Witte, M.B. and A. Barbul. 1997. General principles of wound healing. *Surgical Clinics of North America*. **77**:509

Wollenberg, A. et al. 2002. Plasmacytoid Dendritic Cells: A New Cutaneous Dendritic Cell Subset with Distinct Role in Inflammatory Skin Diseases. *Journal of Investigative Dermatology*. **119**:1096

Wolowczuk, I. et al. 1997. Interleukin-7 in the skin of *Schistosoma mansoni*-infected mice is associated with a decrease in interferon-gamma production and leads to an aggravation of the disease. *Immunology*.**911**:35

Wu, W-K. et al. 2010. IL-10 regulation of macrophage VEGF production is dependent on macrophage polarisation and hypoxia. *Immunobiology*. **215**:796

Xin, X et al. 2001. Hepatocyte Growth Factor enhances Vascular Endothelial Growth Factor-induced angiogenesis *in vitro* and *in vivo*. *American Society for Investigative Pathology*. **158**:1111

Xu, J. et al 2001. Proteolytic exposure of a cryptic site within collagen type IV is required for angiogenesis and tumour growth *in vivo*. *The Journal of Cell Biology*. **154**:1069

Yang, X., S.Wang et al. 2000. IL-10 deficiency prevents IL-5 overproduction and eosinophilic inflammation in a murine model of asthma-like reaction. *European Journal of Immunology*. **30**:382

Yano, H. et al. 1999. Mast cell infiltration around gastric cancer cells correlates with tumour angiogenesis and metastasis. *Gastric cancer*. **2**:26

Yoo, S.A. et al. 2009. Role of placental growth factor and its receptor flt-1 in rheumatoid inflammation: a link between angiogenesis and inflammation. *Arthritis & Rheumatism*. **60**:345

Yu, L.J. and J.W. Rak. 2003. Inflammatory and immune cells in tumour angiogenesis and arteriogenesis. *Breast Cancer Research*. **5**:83

Zhang, X and D.M. Mosser. 2008. Macrophage activation by endogenous danger signals. *The Journal of Pathology*. **241**:161

Zarnegar, R. and G.K. Michalopoulos. 1995. The many Faces of Hepatocyte growth factor: from hepatopoiesis to hematopoiesis. *The Journal of Cell Biology*. **129**:1177